Process development for symbiotic culture of Saccharomyces cerevisiae and Chlorella vulgaris for in situ CO2 mitigation

Angéla La

université PARIS-SACLAY

CentraleSupélec

NNT : 2019SACLC031

Process development for symbiotic culture of *Saccharomyces cerevisiae* and *Chlorella vulgaris* for *in situ* CO_2 mitigation

Thèse de doctorat de l'Université Paris-Saclay
Préparée à CentraleSupélec

École doctorale n°579 Sciences mécaniques et énergétiques, matériaux et géosciences (SMEMAG)
Spécialité de doctorat : Génie des procédés

Thèse présentée et soutenue à Gif-Sur-Yvette, le 22 Mai 2019, par

Mme Angéla LA

Composition du Jury :

M. Théodore Bouchez Responsable d'équipe, IRSTEA	Président du jury
Mme Patricia Taillandier Professeur, INP-ENSIACET, Université de Toulouse	Rapporteur
M. Olivier Bernard Directeur de recherche, INRIA Sophia-Antipolis Méditerranée	Rapporteur
Mme Marina Bely Maître de Conférences HDR, Université de Bordeaux	Examinatrice
Mme Filipa Lopes Professeur, CentraleSupélec, Université Paris-Saclay	Examinatrice
M. Patrick Perré Professeur, CentraleSupélec, Université Paris-Saclay	Directeur de thèse
M. Behnam Taidi Professeur, CentraleSupélec, Université Paris-Saclay	Co-Directeur de thèse

Thèse de doctorat

Résumé

Titre : Développement d'un procédé symbiotique entre *Saccharomyces cerevisiae* et *Chlorella vulgaris* en photo-bioréacteur pour une limitation en rejet de CO_2 *in situ*

La levure et la microalgue sont des microorganismes très étudiés pour la production de composés à haute valeur ajoutée pour des secteurs tels que l'agroalimentaire et l'énergie. Ce travail de thèse propose un procédé de culture mixte entre la levure *Saccharomyces cerevisiae* et la microalgue *Chlorella vulgaris* pour la croissance des deux espèces tout en limitant le rejet en CO_2. Le procédé repose sur la symbiose mutuelle entre les deux organismes autour des échanges de gaz, qui est rendu possible en imposant une co-dominance en termes de population. Les populations doivent être équilibrées pour que les microalgues puissent gérer la production de CO_2. Le procédé est réalisé en photo-bioréacteur de 5 litres non-aéré et fermé, afin d'éviter les échanges gazeux avec l'environnement externe. Dans cette configuration, le CO_2 est produit sous forme dissoute et directement accessible aux microalgues, évitant les phénomènes de dégazage et de dissolution. Les populations de levures et de microalgues atteignent une concentration égale ($2x10^{10}$ cellules. l^{-1}) au bout de 24 heures de culture, restent stables jusqu'à la fin de la culture (168 heures) et les microalgues recyclent 12% du CO_2 produit par les levures. Un modèle cinétique de la levure et de la microalgue en culture mixte est développé en combinant le modèle individuel de la levure et celui de la microalgue. Le modèle prédictif de la levure prend en compte les possibles voies métaboliques impliquées dans la fermentation et la respiration de ces voies est prédite en y intégrant des facteurs de limitation. Le modèle de la microalgue est basé sur l'activité photosynthétique. Les résultats de ce travail montrent la faisabilité du procédé de culture mixte entre hétérotrophe et autotrophe et pourrait apporter les bases pour le développement d'un procédé écologique à faible impact environnemental.

Mots-clés : consortium microbien, culture mixte et co-dominante, échange de gaz, modèle de croissance, photo-bioréacteur, métabolisme

Abstract

Title: Process development for symbiotic culture of *Saccharomyces cerevisiae* and *Chlorella vulgaris* for in situ CO_2 mitigation

Yeast and microalgae are microorganisms widely studied for the production of high-value compounds used in food and energy area. This work proposes a process of mixed culture of *Saccharomyces cerevisiae* and *Chlorella vulgaris* for both growth and CO_2 mitigation. The process relies on mutual symbiosis between the two organisms through gas exchange, which is possible by engineering the co-dominance of populations. The two populations must be balanced in such a way so that microalgae can cope with the rate of CO_2 production by the yeast activity. The process is performed in non-aerated 5l-photo-bioreactor fitted with a fermentation lock to prevent gas exchange with the outside atmosphere. With this set-up, the CO_2 is produced in dissolved form and is available to the microalgae avoiding degassing and dissolution phenomena. The two organism populations are balanced at approximately $2x10^{10}$ cells. l^{-1}, 12% CO_2 produced by yeast was reutilized by microalgae within 168 hours of culture. A yeast and microalgae growth model in mixed culture is developed by combining each individual growth model. The predictive yeast model considers the possible metabolic pathways involved in fermentation and respiration and imposes limitation factors on these pathways, in this manner, the model can predict the partition of these pathways. The microalgae individual model is based on the photosynthetic activity. The results of this work show the feasibility of such process and could provide a basis for the development of a green process of low environmental impact.

Keywords: microbial consortium, co-dominant mixed culture, gas exchange, growth model, photo-bioreactor, metabolism

Remerciements

Je tiens tout d'abord à exprimer toute ma reconnaissance envers Patrick Perré, mon directeur de thèse. Je le remercie de m'avoir accueillie dans son laboratoire et de m'avoir guidée durant ces années de thèse. Travailler à ses côtés aura été une expérience extrêmement riche et stimulante. Je le remercie pour son encadrement, son efficacité et d'avoir pris le temps de partager ses nombreuses compétences et sa rigueur intellectuelle et tout cela m'a beaucoup aidée à dépasser mes limites.

Mes remerciements viennent naturellement à Behnam Taidi, mon co-directeur de thèse, qui a été le tout premier à me donner ma chance et qui a énormément contribué à mon initiation à la culture en bioréacteur. Je le remercie pour sa disponibilité et de m'avoir accompagnée pendant toute cette aventure semée d'embûches.

J'adresse également mes remerciements aux membres du jury : Théodore Bouchez pour avoir présidé ce jury, Patricia Taillandier et Olivier Bernard pour avoir accepté d'être les rapporteurs de ce manuscrit et pour le temps consacré à son étude, Marina Bely et Filipa Lopes pour leur implication en tant qu'examinatrices.

Je remercie chaleureusement toute l'équipe du LGPM du campus de Gif et de Pomacle. Merci à Fanny et Cédric pour toutes les analyses d'échantillons, à Cyril et Thierry pour m'avoir aidée dans le montage des dispositifs expérimentaux, à Mathilde pour toutes les fois que j'ai eu besoin d'azote. À toutes ces personnes qui font du LGPM un laboratoire où il fait bon d'y travailler. Je pense, entre autres, à mes chers collègues docteurs et camarades de promotion (John et Arnaud), aux doctorants pour qui il reste encore du chemin et à qui j'adresse tout mon soutien (Julia, Claire, Jing, Jérôme, Yong, Yuanyuan, Manasa…). Une pensée également à Clarisse pour sa super bonne humeur, à Barbara pour toute l'énergie qu'elle dégage et surtout pour ses mots tendres et réconfortants le jour de ma soutenance, à Pin qui m'a beaucoup aidée dans mes premiers pas au LGPM, et enfin aux personnels permanents de la fine équipe du midi, toujours présents pour manger au CROUS (Magali, Nathalie, Marie-Laurence et Hervé).

Un immense merci à la famille Vandewalle de m'avoir acceptée si chaleureusement et grâce à qui je peux toujours célébrer les fêtes de famille en France, et je remercie plus particulièrement Mamie Annie, Thierry et Dominique de s'être déplacés pour assister à ma soutenance de thèse.

Je tiens à remercier profondément ma famille et plus particulièrement mon père et ma mère à qui je dois tellement de choses. Je leur dédie ce travail en signe de remerciement pour tout leur soutien et leur amour. Je ne serais pas devenue le petit bout de femme que je suis aujourd'hui sans eux.

J'adresse mes derniers remerciements à Thomas. Je ne le remercierais jamais assez pour toutes ses relectures, ses corrections et ses critiques constructives qui ont contribué à l'aboutissement de ce travail. Son soutien, sa patience et son amour ont été si précieux durant tout ce périple. Je suis fière et heureuse de l'avoir à mes côtés et que l'on puisse continuer à grandir ensemble.

" LA VIE, C'EST COMME UNE BICYCLETTE, IL FAUT AVANCER POUR NE PAS PERDRE L'ÉQUILIBRE. "

A. EINSTEIN

Contents

Nomenclature

Latin symbols

b	extinction coefficient of microalgae (143)	l. g^{-1} m^{-1}
dr	distance from the edge of photo-bioreactor	m
$C_{content}$	carbon content	%
$C_{glucose}$	moles of carbon of 1 mole of glucose (6)	mole
DW	dry weight	g. l^{-1}
H_{O_2}	Henry's constant for O_2 at 25°C (769.23)	atm l. $mole^{-1}$
H_{CO_2}	Henry's constant for O_2 at 25°C (29.41)	atm l. $mole^{-1}$
h_m	diffusion coefficient gas/liquid phase (1×10^{-2})	m. s-1
I	light intensity	µmole. m^{-2} s^{-1}
I_0	intensity of the light source (1800)	µmole. m^{-2} s^{-1}
I_{opt}	light intensity for maximal microalgae growth (275)	µmole. m^{-2} s^{-1}
K_1	dissociation constant of CO_2/ HCO_3^-	-
K_2	dissociation constant of HCO_3^-/ CO_3^{2-}	-
K_i	half-saturation of compound i	g. l^{-1}
K_La	volumetric gas transfer	h^{-1}
m_i	mass of compound i	g
M_i	molar mass of compound i	g. $mole^{-1}$
N	cells concentration	cells. l^{-1}
N_0	initial concentration	cells. l^{-1}
P_{O2}	partial O_2 pression	% (v/v)
P_{CO2}	partial CO_2 pression	% (v/v)
r	length path	m
R	radius of the photo-bioreactor (0.08)	m
R_{gas}	gas constant (8.314)	m^3 Pa. mol^{-1} K^{-1}
S	area exchange of gas/liquid phase (2×10^{-2})	m^2
T	temperature culture (298)	K
td	doubling time	h
V_{gas}	volume of headspace ($1.3x10^{-3}$)	m^{-3}
V_{liq}	volume of liquid phase (5)	l

Greek symbol

α	initial slope of the light response curve (2.1×10^{-3})	h^{-1}
β_{CO2}	mass CO_2 consumed per mass of microalgae	g. g^{-1}
β_{O2}	mass O_2 produced per mass of microalgae	g. g^{-1}
γ	mass iron consumed per mass of microalgae	g. g^{-1}
ε	mass iron consumed per mass of yeast	g. g^{-1}
λ_i	kinetics parameter of compound i	h^{-1}
μ	specific growth rate	h^{-1}
μ_{yeast}	maximal yeast growth rate (0.3)	h^{-1}
μ_{max_algae}	maximal microalgae growth rate (0.04)	h^{-1}

Abbreviations

2PG	2-phosphoglycolate
3PG	3-phosphoglycerate
aa	amino acids
ADP	adenosine di-phosphate
ATP	adenosine tri-phosphate
auto	autotrophy
coA	coenzyme A
coQ	coenzyme q10
coQH2	ubiquinol
DHAH	dihydroxyacetone phosphate
DW	dry weight
EM	Embden-Meyerhof
eth	ethanol
ER	endoplasmic reticulum
FAD^+	flavin adenine dinucleotide (oxidized form)
FADH	flavin adenine dinucleotide (reduced form)
FAN	free amino nitrogen
Fe-FeEDTA	iron Fe from Ferric EDTA
FS	forward scatter
G3P	glyceraldehyde 3-phosphate
GFP	green fluorescent protein
glu	glucose
gly	glycerol
hetero	heterotrophy
MBM	modified Bristol medium
mixo	mixotrophy
NAD^+	nicotinamide adenine dinucleotide (oxidized form)
NADH	nicotinamide adenine dinucleotide (reduced form)
NADP	nicotinamide adenine dinucleotide phosphate (oxidized form)
NADPH	nicotinamide adenine dinucleotide phosphate (reduced form)
$N\text{-}NH_4^+$	nitrogen from NH_4^+
$N\text{-}NO_3^-$	nitrogen from NO_3^-
OD	optical density
OUR	oxygen uptake rate
P	product
PBR	photo-bioreactor
PGA	3-phosphoglycerate
RuBisCo	ribulose 1,5-biphosphate carboxylase oxygenase
RuBP	ribulose 1,5-bisphosphate
S	substrate
SS	side scatter
TCA	tricarboxylic acid
X	biomass
Y	yield coefficient
YPG	yeast extract-peptone-glucose

General introduction

The world is shifting its production processes from a linear, petrol-based economy towards an agricultural circular bio-economy. The harmful effects of atmospheric CO_2 and other greenhouse gases are increasingly evident. In this context, the development of "green" biotransformation processes that use the minimum amount of energy in the most efficient manner and that produce the least quantity of noxious waste is of utmost important. CO_2 is produced as a waste product from many biotransformation processes. Once released, the CO_2 exerts its damaging influence before it can be captured again though agricultural cultures. The chemical and physical processes for the capture of CO_2 before its release into the atmosphere are accompanied with fossil fuel consumption. Even agricultural recapture of CO_2 entails all the energy costs associated with the culture, harvest and processing of crops. All in all, once the CO_2 leaves the bioreactor, its capture is always associated with the use of energy that is often from fossil fuel sources and hence the release of more CO_2 from fossil sources. Therefore, *in situ* biological sequestration of this gas has the potential advantage of decreasing fossil carbon release into the atmosphere and limiting the environmental damage that can be brought about before the CO_2 is recaptured.

Commercially, the loss of a considerable part of the substrate in the form of CO_2 is an inefficient practice that cannot be avoided with microbial cultures. With many biotransformation processes, a large part of the substrate (30-50%) is converted to CO_2 rather than product. In economic terms, the producer "wastes" almost half of its substrate. *In situ* recapture of CO_2 could reduce this financial loss by providing an opportunity where the substrate would be entirely used, at the same time rendering the process sustainable. To this end, photosynthesis is the best candidate to be associated to the normal production process. This natural process is often based on symbiotic relationships between organisms.

Systems based on symbiosis between microbial species have been attempted for biotechnological applications in bioprocess and environmental protection (Santos and Reis 2014; Magdouli et al. 2016). The choice of microbial species (microalgae, bacteria or yeast) depends on the final aims of co-culture: harvesting by bioflocculation (Subashchandrabose et al. 2011; Rai et al. 2012), wastewater treatment (Arumugam et al. 2014), production of extracellular polymeric substances (Haggstrom and Dostalek 1981) or growth promotion and lipid production (Milledge and Heaven 2013; Pragya et al. 2013). The creation and control of specific consortia, with the desired microbial ecology, to perform biotransformation is key to the use of these consortia in industrial biotechnology.

The heterotrophic CO_2 production rate is usually largely superior to it autotrophic consumption rate, hence from a CO_2 mitigation viewpoint the mixed populations must be balanced in such way so that the photosynthetic population can cope with the rate of CO_2 production. In other words, the heterotrophic activity must be in step with the CO_2 removal rate. This could be achieved though co-dominance of the populations allowing synergy between the two organisms based on gaseous exchange. To the author's knowledge, no scientific studies have been published with the stated aim of developing co-dominant symbiotic mixed cultures. Most studies have simply demonstrated that by increasing the CO_2 concentration in a photobioreactor, albeit from a heterotrophic culture, the production rate of photosynthesis increases.

The study exposed in this thesis details the strategy used to develop a co-dominant mixed culture i.e. a batch process based on a constructed consortium of yeast and microalgae so that CO_2 mitigation becomes an integral part of the process. Yeast and microalgae were targeted since they are used in bioprocesses for high value oil production and the species *Saccharomyces cerevisiae* and *Chlorella vulgaris* were chosen for this study as model organisms due to the vast literature that exists in connection with their metabolisms. A kinetic growth model of yeast and microalgae in the mixed culture (consortium) is also presented in this thesis.

This thesis starts with a literature review (Chapter 1) describing the possible metabolisms adopted by the yeast *S. cerevisiae* and the microalga *C. vulgaris* according to culture conditions. An inventory of studies of consortia of yeast and microalgae is also described to outline the advantages and the challenges in developing co-dominant mixed cultures of yeast and microalgae.

The techniques and methodologies used in this study for the acquisition of experimental data and their analysis is presented in the chapter "Material and methods" (Chapter 2).

The following chapters concern the development of the process of mixed culture, which was conducted through an approach based on interactions between the experimental and the modeling part (Figure 1).

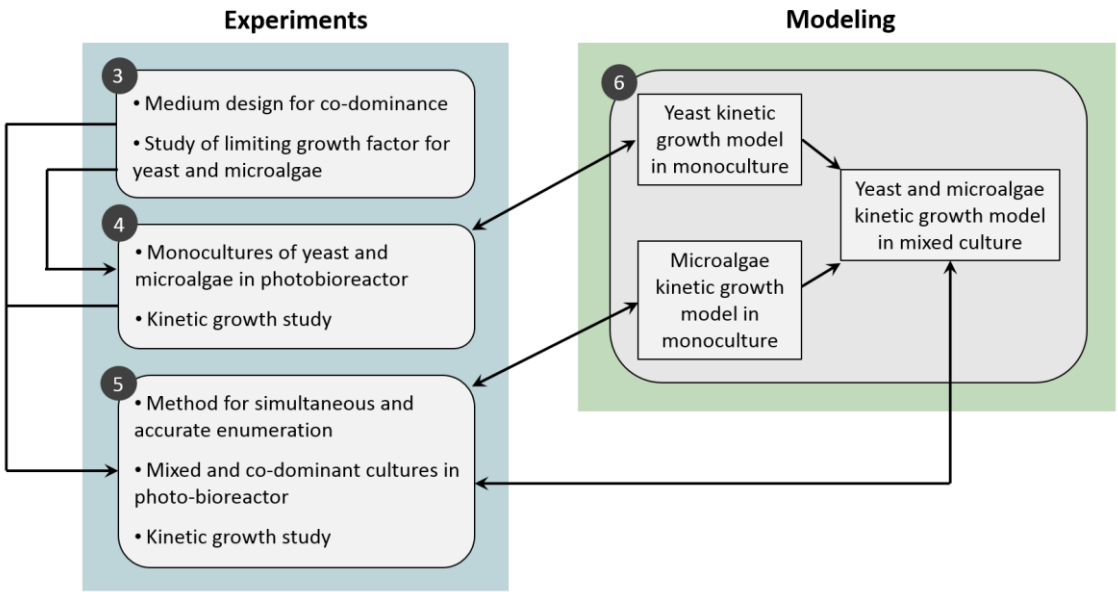

Figure 1. Interaction between experimental and modelling part for the development and the study of mixed and co-dominant culture (consortium) of yeast *S. cerevisiae* and microalga *C. vulgaris*. Corresponding chapters are specified in grey circles.

In Chapter 3, key tools for the development of a co-dominant mixed culture are presented: definition of culture parameters and the design of a medium suited for both yeast and microalgae growth. Components from this newly designed medium are studied to assess their impact on yeast and microalgae growth and with a view to optimize the medium.

S. cerevisiae and *C. vulgaris* monoculture were then grown in the newly designed medium and in photo-bioreactors with the closest culture conditions possible to those of the mixed culture. The study of experimental data, presented in Chapter 4, allowed to provide mass balances, to determine metabolisms adopted by yeast and microalgae and to estimate yeast and microalgae behaviors in mixed culture.

Chapter 5 presents results of two mixed cultures in photo-bioreactor. The mixed cultures were performed using the newly designed medium (Chapter 3) and *S. cerevisiae* and *C. vulgaris* growth were followed thanks to the enumeration method presented in Chapter 3. The mass balances and the growth kinetics in yeast and microalgae monocultures were compared to mixed cultures in order to identify the interactions between *S. cerevisiae* and *C. vulgaris* in mixed culture. A method for simultaneous and accurate enumeration of the two species in a mixed suspension is also presented.

Chapter 6 presents the development of the kinetic growth models of *S. cerevisiae* and *C. vulgaris* in monoculture. The stoichiometric reactions are formulated according possible metabolisms adopted by yeast and microalgae in monoculture (Chapter 4). The stoichiometric coefficients are well-known from literature and the coefficients of the reaction kinetics were adjusted with experimental data and confirmed with the literature. The yeast and microalgae kinetic growth model in mixed culture is based on the combination of their respective individual model and by taking account the interactions between the two species. Simulation results are then compared to the experimental data. Modeling is a tool for data analysis from experimental part and a mean for better understanding of the yeast and microalgae metabolisms.

Through this study, we propose a general methodology for the development and the study of a co-dominant symbiotic mixed culture of a heterotroph and an autotroph and assess the success and the challenges of such strategy. The work presented here was performed on well-known model organisms but can provide the basis for more applied studies. The potential advantage of this work is that a symbiotic mixed culture would self-regulate the speed of the bioconversion hence the CO_2-production and -utilization rates; it could potentially eliminate the need for gas supply and can lead to full utilization of the substrate. The potential savings would be those of recovering the cost of the portion of the substrate that is normally lost as CO_2, making considerable savings in terms of gas supply avoidance and reducing environmental CO_2 emissions. In an economical assessment, all these savings would have to be weighed against the losses incurred by moderating the bioconversion speed in step with the photosynthetic rate.

Chapter 1. Literature review

This literature review outlines the possible metabolisms of both *Saccharomyces cerevisiae* and *Chlorella vulgaris* including their specific nutrient requirement. This approach helps to understand and predict potential exchanges between yeast and microalgae when grown together in a mixed culture. A review of previous studies on mixed cultures of yeast and microalgae is also presented in this chapter to identify the improvements needed for the development of the mixed culture processes.

Contents

1.1 Presentation of the yeast *Saccharomyces cerevisiae*

1.1.1 Yeast structure

S. cerevisiae is a unicellular eukaryote fungus with generally an ellipsoid shape with a diameter of 5–10 µm. A yeast cell is also composed of a bud with a smaller diameter of around 5 µm. The yeast ultrastructure and organelles are comparable to that of higher eukaryotic cells: cell wall, nucleus, mitochondria, endoplasmic reticulum (ER), Golgi apparatus, vacuoles and secretory vesicles (Figure 2).

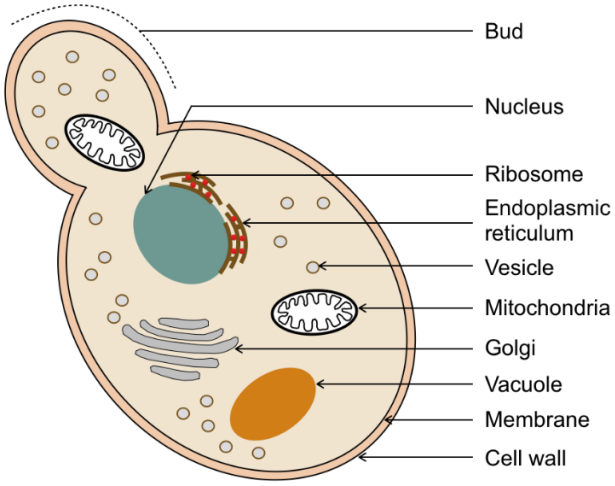

Figure 2. Yeast cell ultrastructure.

The yeast cells propagate by budding from the mother cell, leading to the formation of two cells of unequal size. After the separation of the daughter cell, a scar made of chitin is formed on each cell. The generation (doubling) time is approximately 3 hours at 28°C under optimal conditions. After 30 to 40 budding processes, the yeast cells age and die.

The yeast is a facultative aerobic-anaerobic microorganism, i.e. it can grow in presence of oxygen (respiration) or in absence of oxygen (fermentation). Under fermentative metabolism, *S. cerevisiae* still requires a small amount of molecular oxygen to produce ergosterol and unsaturated fatty acids; key components of its cell membrane.

1.1.2 Yeast metabolism

Three different catabolic pathways can be adopted by the yeast *S. cerevisiae*: strict respiration, strict fermentation and aerobic fermentation (Figure 3).

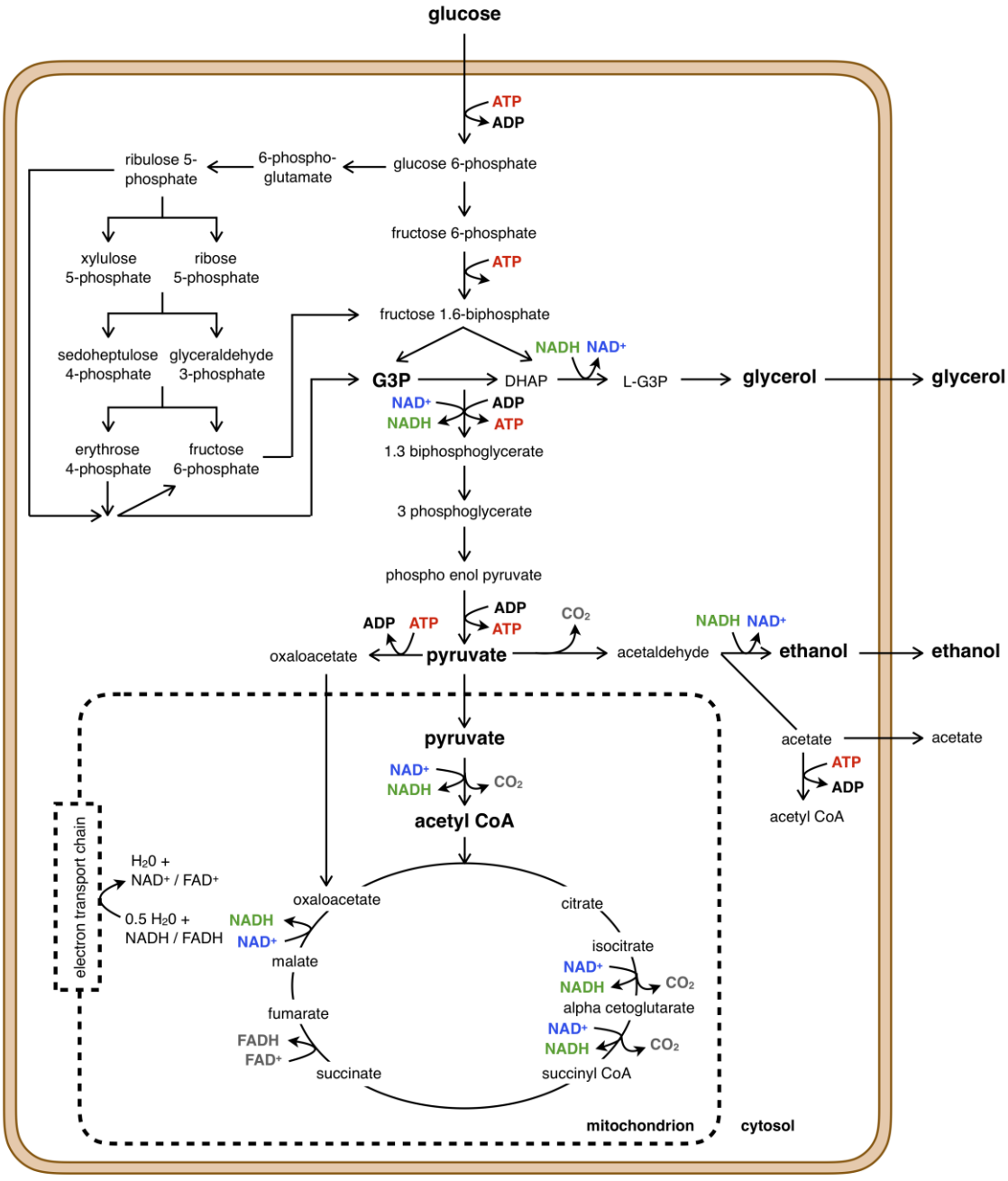

Figure 3. Metabolic pathways possible in *Saccharomyces cerevisiae* (Lannig 2015).

2.1.1.1 Metabolism under aerobic growth culture: respiration

Aerobic respiration or cellular respiration is the process where the sugar substrate is oxidized completely to CO_2, water and Adenine Tri-Phosphate (ATP). ATP is the energy currency of the cell and is produced to provide energy for others cellular activities such as anabolism and biomass production.

Respiration with O_2 occurs under aerobic conditions and involves four successive metabolic pathways: glycolysis, the transition reaction into the tricarboxylic acid cycle (TCA cycle) and oxidative phosphorylation (Figure 3).

During glycolysis, the carbohydrate (glucose or fructose) molecule is oxidized into pyruvate in the cytosol. The glycolysis of each glucose molecule requires two ATP molecules to begin with but produces four ATP in the latter part of glycolysis with a net gain of two ATP molecules. Glycolysis is accompanied by the transfer of electrons. During glycolysis, two NAD^+ (nicotinamide adenine dinucleotide) molecules carry two electrons each and bind with two protons (H^+) respectively from glucose to be reduced into NADH. In aerobic condition, NADH enters mitochondria for following stages of oxidative metabolism.

During the transition reaction, the two pyruvate molecules produced from glycolysis move from cytosol to mitochondria matrix, are metabolized into Acetyl-CoA: the pyruvate transport from the cytosol to mitochondria allows the release of two CO_2 molecules, then two NAD^+ molecules are reduced into NADH. The final products are two molecules of acetyl-CoA.

The two acetyl-CoA molecules produced from the transition reaction enter in TCA cycle to be oxidized inside mitochondria. During this metabolic pathway, NAD^+ and a new electron carrier molecule FAD^+ (Flavin Adenine Dinucleotide) are reduced to NADH and $FADH_2$ respectively, breaking Acetyl-CoA molecules for H^+ use. At the end of TCA cycle, two ATP molecules and four CO_2 molecules are generated. The Acetyl-CoA molecules are fully dismantled.

During the first step of oxidative phosphorylation pathway (Figure 4), called electron transport chain, NADH and $FADH_2$ produced during previous metabolic pathways are oxidized into NAD+ and FAD^+, releasing H^+ and electron, and creating an H^+ gradient across the intermembrane of mitochondria. During this step an O_2 is used to release a H_2O molecule and no ATP is produced (Figure 4). During the second step of oxidative phosphorylation pathway, called chemiosmosis, an ATP is synthesized through the flow of H^+ back across the

intermembrane of mitochondria. From one glucose molecule, chemiosmosis generates 38 ATP molecules.

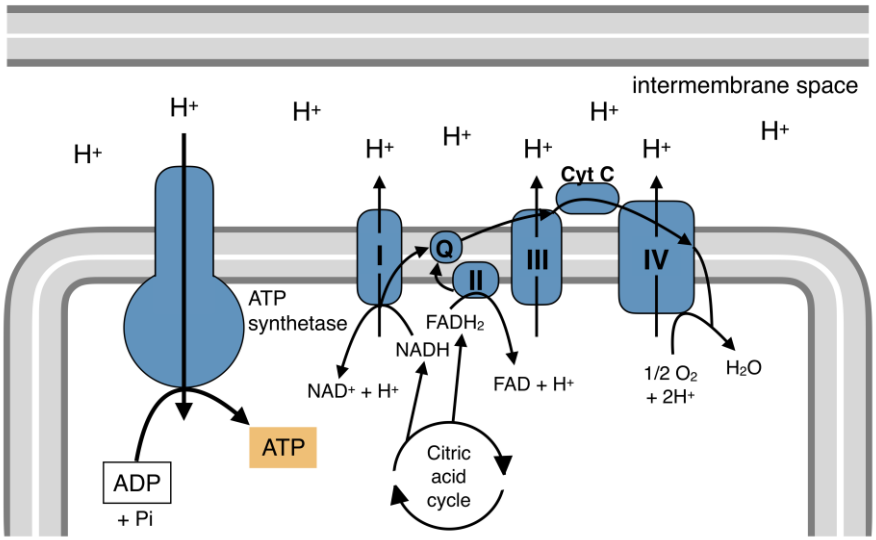

Figure 4. Oxidative phosphorylation.

Table 1. Energy balance of glucose metabolization through cellular respiration. coASH, co enzyme A ; CoQ, co enzyme q10 ; CoQH2, ubiquinol.

glycolysis
glucose + $2NAD^+$ + 2ADP ⟶ 2pyruvate + 2NADH + $2H^+$ + 2ATP + $2H_2O$
transition reaction
2pyruvate + $2NAD^+$ + 2CoASH + $2H_2O$ ⟶ 2Ac-CoA + 2NADH + $2H^+$ + $2CO_2$
TCA cycle
2Ac-CoA + $6NAD^+$ + 2ADP + $8H_2O$ + 2CoQ + $8H_2O$ ⟶ 2CoASH + 6NADH + $8H^+$ + 2ATP + 4 CO_2 + $2CoQH_2$
oxidative phosphorylation
10NADH + $5O_2$ + 30ADP + $40H^+$ ⟶ $10NAD^+$ + $40H_2O$ + 30ATP
$2CoQH_2$ + O_2 + 4ADP + $4H^+$ ⟶ 2CoQ + $6H_2O$ + 4ATP
glucose + $6O_2$ + 38ADP + $32H^+$ ⟶ $38H_2O$ + 38ATP + $6CO_2$

In oxidative metabolism, ATP, biomass, CO_2 and H_2O are the only products from glucose and oxygen (Table 1). The maximal biomass yield coefficient on glucose is 0.5 g_{yeast}. $g_{glucose}^{-1}$ (Verduyn et al. 1990b).

S. cerevisiae is a facultative anaerobe, i.e. it can also produce energy in anaerobic conditions using a fermentative metabolism.

2.1.1.2 Metabolism under anaerobic growth conditions: fermentation

Complete fermentation of carbohydrate occurs under strict anaerobic conditions and is characterized by the production of ethanol. The production of the latter provides the energy (ATP) required for biomass formation and cell maintenance. Although ATP is produced during fermentation, the yield is much lower than during respiration (2 and 38 $mole_{ATP}$. $mole_{glucose}^{-1}$ respectively).

The glycolysis, the transition reaction, the TCA cycle and the ethanol production pathways are the main catabolic pathways of the complete fermentation. The oxidative phosphorylation pathway is not involved as there is no molecular oxygen available (Figure 3).

Glycolysis occurs without direct implication of O_2. In the absence of O_2, the glucose molecule follows another metabolic pathway than in oxidative metabolism. The two pyruvates produced at the end of glycolysis are broken down into two acetaldehyde molecules releasing two CO_2 molecules. Then the acetaldehyde is reduced into ethanol oxidizing NADH oxidation into NAD^+. The NAD^+ is then reused during glycolysis.

During fermentation of glucose, glycerol can be produced in the cytosol of *S. cerevisiae* in order to close the NADH/NAD^+ redox reaction. During glycolysis, glucose is converted into glyceraldehyde-3-phosphate and dihydroxyacetone phosphate in equimolar amounts. Most of dihydroxyacetone is converted into glyceraldehyde-3-phosphate by the enzyme triose phosphate isomerase and the excess dihydroxyacetone phosphate is converted into glycerol. The conversion of dihydroacetone phosphate into glycerol is a two-step reaction involving oxidation of NADH and two enzymes (glycerol-3-phosphate dehydrogenase and phosphatase) (Scanes et al. 1998)

In fermentative metabolism, the carbon flow through the TCA cycle clearly decreases compared to oxidative metabolism (Nissen et al. 1997; Jouhten et al. 2008). The biomass yield coefficient also decreases to around 0.1 g_{yeast}. $g_{glucose}^{-1}$, compensating with production of byproducts (ethanol, glycerol and fusel alcohols) (Verduyn et al. 1990b).

Cell proliferation is the first aim of yeast and ethanol is a byproduct of this process linking alcohol production and yeast growth. While ethanol is produced, cells strive to maintain

their redox balance and make enough ATP to maintain growth. In fact, ethanol cannot be produced efficiently without significant growth of yeast cells. Non-growing yeast cells will ferment only enough sugar to produce energy for cell maintenance and accumulate glycogen and trehalose. The challenge in the fermentation process is to provide enough nutrients for yeast to promote ethanol production while avoiding excessive yeast growth which will represent an alcohol-yield loss (Walker and Stewart 2016).

S. cerevisiae is capable of generating energy under strict fermentative metabolism i.e. in complete absence of O_2 and without respiration, however, molecular O_2 is required for the biosynthesis of compounds required for yeast growth: ergosterol and unsaturated fatty acids (van Dijken et al. 1993). Anaerobic yeast growth can be ensured by the artificial addition of these compounds and absence in the culture medium would lead to a reduction in the specific growth rate and the growth yield (Macy and Miller 1983).

2.1.1.3 Aerobic fermentation referred as Crabtree effect

The aerobic fermentation is characterized by the production of ethanol in presence of oxygen, hence both oxidative phosphorylation and ethanol production pathways are possible. This metabolism occurs when external glucose concentration exceeds a certain variant-dependent threshold concentration.

The energy production comes from glycolysis, the TCA cycle and oxidative phosphorylation. The co-factor NADH is oxidized by both oxidative phosphorylation and ethanol production pathways. The carbon flow through TCA cycle is still lower than in strict respiration but is higher than in fermentative metabolism. The biomass yield coefficient is lower than in strict respiration with values between 0.10 and 0.16 $g_{yeast}. g_{glucose}^{-1}$ (Franzén 2003) but higher than the biomass yield of pure fermentation.

In 1929, Herbert Crabtree showed that the addition of glucose to suspension of rat tumor cells lead to a decrease in respiratory activity and production of lactic acid. This phenomenon was also used to explain the alcoholic fermentation in yeast in aerobic condition (Alexander and Jeffries 1990).

Under aerobic conditions and with an external glucose concentration above 0.10 – 0.15 $g. l^{-1}$ (Verduyn et al. 1984), *S. cerevisiae* ferments glucose during the logarithmic phase of growth releasing ethanol (De Deken 1966); therefore, *S. cerevisiae* is a Crabtree-positive yeast (Figure 5). A high concentration of glucose seems to have an impact on the activities of some

enzymes involved in TCA cycle and oxidative phosphorylation (Beck and Kaspar von Meyenburg 1968; Fiechter and Seghezzi 1992). At low external glucose concentration and in presence of oxygen, *S. cerevisiae* is in strict cellular respirative metabolism, so does not produce ethanol (Käppeli et al. 1985).

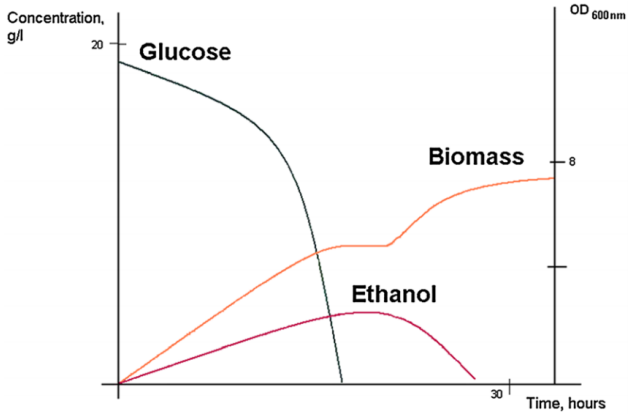

Figure 5. Batch culture of a Crabtree-positive yeasts (Schifferdecker et al. 2014).

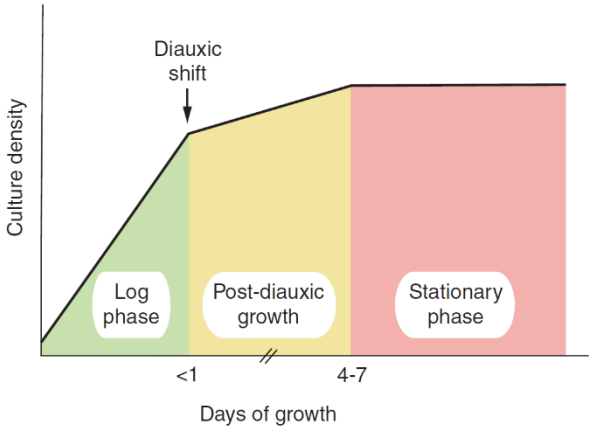

Figure 6. Schematic diauxic growth profile of *Saccharomyces cerevisiae* on glucose-based media (Herman 2002).

S. cerevisiae can respire both ethanol and glycerol and switches to respiration on ethanol when glucose is depleted. Finally, when ethanol is fully exhausted, yeasts cells enter the stationary growth phase (Figure 6). This phenomenon that involves two successive growth phases, is called diauxie and the period of transition in the metabolism is called diauxic shift. The diauxic phase occurs generally within the first 24 hours (Werner-Washburne et al. 1993; Herman 2002), although the duration of this period varies according the concentration of the

preferred substrate. The entry of *S. cerevisiae* in a diauxic shift is characterized by a decrease of the growth rate (Albers et al. 2002).

2.1.1.4 Reoxidation of NADH into NAD^+ under aerobic and anaerobic conditions

NADH is the reduced form of the co-enzyme nicotinamide adenine dinucleotide (NAD^+). NAD^+ is mainly involved as an electron transporter in reduction-oxidation reactions such as glycolysis and TCA cycle. During these reactions, NAD^+ is used generating NADH and the reoxidation of the latter is required to close the NADH/NAD^+ redox balance in *S. cerevisiae* and regenerate NAD^+ allowing glycolysis to proceed.

In strict respiration metabolism, NADH is generated in the cytosol during glycolysis and in the mitochondria during the TCA cycle. Both cytosolic and mitochondrial NADH are reoxidized by the respiratory chain if the conditions permit respiration. The mitochondrial inner membrane is impermeable to NADH and NAD^+ so the cellular redox balance dictates that reduced coenzymes must be reoxidized in the compartment where they are generated. Respiration of intramitochondrial NADH occurs via internal mitochondrial NADH dehydrogenase (Figure 7). The cytosolic NADH can be oxidized via external mitochondrial NADH dehydrogenase or via the glycerol-3-phosphate shuttle (Figure 7).

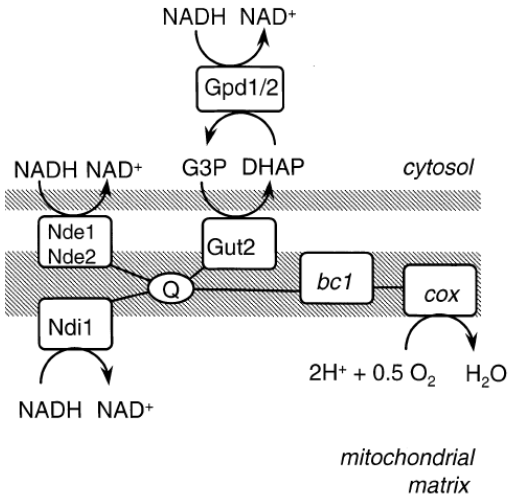

Figure 7. Scheme of NADH reoxidation in the respiratory chain of *S. cerevisiae*. bc1, bc1 complex; cox, cytochrome c oxidase; Gpd, soluble glycerol-3-phosphate dehydrogenase; Gut2, membrane-bound glycerol-3-phosphate dehydrogenase; Nde, external NADH dehydrogenase; Ndi1, internal NADH dehydrogenase; Q:ubiquinone (Bakker and Overkamp 2001).

In strict fermentative metabolism (without aeration), NADH is only generated during glycolysis. The redox balance for the co-enzyme system NAD^+/NADH is closed through the production of ethanol and glycerol (Figure 8).

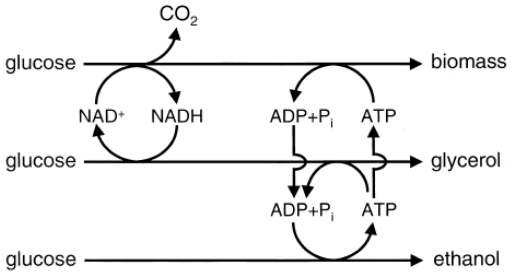

Figure 8. Schematic overview of NAD^+/NADH turnover in respiring (top) and fermentative (bottom) cultures of *S. cerevisiae*. Depending on the concentrations of sugar and oxygen, intermediate situations are possible. In addition to biomass formation, production of low-molecular-mass metabolites, such as acetate, pyruvate, acetaldehyde or succinate may affect turn-over of NAD^+/NADH (Bakker and Overkamp 2001).

In aerobic fermentation, the NADH is still only generated through glycolysis but the cytosolic NADH is reoxidized through external mitochondrial NADH dehydrogenase (respiratory chain), in addition to the production metabolic pathways of ethanol and glycerol.

1.1.3 Nutrition and culture parameters

1.1.3.1 Carbon

Carbon is a major constituent element of *S. cerevisiae* as it represents approximatively 47% of *S. cerevisiae* dry weight (Verduyn et al. 1990b). Glucose is the preferred carbon substrate of *S. cerevisiae* and the presence of glucose inhibits assimilation of other sugars when a mixed source of carbohydrates is supplied to the yeast (Klein et al. 1998; Meijer et al. 1998).

1.1.3.2 Nitrogen

S. cerevisiae is not capable of assimilating nitrogen from atmosphere and requires assimilable organic nitrogen such as α-amino acids or inorganic nitrogen like ammonium for growth and ethanol production. Urea can also be used by yeast, but not recommended for food and feed applications as it can lead to the formation of carcinogenic ethyl carbamate. Nitrogen in yeast fermentation is mainly involved the synthesis of amino acids, proteins (enzymes) and nucleic acids. Levels of free alpha-amino nitrogen (FAN) (individual amino acids and small

peptides) can be growth limiting and *S. cerevisiae* growth (yield) increases almost linearly with increasing FAN levels up to 100 mg. l^{-1} (Walker and Stewart 2016).

Amino acids are the preferred energetically nitrogen source for *S. cerevisiae* in fermentation but with nitrogen catabolite repression, the presence of ammonium ions may inhibit amino acids uptake. In *S. cerevisiae*, two classes of energy-dependent amino acid uptake systems are involved: one is broadly specific (the general amino acid permease, GAP) and effects the uptake of all naturally occurring amino acids, whilst the other includes a variety of transporters that display specificity for particular amino acids. *S. cerevisiae* can also dissimilate amino acids (by decarboxylation, transamination, or fermentation) to yield ammonium, glutamate, and higher alcohols (Walker and Stewart 2016).

In yeast, ammonia (NH_3) reacts with alpha-ketoglutarate from the Krebs cycle to form glutamate and then from the onwards all the other amino acids are made through transamination reactions.

1.1.3.3 Molecular oxygen O_2

Molecular oxygen O_2 is necessary for yeast growth and maintaining the yeast viability in both respiration and fermentation metabolisms. Under strict respiration, O_2 plays a key role in the respiratory chain activity for the generation of ATP.

Although strict fermentation occurs under anaerobic condition, O_2 is manstill required for the synthesis of yeast membrane compounds, i.e. sterols and unsaturated fatty acids. For strict fermentation in winemaking, the average amount of O_2 needed is between 5-10 mg. l^{-1} (Sablayrolles J.M. 1986). O_2 is more used for the synthesis of sterols (75 % of O_2 used) than for that of unsaturated fatty acids (Salmon 2006). The content of lipid compounds in the medium can decrease the O_2 requirement.

1.1.3.4 Temperature and pH

Regarding temperature and pH requirements for alcoholic fermentations, yeasts thrive in warm and acidic environments with most *S. cerevisiae* strains growing well between 20 and 30°C. The optimal pH for yeast growth is from 5 to 5.2 but some yeast strains are able to grow at pH of 3.5-6 (Boulton and Quain 2001).

Temperature has an impact on yeast cell growth, population viability, ethanol production and the substrate yield coefficient (Gervais and de Marañon 1995). The biomass yield coefficient ($Y_{X/S}$) and the ethanol yield coefficient ($Y_{P/S}$) both change for the same substrate depending on the temperature of the aerated fed-batch culture (Aldiguier et al. 2004). The $Y_{X/S}$ decreases with increase in temperature from 27°C (Aldiguier et al. 2004).

1.1.4 Nutrient limitation resulting in stuck and sluggish fermentations

A stuck fermentation is characterized by a premature cessation of fermentation, resulting in an excessive residual sugar concentration in the wine. A wine fermentation is considered as complete when the residual sugar concentration is below 4 g. l^{-1}. Stuck fermentations directly decrease productivity and can reduce wine quality with the formation of off-flavors for example (Bisson, 1999; Henschke, 1997).

A sluggish fermentation is one in which the rate of fermentation is considered as too low for commercial purposes. In winemaking, a sluggish fermentation can take several months to finish instead of the more usual two to three weeks (Bisson 1999).

The rate of fermentation of carbohydrate depends on two factors: the total yeast population and the yeast fermentation capacity. A typical industrial fermentation requires roughly 10^{11} cells. l^{-1} and if the total biomass is lower than this level, the fermentation rate will be slower since there are fewer fermenting cells in the medium. The yeast fermentation capacity can differ for different yeast strains (variants) and depends on the growth conditions. The main factors influencing the total biomass and the fermentation capacity are (Bisson 1999):

- nutrients availability (nitrogen, molecular oxygen and sterols)
- ethanol toxicity
- pH
- extremes of temperature
- toxins

Nitrogen and molecular oxygen limitation are of major importance (Blateyron and Sablayrolles 2001). Nitrogen sources such as ammonium salts and α-amino acids are necessary for proteins synthesis and yeast growth. Molecular oxygen is mandatory for the synthesis of yeast membrane compounds, particularly sterols and unsaturated fatty acids.

Figure 9 represents a typical stuck fermentation due to nitrogen deficiency. When the culture is limited in nitrogen, the total biomass decreases leading to reduction of the fermentation rate.

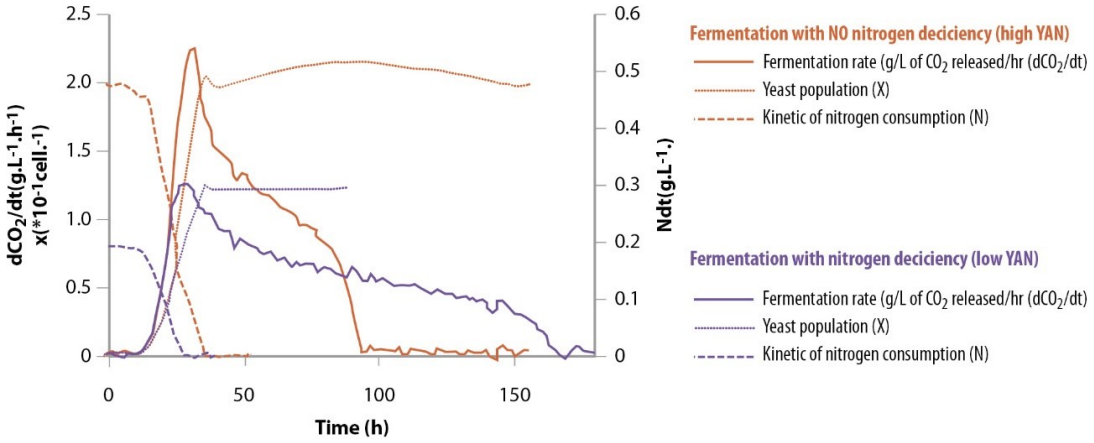

Figure 9. Growth profile of yeast in a stuck fermentation (Sablayrolles, J.M., Sitevi Conference, 2015).

1.2 Presentation of the microalga *Chlorella vulgaris*

1.2.1 Structural presentation of microalgae

Chlorella vulgaris is a unicellular eukaryotic organism firstly identified by Martinus Willem Beijerinck in 1890. The species *C. vulgaris* has a round or ellipsoid form with a diameter of around 2-10 µm and contains similar organelles to plant cells (Safi et al. 2014) (Figure 10).

The cytoplasm is composed of water, soluble proteins, minerals and hosts internal organelles: mitochondria, nucleus, endoplasmic reticulum vacuoles, chloroplast and Golgi apparatus. *C. vulgaris* contains a single chloroplast, which is the key element for photosynthesis such as thylakoids wherein the chlorophyll a and b are synthesized and housed. The pyrenoid is at the center of carbon dioxide fixation as it contains high levels of ribulose 1,5-biphosphate carboxylase oxygenase (RuBisCo). The chloroplast also contains starch granules, the principal energy and carbon reserve of this organism. The starch granules, composed of amylose and amylopectin are formed in the chloroplast under stress growth conditions (Safi et al. 2014).

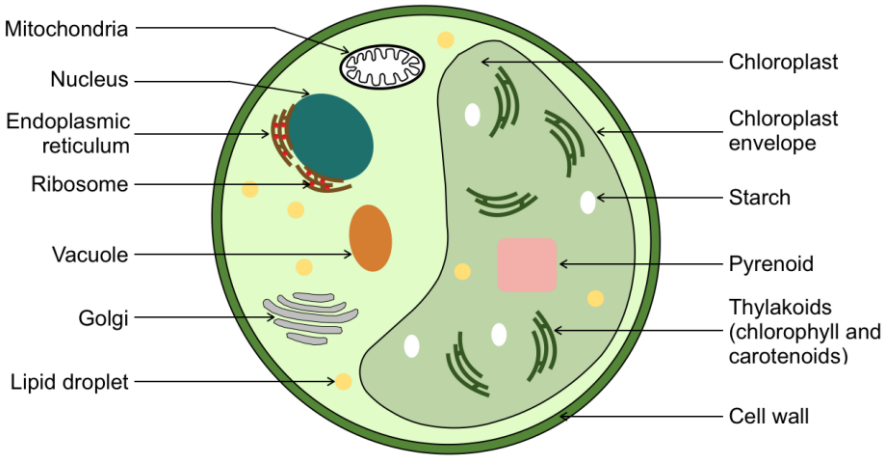

Figure 10. Microalga cell ultrastructure

C. vulgaris reproduction is rapid, asexual by autosporulation (non-motile reproduction) (Safi et al. 2014). Four daughter cells having their own cell wall are formed within the mother cell and after maturation the mother cell wall disrupts, releasing daughter cells, debris and internal nutrients that could be used by daughter cells (Yamamoto et al. 2004) (Figure 11).

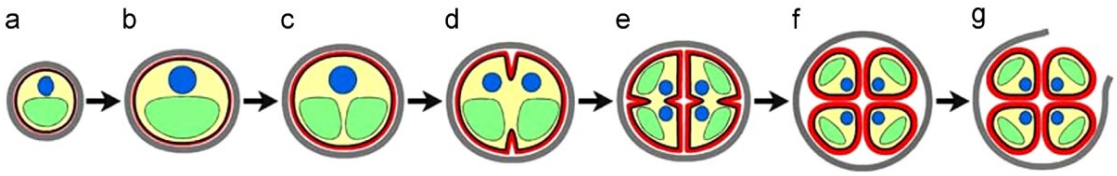

Figure 11. *C. vulgaris* cell division. (a) early cell-growth phase; (b) late cell-growth phase; (c) chloroplast dividing phase; (d) early protoplast dividing phase; (e) late protoplast dividing phase; (f) daughter cells maturation phase and (g) hatching phase. (Safi et al. 2014).

1.2.2 Microalgae metabolism

1.2.2.1 Autotrophic metabolism

A photo-autotrophic growth occurs in mineral medium without any organic carbon when the culture is exposed to sufficient light. Under these conditions, microalgae are capable to synthesize their own organic carbon through photosynthesis. Photosynthesis is a key process in which CO_2 and water are converted into carbohydrates and oxygen through redox reactions supplied by light energy (harvested by chlorophyll molecules).

Photosynthesis is composed of two successive stages: the light reactions (light dependent) and the dark reactions (light independent).

The light reactions occur in the thylakoid membrane of chloroplasts (Figure 12). The light is harvested by two photosystems (proteins and pigments complexes): photosystem I (PSI) and photosystem II (PSII). In both systems, the light is collected through pigments and chlorophyll molecules localized in the center of the photosystem (reaction center). The reaction center of photosystem I and II are respectively P700 and P680. Electrons are removed from water and pass through PSII and PSI, requiring light to absorbed once in each system regenerating NADPH and ATP.

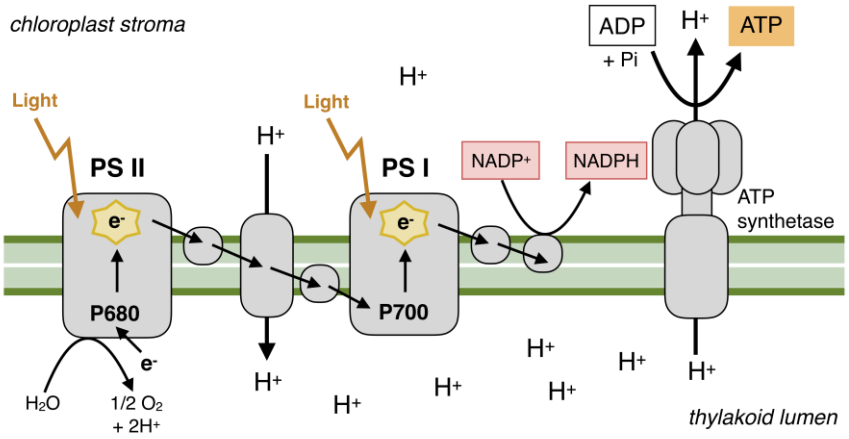

Figure 12. Light reactions of photosynthesis at the thylakoid membrane.

During the light reactions, light energy is converted to chemical energy allowing reduction of $NADP^+$ to NADPH and production ATP; both are used later for the dark reactions as energy source (Figure 13). ATP is the energy currency of cells, i.e. hydrolysis of ATP to ADP releases energy. $NADP^+$ is reduced to NADPH, which is a strong reducing agent that can be oxidized, i.e. it can give away electrons associated with the hydrogen, reducing another molecule. When oxidize, the NADPH goes to a lower energy state and the energy released can be used in the dark reaction.

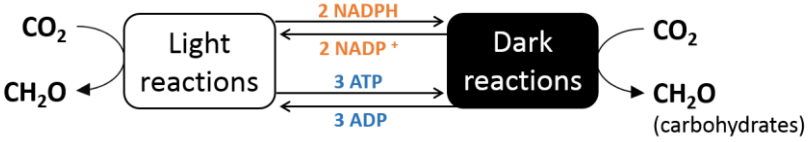

Figure 13. Interactions between light and dark reactions (adapted from Masojídek et al. (2013)).

The dark reactions still occur in presence of light in the chloroplast stroma and the aim of this stage is to fix CO_2 through the Calvin cycle using products from the light reactions (ATP and NADPH) (Figure 14). This stage can be expressed as:

$CO_2 + 4H^+ + 4e^- + 2\ NADPH + 3\ ATP \rightarrow (CH_2O) + H_2O$ **Reaction 1**

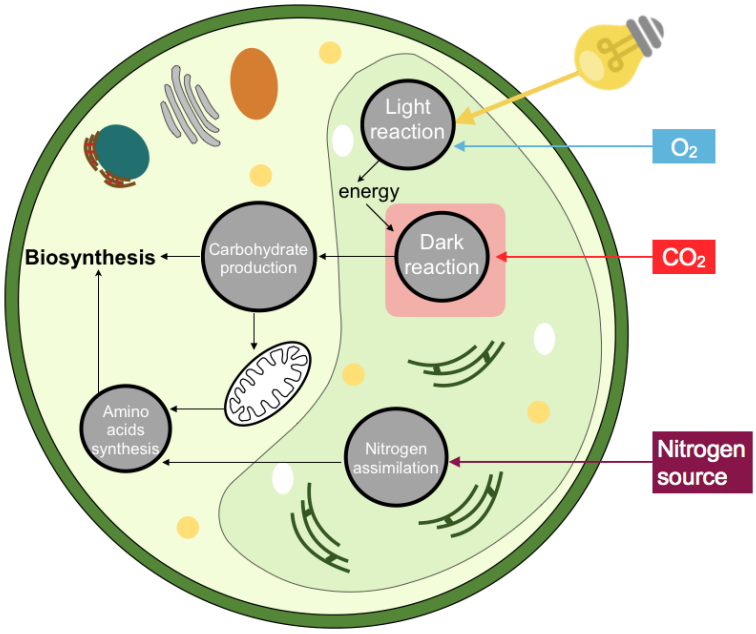

Figure 14. Pathways involved in microalgae photo-autotrophic growth.

Fixation of one molecule of CO_2 required energy from three molecules of ATP and two molecules of NADPH (Richmond 2017) and 95 % of NADPH together with 60 % of ATP from the light reactions are used in the dark reactions (Falkowski and Raven 2007). The Calvin cycle is composed of four distinct phases (Figure 15):

1. Carboxylation phase: the enzyme RuBisCo catalyzes the carboxylation of RuBP with CO_2 to form two molecules of 3-phosphoglycerate (3PG)

2. Reduction phase: phosphorylation of 3PG required ATP and NADPH to form diphosphoglycerate (GBP) and the latter is reduced to form G3P

3. Regeneration phase: 5/6 of G3P molecules produced are recycled within the Calvin cycle for regeneration of RuBP

4. Production phase: 1/6 of G3P molecules are used for carbohydrate production (Falkowski and Raven 2007).

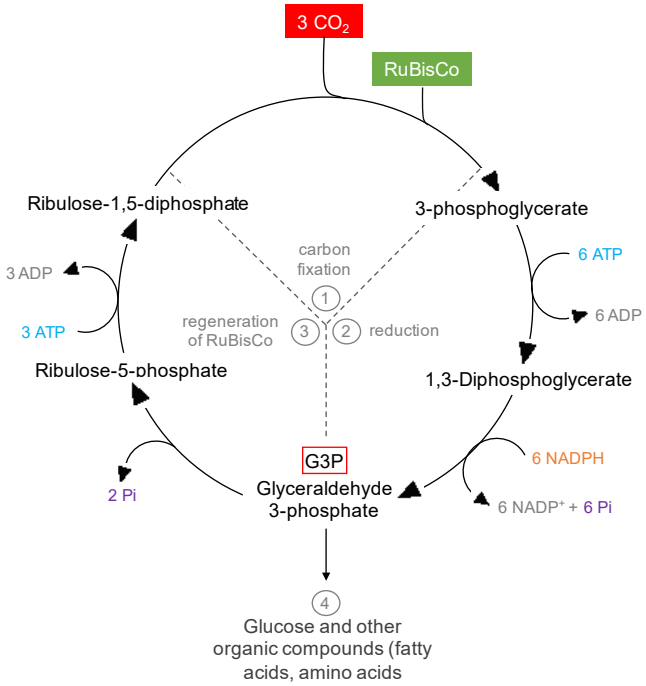

Figure 15. Calvin Cycle (carbon fixation) occurs in the chloroplast.

The enzyme RuBisCo can also fix O_2 into the RuBP to give 3-phosphoglycerate (PGA) and 2-phosphoglycolate (2PG) during photosynthesis: this phenomenon is called the photorespiration (Figure 16).

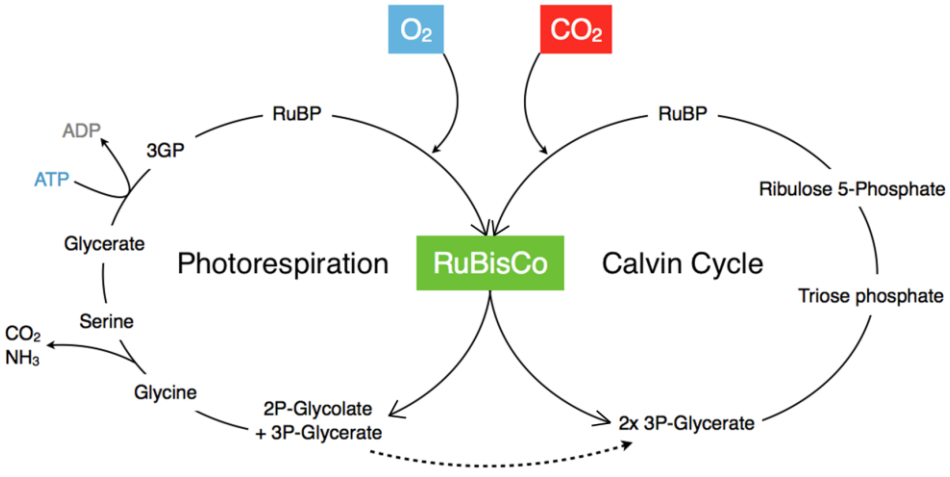

Figure 16. Photorespiration (adapted from Xu et al. (2015)).

In autotrophic conditions, the photosynthesis step allows the production of carbohydrate, hence, the respiration of organic carbon processes is also involved; glycolysis, the TCA cycle, the pentose phosphate pathway and respiration in mitochondria (Figure 14):
1. TCA cycle: in the mitochondrion, pyruvate (from G3P) is oxidized into CO_2 and byproducts from TCA cycle are used as substrate for the synthesis of essential elements.
2. Pentose phosphate pathway: NADPH and pentoses phosphates are produced from glucose. The production of NADPH in this pathway is necessary for the synthesis of lipids and reduction of NO_2^- (Turpin et al. 1988; Falkowski and Raven 2007).
3. Respiration in mitochondrion: NADH from the TCA cycle is oxidized by NADH dehydrogenase. This reaction is coupled to an electron transport chain allowing the formation of a H^+ gradient. The latter provides energy for the ATP synthesis. The high quantity of ATP produced allows proper cell development including nitrogen assimilation for proteins synthesis (Turpin et al. 1988). According to Yang et al. 2000, in *Chlorella pyrenoidosa* the respiration in mitochondrion produces 40 % of ATP in the cell.

1.2.2.2 Heterotrophic metabolism

Microalgae growth in heterotrophic conditions can occur in the presence of organic carbon substrate, O_2 and in the absence light. The presence of organic carbon source such as glucose is used to provide energy to replace the traditional support of light energy.

In heterotrophic conditions, there is no photosynthesis (light and dark reaction). Glucose is used as organic carbon source and metabolized through glycolysis. Glucose is assimilated from medium (extracellular space) to the cytosol of microalgae through the hexose/H^+ inducible active transport (Figure 17).

Microalgae growth under heterotrophic conditions induces physiological changes such as cells size, storage materials content (starch and lipids grains) (Boyle and Morgan 2009), protein, chlorophyll, RNA, and vitamin contents (Martinez et al. 1991). Under autotrophic conditions, chloroplasts and starch granule appear clearly visible in photosynthetic cells as reported Lebsky et al. (2001). Under heterotrophic conditions, the thylakoid membranes disappear while large lipid droplets are formed (de-Bashan et al. 2002), suggesting chlorophyll breakdown and chloroplasts degeneration, associated with lipogenesis during the heterotrophic growth (Xiong et al. 2010).

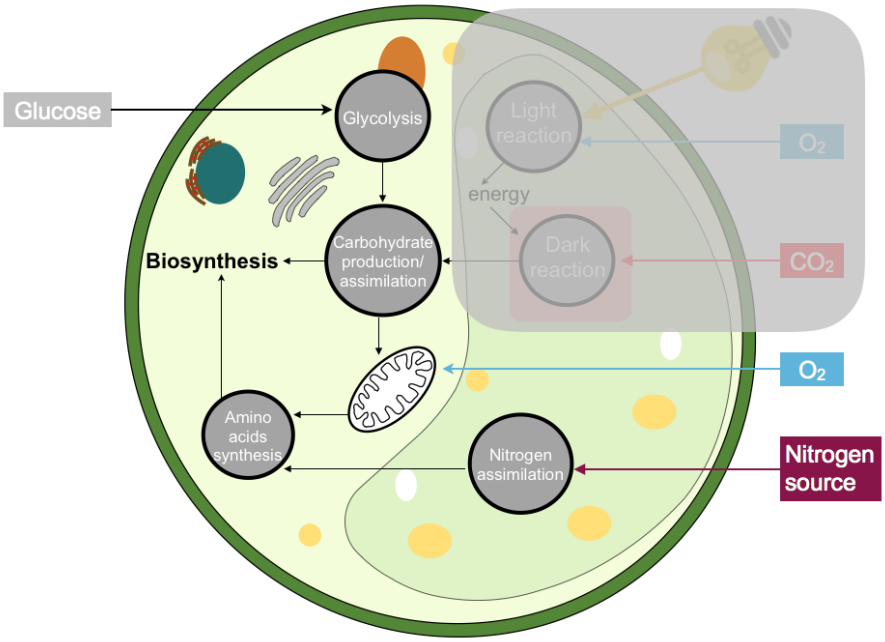

Figure 17. Pathways involved in microalgae heterotrophic growth. The grey square indicates the pathways not involved during this type of growth.

Heterotrophic growth provides an alternative energy source to light and boost cell growth. Maximum growth rates observed in heterotrophic cultures of microalgae range from 0.2 to 0.7 day^{-1} (Perez-Garcia and Bashan, 2015). Compared to the autotrophic conditions, heterotrophic conditions have enhanced concentration of *Chlorella protothecoides* up to 3.4 times (Shi et al. 1999), of *Chlorella vulgaris* up to 4.8 times (Liang et al. 2009) and of *Chlorella sorokiniana* up to 3.3 times (Zheng et al. 2012).

1.2.2.3 Mixotrophic metabolism

Microalgae are able to simultaneously adopt an autotrophic metabolism and a heterotrophic metabolism under mixotrophic conditions, reducing their dependency on light. As under heterotrophic conditions, aerobic glycolysis by microalgae involves the Embden-Meyerhof (EM) and the Pentose Phosphate pathways. The EM pathway is the main glycolytic process of cells in mixotrophic growth with light (Neilson and Lewin 1974; Yang et al. 2000; Hong and Lee 2007; Perez-Garcia et al. 2010) (Figure 18).

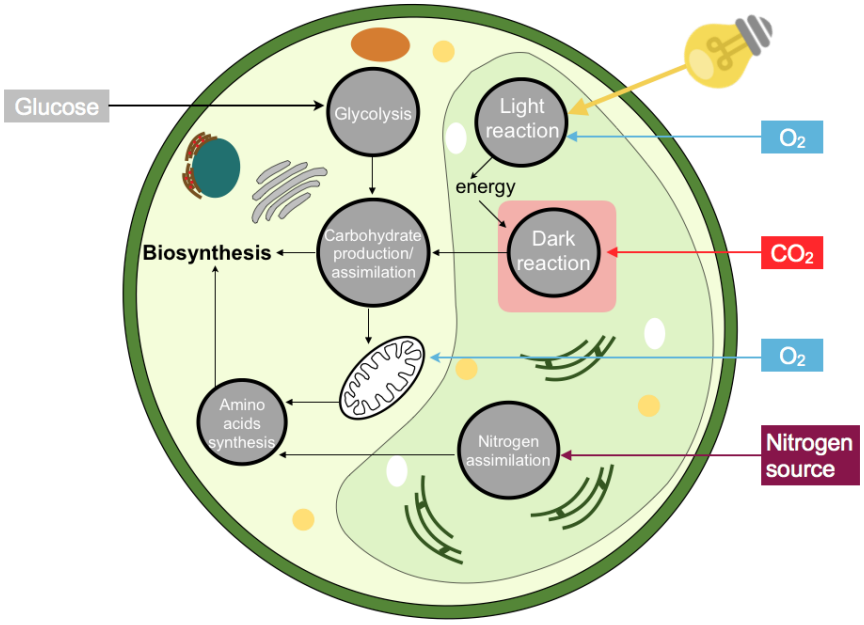

Figure 18. Pathways involved in microalgae mixotrophic growth

Under mixotrophic conditions, the autotrophic mode is regulated by the metabolite concentration and enzyme affinity to substrates and not by factors at the genetic or transcriptional level (Yang et al. 2002). Different hypothesis could describe the interactions between autotrophic and heterotrophic metabolism in mixotrophic conditions:

1) the growth rate under mixotrophic regime (μ_{mixo}) corresponds approximately to the sum of the maximum growth rates obtained under the photo-autotrophic and heterotrophic modes ($\mu_{mixo} = \mu_{hetero} + \mu_{auto}$) (Marquez et al. 1993; Girard et al. 2014). As the mixotrophic specific growth rate equals the sum of the autotrophic and heterotrophic growth rates, the autotrophic and the heterotrophic metabolisms probably act non-competitively under mixotrophic growth (Smith et al. 2015). This relationship has been reported in different microalgae species as *Chlorella regulis* (Endo et al. 1977), *C. vulgaris* (Ogawa and Aiba 1981; Martinez et al. 1991), *Haematococcus pluvialis* (Kobayashi et al. 1992) and *Chlamydomonas humicola* (Lalibertè and de la Noüie 1993). The degree of regulation of autotrophy and heretrophy activities allows non-competitive growth between the two metabolic pathways and is established through the inhibition of chlorophyll production by organic carbon assimilation and through the production of organic carbon uptake enzyme (Ogawa and Aiba 1981; Smith et al. 2015). On the other hand, the presence of light can photo-inhibit the uptake of organic carbon by affecting the balance between reduced and oxidized energy carrying molecules (ATP and

NADH), as a consequence of photosynthetic activity (Perez-Garcia and Bashan, 2015) and by inhibiting expression of the hexose/H^+ system (Perez-Garcia et al. 2010).

2) the autotrophy and heterotrophy activities could interact through synergetic effects rather than non-competition mechanisms (Smith et al. 2015). The addition of external organic carbon generates a CO_2 rich environment that promotes growth of algae. The assimilation and metabolism of organic carbon provides an endogenic source of CO_2 to fuel photosynthesis, which in turn provides an enriched source of O_2 for respiration. This synergistic effect could reduce gaseous growth limitations and enhance growth. Hence, mixotrophic cultivation is associated with lower emission of CO_2 than heterotrophic cultivation on the basis of per unit biomass/lipid production. This happens because part of the CO_2 release can be compensated by photosynthesis (Xiong et al. 2010; Chen et al. 2011). Compared with heterotrophic cultivation, mixotrophic cultivation of C. protothecoides released 61.5 % less CO_2 with production of the same yield of lipid (Xiong et al. 2010). Nevertheless, the enzyme Rubisco, which is responsible for CO_2 fixation, remains functional in cells at the heterotrophic phase (Xiong et al. 2010). During mixotrophy, growth is influenced by the medium supplement of glucose during both the light and dark phases (photoperiod); hence, there is decreased loss of biomass during the dark phase characterized by CO_2 emission (Wang et al. 2014).

The combination of autotrophic and heterotrophic metabolisms allows higher cell densities than autotrophy, while using considerably less organic material per unit of biomass for heterotrophic growth in the dark. Mixotrophic growth enable 20-40% higher growth rate compared with autotrophic condition (Wang et al. 2014) and allows to significantly enhance the biomass productivity, which in turn leads to enhanced lipid productivity.

The increase in cell density under mixotrophic growth conditions seems to be due to higher energy availability, released through aerobic respiration, and catabolism of carbohydrates through photosynthesis (Mitra et al. 2012). Under certain mixotrophic culture conditions, *C. vulgaris* breaks down all glucose in the medium within 2 days (Mitra et al. 2012). On the other hand, according to Santos et al. 2011, mixotrophic growth consumed only one-third of (31.6%) of the initial glucose within 7 days of culture. The Figure 19 shows how microalgae assimilate carbon and produce energy in mixotrophic conditions: both heterotrophic and autotrophic metabolic pathways are involved.

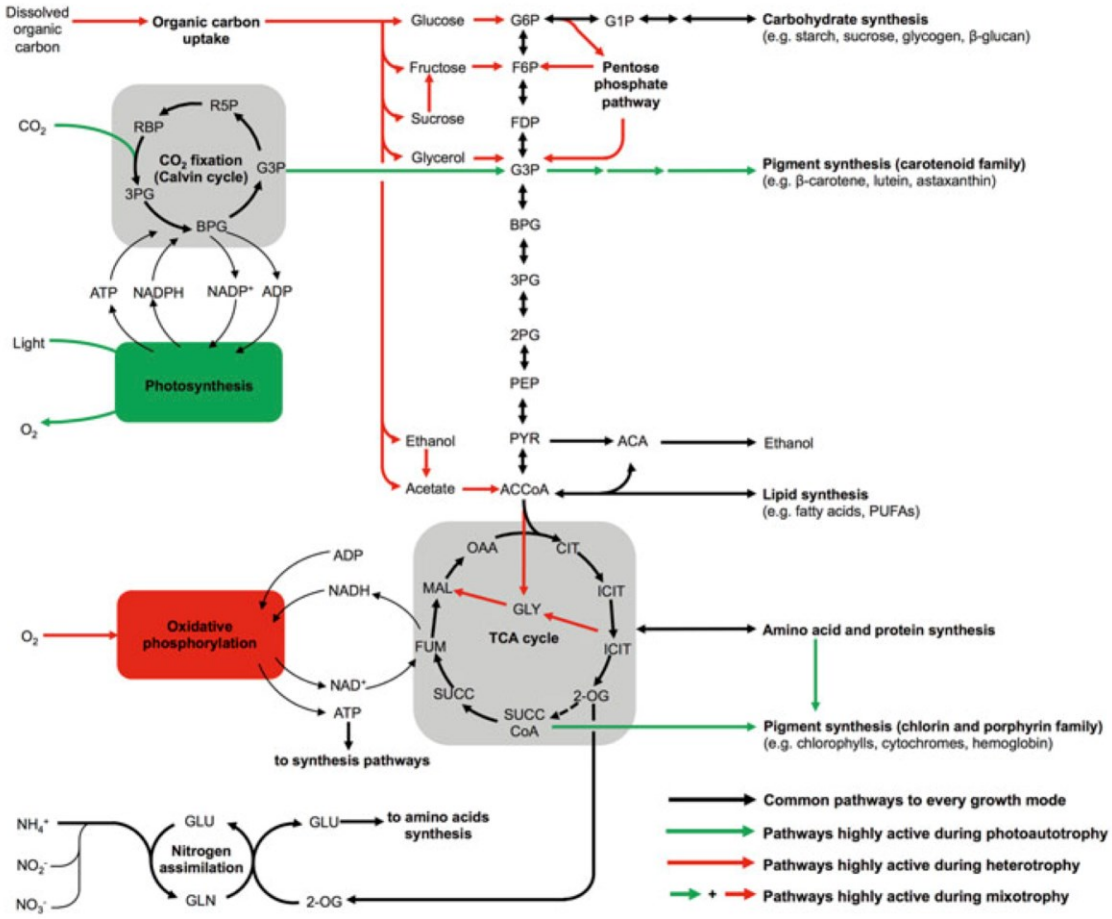

Figure 19. Metabolic pathways for assimilation of carbon and production of energy in photo-autotrophic, heterotrophic and mixotrophic microalgae metabolism (Perez-Garcia and Bashan 2015).

Maximum growth rates observed in mixotrophic cultures of microalgae range from 0.25 to 1.0 day^{-1}, which are higher than heterotrophic growth (Perez-Garcia and Bashan, 2015). Mixotrophic cultivation of microalgae shows the highest growth rate, followed by autotrophic cultivation and then heterotrophic cultivation (Santos et al. 2011). Culture of *Scenedesmus obliquus* in medium containing cheese whey permeate as organic source for mixotrophic and heterotrophic conditions, showed that maximum growth under mixotrophic condition corresponds approximately to the sum of the maximum growth rates under heterotrophic and autotrophic conditions (Girard et al. 2014).

Cultures in mixotrophic conditions increase the proportion of lipid storage (Liang et al. 2009; Mitra et al. 2012). This increase could be attributed to the excess organic carbon in the medium and exposure to low irradiance at the same time (Liang et al. 2009; Mitra et al. 2012).

Santos et al. (2011) confirmed this statement when mixotrophic growth was compared to autotrophic cultivation: in their study, the mixotrophic cultivation showed a lipid productivity 8 times higher than the autotrophic growth (0.071 and 0.009 g. l^{-1} day^{-1} respectively). However, mixotrophic incubation showed a lipid productivity 5 time lower than a heterotrophic culture (0.071 g. l^{-1} day^{-1} and 0.349 g. l^{-1} day^{-1} respectively).

1.2.3 Nutrition and culture parameters

1.2.3.1 Carbon

Microalgae require CO_2 as carbon source for photosynthesis but above a certain concentration it becomes inhibitory to microalgae growth and could be harmful: *C. vulgaris* can tolerate up to 12% CO_2 at a temperature of 35°C (Dong and Zhao 2004).

Microalgae can also assimilate the bicarbonate HCO_3^-. Once HCO_3^- passes the plasma membrane, it can be converted into CO_2 by the action of carbonic anhydrase (CA) because the enzyme RuBisCo reacts only with CO_2 and not HCO_3^-. HCO_3^- can also be concentrated through the CO_2 concentrating mechanism (CCM) (mostly when CO_2 concentration is low), and be later converted into CO_2 by CA (Larsson and Axelsson 1999; Matsuda et al. 2001) (Figure 20).

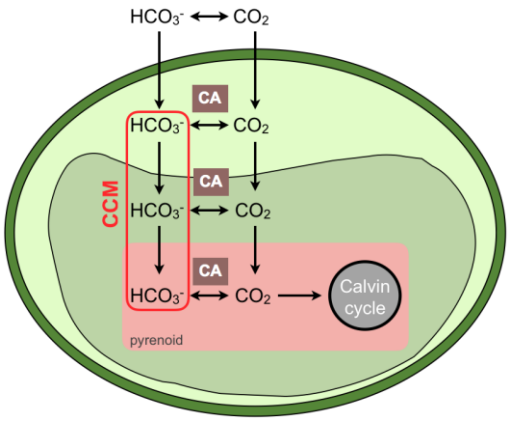

Figure 20. HCO_3^- and CO_2 assimilation in microalgae (CA carbonic anhydrase, CCM CO_2 concentrating mechanism).

For heterotrophic or mixotrophic culture conditions, microalgae can metabolize several kinds of monosaccharides (glucose, fructose, galactose and mannose) and disaccharides (lactose and sucrose) (Perez Garcia and Bashan, 2015). Each microalgal species and strain has different capacities to assimilate different organic compounds (Kröger and Müller-Langer 2011) but

glucose is the most commonly used carbon source and microalgae growth on this substrate provides higher growth and respiration rates (Griffiths et al. 1960) than other substrates as glucose provides high energy content per mole. For example, glucose produces 2.8 kJ. mole^{-1} of energy compared to 0.8 kJ. mole^{-1} for acetate (Boyle and Morgan 2009).

1.2.3.2 Nitrogen

Nitrogen, after carbon, is the second major cell constituent. The quantity of N varies according species and medium conditions but it is around 7% of cell dry mass (Bhola et al. 2011; A W Hom 2015). Despite the higher carbon content in microalgae cells, the ratio C/N is important in optimizing a culture because microalgae growth is controlled by the interaction between organic carbon and nitrogen (Pagnanelli et al. 2014; Silaban et al. 2014).

The most preferred nitrogen source for microalgae is ammonium NH_4^+. N incorporation into biomass from ammonium is the most energetically efficient, since less energy is required for its uptake (Syrett and Morris 1963; Goldman 1977; Shi et al. 1999; Wilhelm et al. 2006). The ammonium can be assimilated directly, transported into the nitrogen assimilation system (Figure 21). In mixotrophic cultivation, ammonium consumption is greater than in autotrophic conditions due to the higher affinity of the cells for ammonium in mixotrophic conditions: more ATP and NADPH are available for ammonium metabolic processes (Perez-Garcia et al. 2010).

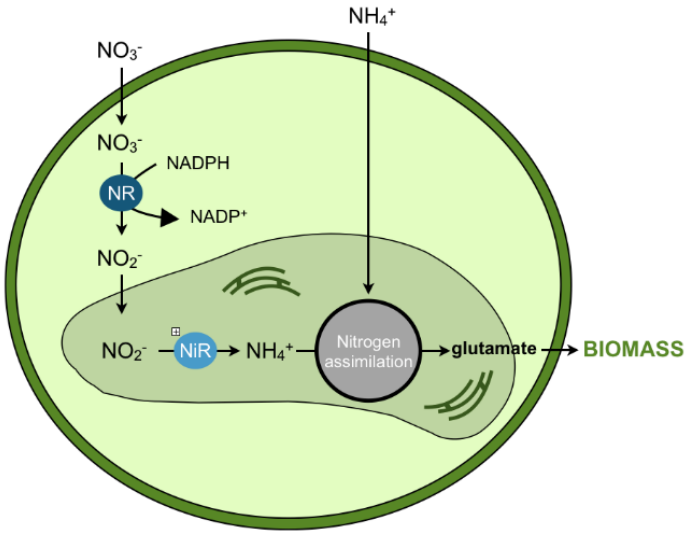

Figure 21. Ammonium, nitrate and nitrite assimilation in microalgae (NH_4^+ ammonium, NO_3^- nitrate, NO_2^- nitrite, NR nitrate reductase, NiR nitrite reductase).

Microalgae are also capable of assimilating nitrate NO_3^-, nitrite NO_2^- , urea and amino acids. In microalgae cell, ammonium can be directly incorporated into nitrogen assimilation while nitrate and nitrite must be converted into ammonium to enter in the nitrogen assimilation pathway (Scherholz and Curtis 2013; Sanz-Luque et al. 2015) (Figure 21).

In unicellular green algae, the assimilated amino acids can be incorporated in the microalgae metabolism through three different mechanisms (McAuley 1987; Muñoz-Blanco et al. 1990; Zuo et al. 2012; Murphree et al. 2017) (Figure 22).

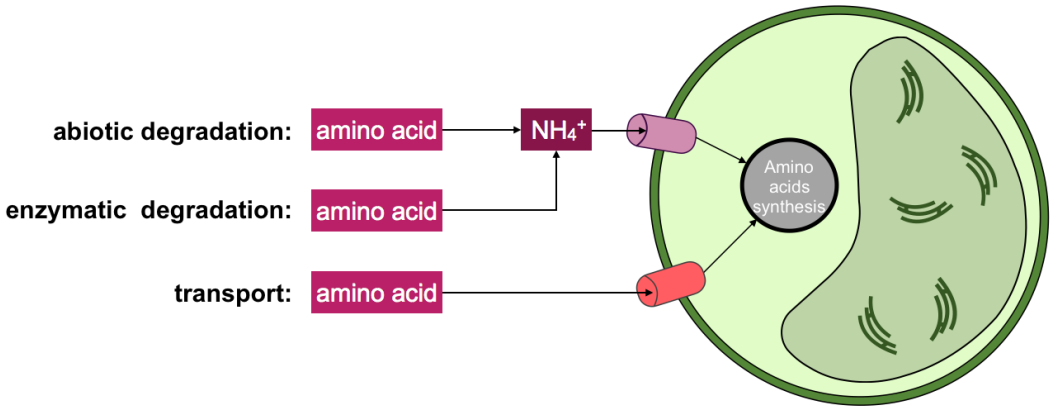

Figure 22. Assimilation of amino acids by microalgae (adapted from Murphree et al. (2017)).

During abiotic degradation, the enzymatic degradation and the transport of amino acids occur across the cell membrane. The abiotic degradation of amino acids results in NH_4^+ production and occurs in the presence of oxygen, heat and light.

Enzymatic degradation involves the oxidative deamination of amino acids outside the microalgal cell catalyzed by a periplasmic amino acid oxidase, resulting in NH_4^+ production and assimilation and oxoacid production, which is not taken up.

During amino-acid transport, amino acids do not undergo any extracellular degradation, they are transported across the membrane to reach the cytosol where they are enzymatically degraded either by conversion into other amino acids via transamination or by the release and subsequent assimilation of NH_4^+. In *C. vulgaris* two amino-acid transport systems are implicated (Cho et al. 1981). One of these is specific for neutral amino acids with small side chains, alanine, glycine, serine, and proline (the proline system) and the other one is specific for the basic amino acids, arginine and lysine (the arginine system). Both these systems are able to transport the corresponding amino acids against an internal free amino acids concentration gradient (Cho et al. 1981). These two transport systems can be induced in *C. vulgaris* in the

presence or absence glucose in nitrogen-rich medium. A third uptake system for amino acids can be induced in *C. vulgaris* when grown in presence of glucose and NH_4C1 (or $NaNO_3$) (Sauer 1984).

1.2.3.3 Light

The light is the main energy source in photo-autotrophic conditions, hence light is required for any photo-autotrophic culture and can become quickly the growth limiting factor depending on photo-bioreactor geometry. Multiple designs of closed photo-bioreactors have been tested and studied in order to optimize the culture exposition to light: flat-plate photo-bioreactor (Qiang and Richmond 1996; Zhang et al. 2001), tubular photo-bioreactor (Molina Grima et al. 1994), and column photo-bioreactor (Kojima and Zhang 1999). In mixotrophic culture, the light is a non-negligible source of energy to increase microalgal biomass.

Light intensity has a great impact on microalgae growth and can even be inhibitory. During photo-inhibition, photosynthesis is inhibited and microalgae growth declines (Subba Rao et al. 2005).

1.2.3.4 Temperature and pH impact on the repartition of carbon species

CO_2 dissolution depends on two phenomena: physical dissolution in the liquid phase and the chemical reaction with water that leads to the repartition of the different carbon species.

The concentration of dissolved CO_2 in the liquid phase can be expressed by Henry's law when the gaseous phase is in equilibrium with the liquid phase and varies according to the temperature (a decrease in temperature leads to an increase in the concentration of dCO_2).

In the liquid phase, the dissolved CO_2 is hydrated to form carbonic acid H_2CO_3, which then dissociates into HCO_3^- and carbonate CO_3^{2-} (Baba and Shiraiwa 2007):

$H_2O + CO_2 \leftrightarrow H_2CO_3$ **Reaction 2**

$H_2CO_3 \leftrightarrow H^+ + HCO_3^-$ **Reaction 3**

$HCO_3^- \leftrightarrow H^+ + CO_3^{2-}$ **Reaction 4**

The dissociation constants of the couples CO_2/ HCO_3^- and HCO_3^-/ CO_3^{2-} are respectively K_1 and K_2, and the repartition of dissolved CO_2, HCO_3^-, and CO_3^{2-} depends on pH (Figure 23):

$$K_1 = \frac{[HCO_3^-][H^+]}{[CO_2]} \quad (1)$$

$$K_2 = \frac{[CO_3^{2-}][H^+]}{[HCO_3^-]} \quad (2)$$

$$K_1 = 10^{-pK1} \quad (3)$$

$$K_2 = 10^{-\mathrm{pK2}} \quad (4)$$

with (Edwards et al. 1978):
$pK_1 = 6.36$ at 25°C
$pK_2 = 10.33$ at 25°C

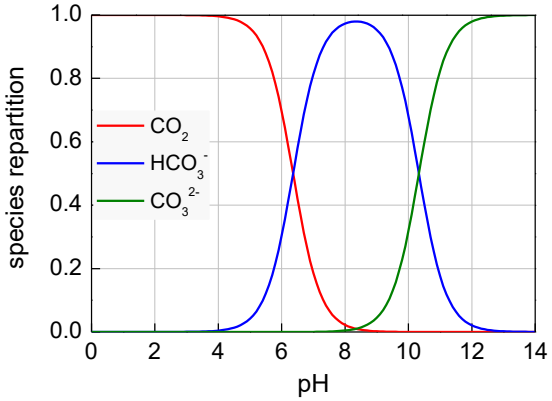

Figure 23. Carbon species repartition according pH at 25°C.

1.3 Batch culture in photo-bioreactor: growth kinetic and gas transfer

1.3.1 Growth kinetic

In batch culture, the key elements necessary for yeast or microalgal cell growth (carbon, nitrogen) are all present at the beginning of the culture. Gaseous substrates and light are "fed" continuously during the culture period., and normally at a constant rate. During growth, the nutrients are consumed and their dissolved concentration in the growth medium decreases with time. The cell growth stops when one key nutrient is depleted (limiting nutrient). The

biochemical composition, the physiological abilities and growth rate are then modified (Cullen et al. 1992).

In a stirred batch bio-reactor, biomass (biomass yield) and product formation can be described quantitatively by the specific yield coefficient expressed as the number of cells or the mass of product formed per unit of substrate consumed, $Y_{X/S}$ and $Y_{P/S}$ respectively. The balance of the cells number between the time t and t+dt are given by:

$$V\ dX = r\ V\ dt \tag{5}$$

with:
V: working volume (l)
r: growth speed (cell. l^{-1} h^{-1})
X: population (cell. l^{-1})
The growth speed r is directly linked by the specific growth rate (μ) and the microbial population:

$$\mathrm{r} = \mu \mathrm{X} \tag{6}$$

with:
μ: specific growth rate (h^{-1})

Then the balance of the cells number is given by:

$$\frac{dX}{dt} = \mu X \tag{7}$$

The balance of the product mass and the substrate mass depends on the balance of the cells number:

$$\frac{dP}{dt} = \frac{Y_{P/S}}{\mathrm{Y_{X/S}}}\frac{dX}{dt} = \frac{Y_{P/S}}{\mathrm{Y_{X/S}}}\mu X \tag{8}$$

$$\frac{dS}{dt} = \frac{1}{\mathrm{Y_{X/S}}}\frac{dX}{dt} = \frac{1}{\mathrm{Y_{P/S}}}\frac{dP}{dt} \tag{9}$$

with:
P: product concentration (g. l^{-1})
S: substrate concentration (g. l^{-1})

The doubling time *td* (h) can be calculated as:

$$td = \frac{ln2}{\mu} \tag{10}$$

1.3.2 Gas transfer

The study of the gas-liquid transfer in bioreactor is essential as gas is one of the most important substrates for yeast and microalgae. Yeast needs O_2 for respiration and microalgae requires CO_2 for photosynthesis under photo-autotrophic conditions and both O_2 and CO_2 under mixotrophic conditions. The transfer of O_2 and CO_2 is schematized in Figure 24.

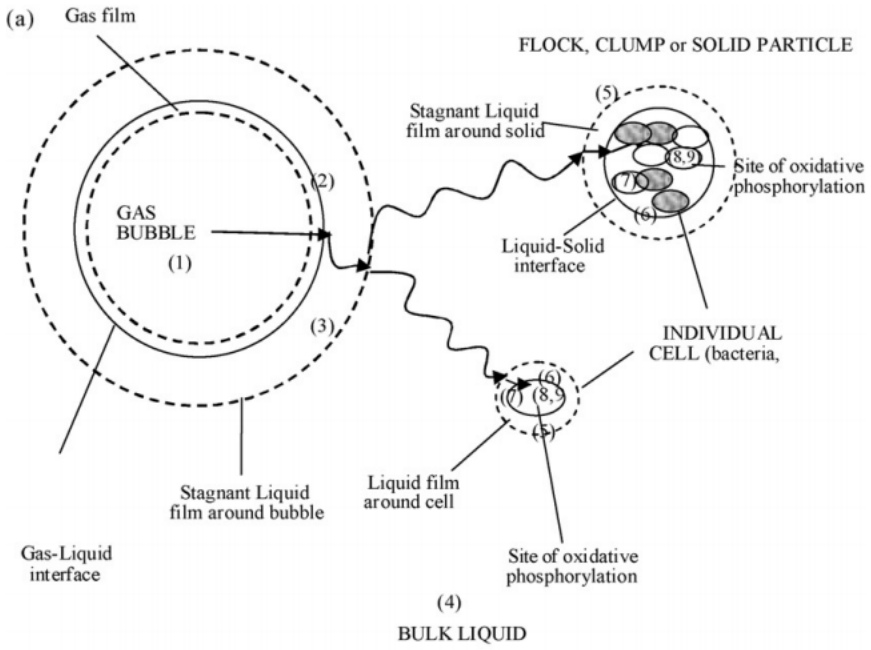

Figure 24. Steps of gas transfer from gas bubble to cell from Garcia-Ochoa et al. (2010). (1) transfer from the interior of the bubble to the gas–liquid interface; (2) movement across the gas–liquid interface; (3) diffusion through the relatively stagnant liquid film surrounding the bubble; (4) transport through the bulk liquid; (5) diffusion through the relatively stagnant liquid film surrounding the cells; (6) movement across the liquid–cell interface; if the cells are in a flock, clump or solid particle, diffusion through the solid to the individual cell; (7) transport through the cytoplasm

till the site where the reactions take place; (8) biochemical reactions involving oxygen consumption and production of CO_2 or other gases; (9) transfer of the produced gases in the reverse direction.

The gas transfer rate depends on the liquid mass transfer coefficient K_L, the total specific surface area available for mass transfer *a*, and the gas concentration. It is difficult to determine K_L and *a* individually so they are usually determined together through one single coefficient called the volumetric gas transfer coefficient K_La, which can be determined experimentally. Then, the K_La allows to obtain the gas balance in the liquid phase in a perfectly homogeneous batch culture.

1.4 Studies on co-cultures of yeast and microalgae

1.4.1 Two types of co-cultures of yeast and microalgae: coupled and mixed cultures

Reports of studies on symbiotic co-cultures of microalgae and yeast have been increasingly appearing in the scientific literature, with the aim of improving biomass and/or target-molecule productivity. These co-cultures fall into two categories: studies with bioreactors in series where the exhaust gases from the heterotrophic culture are fed into the autotrophic culture, and studies where both yeast and microalgae are concomitantly in the same culture. We have decided to refer to the former as coupled cultures and the latter as mixed cultures (Figure 25).

Coupled cultures consists of an upstream heterotrophic yeast-culture connected to an autotrophic culture of microalgae in photo-bioreactor through the exhaust gases from yeast culture (Pisman and Somova 2003; Puangbut and Leesing 2012; Santos et al. 2013; Dillschneider et al. 2014; Gomez et al. 2016). Studies on coupled cultures have mainly suggested an increase in the final microalgae biomass and lipid production that is achieved by effectively enriching the air supply to the microalgae cultures with CO_2 from the heterotrophic culture. In a coupled-culture system, the autotrophic organism benefits from the heterotrophic organism with no positive or negative impact on the latter, which essentially acts as a CO_2 generator.

The principle of mixed cultures of yeast and microalgae is based on the growth of both species in the same liquid phase of a culture. Studies on these mixed cultures are mainly conducted in order to increase the lipid production and shows a mutual benefit between yeast and microalgae as CO_2 produced by the heterotroph is accessible for microalgae photosynthesis and the O_2 released from the autotroph can be used back by yeast.

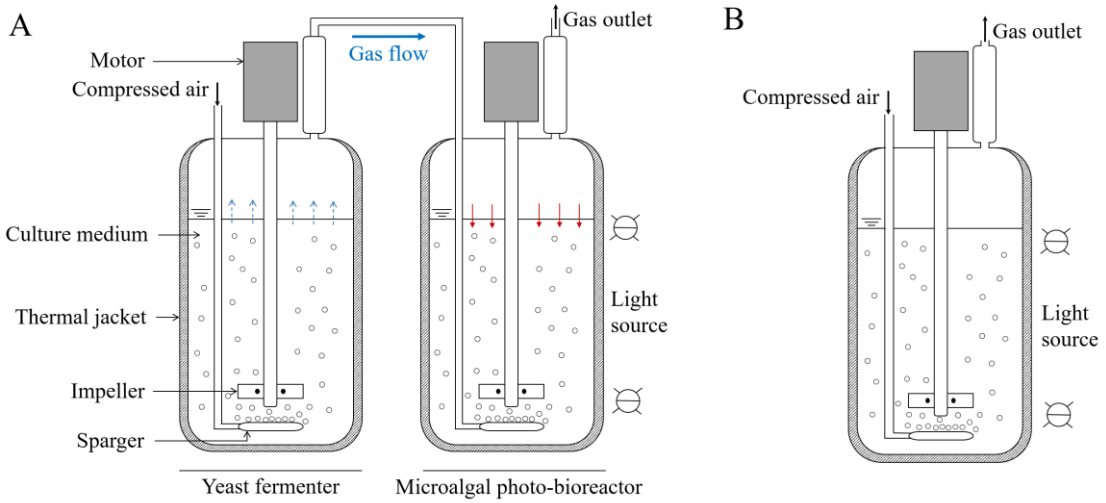

Figure 25. Two types of co-cultures of yeast and microalgae. (A) Coupled-culture and (B) mixed culture; (A) gases pass from the liquid phase of the heterotrophic culture into a gaseous phase (blue dashed arrows) and they then pass from the gaseous phase into the liquid phase of the photo-bioreactor (red solid arrows). (B) Diagram of a mixed culture of heterotrophic and autotrophic organisms; the gases are generated and reused in situ. The CO_2 is produced by heterotrophic metabolism of the organic carbon source. In (B) aeration is optional and can be avoided altogether.

1.4.2 Potential advantages of mixed cultures over coupled cultures

The mixed culture system of microalgae and yeast focuses on the symbiotic potential of associating both organisms in the same culture. This system has an advantage over coupled-cultures in that it provides an opportunity for direct gaseous exchange in dissolved form bypassing the dissolution and degassing rates of the gas supply. Usually, any gas supplied to a bioreactor has to pass from a gaseous phase into a liquid phase (dissolution) and the gases produced by the culture must pass from the liquid phase into the gaseous phase (degassing). These transfers are subject to specific surface limitations as well as mixing phenomena that can limit CO_2 supply to the autotroph and O_2 supply to the heterotroph in a coupled culture. In a mixed culture of microalgae and yeast, each organism would use the dissolved gas produced by the other organism *in situ* and without passing through a gaseous phase, the organisms could benefit from each other.

1.4.3 Principle interactions in symbiotic mixed culture cultures

Symbiosis is the association between two organisms. The term of "symbiosis" is credited to Heinrich Anton de Bary who first used and described it as "the living together of unlike

named organisms" in 1879 (Oulhen et al. 2016). One of the most natural composite organisms, considered as the model of symbiosis is the lichen. Lichens arise from a symbiotic relationship between a fungi and algae or cyanobacteria (Gargas et al. 1995). Six basal interactions can occur in symbiosis (Figure 26).

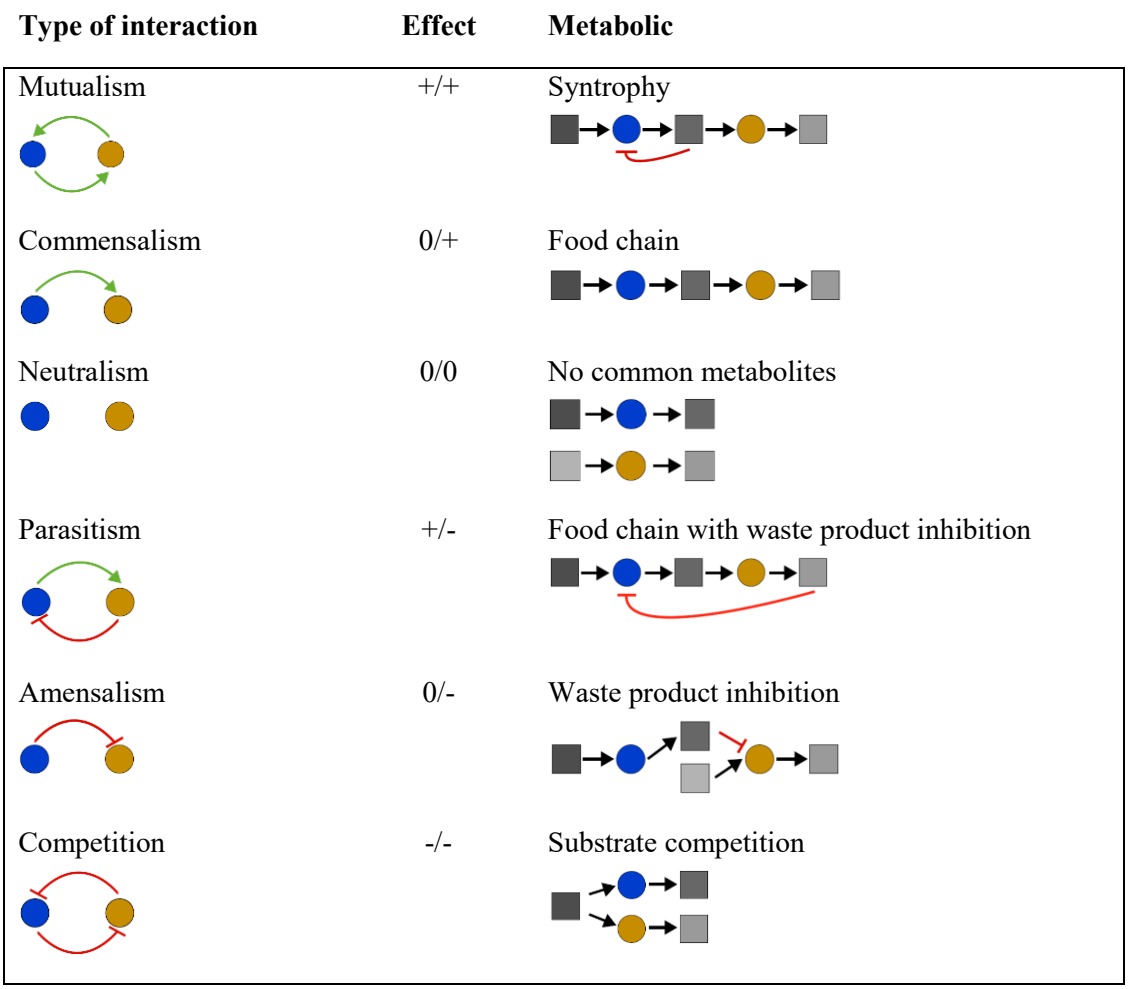

Figure 26. Six potential symbiotic interactions between yeast and microalgae and corresponding metabolic representation. Circles (blue and yellow) represents the organisms and squares are products or substrates (adapted from Großkopf and Soyer (2014)).

Mutualism is the association between two organisms in which each organism benefits from the activity of the other. The interest in a mixed culture of yeast and microalgae is the mutualism that could be installed through the gas supply by one species towards the other one. In the commensalism, one organism helps the growth of the other. Only one organism takes advantage of the relationship and for the other, the effect is neutral. In neutralism there is no

effect on either organism from the presence of the other organism and they grow independently. In parasitism, one organism takes advantage of the association altering the growth of the other one. In amensalism, one organism develops without any positive or negative effect of the association, but the organism inhibits the growth of the other second organism. In competition, both organisms share the same nutrient resulting in growth reduction for both.

1.5 Challenges in developing a mutual symbiotic mixed culture: co-dominance installation and accurate measurement of microbial proportion

From a CO_2 mitigation viewpoint, as the heterotrophic CO_2 production rate is usually largely superior to its autotrophic consumption rate, the two populations must be balanced in such way that the photosynthetic population can cope with the rate of CO_2 production. Hence the heterotrophic activity must be in step with the CO_2 removal rate. This could be achieved though co-dominance of the populations allowing synergy between the two organisms based on gaseous exchange. So far, no scientific studies have been published with the stated aim of developing co-dominant symbiotic mixed cultures.

One of the main challenges for a mixed culture of yeast and microalgae appears to be the dominance of one organism over the other by the end of incubation period. This dominance seems to be caused by the medium composition, which could be more suitable for the growth of one species, at the expense of the other one. The comparison of yeast and microalgae monocultures with mixed cultures of the two organisms is useful to determine whether the medium is favorable to yeast or microalgae. Yeast was the dominant species in most of the studies on mixed culture reviewed in this document (Table 2) probably due to the presence of organic substrates (Table 3) and its faster specific growth rate (μ).

In Papone et al. (2016), the yeast biomass yield was even higher than the total biomass yield in mixed culture (9.43 and 6.9 g. l^{-1} respectively). In Xue et al. (2010) and Zhang et al. (2014), the yeast biomass yield in monoculture was higher than that of microalgae (88 % and 89 %respectively), which supports the hypothesis that the medium used was more adapted for yeast growth than for microalgae growth. However, in these two studies the yeast biomass yield in monoculture was lower than that in mixed culture, which could be explained by positive effects of adding microalgae on yeast growth. In mixed cultures showing a yeast dominance, the media were designed by including key components for yeast growth: organic carbon through glucose,

assimilable nitrogen via ammonium sulfate ($(NH_4)_2SO_4$) and some of the media contained yeast extract (Table 3).

Interestingly, Dong and Zhao (2004) showed a dominance of yeast while their medium contained glucose but neither ammonium sulfate nor yeast extract. In this study *Phaffia rhodozyma* grew on glucose as carbon source and nitrate as nitrogen source since this yeast specie is capable to grow on various types of nitrogen sources including nitrate (Johnson and An 1991; Hu et al. 2005).

In Zuccaro et al. (2019), the yeast yield in mixed culture was higher than in monoculture, which demonstrated the advantage of the consortium for yeast. On the other hand, the microalgae did not draw any advantages from the consortium as the microalgae yield was lower in mixed culture than in monoculture. The authors explained that the capacity of microalgae to use organic carbon lowered the efficiency of the mixed culture compared to the combination of the two monocultures. Hence, the competition for organic substrates between yeast and microalgae must be considered when designing a medium for the consortium.

In the studies showing a dominance of microalgae, the microalgae biomass yield was very similar to the total biomass yield in mixed culture, supposing that the medium was suitable for microalgae growth and not for yeast (Cai et al. 2007; Shu et al. 2013; Wang et al. 2016). The medium designed in these studies contained glucose and nitrate as the only nitrogen source but yeast of the genera *Saccharomyces* and *Ambrosiozyma* are unable to assimilate nitrate (Siverio 2002), which explains why yeast could not grow in the mixed cultures.

Despite the dominance issue, the studies on mixed culture showed globally a higher product yield coefficient than that obtained by combining the yeast and the microalgae monocultures.

Surprisingly, only five studies on mixed cultures of yeast and microalgae presented the microalgae and yeast concentration in mixed cultures while the yeast:microalgae ratio in the mixed culture during the culture time is a key parameter to evaluate the synergetic effects between the two microorganisms. In Zuccaro et al., (2019), the yeast and microalgae populations were enumerated with a Malassez counting chamber. Cell counting methods based on hemocytometer present disadvantages mainly in terms of manipulation errors (improper mix) and human sampling errors (over-counting or under-counting of specific cell types or in specific areas). The difficulty in enumerating simultaneously and precisely yeast and microalgae in the same suspension could explain this lack of measurement of yeast:microalgae ratio in many published studies.

In conclusion, the two main challenges in developing a co-dominant mixed culture of yeast and microalgae appears to be the design of an appropriate medium, to promote both yeast and microalgae growth, and the development of an accurate method for simultaneous enumeration of yeast and microalgae. The design of an appropriate medium requires knowledge of the capacity of each species to use the different compounds in the medium, hence potential competition(s) for nutrient(s) must be taken account.

Table 2. List of mixed culture of yeast and microalgae studied in the literature. A specie is in bold when it was the dominant specie in the mixed culture (*value calculated from data in publication, • cells. ml^{-1}, º g. $cell^{-1}$)

			yeast monoculture		algae monoculture		mixed culture				$Y_{P/X}$ (g. g^{-1})		Ref.
yeast specie	algae specie	molecule of interest	biomass yield (g. l^{-1})	product yield (g. l^{-1})	biomass yield (g. l^{-1})	product yield (g. l^{-1})	total biomass yield (g. l^{-1})	product yield (g. l^{-1})	yeast proportion (%)	algae proportion (%)	mixed culture	yeast and microalgae monocultures	
Ambrosiozyma cicatricosa	***Isochrysis galbana***	lipids	0.17	0.01*	1.17	0.2*	1.32	0.15*	3.36	96.64	0.11*	0.14*	Cai et al. (2007)
Saccharomyces cerevisiae	***Chlorella sp.***	lipid	.	_	1.44	0.261	1.834	0.358	12.5	87.5	0.20*	_	Shu et al. (2013)
Saccharomyces cerevisiae	***Scenedesmus obliquus***	lipid	_	_	3.30	3.894	3.4	4.1	_	_	1.21*	_	Wang et al. (2015)
Phaffia rhodozyma	*Haematococcus pluvialis*	astaxanthin	3.22	0.0020	0.69	0.0023	3.32	0.007	_	_	0.002*	0.001*	Dong and Zhao (2004)
Rhodotorula glutinis	*Spirulina platensis*	lipid	1.70	0.135	0.20	0.013	3.67	0.467	_	_	0.13*	0.08*	Xue et al. (2010)
Rhodotorula glutinis	*Chlorella vulgaris*	lipid	2.10	1.4	1.00	0.75	2.12	1.75	86*	14*	0.83*	0.69*	Cheirsilp et al. (2011b)
Rhodotorula glutinis	*Chlorella vulgaris*	lipid	_	_	_	_	2.5	1.05	60*	40*	0.42*	_	Cheirsilp et al. (2011a)
Torulaspora maleeae	*Chlorella sp.*	lipid	8.27	0.92	1.93	0.052	8.73	1.564	_	_	0.18*	0.10*	Papone et al. (2016b)
Torulaspora maleeae	*Chlorella sp.*	lipid	6.4	0.466	2.53	0.132	7.33	0.808	_	_	0.11*	0.07*	Leesing et al. (2012)
Rhodotorula glutinis	*Chlorella vulgaris*	lipid	14	2	1.60	0.3	19.4	3.400	_	_	0.18*	0.15*	Zhang et al. (2014)
Torulaspora globosa	*Chlorella sp.*	lipid	9.43	0.2	3.30	0.12	6.9	0.33	_	_	0.05*	0.03*	Papone et al. (2016)
Lipomyces starkeyi	*Chlamydomonas reinhardtii*	lipids	25×10^{6}•	0.19	9×10^{6}•	0.16	44×10^{6}* •	0.21	90*	10*	5×10^{-12}* º	0.35*	Zuccaro et al., (2019)

Table 3. Medium composition for mixed culture. A specie is in bold when it was the dominant specie in the mixed culture

yeast specie	algae specie	medium composition for mixed culture (g. l^{-1})		Ref.
		organic carbon	other nutrients	
A. cicatricosa	***I. galbana***	glucose, 2	Aged seawater + f/2 medium	Cai et al. (2007)
S. cerevisiae	***Chlorella sp.***	Not specified		Shu et al. (2013)
S. cerevisiae	***S. obliquus***		BG11 medium	Wang et al. (2016)
P. rhodozyma	*H. pluvialis*	glucose, 10	BBM medium	Dong and Zhao (2004)
R. glutinis	*S. platensis*	glucose, 40	$(NH_4)_2SO_4$, 1.0; $MgSO_4 \cdot 7H_2O$, 1.0; $NaNO_3$, 2.5; K_2SO_4, 1.5; NaCl, 1.0; KH_2PO_4, 5.0; $NaHCO_3$, 10.0; $FeSO_4 \cdot 7H_2O$, 0.01; EDTA, 0.08; $CaCl_2$, 0.004; H_3BO_3, 0.00286; $(NH_4)_6MO_7O_{24}$, 0.00002; $MnCl_2 \cdot 4H_2O$, 0.0018; $CuSO_4 \cdot 5H_2O$, 0.000125; $ZnSO_4 \cdot 7H_2O$, 0.00022	Xue et al. (2010)
R. glutinis	*C. vulgaris*	Industrial wastes (effluent from steamed fish process)		Cheirsilp et al. (2011)
R. glutinis	*C. vulgaris*	glycerol, 10	$(NH_4)_2SO_4$	Cheirsilp et al. (2012)
T. maleeae	*Chlorella sp.*	glucose, 20	$(NH_4)_2SO_4$, 0.1; KH_2PO_4, 0.4; $MgSO_4.7H_2O$, 1.5; $ZnSO_4$, 0.0044; $CaCl_2$, 0.0025; $MnCl_2$, 0.0005; $CuSO_4$, 0.0003; yeast extract, 0.75	Papone et al. (2016b)
T. maleeae	*Chlorella sp.*	glucose, 20	$(NH_4)_2SO_4$, 0.1; KH_2PO_4, 0.4; $MgSO_4.7H_2O$, 1.5; $ZnSO_4$, 0.0044; $CaCl_2$, 0.0025; $MnCl_2$, 0.0005; $CuSO_4$, 0.0003; yeast extract, 0.75	Leesing et al. (2012)
R. glutinis	*C. vulgaris*	glucose, 20	$(NH_4)_2SO_4$, 2; KH_2PO_4, 7; $NaSO_4$, 2; $MgSO_4$ $7H_2O$, 1.5; BG-11 medium; yeast extract, 1.5	Zhang et al. (2014)
T. globosa	*Chlorella sp.*	glucose, 20	$(NH_4)_2SO_4$, 0.1; KH_2PO_4, 0.4; $MgSO_4.7H_2O$, 1.5; $ZnSO_4$, 0.0044; $CaCl_2$, 0.0025; $MnCl_2$, 0.0005; $CuSO_4$, 0.0003; yeast extract, 0.75	Papone et al. (2016)
L. starkeyi	*C. reinhardtii*	glucose, 10 yeast extract, 5 sodium acetate, 18 mM (Ac)	Tris buffer, 20 mM; Na-acetate, 18 mM; KPO_4, 1 mM; NH_4Cl, 7.5 mM; $MgSO_4$, 1 mM; $CaCl_2$, 0.5 mM; trace elements	Zuccaro et al., (2019)

1.6 Conclusion

From a CO_2 mitigation viewpoint, microalgae and yeast population must be balanced in activity to ensure that the photosynthetic population can cope with the rate of CO_2 production. Hence the heterotrophic activity must be in step with the CO_2 removal rate. This balance could be achieved though co-dominance of the populations.

In previous studies, the processes of mixed culture between yeast and microalgae has shown the dominance of one of the species over the other and the present thesis aims to enhance these processes by proposing a co-dominant mixed culture of yeast *S. cerevisiae* and microalga *C. vulgaris* that should allow the growth of both species through mutual synergetic effects. The co-dominance can be achieved by designing a medium suitable for growth of both yeast and microalgae to the desired extents for each organism. An appropriate choice of the carbon and nitrogen sources is important for their assimilation by *S. cerevisiae* and *C. vulgaris*. The non-negligible difference in growth rates should also be compensated by other parameters to avoid any yeast dominance.

Different interactions can occur in mixed culture of yeast and microalgae. Mutualism can happen through gas exchange and competition in nutrient can also occur as yeast and microalgae have common assimilable nutrients (glucose, amino acids, ammonium). A method for simultaneous enumeration of yeast and microalgae is then required to study and evaluate the interactions between the species.

By using the model strains *S. cerevisiae* and *C. vulgaris*, the strategy to develop a co-dominant mixed culture of yeast and microalgae could be applied to any mixed culture of a heterotroph and an autotroph.

Chapter 2. Materials and methods

Part of experiments were conducted in shake-flask in order to develop the medium suited for both S. cerevisiae and C. vulgaris growth, and to evaluate the impact of the key components on yeast and microalgae growth. Experiments in photo-bioreactor (PBR) were also carried out to study the metabolisms of each organism in monoculture and mixed culture. The evolution of what was produced and consumed was followed through analytical methods.

Contents

2.1 Strategy of the experimental part of this study

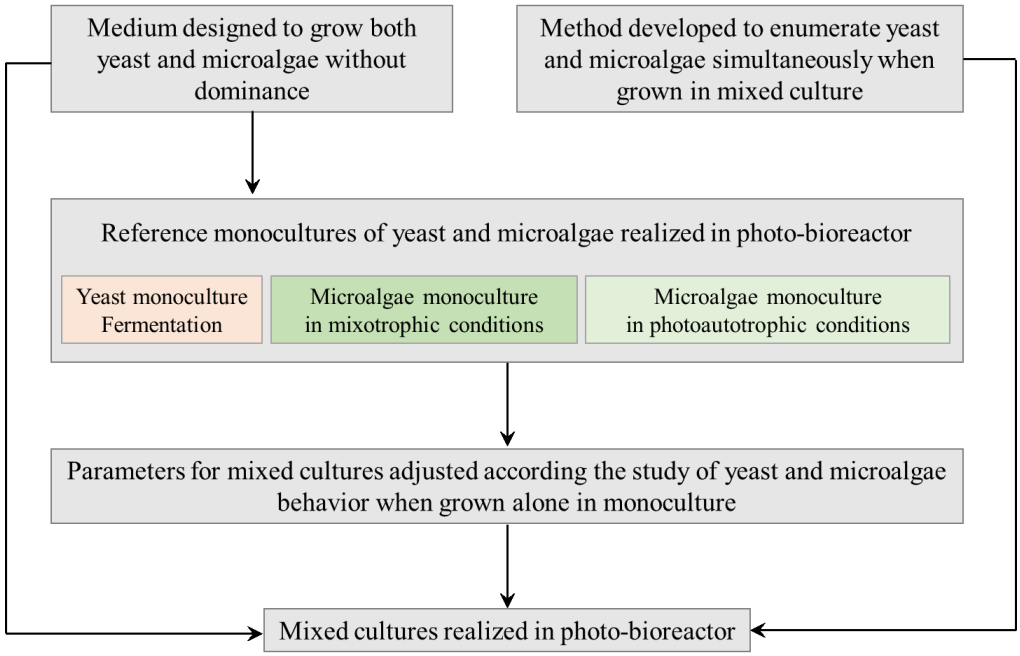

Figure 27. Development of a mixed culture of the yeast *S. cerevisiae* and the microalga *C. vulgaris*

The medium design was the first step of this project. The impact of each medium component was tested on *S. cerevisiae* and *C. vulgaris* in order to evaluate the potential competitions between these microorganisms. Then, the yeast and microalgae were grown in monoculture in the newly designed medium in 5l-photo-bioreactor to be in the closest conditions as possible to the mixed culture planned for the later part of the project. The studies of yeast and microalgae behaviors from these monocultures allowed the adjustment of other parameters for the mixed culture. Finally, the comparison of yeast and microalgae behavior in monocultures and in mixed culture allowed the exploration of the interactions between these two microorganisms.

2.2 Microbial strains and their maintenance

S. cerevisiae strain ID YLR249W was supplied by Life Technologies-University of California San Francisco. This clone expresses a cytoplasm fusion protein PRM1 coupled to a green fluorescent protein (GFP). The strain was maintained on YPG agar stock plates incubated at 25°C for 3 days and subsequently stored at 4°C. The YPG agar medium was composed of ($g.\ l^{-1}$): yeast extract (10), peptone (20) glucose (10) and agar (15) and the stock plates were renewed every three months.

C. vulgaris SAG 211-12 was obtained from the Culture Collection of Algae (SAG), University of Göttingen, Germany. The strain was maintained in liquid culture (50 ml in 250 ml flask) through weekly subculture into fresh medium, incubated at 25°C on an orbital shaker (120 rpm) with continuous lighting at 20 µmol. m^{-2} s^{-1} at the surface of the culture and in air enriched with 1.5% (v/v) CO_2. The liquid inorganic medium used was autotrophic MBM (modified 3N-Bristol medium) (Clément-Larosière et al. 2014), with the following composition (mg. l^{-1}): $NaNO_3$ (750); $CaCl_2.2H_2O$ (25); $MgSO_4.7H_2O$ (75); FeEDTA (20); K_2HPO_4 (75); KH_2PO_4 (175); NaCl (20); H_3BO_3 (2.86); $MnCl_2.4H_2O$ (1.81); $ZnSO_4.7H_2O$ (0.220); $CuSO_4.7H_2O$ (0.08); MoO_3 85% (0.036); $CoSO_4.7H_2O$, (0.09).

2.3 Shake-flask cultures

2.3.1 Specific medium design for mixed culture

Monocultures of *S. cerevisiae* and *C. vulgaris* were grown in three different media in order to define a medium suitable for co-dominance of the organisms in mixed culture. The media were based on different combinations of microalgae autotrophic growth medium (MBM) and components from the commonly used yeast growth YPG (yeast extract, peptone and glucose) medium (g. l^{-1}) (Table 4)

Table 4 Candidate media tested for mixed culture of yeast and microalgae

candidate medium	MBM medium	glucose (10 g. l^{-1})	yeast extract (20 g. l^{-1})	peptone (20 g. l^{-1})
1	x	x		
2	x	x	x	
3	x	x		x

Erlenmeyer flasks (50 ml working volume; 250 ml total volume) were used for the monoculture of *C. vulgaris* and *S. cerevisiae* in the above media and the inoculation ratio was 1% (v/v) from a fully-grown culture. The flasks were incubated at 25°C on an orbital shaker (120 rpm) with continuous lighting at 80 µmol. m^{-2} s^{-1} (LI250A Light Meter; LI-COR, USA) at the surface of the cultures.

The medium finally selected and specifically designed for the mixed culture was named **Mix medium** and the composition is described is Table 5.

Table 5 Composition of the Mix medium

	concentration g. l^{-1}	mole. l^{-1}
$NaNO_3$	1.5	1.8×10^{-2}
$CaCl_2.2H_2O$	5.0×10^{-2}	3.9×10^{-4}
$MgSO_4.7H_2O$	1.5×10^{-2}	6.1×10^{-4}
FeEDTA	4.0×10^{-2}	1.2×10^{-4}
K_2HPO_4	7.5×10^{-2}	4.3×10^{-4}
KH_2PO_4	1.8×10^{-1}	1.3×10^{-3}
NaCl	2.0×10^{-2}	3.4×10^{-4}
Trace elements:		
H_3BO_3	2.9×10^{-3}	4.6×10^{-5}
$MnCl_2.4H_2O$	1.8×10^{-3}	1.2×10^{-5}
$ZnSO_4.7H_2O$	2.2×10^{-4}	1.2×10^{-6}
$CuSO_4.7H_2O$	8.0×10^{-5}	4.2×10^{-7}
MoO_3 85%	3.6×10^{-5}	2.5×10^{-7}
$CoSO_4.7H_2O$	9.0×10^{-5}	4.9×10^{-7}
Peptone:	20	--
total nitrogen	3.0	2.1×10^{-1}
free amino nitrogen	5.4×10^{-1}	4.5×10^{-3}*
NH_4	6.0×10^{-2} **	3.3×10^{-3}
glucose	10	5.6×10^{-2}

* average molar mass of an amino acids is 118.9 g. mol^{-1} (Hachiya et al. 2007)

** measured by ion chromatography

2.3.2 Influence of glucose on yeast

To test the impact of glucose on yeast, *S. cerevisiae* was grown in Mix medium containing different concentration of glucose: 5, 10 and 15 g. l^{-1}. *S. cerevisiae* grew in aerated shake flask, incubated at 25°C on an orbital shaker (120 rpm) with a working volume of 50 ml. The yeast inoculum was prepared using 50 ml of Mix medium in shake flask, incubated at 25°C on an orbital shaker (120 rpm).

2.3.3 Influence of the peptone component on yeast

To test the impact of peptone on yeast, *S. cerevisiae* grew in Mix medium containing different concentration of peptone: 10, 20 and 30 g. l^{-1} with 20 g. l^{-1} which is the peptone concentration in Mix medium. Each experiment condition was conducted in duplicate, in 250-ml shake flash with a working volume of 50 ml and incubated at 25°C on an orbital shaker (120 rpm). The yeast inoculum was prepared using 50 ml of Mix medium in shake flask, incubated at 25°C on an orbital shaker (120 rpm).

2.3.4 Influence of peptone on microalgae

C. vulgaris grew in autotrophic MBM medium containing different concentration of peptone to assess the impact of peptone on microalgae growth: 10, 20 and 30 g. l^{-1} with 20 g. l^{-1} which is the peptone concentration in Mix medium. Each experiment condition was conducted in duplicate, in 250-ml shake flash with a working volume of 50 ml and incubated at 25°C on an orbital shaker (120 rpm) with continuous lighting at 80 µmol. m^{-2} s^{-1} (LI250A Light Meter; LI-COR, USA) at the surface of the cultures. The microalgae inoculum was prepared using 50 ml of Mix medium in shake flask, incubated at 25°C on an orbital shaker (120 rpm) with continuous lighting at 80 µmole. m^{-2} s^{-1} (LI250A Light Meter; LI-COR, USA) at the surface of the cultures.

2.3.5 The impact of iron concentration on yeast growth

The Mix medium contained iron in the form of FeEDTA, a form of iron assimilable by *S. cerevisiae*. The impact of the iron concentration on yeast growth was assessed. *S. cerevisiae* was grown in Mix medium in presence (6.7×10^{-3} $g_{Fe\text{-}FeEDTA}$. l^{-1}) or absence of iron (0 $g_{Fe\text{-}FeEDTA}$. l^{-1}), in aerated shake flask, incubated at 25°C on an orbital shaker (120 rpm) with a working volume of 50 ml. The yeast inoculum was prepared using 50 ml of Mix medium containing the normal concentration of iron in shake flask, incubated at 25°C on an orbital shaker (120 rpm).

2.3.6 The impact of iron concentration on microalgae growth

The impact of iron on *C. vulgaris* growth was also studied. *C. vulgaris* was grown in autotrophic MBM medium in presence of low concentration of iron (6.7×10^{-4} $g_{Fe\text{-}FeEDTA}$. l^{-1}) or in presence of the original concentration of iron in Mix medium (6.7×10^{-3} $g_{Fe\text{-}FeEDTA}$. l^{-1}). Microalgae were grown in aerated shake flask, incubated at 25°C on an orbital shaker (120 rpm) with a working volume of 50 ml and continuous lighting at 20 µmole. m^{-2} s^{-1} (LI250A Light

Meter; LI-COR, USA) at the surface of the cultures. The microalgae inoculum was prepared using 50 ml of MBM medium in shake flask, incubated at 25°C on an orbital shaker (120 rpm) with continuous lighting at 80 µmole. m^{-2} s^{-1} (LI250A Light Meter; LI-COR, USA) at the surface of the cultures.

2.3.7 The impact of trace elements concentrations on microalgae growth

The trace elements composition of Mix medium and its impact on microalgae growth was investigated. Microalgae grew autotrophic MBM medium with or without trace elements, in aerated shake flask, incubated at 25°C on an orbital shaker (120 rpm) with a working volume of 50 ml and continuous lighting at 20 µmol. m^{-2} s^{-1} (LI250A Light Meter; LI-COR, USA) at the surface of the cultures. The microalgae inoculum was prepared using 50 ml of MBM medium containing trace elements in shake flask, incubated at 25°C on an orbital shaker (120 rpm) with continuous lighting at 80 µmole. m^{-2} s^{-1} (LI250A Light Meter; LI-COR, USA) at the surface of the cultures.

2.3.8 The impact of ethanol on microalgae growth

C. vulgaris was grown on MBM medium in Erlenmeyer flasks (50 ml working volume; 250 ml total volume) and the flasks were incubated at 25°C on an orbital shaker (120 rpm) with continuous lighting at 20 µmole. m^{-2}. s^{-1} and in air enriched with CO_2 1.5% (v/v). Four ethanol concentrations were tested (0, 2, 4 and 6 g. l^{-1}) (ethanol 96%).

2.3.9 Mixed cultures

The system of closed shake flask (Figure 28) was designed in order to reproduce mixed cultures of yeast and microalgae in the closed culture conditions as mixed cultures in 5l-photo-bioreactor (Figure 30). Overpressure inside the shake flask was avoided through a small pipe formed by the syringe. The gas flow could continue to a safety valve formed by a tube containing a glycerol solution (20% v/v). This safety valve allowed a hermetical close of the shake flask while ensuring safety in case of overpressure and a glycerol solution was used instead of water to diminish liquid evaporation rate. A 0.2 µm filter was added at the external end of the syringe to avoid any contamination from the environment.

The shake flasks were incubated an orbital shaker (120 rpm) with continuous lighting at 20 µmole. m^{-2} s^{-1} at 25 °C. The cultures were conducted with 50 ml of working volume.

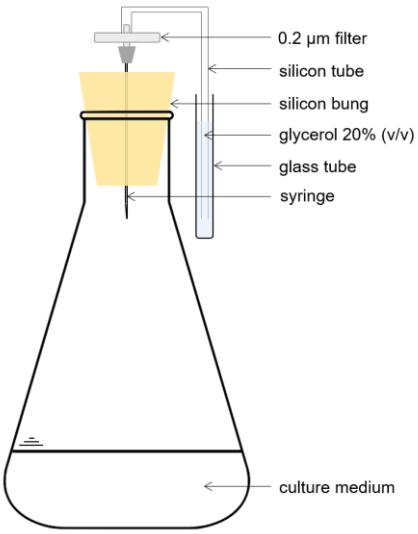

Figure 28. Closed shake flask.

2.4 Cultures in photo-bioreactor

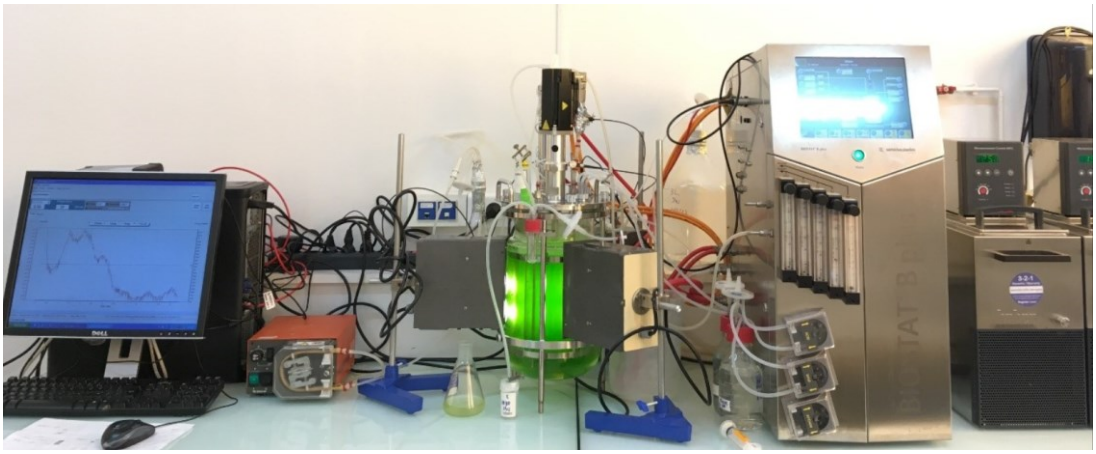

Figure 29. Picture of a culture in 5l-photo-bioreactor.

All experiments in photo-bioreactor (PBR) were conducted in a stirred bioreactor (5-liter working volume) (BIOSTAT Bplus – 5 L CC; Sartorius Stedim biotech). The PBR was lit with six LED lamps (Ledare 130 lumen, 2700 Kelvin, 27° dispersion angle, IKEA). The light intensity at the inner surface of the bioreactor for each lamp was measured at 1,800 µmole. m^{-2} s^{-1} (LI250A Light Meter; LI-COR, USA) and the peak emission is at 600 nm (Appendix 9). The stirring speed was 750 rpm, the temperature was maintained at 25°C and the pH was controlled at 6.5 with automatic alkaline or acid solutions addition based on the

continuous measurements made by an internal pH probe (EasyFerm PLUS K8 325, Hamilton). The alkaline solution was composed of potassium hydroxide (1 M KOH) and the acid solution was composed of phosphoric acid (1 M H_3PO_4). Dissolved oxygen (pO2) in both mixed cultures was measured with an internal probe (VisiFerm DO H2, Hamilton). The pO2 was expressed in terms of % of O2 partial pressure in the liquid phase of the culture.

The *S. cerevisiae* and *C. vulgaris* specific growth rates μ were calculated as the slope of the linear part of the logarithm of cell concentration plotted versus time.

2.4.1 Mixed cultures of yeast and microalgae

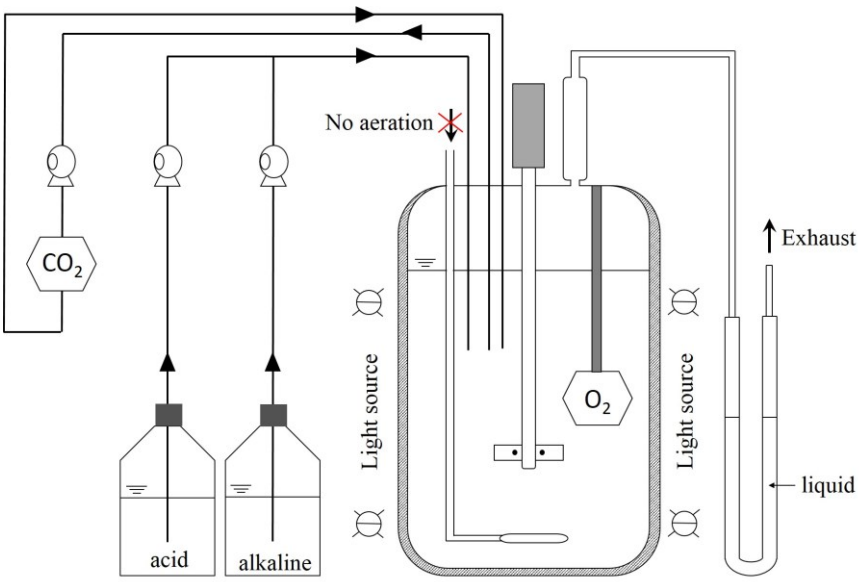

Figure 30. Diagram of a closed 5l-photo-bioreactor.

Two non-aerated mixed cultures in PBR were grown using Mix medium. The experimental set up (Figure 30) involved hermetically isolating the bioreactor to limit the exchange of gases with the atmosphere at the exterior of the bioreactor. Dissolved CO_2 (pCO_2) was measured only in the mixed culture 2 with an external minisensor integrated in a flow cell (CO2 Flow-Through Cell FTC-CD1, PreSens). The culture was circulated (90 ml. min^{-1}) through the flow cell with the aid of a peristaltic pump (520S/R, Watson Marlow) and back into the bioreactor. The flow-through cell was placed as close to the outlet from the bioreactor as possible. The passage of the culture over the sensor in the flow cell allowed the continuous

measurement of pCO_2 via an optical fiber. As with the pO_2, the pCO_2 was expressed in % of CO_2 partial pressure in the liquid phase of the culture.

S. cerevisiae inoculum preparation was the same for both mixed cultures*; S. cerevisiae* was grown on Mix medium, at 25°C, for 2 days. The preparation of the *C. vulgaris* inoculum for the two mixed cultures differed; for the mixed culture 1, the *C. vulgaris* inoculum was grown on Mix medium under continuous illumination, for 15 days, at 25°C and for mixed culture 2 the *C. vulgaris* inoculum was grown autotrophically using Mix medium **without** glucose and peptone under continuous lighting, for 15 days, at 25°C.

2.4.2 Monoculture of *S. cerevisiae*

The monoculture of *S. cerevisiae* was grown in a non-aerated PBR in Mix medium, with culture parameters as described above and the photo-bioreactor configuration was the same as for mixed culture (Figure 30), there was no aeration and gas outlet was closed as described with a fermentation lock. The culture was lit as for the mixed culture. The *S. cerevisiae* inoculum was grown in YPG medium, at 25°C, for 2 days.

2.4.3 Monocultures of *C. vulgaris*

Two monocultures of *C. vulgaris* in PBR were grown, one in Mix medium and the other autotrophically in Mix medium **without** glucose and peptone. Both culture conditions were set up as described above and the photo-bioreactor was continuously aerated with sterile air (Midisart 2000 0.2 µm PTFE, Sartorius) at 500 ml. min^{-1} (0.1 vvm) (1 atm, 25°C). To inoculate both monocultures of *C. vulgaris*, microalgae inoculum was grown in autotrophic MBM medium under continuous light at 25°C for 15 days.

2.5 Analytical methods

2.5.1 Enumeration with Thoma counting chamber

For enumeration with Thoma counting chamber, 10 µl of culture sample is put on the chamber and observed through optical microscopy (ZEISS). The number of cells counted in the area 1 (Figure 31) is then used in the formula below to obtain the cell concentration:

$$\text{cell concentration}(\text{ cells. } l^{-1}) = 16 \times N \times 10^4 \quad (11)$$

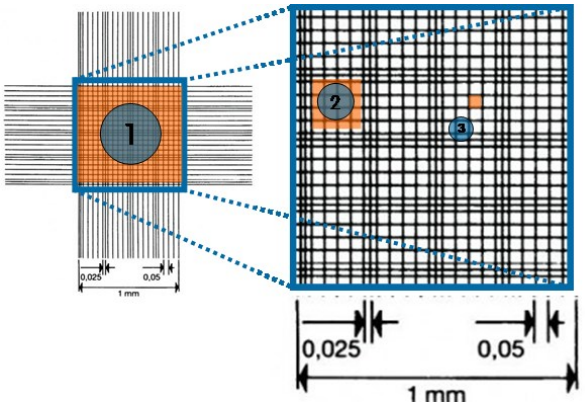

Figure 31. Thoma counting chamber.

2.5.2 Enumeration of *S. cerevisiae* and *C. vulgaris* by flow cytometry

Flow cytometry is a technology used to enumerate cell population in a sample and to analyze physical and chemical characteristics of the cells. In the flow cytometer Guava easyCyte™ (EMD Millipore), a microcapillary allowed direct cells sampling by aspiration (no sheath fluid was used) and with this flow, each cell passing through the laser (488 nm) scattered light, which was detected as Forward Scatter (FS) and Side Scatter (SS) (Figure 32). FS was proportional to the cell size and SS to the internal cell structure.

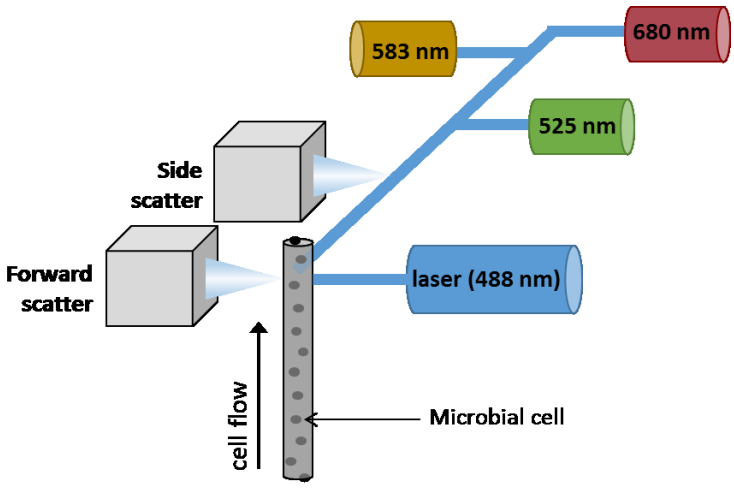

Figure 32. Flow cytometry in Guava easyCyte™. Sample flow through a microcapillary and laser scatter by cells (A) and detection of Forward Scatter, Side Scatter and fluorescence of cells (B).

Our *S. cerevisiae* strain and *C. vulgaris* contained respectively GFP protein and chlorophyll, that emitted respectively a green and red fluorescence after excitation by the laser of 488 nm. These fluorescences were detected by sensors integrated into the flow cytometer (Figure 32). In this manner, yeast and microalgae population could be distinguished based on their autofluorescence.

Samples were diluted so that the cell enumeration was always performed at cell concentrations between 1×10^5 and 1×10^6 cells. ml^{-1}. The method for cell enumeration by flow cytometer suspensions containing only one of the microorganisms was previously validated against a Thoma counting chamber as the referent method. *C. vulgaris* viability was also determined by flow cytometry using the Guava ViaCount Reagent (EMD Millipore).

2.5.3 Dry weight

Dry weight was performed by sampling and centrifuging 10 ml of culture (10 min and 1800 g). The pellet was washed with equal volume of deionized water, and was centrifuged again (10 min, 1800 g) and the final pellet was transferred into a dry pre-weight ceramic cup (24 h, 105°C). The pellet was dried overnight at 105 °C and cooled in a desiccator containing dry silica gel prior to weighing. A correlation between the dry weight and the cell concentration was established for *S. cerevisiae* and *C. vulgaris*:

$$DW_{yeast} = 3.25 \times 10^{-11}\, N_{yeast} \quad (12)$$

$$DW_{microalgae} = 1.5 \times 10^{-11}\, N_{microalgae} \quad (13)$$

with:
DW_{yeast}: *S. cerevisiae* dry weight (g. l^{-1})
$DW_{microalgae}$: *C. vulgaris* dry weight (g. l^{-1})
N_{yeast}: *S. cerevisiae* cells concentration (cells. l^{-1})
$N_{microalgae}$: *C. vulgaris* cells concentration (cells. l^{-1})

The correlation for yeast was based on experimental data points from a monoculture of *S. cerevisiae* in PBR using Mix medium (9 data points and $R^2 = 0.91$) (Figure 33A) and the correlation of microalgae was based on experimental data from an autotrophic monoculture in PBR using the Mix medium **without** glucose and peptone (13 data points and $R^2 = 0.96$) (Figure 33B).

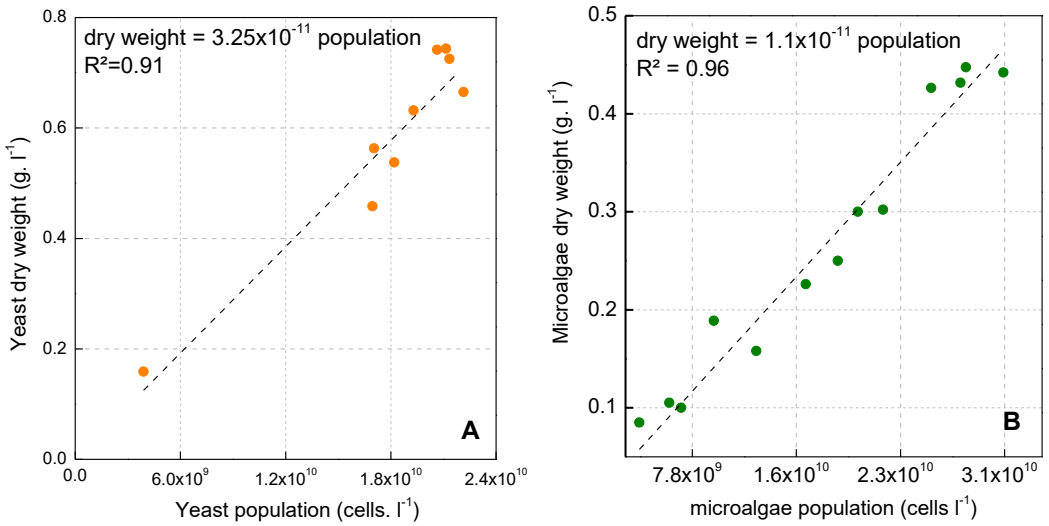

Figure 33. Correlation between dry weight and population for *S. cerevisiae* (A) and *C. vulgaris* (B).

2.5.4 Glucose, ethanol and glycerol measurements

The measurements of glucose, ethanol and glycerol were performed by high-performance liquid chromatography (HPLC) (Ultimate 3000, Thermo Scientific), for concentration between 0 and 10 g. l^{-1}. A cationic column (Aminex HPX-87H, Bio-Rad) was used with 2 mM sulfuric acid as the mobile phase with a flow rate of 0.5 ml. min^{-1}, an injection volume of 10 µl, a temperature of 45°C and a pressure of 60 bar. The refractive index (RI) detector (RI 101, Shodex) at the end of the column, detected the products in the solution in the form of distinct chromatogram peaks. According to their retention time, peaks were identified and integrated (area under the signal) by the software Chroméléon 6.8. The integration of the peaks indicated the product concentration based on range of standards.

Culture supernatants were prepared by sample centrifugation (10 min, 3500 g) and filtration (PTFE Syringe Filter 0.2 µm, Fisherbrand). If necessary, dilution with milliQ water was performed to reach a concentration between 0 and 10 g. l^{-1}.

2.5.5 Ions measurements

Evolution of anions (Cl^-, NO_3^-, SO_4^{2-}, $PO4^{3-}$) and cations (Na^+, NH_4^+, K^+, Mg^{2+}, Ca^{2+}) were studied for cultures in PBR. The measurements of ions were performed by ion

chromatography (Dionex ICS-5000 + HPCI System, Thermo Scientific) for concentration between 0.05 and 50 mg. l^{-1}. A pre-column anionic column IONPAC AG11-HC (2x50 mm) was coupled to an anionic column IONPAC AS11-HC (2×250 mm) for the detection of anions and the detection of cations was performed with the association of a pre-column IONPAC CG16 (3×50 mm) and a cationic column IONPAC CS16 (3×250 mm). The elution of anions was performed with 30 mM hydroxy potassium, a flow rate of 0.3 ml min^{-1}, the elution for cations was performed with 30 mM methanesulfonic acid and a flow rate of 0.36 ml. min^{-1}. Analysis were performed at 35°C with a detection by conductimetry.

Culture supernatants were prepared by sample centrifugation (10 min, 3500×g) and filtration (PTFE Syringe Filter 0.2 µm, Fisherbrand). If ions concentration was too high, dilution with milliQ was performed to decrease the concentration to 0.05 and 50 mg. l^{-1}.

2.5.6 Total chlorophyll measurements

The total chlorophyll (chlorophyll a and b) concentration of *C. vulgaris* was determined according to the method of Porra (1990) and Ben Amor-Ben Ayed et al. (2015). For each replicate, an Eppendorf tube was filled with 1 ml of sample. After centrifugation (5 min, 6400×*g*), 1 ml of an aqueous solution of 85% methanol and 1.5 mmol. l^{-1} of sodium dithionite was added to the pellet of each tube. The tubes were incubated at 40°C for 32 min in the dark. After centrifugation (5 min, 6400×*g*), the absorbance of the supernatants was measured at 650 nm and 664 nm (UV-Visible Spectrophotometer EVOLUTION 60S, Thermo Scientific), and the concentration of total chlorophyll in the culture was calculated as follows:

$$\text{Chl a (mg. } l^{-1}) = 16.41 \times \text{OD 664 nm} - 8.09 \times \text{OD 650 nm} \quad (14)$$

$$\text{Chl b (mg. } l^{-1}) = 30.82 \times \text{OD 650 nm} - 12.57 \times \text{OD 664 nm} \quad (15)$$

$$\text{Chl tot (mg. } l^{-1}) = \text{Chl a} + \text{Chl b} \quad (16)$$

The total chlorophyll content (mg. $cell^{-1}$) corresponds to total chlorophyll amount per cell.

2.5.7 Elementary analysis

The elementary composition of *S. cerevisiae* and *C. vulgaris* biomass were analyzed by CHNS/O analysis. This elemental analysis provides the mass percentage of carbon, hydrogen,

nitrogen, sulfur and oxygen in a solid sample. The elementary analysis was performed by the analyzer CNHS FLASH 2000 (ThermoFisherScientific) with two distinct analysis circuit: CHNS and O.

Yeast and microalgae biomass were prepared as for dry weight (section 2.5.3), while peptone samples were not prepared as peptone was already in form of dried powder. For the CHNS analysis of one sample, 1 mg of the sample was weighed (Mettler XP6, precision 1 μg) in a tin capsule with 1 mg of vanadium(V) oxide (V_2O_5), to ensure the complete combustion. For the O analysis of one sample, 1 mg was weighed in a silver capsule without any catalyst.

The CHNS analysis was performed by a "Flash" (quick) combustion of the sample in a reactor maintained at 930°C. The gaseous combustion products were separated on chromatographic column and detected by the katharometer, hence C, H, N and S were respectively detected in the form of CO_2, H_2O, N_2, and SO_2. The O analysis was performed by pyrolysis in reactor maintained at 1000°C. Oxygen was detected by a katharometer in form of carbon monoxide (CO). In both CNHS and O analysis, the detection by katharometer was based on the measurement of variations in thermal conductivity of a gas flow. The response of the katharometer was proportional to the gas concentration in the mixture.

Chapter 3. Strategy for the development of a co-dominant mixed culture of yeast and microalgae

This chapter describes the strategy adopted to limit co-dominance of one microorganism over the other in mixed culture of yeast S. cerevisiae and microalgae *C. vulgaris*. The strategy included the design of a medium that allowed both yeast and microalgae growth in co-dominance in mixed culture. The impact of each component from the newly designed medium was assessed on yeast and microalgae in order to: firstly, evaluate potential nutrients competition between the two organisms and, secondly to optimize the medium for yeast and microalgae growth. The experiments in this chapter were conducted in shake-flask culture. The strategy for a co-dominant mixed culture of yeast and microalgae in photo-bioreactor also involved the definition of suitable growth parameters. These parameters are defined and explained in this chapter.

Contents

3.1 Design of a specific medium for mixed culture: test of candidate media

A growth medium that allowed the growth of both yeast and microalgae was necessary for a mixed culture of these microorganisms. The strategy for designing a medium suitable for a co-dominant mixed culture of yeast and microalgae was to combine the YPG medium, a standard medium used for yeast, and the MBM medium, a standard medium for autotrophic microalgae growth (Clément-Larosière et al. 2014; Ben Amor-Ben Ayed et al. 2015). As the specific growth rate (μ) of *C. vulgaris* is smaller than that of *S. cerevisiae*, the growth medium was designed to slightly favor *C. vulgaris* development and limit *S. cerevisiae* growth. Three candidate media were then assessed by focusing on their impact on yeast or microalgae final yield when grown in monoculture (Figure 34).

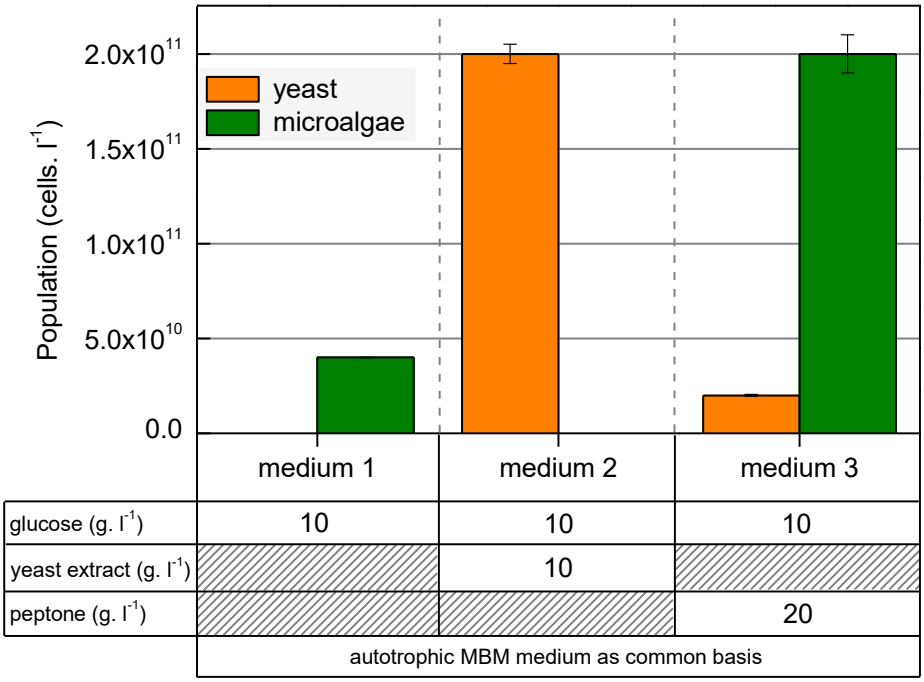

Figure 34. Maximum population of yeast and microalgae in monoculture using three candidate media for mixed culture. Yeast population was measured after 3 days of incubation and microalgae population after 5 days of incubation. Each monoculture was performed in duplicate and average values are shown. Where no values are shown, there was no measurable growth.

Medium 1, which contained MBM medium and glucose allowed only *C. vulgaris* growth (4×10^{10} cells. l^{-1}) and *S. cerevisiae* growth was barely detectable. Medium 1 contained glucose, which can be used by both microalgae and yeast. Nitrate in the form of $NaNO_3$ was the main

nitrogen source for *C. vulgaris* as *S. cerevisiae* is unable to use nitrate as nitrogen source (Siverio 2002). We can postulate that *S. cerevisiae* could not grow on the medium 1 because of the lack of a suitable nitrogen source in this medium.

Monocultures of *C. vulgaris* and *S. cerevisiae* in medium 2 showed the opposite results from those in medium 1: the yeast grew but not the microalgae. The yeast extract in this medium provided additional components that could be used by the yeast. *C. vulgaris* did not grow in this medium and the formation of cell aggregates suggests a toxicity/stress from yeast extract for the *C. vulgaris* strain used in this study.

In medium 3, both *C. vulgaris* and *S. cerevisiae* could grow: the maximum *C. vulgaris* population was 2×10^{11} cells. l^{-1} and the maximum yeast population was 10 times lower (2×10^{10} cells. l^{-1}). This medium allowed both yeast and microalgae growth because it contained nitrogen and carbon sources available to both yeast and microalgae. Yeast could use glucose as a carbon source and peptone components as a nitrogen source (5.4×10^{-1} g. l^{-1} of free amino nitrogen and 6.0×10^{-2} g. l^{-1} NH_4). Microalgae could use CO_2 (from the air) and glucose according their metabolism (autotrophic and heterotrophic respectively), then nitrate and peptone components as nitrogen sources.

These results indicate that medium 3 was a good candidate for a co-dominant mixed culture of yeast and microalgae: the microalgae maximal population was enhanced in medium 3 compared to the standard autotrophic MBM medium for microalgae. On the other hand, the yeast maximal population decreased in medium 3 compared to the standard YPD medium, commonly used for yeast fermentation (Figure 35).

Even if the maximal microalgae population was 10 times higher than that of yeast, these results were obtained from monocultures wherein yeast and microalgae grew separately. In the case where yeast and microalgae grew in mixed culture, there would be a competition for common assimilable nutrients (glucose, amino acids and components from peptone). As the μ of yeast is higher than that of microalgae, yeast would use the common nutrients to the detriment of microalgae and compromising the co-dominance in the mixed culture. The higher maximal microalgae population obtained with medium 3 could allow to compensate the higher μ of yeast.

To conclude, medium 3 was the best candidate-medium tested for a mixed culture of yeast and microalgae. This medium was named **Mix medium** and used for the rest of this research work.

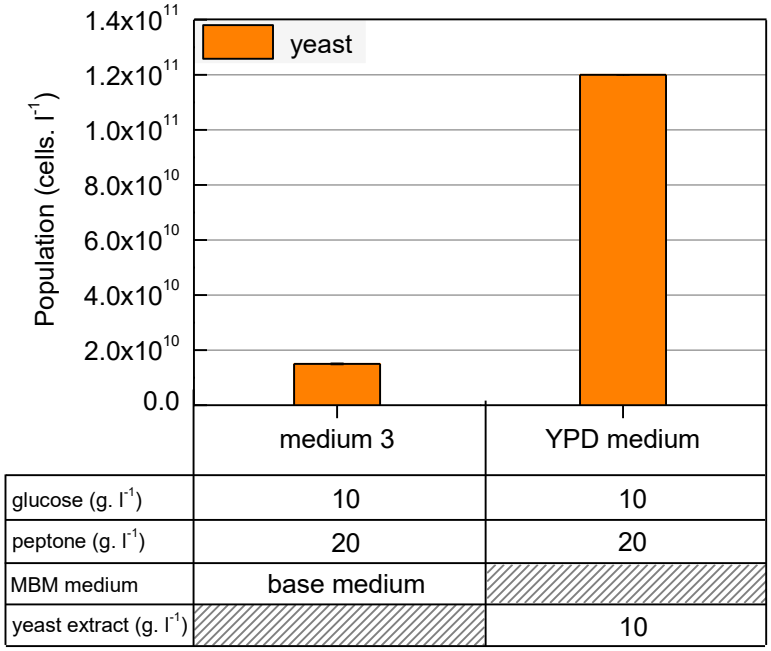

Figure 35. Yeast maximal population in monoculture using medium 3 or YPD medium. The yeast population was measured at the end of the exponential phase (25 hours). Each monoculture was performed in duplicate.

3.2 Optimization of the Mix medium for co-dominance of *S. cerevisiae* and *C. vulgaris*

Mix medium was chosen as the most suitable candidate for co-dominance of yeast and microalgae in mixed culture. Mix medium was composed of three components: mineral medium, glucose and peptone. The composition of the mineral medium was kept constant and the effect the other two components were tested on the growth of the microorganisms. Glucose and peptone are two components that can be assimilated by both yeast and microalgae so the study of their impact on both organisms was essential. *C. vulgaris* is capable of heterotrophic growth using glucose as a carbon source. *S. cerevisiae* is capable of respiration or fermentation of glucose. Additionally, this study would give an indication on the maximal yeast and microalgae population in mixed culture where the two organisms would be both competing for peptone nutritive components and glucose.

3.2.1 Impact of glucose concentration on *S. cerevisiae* growth

To assess the impact of glucose on *S. cerevisiae* growth in Mix medium, yeast was grown with three different concentrations of glucose: 5, 10 and 15 g. l^{-1}. The peptone concentration

was fixed at 20 g. l^{-1} as in the original recipe of Mix medium. The experiments were performed in shake flask with constant aeration and bungs that allowed sterile gas exchange with the atmosphere outside the flasks.

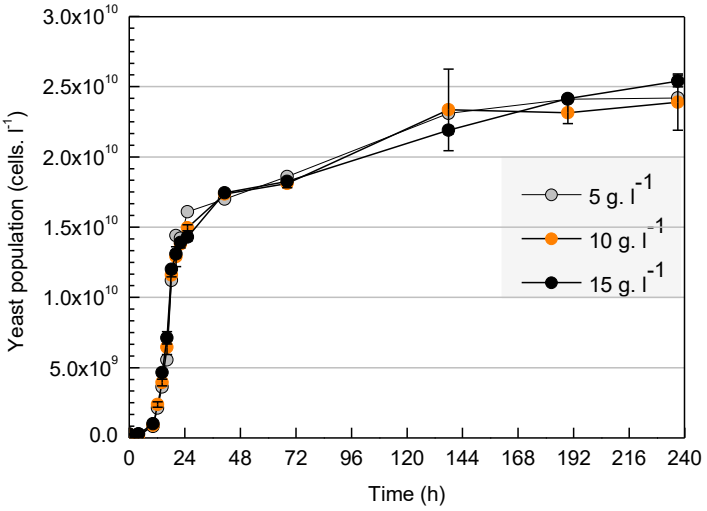

Figure 36. Yeast growth profile at different initial glucose concentrations. Each monoculture was performed in duplicate and the error bars indicate the standard deviation of the two points.

The yeast growth profile in the three conditions were identical. The μ and the yeast yield reached at the end of the exponential phase (around 22 hours) were similar, followed by a second growth phase that was probably a resulted of ethanol respiration once glucose was exhausted as carbon source (Figure 36). The higher the initial glucose concentration, the higher the ethanol yield although, unsurprisingly, the ethanol yield coefficient $Y_{eth/glu}$ was similar in the three cultures (around 0.39 $g_{ethanol}$. $g_{glucose}^{-1}$) (Figure 37). The fermentation activity was the same at all initial glucose concentrations, which suggests that increasing the glucose initial concentration enhanced the amount of glucose converted into ethanol as well as the amount of glucose available for biomass (and by-products like fusel alcohols) formation. However, increasing the initial glucose concentration did not affect the final yield of yeast, suggesting that glucose was not the growth-limiting factor. Glucose provided organic carbon, so yeast growth may have been limited by oxygen or nitrogen from peptone. Since a second growth phase was observed after exponential growth on glucose, it can be concluded that oxygen was not the nutrient that limited the extent of yeast growth. By process of elimination, nitrogen-based compound from peptone was most likely to be the growth-limiting nutrient.

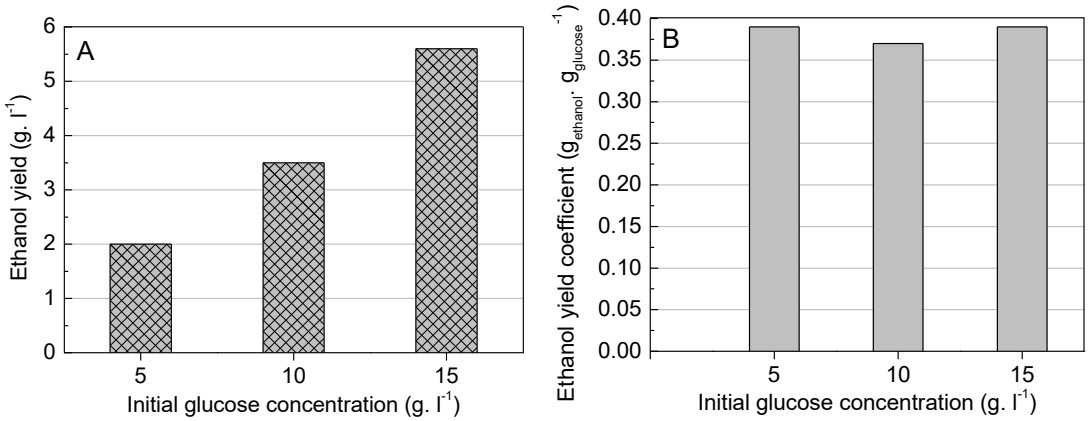

Figure 37. Ethanol yield produced by *S. cerevisiae* at different initial glucose concentrations in yeast monoculture (a) and ethanol yield coefficient on glucose (b). Yield coefficients were calculated from duplicate experiment.

The above experiments were all performed with pure cultures (monocultures) of *S. cerevisiae*. In a mixed culture situation, the glucose may be shared between the yeast and the microalgae. This would affect the ethanol yield but not the yield of yeast, as the glucose is not the limiting nutrient for yeast extent of growth. It is also possible that *S. cerevisiae* with its faster μ could use all glucose in mixed culture forcing the microalgae to grow photo-autotrophically (without glucose).

3.2.2 Effect of peptone concentration on yeast *S. cerevisiae*

To evaluate the impact of peptone on *S. cerevisiae*, yeast was grown at three different concentrations of peptone in the Mix medium (10, 20 and 30 g. l^{-1}) with the glucose concentration fixed at 10 g. l^{-1}. The experiments were performed in shake flask with constant aeration through agitation.

The pattern that emerged was that the higher the initial peptone concentration, the higher the yeast population at the end of the exponential phase (Figure 38). Despite the difference in yeast yield, the shape of the growth curves was similar for the three conditions: a first exponential phase (same μ for the three conditions) was followed by a second growth phase, resembling diauxic growth. The second growth phase was slower and almost linear in nature suggesting that ethanol was used respiratively as sole carbon source and that the constant supply rate of O_2 was responsible for the linear growth.

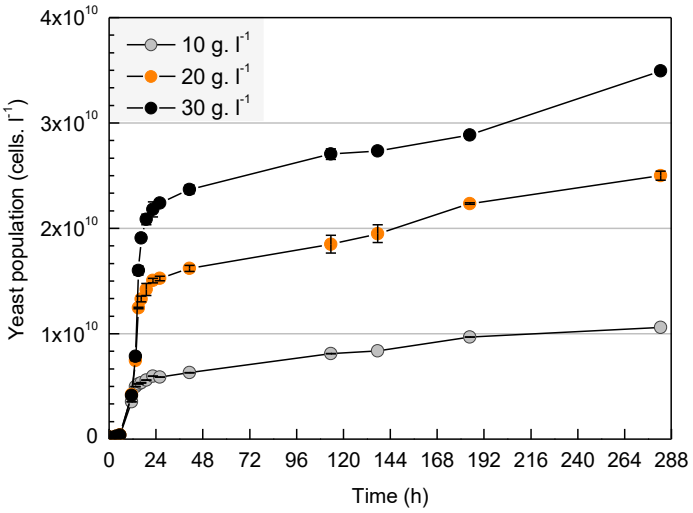

Figure 38. Yeast growth profiles with different initial peptone concentrations. Each monoculture was performed in duplicate.

Peptone provided nitrogen (15% w/w of peptone) in different forms but only part of the total nitrogen is assimilable by *S. cerevisiae*: NH_4^+, individual amino acids and small peptides (up to three-unit oligomers). In fermentation, amino acids and small peptides are energetically preferred sources of nitrogen for *S. cerevisiae* and their concentration is collectively called free amino nitrogen (FAN). Increasing the initial peptone concentration enhanced the yeast yield, demonstrating that the assimilable nitrogen was the limiting growth factor for yeast. The nitrogen concentration calculated from the FAN was coherent with that in found in the yeast biomass, even at the highest peptone concentration (30 g. l^{-1}) tested. This again confirmed that amino acids and short peptides from peptone were the limiting growth factors for yeast growth (Table 6). Although these results suggest amino acid assimilation by yeast, the assimilation of some NH_4^+ cannot be ruled out.

Table 6. Nitrogen content in the medium and biomass formed according the initial peptone concentration

Medium compounds			Yeast biomass formed		
Peptone	FAN*	**N from FAN**	Yeast yield		**N in yeast**
g. l^{-1}	g.l^{-1}	**g. l^{-1}**	cells. l^{-1}	g. l^{-1}	**g. l^{-1}**
10	2.6×10^{-1}	**3.0×10^{-2}**	6.7×10^{9}	2.1×10^{-1}	**2.2×10^{-2}**
20	5.2×10^{-1}	**6.1×10^{-2}**	1.7×10^{10}	5.5×10^{-1}	**5.5×10^{-2}**
30	7.8×10^{-1}	**9.2×10^{-2}**	2.6×10^{10}	8.5×10^{-1}	**8.5×10^{-2}**

The nitrogen concentration from FAN (N_{FAN}) and that from yeast biomass (N_{yeast}) were calculated as:

$$N_{FAN} = \frac{Peptone \times FAN_{content}}{M_{aa}} \times M_N \quad (17)$$

with:
N_{FAN}: nitrogen concentration from FAN (g. l^{-1})
$Peptone$: initial peptone concentration (g. l^{-1})
$FAN_{content}$: individual amino acids and small peptides content in peptone (2.7 %)
M_{aa}: mean of the different amino acids molecular weight (118.9 g. $mole^{-1}$)
M_N: nitrogen molecular weight (14 g $mole^{-1}$)

$$N_{yeast} = DW_{yeast} \times N_{content} \quad (18)$$

with:
N_{yeast}: nitrogen content from yeast biomass (g. l^{-1})
DW_{yeast}: yeast dry weight (g. l^{-1})
$N_{content}$: nitrogen content in yeast biomass (10% w/w)

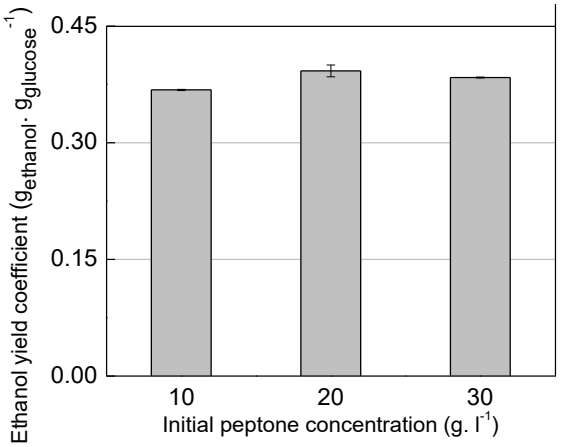

Figure 39. Ethanol yield coefficient on glucose according the initial peptone concentration. Yield coefficients were calculated from duplicate experiments.

The increase in initial peptone concentration was accompanied by an increase in yeast population yield but the $Y_{eth/glu}$ remained the same (Figure 39): the concentration of ethanol produced was the same (Appendix 4, 5 and 6). This observation suggests that the amount of organic carbon, largely from glucose, available for the formation of biomass and by-products remained the same regardless the initial concentration of peptone, which emphasizes that assimilable nitrogenous compounds from peptone were the limiting-growth factors and not glucose.

3.2.3 Impact of peptone concentration on microalgae *C. vulgaris*

To assess the impact of peptone on *C. vulgaris*, the microalgae was grown with three different concentrations of peptone (10, 20 and 30 g. l^{-1}) in the Mix medium without glucose. The Mix medium was hence composed of only the autotrophic medium, and peptone.

The impact of the peptone concentration on microalgae was investigated in the absence of glucose because in a mixed culture, it seemed reasonable to assume that with the high μ of yeast, the glucose would be exclusively used by yeast leaving *C. vulgaris* to grow photo-autotrophically. The experiments were performed in shake flask cultures with constant aeration to supply atmospheric CO_2.

The addition of peptone increased the microalgae yield but the latter was not in step with the increase in the peptone concentration (Figure 40). The addition of 10 and 20 g. l^{-1} peptone only slightly increased the final microalgae concentration, but the peptone accelerated the speed of growth (Figure 40) suggesting that it supplied nitrogenous compounds not present in the autotrophic MBM medium (NH_4^+, individual amino acids and small peptides). Significant increase in the μ and final biomass concentration was observed by the addition of 30 g. l^{-1}, again reinforcing the idea that the peptone supplied a growth-limiting factor to the microalgae, as well as the yeast as discussed above. (Figure 40).

In absence of peptone, *C. vulgaris* could still grow reaching around the same final concentration as in presence of the lower concentrations of peptone (10 and 20 g. l^{-1}) tested. Therefore, in a mixed culture situation if *S. cerevisiae* used principally the specific peptone components as well as the glucose (all organic compounds), *C. vulgaris* would still grow autotrophically.

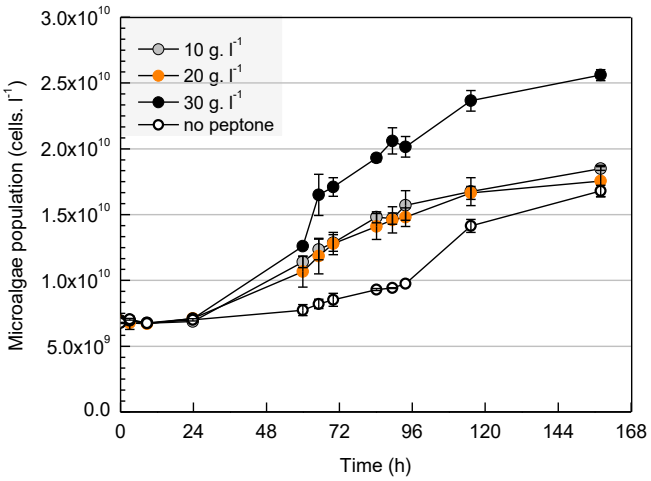

Figure 40. Microalgae growth profile at different initial peptone concentrations. *C. vulgaris* was grown without glucose. Each monoculture was performed in duplicate and the error bars represent the standard deviation around the average points.

3.2.4 Adjustment of the peptone concentration for an optimized Mix medium

The *S. cerevisiae* and *C. vulgaris* monocultures in shake flask showed that the yield of yeast was independent of that of microalgae whatever the initial peptone concentration. Their respective population yields under each condition were compared in order to determine the most suitable peptone concentration for a co-dominant mixed culture.

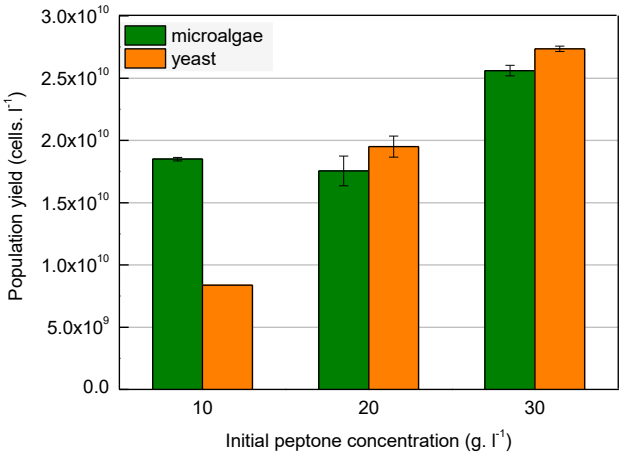

Figure 41. Summary of yeast and microalgae population yields in monoculture according the initial peptone concentration. The yields correspond to the population reached at 138 and 158 hours respectively for *S. cerevisiae* and *C. vulgaris*. The yields were calculated from duplicate experiment the error pars represent the standard deviation around the average points.

With an initial peptone concentration of 10 g. l^{-1}, the yeast and the microalgae population yields were significantly different as the microalgae population was twice higher than yeast population (Figure 41). From 20 g. l^{-1} of peptone, the yeast and the microalgae population yield were roughly similar, and both increased with a rise in initial peptone concentration. An excessively high population density is unfavorable to light penetration into a photosynthetic culture. For this reason, a concentration of 20 g. l^{-1} peptone was chosen as the concentration to use for mixed cultures (more explanation below).

The aim of medium design was to define the conditions that would result in co-dominance between yeast and microalgae in mixed culture. The peptone concentration of 10 g. l^{-1} was not a suitable value as microalgae would dominate the population. At best, yeast would use all peptone components necessary and would reach 8.4×10^{9} cells. l^{-1} (Figure 41), but this population yield would remain twice lower than the microalgae population yield reached without any uptake of components from peptone (1.7×10^{10} cells. l^{-1}) (Figure 40).

With 20 or 30 g. l^{-1} peptone, parity of the populations could be reached if they equally shared the peptone. However, the yeast μ was higher than that for the microalgae so in the worst-case scenario, *S. cerevisiae* would consume all limiting-components of peptone and *C. vulgaris* would grow without using any of them. In this situation and with an initial peptone concentration of 30 g. l^{-1}, the yeast population yield would be 63 % higher than microalgae if the latter grew without peptone and the co-dominance would not be reached (2.7×10^{10} cells. l^{-1} and 1.7×10^{10} cells. l^{-1} respectively) (Figure 41 and Figure 40).

The co-dominance could be reached with 20 and 30 g. l^{-1} peptone but any more concentrated culture would risk auto-shadowing so the minimum concentration of peptone, considering that parity of population is reached in a mixed culture situation; 20 g. l^{-1} peptone seems to be a good compromise. Moreover, with a peptone concentration of 20 g. l^{-1} if yeast used all peptone, the yeast and microalgae population yield would remain similar (1.9×10^{10} cells. l^{-1} and 1.8×10^{10} cells. l^{-1} respectively) as microalgae could also grow autotrophically without peptone and glucose (Figure 40).

Finally, the peptone concentration of 20 g. l^{-1} is a good compromise compared to the other concentrations as it would allow the co-dominance between yeast and microalgae in mixed culture using Mix medium. The peptone concentration was then was kept at 20 g. l^{-1} in the Mix medium for subsequent experiments.

3.3 Nutrient competition between yeast and microalgae in mixed culture using Mix medium

Figure 42 shows the hypothetical scenarios that could occur in mixed culture of the two organisms if they each behaved as their respective monocultures. These hypotheses were based on the study of the peptone and glucose influences on *S. cerevisiae* and *C. vulgaris* growth.

S. cerevisiae will need to assimilate both glucose and peptone for growth, the absence of any one of these two nutrient sources would prevent yeast growth. On the other hand, *C. vulgaris* could grow without either glucose or peptone, or both, using a photo-autotrophic metabolism with nitrate as source of nitrogen and CO_2 as carbon source. Only the hypothetical scenario A could lead to a co-dominance between yeast and microalgae in mixed culture: if the yeast would use all of the glucose and peptone while the microalgae grew photo-autotrophically using nitrate as nitrogen source.

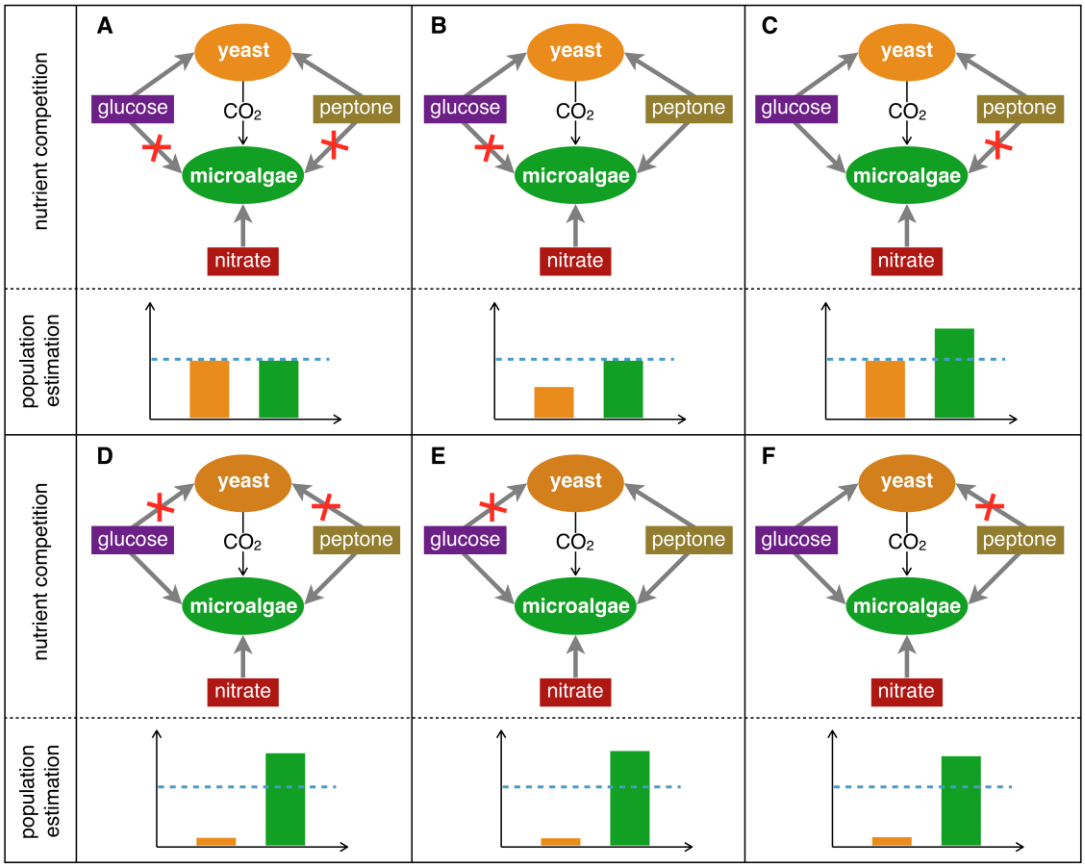

Figure 42. Six hypothetical scenarios representing the possible influence of nutrient competition on yeast and microalgae population yield in case of mixed culture using the Mix medium.

Examining the various hypothetical scenarios:

A. The yeast uses all the glucose and nutrients from the peptone; microalgae consume CO_2 and nitrate as nitrogen source. Based on the monoculture results the growth of the two organisms would be to an equal extent. Hence the condition of co-dominance would be achieved.
B. The yeast uses all the glucose and the nutrients from the peptone are shared between yeast and microalgae; microalgae additionally consume CO_2 and nitrate as nitrogen source. Based on the monoculture results the yeast yield would decrease since less nutrients from peptone would be available to the organisms. Microalgae yield would not increase despite the use of part of components from peptone.
C. The yeast uses all nutrients from peptone, and glucose is shared between yeast and microalgae; microalgae also consume CO_2 and nitrate as nitrogen source. Based on the monoculture results the glucose sharing would not impact on the yeast yield but would increase that of microalgae as glucose is another carbon source for microalgae metabolized through respiration.
D. The microalgae use all the glucose and nutrients from the peptone. Based on the monoculture results the growth of microalgae would increase as glucose and nutrients from peptone are available for a heterotrophic growth. Yeast would not grow as glucose and nutrients from peptone are mandatory for its growth.
E. Microalgae use all the glucose and nutrients from the peptone are shared between yeast and microalgae. Based on the monoculture results the growth of microalgae would increase as glucose and nutrients from peptone are available for a heterotrophic growth. Yeast would not grow as glucose (organic carbon source) is mandatory for its growth.
F. Microalgae use all nutrients from peptone and glucose is shared between yeast and microalgae. Based on the monoculture results the growth of microalgae would increase as glucose and nutrients from peptone are available for a heterotrophic growth. Yeast would not grow as nutrients from peptone are mandatory for growth.

A last hypothetical scenario would be where glucose and nutrients from peptone are shared by both yeast and microalgae. With this scenario, the growth of each organism would depend on the proportion of nutrient used by each organism, so it seems to be difficult to estimate the growth of yeast and microalgae. Overall, yeast growth would decrease because of a lower amount of nutrient from peptone would be available to this organism and microalgae growth would increase with the utilization of some glucose.

3.4 Definition of parameters for mixed culture in photo-bioreactor

The temperature and pH in photo-bioreactor were adjusted to promote co-dominance of yeast and microalgae in mixed culture by favoring *C. vulgaris* growth and restricting *S. cerevisiae* growth. According to Kumar et al. (2010), temperatures of 15-26°C and neutral pH are optima for microalgae growth. The form of the dissolved CO_2 concentration and the pH of the culture are directly linked so we chose to control the pH at 6.5 to achieve a good compromise between having a neutral pH and the dissolved CO_2 and bicarbonate species proportioned at around 0.5 at 25°C (Edwards et al. 1978) (Chapter 1).

The inoculum ratio was set up in an inverse manner to compensate for the higher yeast μ and favor microalgae growth:

$$N_{0C.vulgaris} = \frac{N_{0S.cerevisiae}\ exp(\mu_{S.cerevisiae} t)}{exp(\mu_{C.vulgaris} t)} \quad (19)$$

with:
$N_{0C.vulgaris}$: initial *C. vulgaris* population (cells. l^{-1})
$N_{0S.cerevisiae}$: initial *S. cerevisiae* population (cells. l^{-1})
$\mu_{S.cerevisiae}$: *S. cerevisiae* specific growth rate (h^{-1})
$\mu_{C.vulgaris}$: *C. vulgaris* specific growth (h^{-1})
t: duration of the *S. cerevisiae* exponential phase (h)

The yeast and microalgae μ and the duration of the *S. cerevisiae* exponential phase were experimentally obtained from separate monocultures in photo-bioreactor (5 l) cultures, with the adjusted parameters to be in the closest conditions as the subsequent mixed culture in photo-bioreactor. Monocultures of *S. cerevisiae* and *C. vulgaris* in photo-bioreactors were then studied in Chapter 4.

In mixed culture, *S. cerevisiae* would produce CO_2 necessary for microalgae photosynthesis and microalgae would produce O_2 that could be used by yeast. To promote these synergetic effects, the gas produced was kept *in situ* by closing the photo-bioreactor and avoiding the aeration.

3.5 Conclusions

The Mix medium designed for a co-dominant mixed culture of yeast *S. cerevisiae* and microalgae *C. vulgaris* was composed of carbon source (glucose, 10 g. l^{-1}) and nitrogen source (peptone, 20 g. l^{-1}) that could be assimilated by both microorganisms. The competition between the organisms in using each component influenced the biomass production yield of yeast and/or microalgae. The strategy for a co-dominant mixed culture also implies the adjustment of the culture parameters in photo-bioreactor.

Chapter 4. Study of *S. cerevisiae* and *C. vulgaris* monocultures in photo-bioreactor

The yeast *S. cerevisiae* and the microalga *C. vulgaris* where studied to compare their behaviors when grown in monoculture and in mixed culture. Three monocultures were conducted in photo-bioreactor under the closest conditions possible to mixed cultures: yeast and microalgae monocultures were realized in Mix medium and a microalgae monoculture was conducted in photo-autotrophic MBM medium without glucose and peptone. Mass balances were realized for a better understanding of yeast and microalgae growth, and dry weight concentrations of the yeast and microalgae were calculated from the corresponding cell concentration. The numeric ratios in stoichiometric reactions were expressed in mole.

Contents

4.1 *S. cerevisiae* monoculture using mix medium

S. cerevisiae was grown on Mix medium in a photo-bioreactor without aeration, exactly under the same conditions as for the subsequent mixed cultures (Chapter 5). The photo-bioreactor was closed with a safety valve. The pH was kept constant at 6.5 with the automatic addition of KOH (1 M).

The yeast exponential phase (μ=0.27 h^{-1}) occurred within the first 24 hours of incubation and was accompanied with glucose and oxygen consumption and the population reached was 1.9×10^{10} cells. l^{-1}. *S. cerevisiae* used all glucose within the first 31 hours of incubation producing ethanol (3.9 g. l^{-1}) reaching a maximum population of 2.2×10^{10} cells. l^{-1} (Figure 43). As suggested in Chapter 3, *S. cerevisiae* growth was limited by the concentration of nitrogenous compounds in peptone (mainly amino acids and short peptides).

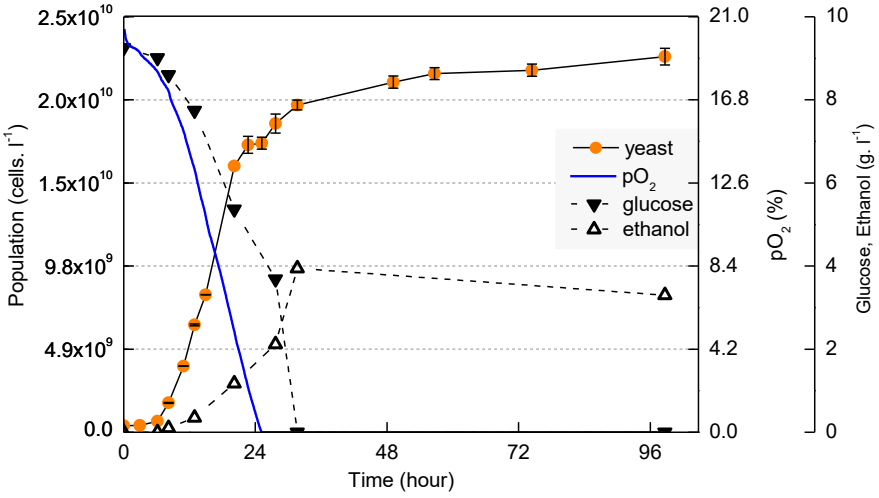

Figure 43. Yeast monoculture using Mix medium in non-aerated and closed photo-bioreactor. The measurement of pO_2 was continuously recorded so the experimental points are fused into a solid blue line.

The ethanol production shows that yeast catabolized glucose fermentatively and was accompanied by glycerol production (up to 0.3 g. l^{-1}, data not shown). Although fermentation activity is known to not require O_2, latter is even so required for synthesis of membrane components (ergosterol, unsaturated fatty acids...). Moreover, the utilization of O_2 through respiration cannot be ruled out as *S. cerevisiae* mixes respiration and fermentation metabolism in the presence of oxygen and when external glucose concentration exceeds 0.8 mmole. l^{-1} (0.1 g. l^{-1}) (Verduyn et al. 1984; Otterstedt et al. 2004): this phenomenon is called the "Crabtree effect". The challenge in studying yeast metabolism was to determine whether glucose was

metabolized through fermentation, respiration, biomass or glycerol formation and in which proportion. The repartition of glucose utilization can be done with a components mass balance, indicating the metabolic pathways used by *S. cerevisiae* in the monoculture.

4.1.1 Study of *S. cerevisiae* metabolism: components mass balance

4.1.1.1 Possible metabolic pathways in *S. cerevisiae*

The main possible metabolic pathways in *S. cerevisiae* are depicted in Figure 44: glycerol, ethanol, biomass and CO_2 can be produced from glucose. The formation of by-products from glucose degradation is neglected in this study.

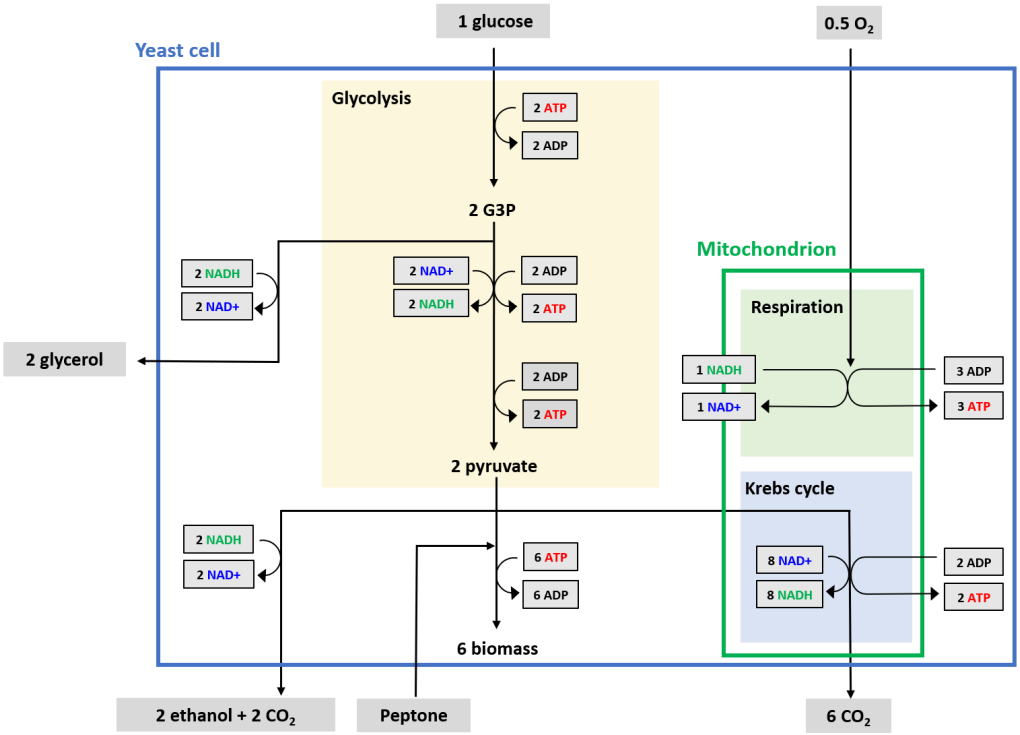

Figure 44. A schematic diagram of the metabolic pathways used in our modeling approach. All numeric ratios are in moles.

The ethanol pathway provides ATP required for biomass formation. Glycerol is produced to close the redox balance for the co-enzyme system NAD^+/NADH of the biomass pathway. The mitochondrial respiration is also involved for regenerating NAD^+ from NADH involving O_2 utilization and ATP production. Mitochondrial respiration can recycle cytosolic and mitochondrial NADH from the Krebs cycle. The latter allows to produce more mitochondrial

NADH, hence more ATP can be generated through the electron transport chain, as long as there is enough O_2. According to Verduyn et al. (1990), during fermentation, *S. cerevisiae* uses glucose principally through alcoholic fermentation and a small part is diverted to anabolic pathway allowing biomass formation. The repartition of glucose into ethanol fermentation and anabolic pathway can be determined from the biomass yield by examining the assimilation equation for biomass formation and ethanol fermentation.

4.1.1.2 Biomass formation

Within 31 hours of incubation, 0.65 g_{DW}. l^{-1} of yeast biomass was produced, i.e. 3.25 g of biomass in total, resulting in a specific biomass yield coefficient on glucose of 0.06 g_{yeast}. $g_{glucose}^{-1}$, which fits with a fermentative metabolism (Verduyn et al. 1990b). Peptone provided nitrogen mainly in the forms of amino acids and short peptides. Glucose was the source of carbon for biomass formation, however, glucose was also used for ethanol, glycerol, CO_2 production and potentially respiration with Krebs Cycle. Therefore, to determine the amount of glucose metabolized into biomass, it was necessary to know the carbon content of *S. cerevisiae* biomass. According to Verduyn et al. (1990b), the composition of 100 g of *S. cerevisiae* biomass is $C_{3.75}H_{6.60}N_{0.63}O_{2.10}$, which gives the ratio of each elements in Table 7. These ratios were very close to the results from elementary CHN/O analysis of dried yeast biomass and these experimental ratios were used for the rest of the thesis.

Table 7. *S. cerevisiae* biomass composition

	Verduyn et al. (1990b) (% w/w)	CHN/O analysis (% w/w)
C	45	46
H	6.6	7
N	8.8	10
O	33.6	34

As *S. cerevisiae* biomass was composed of 46% carbon, 3.7 g of glucose was required to form 3.25 g of biomass:

$$\mathrm{m}_{glucose} = \frac{\mathrm{m}_{yeast}\, C_{\mathrm{content}}}{\mathrm{M_C}\, \mathrm{C_{glucose}}}\, \mathrm{M_{glucose}} = 3.7\ \mathrm{g} \qquad (20)$$

with:

$m_{glucose}$: mass of glucose used for biomass formation (g_{yeast})

m_{yeast} : yeast biomass formed (3.25 g)
$C_{content}$: carbon content in yeast biomass (46%)
M_C : carbon molecular weight (g. mole^{-1})
$C_{glucose}$: moles of carbon of 1 mole of glucose (6 moles)
$M_{glucose}$: glucose molecular weight (g. mole^{-1})

The degradation of 3.7 g of glucose i.e. 0.021 mole, required 0.042 mole NAD^+, and 0.115 mole ATP (yeast yield coefficient on ATP was 28.3 $g_{yeast.}$ $mole_{ATP}^{-1}$ according to Verduyn et al. (1990a)):

0.021 $C_6H_{12}O_6$ + 0.021 N-(amino acids) + 0.115 ATP + 0.042 NAD^+ → BIOMASS + 0.115 ADP + 0.042 NADH **Reaction 5**

The ethanol and glycerol production from fermentation activity provided ATP and NAD^+ (described in section below).

4.1.1.3 Fermentation

S. cerevisiae produced 3.95 g. l^{-1} of ethanol, i.e. 19.8 g ethanol (0.43 mole) in total within 31 hours. This production required 38.6 g glucose (0.215 mole) and generated an estimated 0.43 mole of ATP, part of which would have been used for biomass formation (0.115 mole ATP for 3.25 g_{DW} of yeast) and the rest may have been used for the production of internal reserves (glycogen and trehalose) and a small part for cell maintenance (0.315 mole ATP):

0.215 $C_6H_{12}O_6$ + 0.43 ADP → 0.43 C_2H_5OH + 0.43 CO_2 + 0.43 ATP **Reaction 6**

During yeast fermentation, 0.3 g. l^{-1} (1.5 g in total corresponding to 0.016 mole) of glycerol was also produced from glucose (1.47 g i.e. 0.008 mole) in order to close the redox balance for the co-enzyme system NAD^+/NADH (Gancedo et al. 1968; Verduyn et al. 1990b):

0.008 $C_6H_{12}O_6$ + 0.016 NADH + 0.016 H^+ → 0.016 $C_3H_8O_3$ + 0.016 NAD^+ **Reaction 7**

Under strict fermentative metabolism, *S. cerevisiae* generally produces enough glycerol to generate enough NAD^+ required for yeast biomass formation. In our *S. cerevisiae* monoculture, the glycerol production pathway did not generate enough NAD^+ to completely

compensate the demand in NAD^+ in the biomass formation pathway (0.042 mole NAD^+ was required), hence 0.026 mole NAD^+ needed to regenerate. This necessary amount of NAD^+ was not provided by the ethanol pathway as the co-enzyme system NAD^+/NADH is closed in this pathway. Therefore, another alternative should have been involved to generate the complementary amount of NAD^+: respiration with O_2 utilization though the electron transport chain.

4.1.1.4 Respiration with Krebs cycle for NAD^+ regeneration

Respirative metabolism is well known to involve Krebs cycle, which uses NAD^+ to generate additional NADH from pyruvate. This mitochondrial NADH is then conveyed to the mitochondrial respiratory chain to regenerate NAD^+ and close the system NAD^+/NADH. At this stage, O_2 is required and ATP is produced. Reaction 8 describes the process of respiration with Krebs cycle from 1 mole of glucose:

$1\ C_6H_{12}O_6 + 6\ O_2 + 38\ ADP + 32\ H^+ \rightarrow 6\ CO_2 + 38\ ATP + 38\ H_2O$ **Reaction 8**

In the respirative metabolism with Krebs cycle, the redox balance for the co-enzyme system NAD^+/NADH is closed, hence no extra NAD^+ is produced, the main goal being the increase in ATP yield. Therefore, Krebs cycle could not have been involved during the yeast monoculture to regenerate NAD^+ and supply to the biomass formation pathway. This is could be linked to the fact that Krebs cycle is repressed with the Crabtree effect, favoring glucose degradation through ethanol production.

4.1.1.5 Respiration through external NADH dehydrogenase for NAD^+ regeneration

In *S. cerevisiae*, NAD^+ can be regenerated from cytosolic NADH by the mitochondrial respiratory chain through external NADH dehydrogenase, requiring O_2 and generating some ATP (Reaction 9). This process can occur without mitochondrial NADH produced from Krebs cycle.

$1\ NADH + 1/2\ O_2 + 1\ H^+ \rightarrow 1\ NAD^+ + H_2O$ **Reaction 9**

The NAD^+ regeneration capacity depends on the amount of O_2 available. The total bioreactor volume is the sum of the liquid volume V_{liq} and the PBR headspace V_{gas}, both contained an initial quantity of oxygen. As the bioreactor was closed during the culture, an oxygen balance equation is needed to know how the initial stock can be used by biological activity:

$$m_{O_2\,gas} = \frac{pO_{2gas}\, M_{O_2} V_{gas}}{R_{gas}\, T} = 0.41\ g \quad (21)$$

$$m_{O_2\,liquide} = \frac{pO_{2\,liquide}\, M_{O_2}\, V_{liq}}{H_{O_2}} = 4.4 \times 10^{-2}\ g \quad (22)$$

$$m_{O_2} = m_{O_2\,gas} + m_{O_2\,liquide} = 0.45\ g \quad (23)$$

where:
m_{O_2}: total O_2 available (g)
$m_{O_2\,gas}$: O_2 available from gaseous phase (headspace of the bioreactor) (g)
$m_{O_2\,liquide}$: O_2 available from liquid phase (g)
pO_{2gas}: partial pressure of O_2 in the gaseous phase (21 000 Pa)
M_{O_2}: molar mass of O_2 (32 g. mole^{-1})
V_{gas}: volume of the gaseous phase (1.5×10^{-3} m^3)
R_{gas}: gas constant (8.314 m^3 Pa. mol^{-1} K^{-1})
T: temperature (298 K)
$pO_{2\,liquide}$: partial pressure of O_2 in the gaseous phase (0.21 atm)
H_{O_2}: Henry's constant for O_2 at 25°C (769.23 atm L. mole^{-1})
V_{liq}: volume of the liquid phase (5 l)

From the total amount of O_2 available (0.45 g i.e. 0.014 mole), 0.028 mole NAD^+ could have been regenerated (Reaction 9), which matches with the amount needed to be regenerated, alternatively to the glycerol pathway (0.026 mole NAD^+). All O_2 available in the PBR was used in respiration with external NADH dehydrogenase, in other words, there was no O_2 left for Krebs cycle, which confirms the absence of Krebs cycle in *S. cerevisiae* metabolism.

4.1.2 Addition of acid and alkaline solutions for pH adjustment

The yeast fermentation activity was accompanied by an automatic addition of alkaline solution (1 M KOH). The alkaline solution was added to maintain the pH at 6.5. Any acidic compounds, including CO_2, released into the medium would react with the KOH. After the growth phase, some of the acidic components are either reabsorbed by the yeast or escape the solution as is the case with CO_2. This then results in a rise in pH, which is counteracted by the system of pH control resulting in the addition of mineral acid (1 M H_3PO_4) in order to maintain the pH constant.

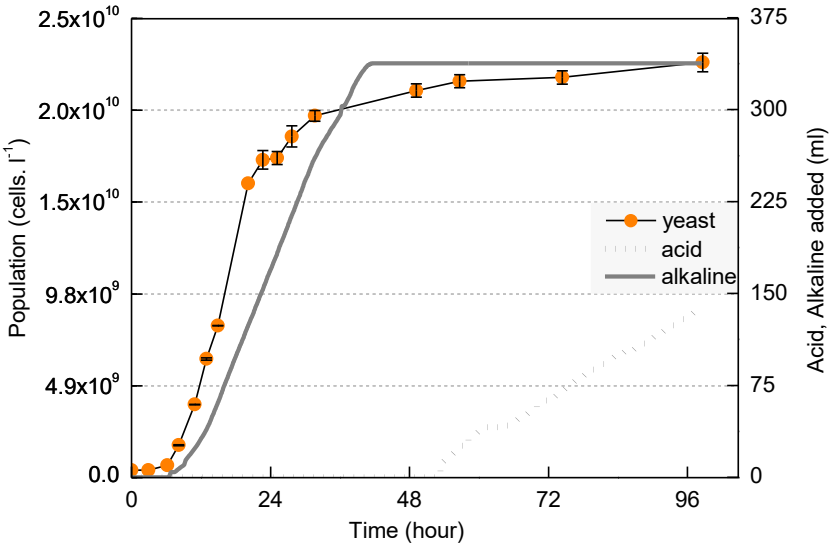

Figure 45. Addition of acid and alkaline solutions to yeast monoculture using Mix medium for automatic pH adjustment at 6.5.

Figure 46 describes the system of pH adjustment according yeast growth. During *S. cerevisiae* growth in Mix medium, biomass and ethanol were produced resulting in the release of carbon dioxide (Reaction 6) and other acid elements such as organic acids, which acidified the culture medium. An alkaline solution was required to compensate the culture medium acidification by increasing the pH value to 6.5; the carbon dioxide was hydrated to carbonic acid H_2CO_3 and then dissociated into proton H^+ and HCO_3^- (Peña et al. 2015), and for an increase in pH value, KOH from the alkaline solution reacted with a proton H^+ to form a water molecule H_2O.

The addition of alkaline solution stopped at the end of the fermentation/growth phase. Since the ethanol production stopped, the CO_2 and organic acids production also stopped, hence there was no need for pH adjustment by addition of alkaline.

After the end of the fermentation phase, the acid solution was added continuously until the end of the culture. The addition of acid to the culture medium indicated an increase in pH that could have been due to the release of alkaline compound by yeast or the removal of acid compound from the culture medium. The removal of protons H^+ from the culture medium could have been due to ethanol stress in yeast *S. cerevisiae* (Charoenbhakdi et al. 2016). Ethanol and other short-chain alcohols are believed to induce loss of membrane integrity, through the association of their aliphatic chains with the hydrophobic interior of membranes, thereby affecting membrane permeability and stability (Weber and Bont 1996). The increase in membrane permeability could have led to an increased passive influx of protons across the membrane, hence inducing removal of protons H^+ from the extracellular environment and alkalization of the culture medium. The addition of acid could also have been due to release of CO_2 to the gaseous phase.

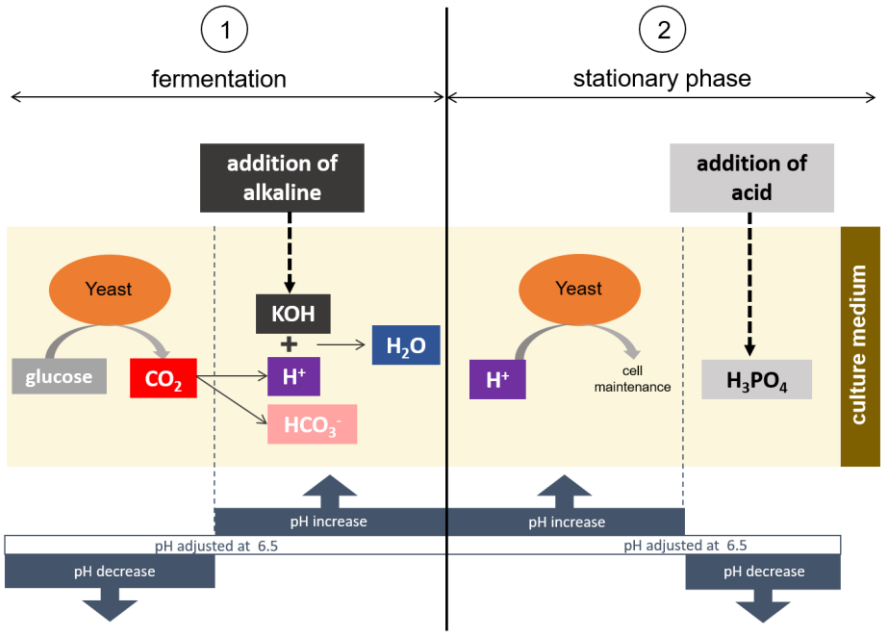

Figure 46. Diagram of pH adjustment to 6.5 by addition of alkaline or acid solution according yeast activity in yeast monoculture using Mix medium.

Using the volume of KOH added to the yeast culture for pH adjustment during yeast monoculture in Mix medium, the concentration of CO_2 produced can be deduced. A KOH

volume of 337 ml was added, and the concentration of the solution was 1 mole. l^{-1}, hence 0.337 mol of KOH was added to 5 liters of working volume in the photo-bioreactor i.e. the concentration of KOH in the culture was 6.7×10^{-2} mole. l^{-1} and was calculated as:

$$[\mathrm{KOH}] = \frac{\mathrm{V}_{KOH}\, C_{\mathrm{KOH}}}{\mathrm{V}_{\mathrm{liq}}} \quad (24)$$

with:
[KOH]: alkaline KOH concentration in the culture medium (mole. l^{-1})
V_{KOH}: volume of KOH added to the culture medium (l)
C_{KOH}: concentration of the KOH solution added to the photo-bioreactor (mole. l^{-1})
V_{liq}: working volume (5 l)

If KOH exclusively reacts with H^+, 6.7×10^{-2} mole. l^{-1} of KOH would have reacted with an equivalent concentration of protons H^+. As 1 mol of proton H^+ came from 1 mol of CO_2, a CO_2 concentration of 6.7×10^{-2} mole. l^{-1} would have been the origin of KOH addition for pH adjustment:

$CO_2 + H_2O \rightarrow H_2CO_3 \rightarrow H^+ + HCO_3^-$ **Reaction 10**

Finally, the CO_2 concentration produced by yeast and that reacted with KOH was 2.97 g l^{-1} and was calculated as:

$$[\mathrm{CO_2}]_{\mathrm{KOH}} = [\mathrm{KOH}]\mathrm{M}_{\mathrm{CO_2}} \quad (25)$$

with:
$[\mathrm{CO_2}]_{\mathrm{KOH}}$: the concentration of CO_2 produced by yeast and reacted with KOH (g. l^{-1})
[KOH]: alkaline KOH concentration in the culture medium (mole. l^{-1})
M_{CO_2}: the CO_2 molar mass (44 g. $mole^{-1}$)

According to Reaction 6, 3.80 g. l^{-1} of CO_2 was produced in yeast monoculture but only 2.97 g. l^{-1} of the CO_2 reacted with H_2O leading to protons H^+ and HCO_3^-, which means that 0.83 g. l^{-1} of CO_2 could have remained in gaseous form and could have passed to the gaseous phase. This is coherent with the overpressure observed during the yeast fermentation process.

4.2 *C. vulgaris* monocultures in aerated photo-bioreactor

Microalgae monocultures in photo-bioreactor were conducted with aeration. This parameter was mandatory in order to supply O_2 and CO_2 to the microalgae as appropriate. In *C. vulgaris* monoculture using Mix medium, microalgae required O_2 for the mixotrophic growth. In microalgae monoculture using the autotrophic medium, *C. vulgaris* needed CO_2 for photo-autotrophic growth. The two monocultures were then supplied with 100% air, composed of 21% of O_2 and 0.035% of CO_2.

The dissolved O_2 and CO_2 were measured continuously in order to evaluate the O_2 uptake rate and the CO_2 biofixation rate by *C. vulgaris*. The O_2 and CO_2 mass balance can be carried out with the volumetric gas transfer K_La.

4.2.1 Study of the CO_2 and O_2 gas transfer in the aerated photo-bioreactor

4.2.1.1 The principle of the volumetric gas transfer coefficient K_La

The K_La is a parameter that allows to quantify the transfer from the gaseous phase to the liquid phase. The determination of the K_La relies on gas measurements as a function of time.

Firstly, the dissolved gases (CO_2 or O_2) in liquid are stripped by vigorously bubbling nitrogen through the liquid phase. Then, a gas mix containing the appropriate O_2 or CO_2 proportions is injected with the same gas flow rate as in microalgae *C. vulgaris* monocultures (500 ml. min^{-1}). The increase in O_2 or CO_2 concentration is followed until saturation value (in equilibrium with gaseous phase).

The gas balance in the liquid phase in a perfectly homogeneous batch culture can be described as:

$$\frac{\mathrm{d[gas]}}{dt} = \mathrm{K_L A}\,([gas]* - [gas]) \tag{26}$$

The integration of the equation gives:

$$\ln \frac{[\mathrm{gas}]* - [\mathrm{gas}]}{[\mathrm{gas}]* - [\mathrm{gas}]_0} = \mathrm{K_L A\,t} \tag{27}$$

where:
[gas]: dissolved gas concentration in the liquid phase (mole. l^{-1})
*[gas]**: maximal gas concentration that can dissolve in the liquid phase (mole. l^{-1}) i.e. gas concentration in equilibrium with gaseous phase-often referred to as saturation
$[gas]_0$: initial dissolved gas concentration in the liquid phase (mole. l^{-1})
K_La: volumetric gas transfer (h^{-1}) with K_L the transfer coefficient and *a* the interfacial area per unit of column volume
t: time (hour)

4.2.1.2 Experimental determination of the volumetric O_2 transfer coefficient K_La

The dissolved O_2 profile was firstly measured over time until equilibrium was established with the gaseous phase. The O_2 concentration was measured in pO_2 (%), percentage of the O_2 partial pressure in the liquid phase. The pO_2 can be converted to O_2 concentration in mol l^{-1} by Henry's law:

$$[O_2] = \frac{pO_2}{H_{O_2}} \quad (28)$$

with:
$[O_2]$: dissolved O_2 concentration in the liquid phase (mole. l^{-1})
pO_2: O_2 partial pressure in the liquid phase (atm)
H_{O_2}: Henry constant for O_2 at 25°C (769.23 atm. L. $mole^{-1}$)

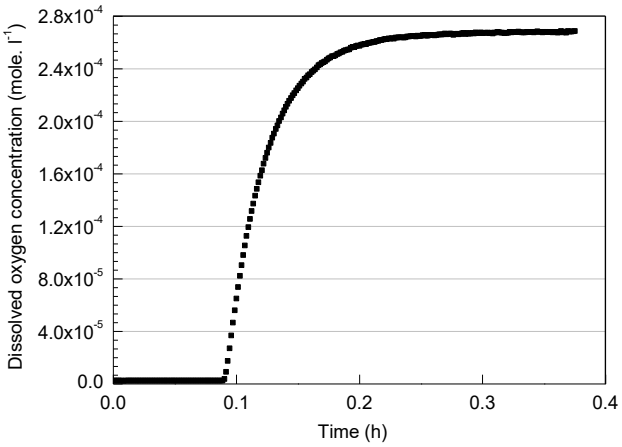

Figure 47. Concentration of dissolved O_2 over time in the photo-bioreactor supplied by air with a flow rate of 500 ml. min^{-1} (0.1 vvm, 1 atm, 25°C).

The K_La for O_2 is obtained from the slope of the linear curve (Figure 48): 29.3 h^{-1}.

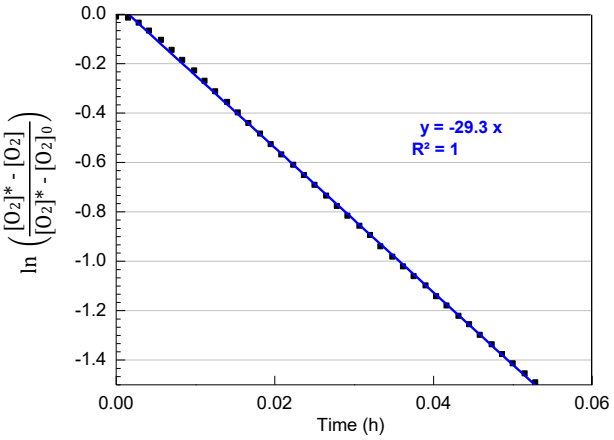

Figure 48. Determination of K_La for O_2.

4.2.1.3 Experimental determination of the volumetric CO_2 transfer coefficient K_La

After degassing the medium with nitrogen, the CO_2 profile was followed over time until equilibrium with the gaseous phase was reached. The CO_2 concentration was measured in pCO_2 (%), percentage of the CO_2 partial pressure in the liquid phase. The pCO_2 can be converted to CO_2 concentration in mol l^{-1} by Henry's law:

$$[CO_2] = \frac{pCO_2}{H_{CO_2}} \quad (29)$$

with:
[CO_2]: dissolved CO_2 concentration in the liquid phase (mole. l^{-1})
pCO_2: O_2 partial pressure in the liquid phase (%)
H_{CO_2}: Henry constant for CO_2 at 25°C (29.41 atm l. $mole^{-1}$)

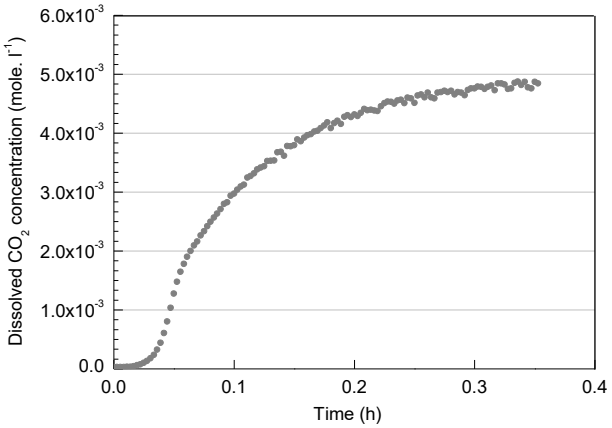

Figure 49. Concentration of dissolved CO_2 over time in the photo-bioreactor supplied by gas mixture composed of 15% of CO_2 and 85% of N with a flow rate of 500 ml min^{-1} (0.1 vvm, 1 atm, 25°C).

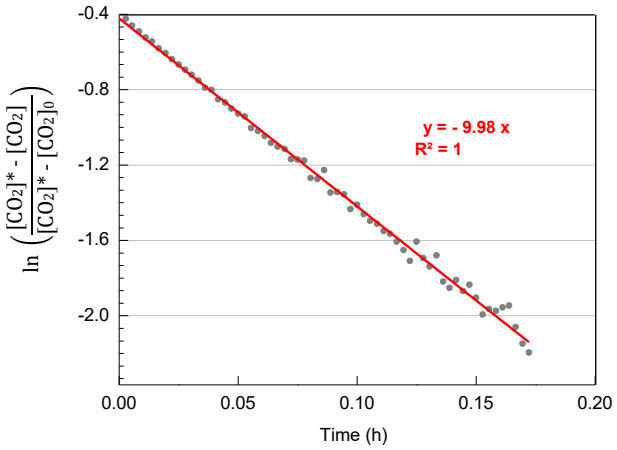

Figure 50. Determination of CO_2 K_La.

The K_La for CO_2 is obtained from the slope of the linear curve (Figure 50): 9.98 h^{-1}.

4.2.1.4 Gas uptake rate from gas concentration data and K_La value

When the gas transfer rate in the liquid phase is known, the O_2 uptake rate OUR or the CO_2 biofixation rate can be determined from equation 30 for OUR and equation 31 for CO_2 biofixation rate (Garcia-Ochoa et al. 2010):

$$\mathrm{OUR} = \mathrm{K_L A}\,([O_2]* - [O_2]) - \frac{d[O_2]}{dt} \qquad (30)$$

with:
OUR: oxygen uptake rate (mol l^{-1} h^{-1}); OUR can also be expressed in gO_2. l^{-1} h^{-1} by multiplying by the O_2 molar mass (32 g. $mole^{-1}$)
$[O_2]$: dissolved O_2 concentration in the liquid phase (mole. l^{-1})
$[O_2]$*: maximal O_2 concentration dissolved in the liquid phase (2.7×10^{-4} mole. l^{-1})
K_La: volumetric O_2 transfer coefficient (28.4 h^{-1})

$$\mathrm{CO_2}\text{ biofixation rate} = \mathrm{K_L A}\,([CO_2]* - [CO_2]) - \frac{d[CO_2]}{dt} \quad (31)$$

where:
CO_2: biofixation rate in mol. l^{-1} h^{-1} and can also be expressed in gCO_2. l^{-1} h^{-1} by multiplying by the CO_2 molar mass (44 g. $mole^{-1}$)
$[CO_2]$: dissolved CO_2 concentration in the liquid phase (mole. l^{-1})
$[CO_2]$*: maximal CO_2 concentration in liquid phase (1.4×10^{-5} mole. l^{-1})
K_La: volumetric CO_2 transfer coefficient (9.98 h^{-1})

4.2.2 Microalgae *C. vulgaris* monoculture using Mix medium

4.2.2.1 Growth study

C. vulgaris was grown on Mix medium in photo-bioreactor in the same way as the *S. cerevisiae* monoculture and, later on, in mixed cultures except that the microalgae monoculture was continuously aerated. Aeration was mandatory for CO_2 provision to *C. vulgaris* for photosynthesis and O_2 supply to microalgae respiration. The pO_2 in the culture was expected to remain stable at 20.9% in the absence of net production or consumption of O_2 by *C. vulgaris*.

During the first 48 hours of *C. vulgaris* growth in Mix medium (Figure 51), the glucose and O_2 concentrations did not decrease while the population increased slightly from 1×10^9 to 1.8×10^9 cells. l^{-1}. The first 48 hours of incubation without any glucose or O_2 consumption was accompanied by a slight amount of cell growth, suggesting photo-autotrophic growth of the organism also reported by Ben Amor-Ben Ayed et al. (2017).

From 48 to 116 hours of incubation, the glucose concentration decreased to complete depletion while the microalgae population increased from 1.8×10^9 to 4×10^{11} cells. l^{-1}.

C. vulgaris grew heterotrophically during this period using glucose and O_2. *C. vulgaris* seems to "privilege" autotrophy as long as the microalgae population is small enough to allow satisfactory light penetration into the photo-bioreactor. After that, *C. vulgaris* seems to have, at least, partly switched to heterotrophic metabolism. Microbial growth leads to an increase in light absorption by the culture and auto-shadowing by the microorganisms (Pfaffinger et al. 2016). The population in the shaded volume (central section of the photo-bioreactor) may have used glucose and O_2 for growth through respiration, while the population in the lit volume (at the edge of the photo-bioreactor and close to the light source) could have grown photo-autotrophically. In a well-mixed culture, as employed in this study, this means that as the average amount of light available to each cell decreases, *C. vulgaris* increasingly progresses towards a more heterotrophic metabolism. The presence of light can also photo-inhibit uptake of glucose by affecting the balance between reduced and oxidized energy carrying molecules (ATP and NADH), because of photosynthetic activity (Perez-Garcia and Bashan, 2015).

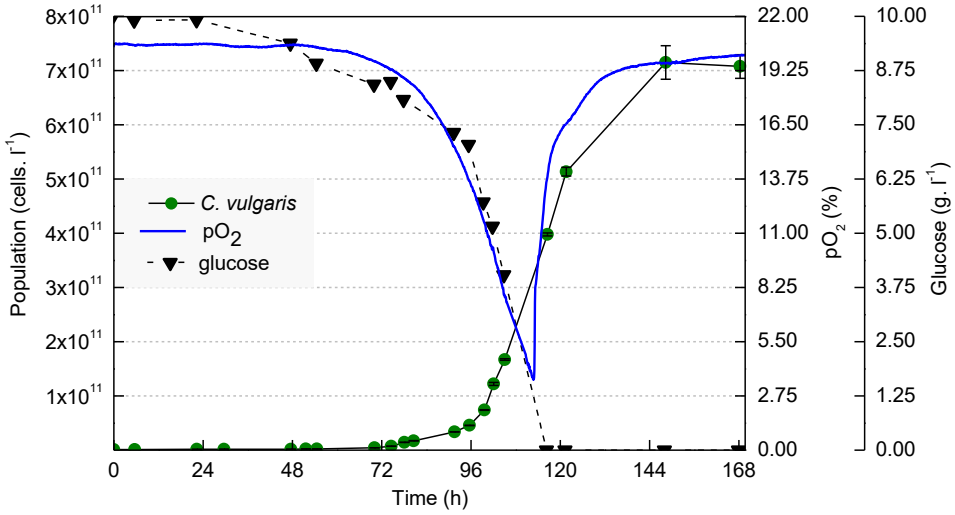

Figure 51. Microalgae growth profile in monoculture using Mix medium in aerated photo-bioreactor.

After 116 hours in incubation, the glucose was depleted and the pO_2 increased until reaching the concentration of saturation. Since glucose was exhausted, no organic carbon source was left to be respired, hence O_2 stopped to be used and the increase in pO_2 was due to the O_2 brought into the bioreactor through continuous aeration. After glucose depletion, *C. vulgaris* grew from 4×10^{11} to 7×10^{11} cells. l^{-1} most likely on photo-autotrophic metabolism as no organic carbon was left in the growth medium, hence the production of O_2 through photosynthesis could have contributed to the increase in pO_2.

The total chlorophyll content can be used as an indicator of the photosynthesis activity of the microalgae culture (Abinandan and Shanthakumar 2016). In microalgae monoculture using Mix medium (Figure 52), the average cell-chlorophyll-content increased at the beginning of the culture, reaching the maximal value of 1.5×10^{-9} mg. cell^{-1} at 48 hours and this occurred in the same period during which no glucose and O_2 were consumed and *C. vulgaris* seemed to have privileged photo-autotrophic growth. After 48 hours of incubation, the average-cell-chlorophyll-content started to decrease at the same time as the beginning of glucose and O_2 consumption, then the total chlorophyll content stabilized from around 120 hours, which corresponded to the end of the microalgae heterotrophy metabolism as glucose was depleted and O_2 stopped to be used. This decrease in total chlorophyll content is coherent with the regulation system of autotrophic-heterotrophic metabolism that involves the inhibition of chlorophyll production by glucose assimilation and through the production of organic carbon uptake enzyme by light source (Ogawa and Aiba 1981; Smith et al. 2015). *C. vulgaris* did not seemed to have adopted a partly photo-autotrophic metabolism during glucose and O_2 utilization.

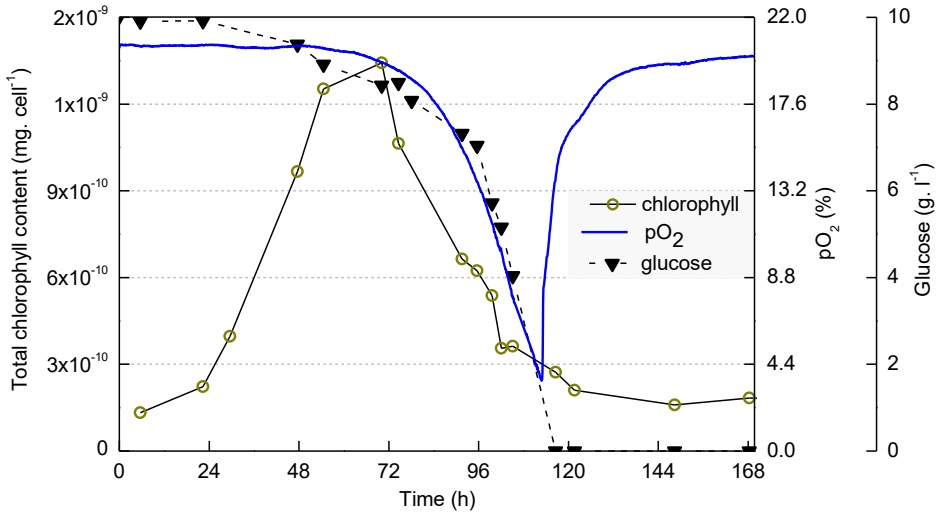

Figure 52. Chlorophyll content, glucose and O_2 concentration in microalgae monoculture using Mix medium in aerated photo-bioreactor.

4.2.2.2 Addition of acid and alkaline solutions for pH adjustment

The addition of acid or alkaline solution for pH adjustment helps to interpret the microorganism's metabolism, as shown for yeast *S. cerevisiae* monoculture (Figure 45). In microalgae monoculture using Mix medium, 5.6 ml of acid solution was added to the culture at the beginning. The alkaline solution was added 37 hours after the beginning of glucose and O_2

uptake and the alkaline addition stopped when glucose was depleted (108 hours) and the addition of acid started 1 hour later (Figure 53).

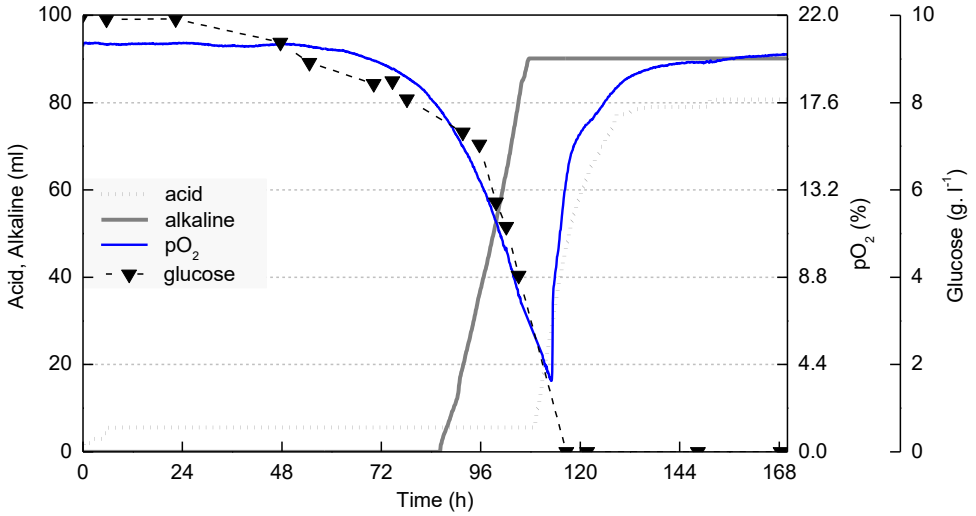

Figure 53. Addition of acid and alkaline solutions to microalgae monoculture using Mix medium for automatic pH adjustment at 6.5.

Figure 54 describes the system of pH adjustment according microalgae growth. The small volume of acid added at the beginning of the culture was coherent with the photo-autotrophic metabolism of *C. vulgaris* during the first 48 hours of incubation. The CO_2 removal from microalgae culture medium led to an increase in pH and to the addition of acid solution for a pH decrease to 6.5.

The alkaline solution was added to the *C. vulgaris* monoculture when the glucose and O_2 concentration entered in a steep linear decrease, leading to a rapid production of CO_2. The CO_2 remaining in the liquid phase, was then hydrated into H_2CO_3 and dissociated to protons H^+ and HCO_3^-, decreasing the pH value. KOH was added to react with the high amount of H^+ to restore the pH value to its set point. Some CO_2 produced by microalgae could also have been stripped out by the continuous aeration.

The acid solution was added after the end of the glucose consumption phase and indicated the beginning of the photosynthetic activity. The pH value increased as CO_2 and HCO_3^- were removed from the culture medium for microalgae photosynthesis and H_3PO_4 was then added to decrease the pH value back to 6.5.

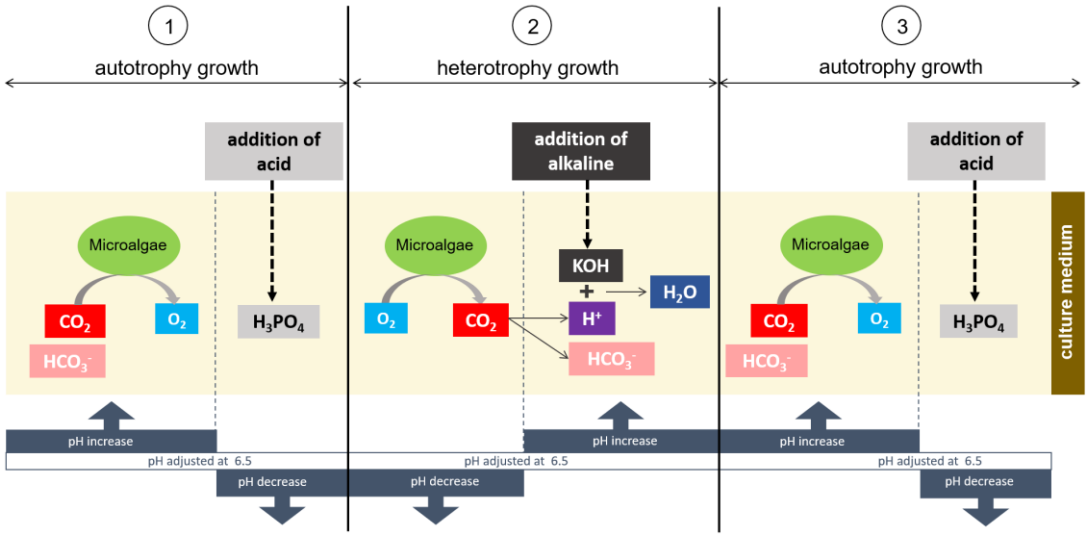

Figure 54. Diagram of pH adjustment to 6.5 by addition of alkaline or acid solution according microalgae activity in monoculture using Mix medium.

4.2.2.3 O_2 uptake rate determination (OUR)

According to equation 30 and from pO_2 data profile over time, OUR could have been calculated (Figure 55). The average microalgae OUR was 0.204 gO_2. l^{-1} h^{-1} and the period of oxygen uptake lasted 53 hours (Figure 51), hence 10.8 g. l^{-1} of O_2 was consumed to respire glucose in microalgae monoculture using Mix medium.

According to the global reaction of cellular respiration on glucose, the respiration of 1 mole of glucose requires 6 moles of O_2:

$C_6H_{12}O_6 + 6O_2 \rightarrow 6\ CO_2 + 6H_2O$ **Reaction 11**

In microalgae monoculture, 10 g. l^{-1} of glucose was used by *C. vulgaris*, corresponding to 0.056 mole. l^{-1}, hence 0.333 mole. l^{-1} of O_2 was required, the equivalent of 10.66 g. l^{-1} of O_2. The concentration of the O_2 consumed calculated from OUR is closed to the O_2 concentration required for glucose respiration, so no additional O_2 was provided to the culture medium, which strongly suggests that *C. vulgaris* did not have photosynthesis activity while using respiring. Consequently, *C. vulgaris* did not mixed autotrophic and heterotrophic metabolisms but only grew using heterotrophy from 48 to 113 hours of incubation.

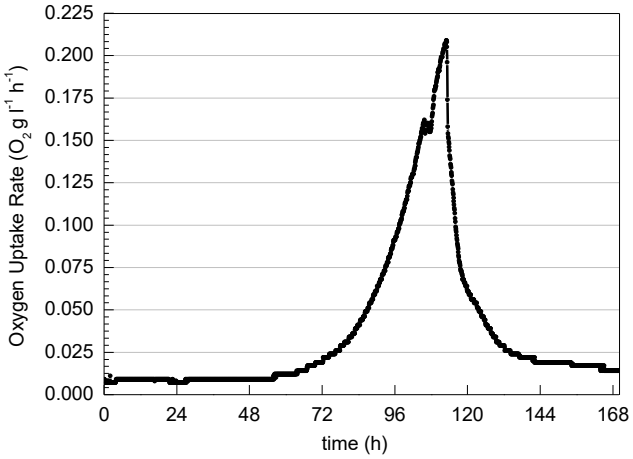

Figure 55. Oxygen Uptake Rate OUR from microalgae monoculture using Mix medium in aerated photo-bioreactor.

The exponential phase of *C. vulgaris* in monoculture was then composed of two successive growth stages: a heterotrophy growth stage (48 to 113 hours) and an autotrophy growth stage (113 to 125 hours). Both growth stages formed the mixotrophic growth with a μ of 0.09 h^{-1} which is high compared to μ from mixotrophic cultures of microalgae reported by Perez-Garcia and Bashan (2015) (μ range from 0.01 h^{-1} to 0.04 h^{-1}).

4.2.3 Microalgae *C. vulgaris* monoculture using autotrophic MBM medium (without glucose and peptone)

4.2.3.1 Metabolism study

C. vulgaris grew on autotrophic medium in photo-bioreactor in the same way as *S. cerevisiae* in monoculture and as mixed cultures except that the microalgae monoculture was continuously aerated. Aeration was required for CO_2 provision to *C. vulgaris* for photosynthesis and O_2 supply to microalgae respiration. The pO_2 in the culture was expected to remain stable at 20.9% in the absence of net production or consumption of O_2 by *C. vulgaris*.

The medium used for this microalgae monoculture was the autotrophic MBM medium without glucose and peptone (Figure 56). The microalgae firstly grew exponentially (μ=0.04 h^{-1}) until around 72 hours, increasing the population from 1.95×10^9 to 1.27×10^{10} cells. l^{-1} accompanied with an increase in pO_2. Starting from a value of 21%, the pO_2 reached 22% at the end of the exponential growth phase then it continued to increase up to 22.3% and remained constant at the same level. Running parallel, pCO_2 showed an opposite profile. The

pCO_2 decreased when the pO_2 increased and they both remained constant at the same time, which suggests microalgae photosynthesis activity. After the exponential growth phase, the growth was almost linear until the end of incubation.

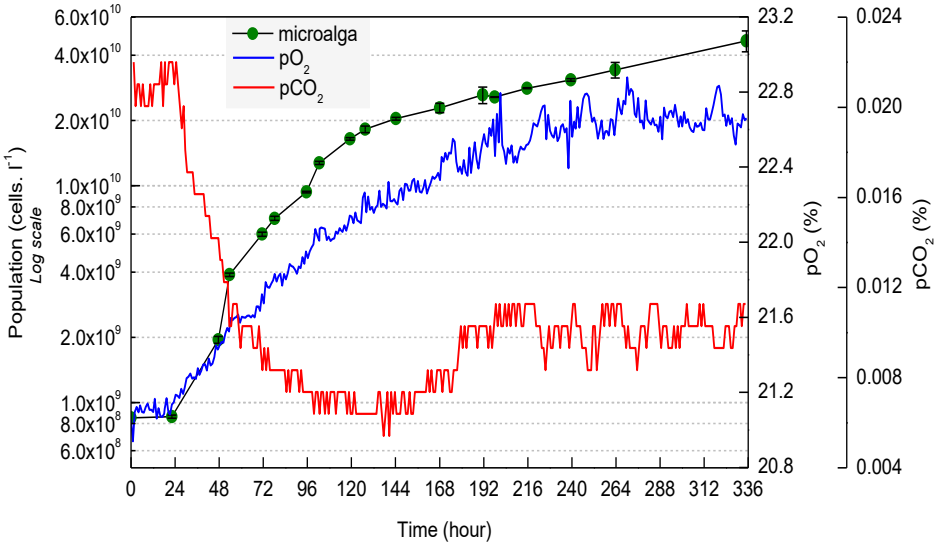

Figure 56. Microalgae growth profile in monoculture using autotrophic MBM medium in aerated photo-bioreactor.

In this microalga photo-autotrophic monoculture, there was no organic substrate (absence of glucose and peptone), hence *C. vulgaris* grew purely on photo-autotrophic metabolism using photosynthesis. Under these conditions, microalgae developed by using light energy and CO_2 in the culture medium as carbon source, resulting in biomass formation and production of O_2. The pO_2 increased up to 22.3% and this is a significant level of O_2 production considering the continuous flow of the air through the photo-bioreactor and the cell concentration in the culture, which means a high microalgae photosynthetic activity. However, the constant pO_2 value at 22.3%, above the saturation value and the almost linear growth, suggest that the *C. vulgaris* photosynthesis activity was limited by a growth limiting factor. CO_2 is a key factor for the photosynthesis process and it was supplied continuously at low concentration, hence CO_2 is likely to have been the growth limiting factor in this microalga photo-autotrophic monoculture.

4.2.3.2 Impact of CO_2 limitation on microalgae growth

The exponential growth occurred while pCO_2 decreased (Figure 56). In this monoculture, *C. vulgaris* grew using photosynthesis, hence the decrease in pCO_2 corresponded to CO_2 biofixation by microalgae. When the evolution of pCO_2 remained stable, the exponential growth phase stopped (96 hours), indicating that the microalgae growth was limited by CO_2 availability.

Despite the beginning of CO_2 limitation, *C. vulgaris* continued to grow linearly thanks to the CO_2 supply through continuous aeration. The microalgal population in the lit volume (at the edge of the photo-bioreactor and closed to the light source) still could have access to light, allowing CO_2 uptake from culture medium and the pCO_2 remained below the value corresponding to the equilibrium with the gaseous phase. The linear phase is also accompanied by a O_2 production, maintaining the pO_2 above equilibrium with the gaseous phase (20.9%).

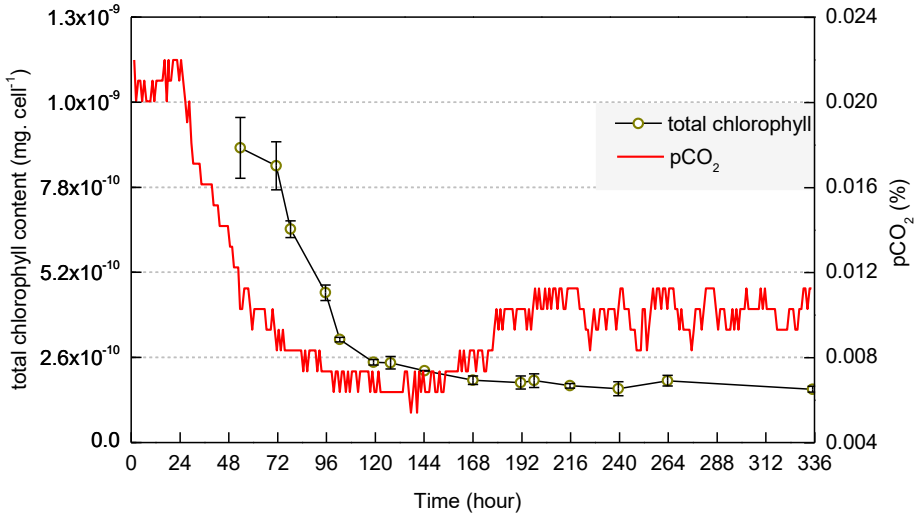

Figure 57. Total chlorophyll content and dissolved CO_2 concentration profiles in microalgae photo-autotrophic monoculture.

As CO_2 limitation influenced *C. vulgaris* growth in photo-autotrophic monoculture, it also had an impact on the total chlorophyll production. The evolution of pCO_2 was concomitant with that of total chlorophyll content: the total chlorophyll content decreased until a minimal value of around 2.4×10^{-10} mg. cell^{-1}, reached when the decrease in pCO_2 stopped (96 hours). Chlorophyll is responsible for the absorption of light energy and its conversion into chemical energy via photosynthesis in algae (da Silva Ferreira and Sant'Anna 2017), therefore the production of chlorophyll decreased because less energy was required to fix CO_2, as the latter became limited.

4.2.3.3 Addition of acid and alkaline solutions for pH adjustment

During *C. vulgaris* growth in the photo-autotrophic monoculture, acid solution was added constantly (Figure 58). The Figure 58 describes the system of pH adjustment in relationship with microalgae growth. *C. vulgaris* grew exclusively on autotrophic metabolism consuming

CO_2 (acid) and the CO_2 removal from the culture medium increased the pH value. The acid solution H_3PO_4 was then added to decrease the pH back to the set point of 6.5.

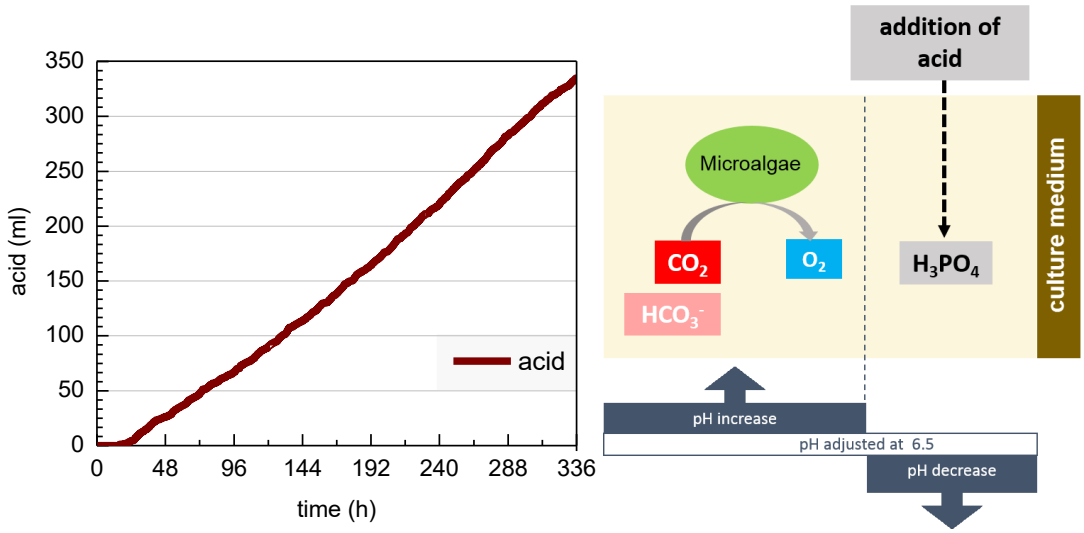

Figure 58. (A) Addition of acid solution to microalgae monoculture using autotrophic MBM medium for automatic pH adjustment at 6.5. (B) Diagram of pH adjustment to 6.5 by addition of alkaline or acid solution according microalgae activity.

4.2.3.4 CO_2 biofixation in microalgae photo-autotrophic monoculture

The CO_2 biofixation rate in microalgae photo-autotrophic monoculture (Figure 59) was calculated over time from equation 30 and from the pCO_2 data profile.

The average CO_2 biofixation rate during microalgae exponential phase was 0.0022 $gCO_2.\ l^{-1}\ h^{-1}$, with a maximal CO_2 biofixation rate of 0.0024 $gCO_2.\ l^{-1}\ h^{-1}$ reached at the end of the exponential phase (96 hours). In Scragg et al. (2002) the CO_2 biofixation rate by *C. vulgaris* was also 0.002 $gCO_2.\ l^{-1}\ h^{-1}$ and microalgae grew in similar conditions as in our *C. vulgaris* photo-autotrophic monoculture as the medium composition was similar and the bioreactor was supplied with air without any addition of CO_2. The CO_2 biofixation rate by *C. vulgaris* can be increase to more than 10 times with CO_2 enrichment to the culture medium. The CO_2 biofixation rate was 0.023 $gCO_2.\ l^{-1}\ h^{-1}$ in a *C. vulgaris* culture enriched with 8% of CO_2 (Adamczyk et al. 2016) and 0.033 $gCO_2.\ l^{-1}\ h^{-1}$ with 13% of CO_2 (Clément-Larosière et al. 2014).

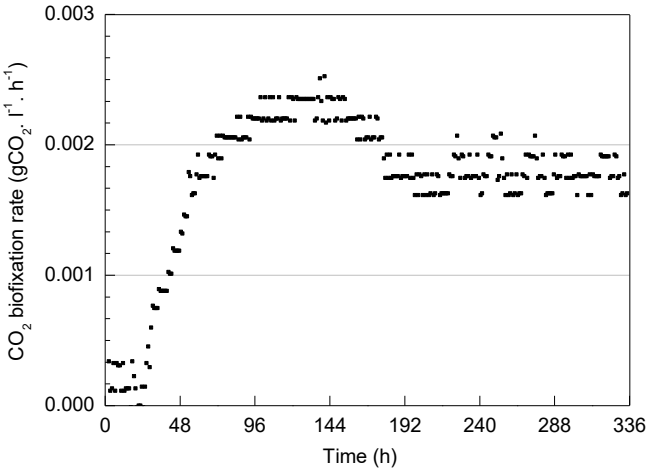

Figure 59. CO_2 biofixation rate from microalgae photo-autotrophic monoculture using Mix medium in aerated photo-bioreactor.

The CO_2 biofixation calculated from the *C. vulgaris* photo-autotrophic monoculture was coherent with the *C. vulgaris* biomass composition in carbon element. During the first 96 hours of incubation, 0.21 g. l^{-1} of CO_2 was consumed by microalgae corresponding to 5.7×10^{-2} g. l^{-1} of carbon assimilated. The microalgal population grew by 1.2×10^{10} cells. l^{-1} corresponding to 0.13 g. l^{-1} of DW. According to Table 8, the carbon content of *C. vulgaris* is 46% (w/w) (Table 8), hence 6×10^{-2} g. l^{-1} of carbon was required to form the microalgae biomass. Carbon element that composed the microalgal biomass came from assimilated CO_2 from the aeration as it was the only carbon source for *C. vulgaris*, hence we can deduce that 0.22 g. l^{-1} of CO_2 was assimilated by microalgae and this value is in accordance with the value calculated from the CO_2 biofixation rate.

Table 8. Composition of 0.13 gDW l^{-1} microalgae at the end of the exponential phase according CHN/O analysis results.

Element	C carbon	H hydrogen	N nitrogen	O oxygen
Content (% w/w)	46	6.7	8	32.5
Concentration (mole. l^{-1})	5×10^{-3}	8.7×10^{-3}	7.4×10^{-4}	2.6×10^{-3}
Concentration (g. l^{-1})	6×10^{-2}	8.7×10^{-3}	1×10^{-2}	4.2×10^{-2}

From Table 8, the elemental composition of 100 gDW of *C. vulgaris* would be $C_{3.8}H_{6.7}N_{0.57}O_2$ and the composition for 26 gDW of *C. vulgaris* can be deduced as

$C_1H_{1.8}N_{0.15}O_{0.53}$, which is coherent the microalgae composition from Scherholz and Curtis 2013 ($C_1H_{1.78}N_{0.165}O_{0.495}$).

4.3 Conclusion

Yeast *S. cerevisiae* and microalga *C. vulgaris* did not use glucose during the same time frame when grown alone in monoculture containing Mix medium. Glucose was fully used by yeast within the first 24 hours of culture while microalgae started to use the carbohydrate from 48 hours of incubation. This suggests that *C. vulgaris* would not use any glucose if both microorganisms grew together in the same mixed culture using Mix medium, so in mixed culture *C. vulgaris* should grow autotrophically and *S. cerevisiae* should grow fermentatively on glucose. Consequently, the yeast monoculture using Mix medium and the microalgae monoculture using autotrophic MBM medium were used as reference cultures for the mixed culture of yeast and microalgae in Mix medium.

CO_2 was the first limiting factor of *C. vulgaris*. CO_2 limitation increases with microbial growth, hence microalgae growth in mixed culture might be altered with yeast growth. Addition of acid or alkaline solution for pH adjustment to 6.5 seems to be a reliable indicator of yeast and microalgae activity by highlighting CO_2 production or consumption and also allows to estimate the amounts of this compound produced/used. The comparison of the pH adjustment process in the yeast and in the microalgae, monocultures should contribute in the evaluation of the proportion of CO_2 released by yeast and subsequently reused by microalgae in mixed culture.

Chapter 5. Mixed culture in closed photo-bioreactor

This chapter presents results of two mixed cultures in photo-bioreactor. The mixed cultures were performed using the newly designed medium (Chapter 3) and *S. cerevisiae* and *C. vulgaris* growth were followed thanks to the enumeration method presented in Chapter 3. The mass balances and the growth kinetics in yeast and microalgae monocultures were compared to mixed cultures in order to identify the interactions between *S. cerevisiae* and *C. vulgaris* in mixed culture. A method for simultaneous and accurate enumeration of the two species in a mixed suspension is also presented.

Contents

5.1 Method for simultaneous enumeration of yeast and microalgae

As a first step, the suitability of the Guava easyCyte™ for the enumeration of *S. cerevisiae* and *C. vulgaris* was tested using shake-flask monocultures of each organism. Each culture was diluted to different concentrations to provide samples for the enumeration. In the absence of a better method, microscopic cell concentration determination was used as a reference method. Cell concentration were determined by flow cytometry, correlated with those made using the Thoma Chamber for both organisms, *S. cerevisiae* and *C. vulgaris,* with a slope of 1 and correlation coefficients of 0.98 and 0.99 respectively (Figure 60). These values confirmed that the method for cell counting with Guava easyCyte™ flow cytometer was valid.

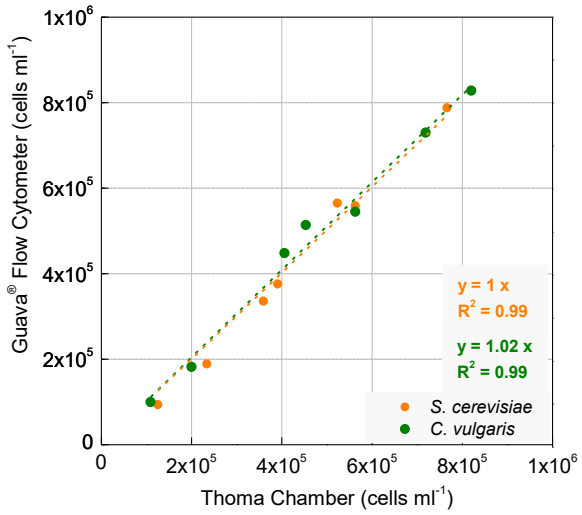

Figure 60. Correlation between two methods for cell counting *S. cerevisiae* and *C. vulgaris* in monoculture.

As a second step, the suitability of the flow cytometer was tested for detecting and discriminating yeast and microalgae in mixed suspensions. The flow cytometer is able to measure the relative size of the cells (detection of forward scatter), to provide information about their internal complexity (detection of side scatter) and the intensity of their autofluorescence detection. The discrimination of *S. cerevisiae* and *C. vulgaris* based on forward and side scatter provided the total cell concentration of the suspension but the distinction of the two populations was weak (Figure 61B). The strategy for a complete discrimination of *S. cerevisiae* and *C. vulgaris* in mixed suspensions with flow cytometer was based on their autofluorescence and relative size. The blue laser (488 nm) of the flow cytometer allowed the excitation of both the GFP protein in the yeast cytoplasm and the chlorophyll in the microalgae. The two molecules emit distinct fluorescence at 510 and 600-700 nm respectively allowing the organisms to be distinguished from one another (Figure 61A). The acquisition according the red/green

fluorescence and the cell relative size allowed clear distinction of the two populations and simultaneously enumerate (Figure 61C and D).

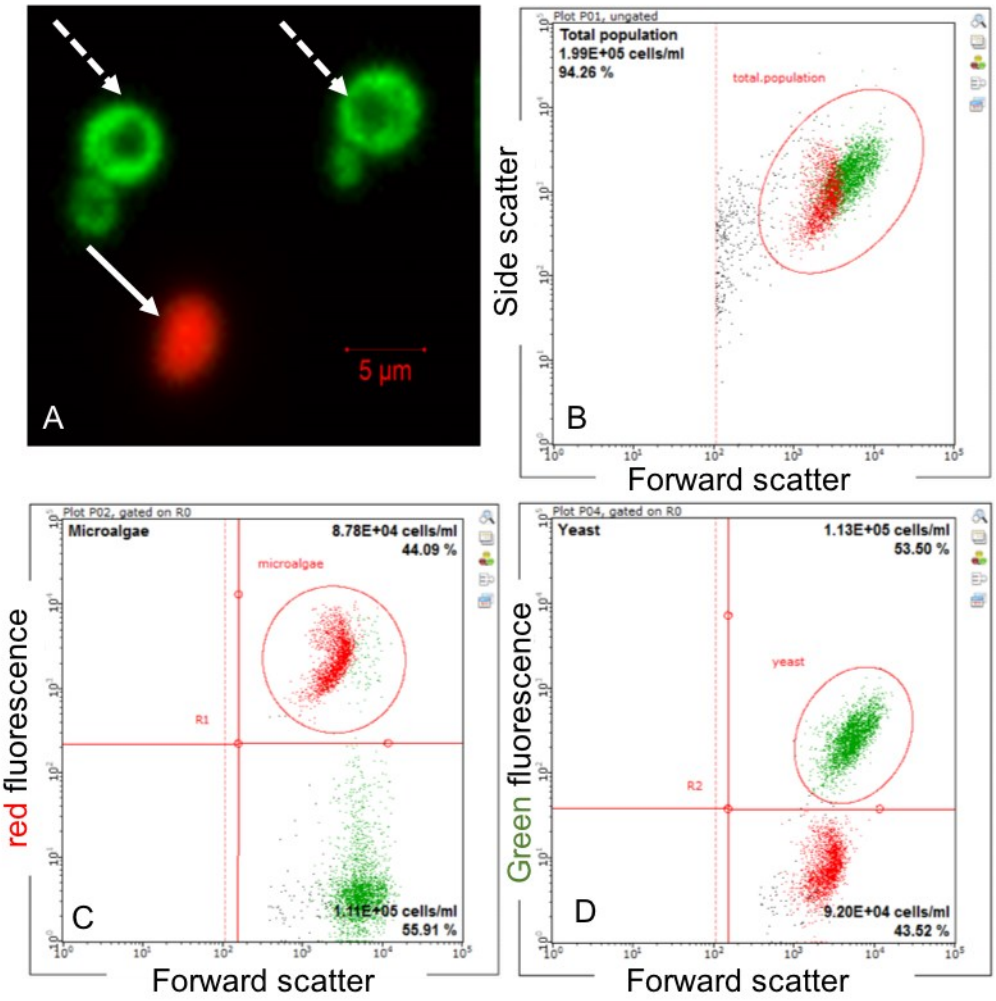

Figure 61. (A) S. *cerevisiae GFP* (dashed arrows) and *C. vulgaris* (solid arrows) cells observation with confocal microscope Zeiss LSM 700 (x20). A 488nm-UV diode laser was used for illumination. GFP protein and chlorophylls fluorescence were captured through a band pass filter at a wavelength of 493−550nm and 615-800nm respectively (B) Screenshot of flow cytometer acquisition; cell complexity versus cell relative size (C) Screenshot of flow cytometer acquisition; red fluorescence versus cell relative size (D) Screenshot of flow cytometer acquisition; green fluorescence versus cell relative size.

To validate the method, eleven mixed suspensions were prepared to obtain different precise yeast:microalgae ratios (calculated ratios) and the two populations in the mixed suspensions were measured with flow cytometry (experimental ratios). By plotting the experimental microalgae ratio as a function of the calculated microalgae ratio (Figure 62A), a

linear relationship was obtained with a slope of 1.048 and a correlation coefficient of 0.997, validating our method for cell counting microalgae from yeast in mixed suspensions.

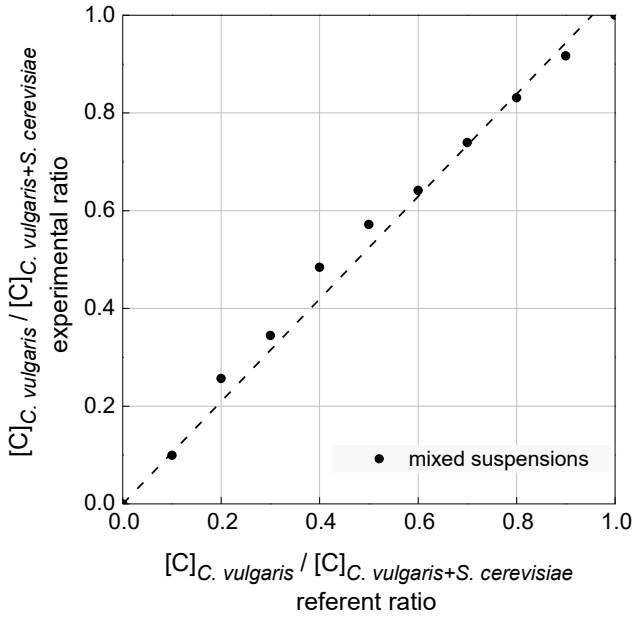

Figure 62. (A) Correlation between experimental (flow cytometry) and calculated *C. vulgaris* proportion in 11 mixed suspensions.

In this study, the *S. cerevisiae* strain was chosen the fluorescence of its GFP protein. For any other studies where the heterotroph would not express any fluorescent molecule, the autotroph autofluorescence from chlorophyll should be enough to distinguish and cell count each population. The heterotroph population could be calculated by subtracting the autotroph population from the total population.

5.2 Definition of yeast:microalgae inoculum ratio for mixed culture

The specific growth rate μ of *S. cerevisiae* and *C. vulgaris* measured from reference monocultures (Chapter 4), were used to define the inoculation microalgae:yeast ratio in mixed culture. The μ of microalgae was smaller than that of *S. cerevisiae* (0.27 and 0.02 h^{-1} respectively) so the inoculation microalgae:yeast ratio was calculated as below to minimize dominance of yeast and favor microalgae growth:

$$X_{0C.vulgaris} = \frac{X_{0S.cerevisiae}\, exp(\mu_{S.cerevisiae} t)}{exp(\mu_{C.vulgaris} t)} \quad (32)$$

with:
$N_{0C.vulgaris}$: initial *C. vulgaris* population
$N_{0S.cerevisiae}$: initial *S. cerevisiae* population (2×10^7 cells. l^{-1})
$\mu_{S.cerevisiae}$: *S. cerevisiae* specific growth rate (0.27 h^{-1})
$\mu_{C.vulgaris}$: *C. vulgaris* specific growth rate (0.04 h^{-1})
t: duration of the *S. cerevisiae* exponential phase (13.5 hours)

5.3 Impact of microalgae inoculum preparation

Two mixed cultures were conducted in order to study the impact of microalgae inoculum preparation on the evolution of mixed culture was studied. In mixed culture 1, the microalgae inoculum was prepared in the Mix medium while in the mixed culture 2, it was prepared in photo-autotrophic conditions using the autotrophic MBM medium. The two mixed cultures only differed in the microalgae inoculum preparation. All other conditions including the microalgae:yeast inoculum ratio was identical and Mix medium was the growth medium used in both PBR cultures.

The microalgae inoculum preparation influenced on the yeast and microalgae yield (Figure 63). Yeast and microalgae yield in mixed culture 1 were similar to that in respective monoculture but both yeast and microalgae yields decreased in mixed culture 2 for which the microalgae inoculum was prepared in autotrophic MBM medium. In the latter, the microalgae yield was 3 times lower than that in mixed culture 1 and microalgae monoculture.

Therefore, the preparation of microalgae inoculum in Mix medium did not impact on *S. cerevisiae* or *C. vulgaris* yield in mixed culture while the preparation in autotrophic MBM medium decreases both yeast and microalgae yield in mixed culture. The way the microalgae inoculum preparation impacted on the two population yields in mixed culture remains unclear at this stage, but the following sections provide clarification.

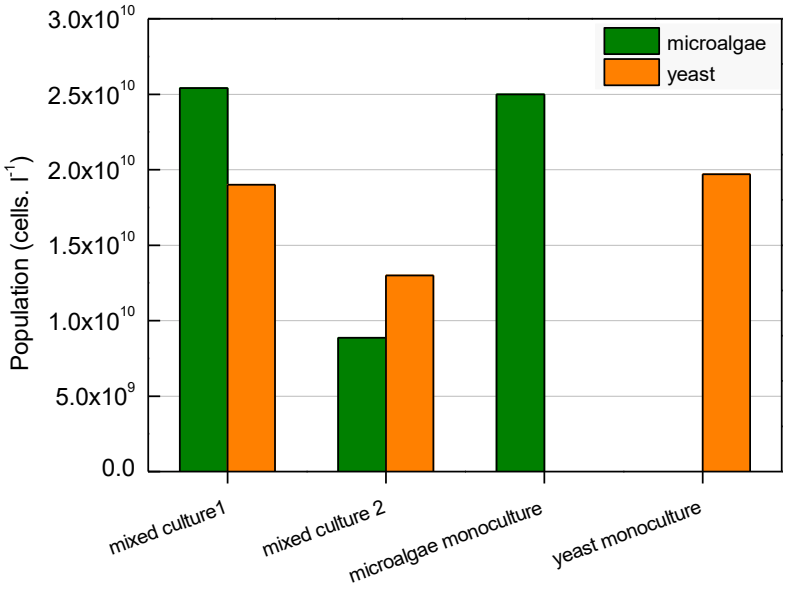

Figure 63. Maximal yeast and microalgae population reached in mixed cultures and yeast and microalgae reference culture in PBR. For mixed culture 1, the microalgae inoculum was prepared using Mix medium and in mixed culture 2 it was prepared in autotrophic MBM medium. The maximal microalgae population in microalgae reference culture corresponds to that at 168 hours of incubation.

5.4 Yeast and microalgae growth in mixed culture in photo-bioreactor

The mixed culture 1 and 2 were conducted in closed and non-aerated photo-bioreactor in order to favor *in situ* gas exchange. The bioreactors were fitted with the equivalent to fermentation lock and the automatic adjustment of the pH with the addition of KOH limited gaseous CO_2 production.

For the mixed culture 1, both the yeast and the microalgae inocula were prepared in the Mix medium (Figure 64), i.e. the medium used for the photo-bioreactor culture. *S. cerevisiae* in mixed culture 1 behaved in the same way as in yeast reference monoculture (Chapter 4) in terms of maximum population, specific growth rate, and ethanol productivity. *C. vulgaris* started to grow from the beginning of incubation period, and without a lag phase, until 24 hours and reached a maximum population of 2.4×10^{10} cells. l^{-1}, then its population remained stable until the end of the experiment. The same population concentration for both organisms was achieved in this mixed culture 1 (around 2×10^{10} cells. l^{-1}), hence co-dominance was reached. This behavior suggested that there was no interference of *C. vulgaris* on *S. cerevisiae* as the latter behaved as it had done in monoculture.

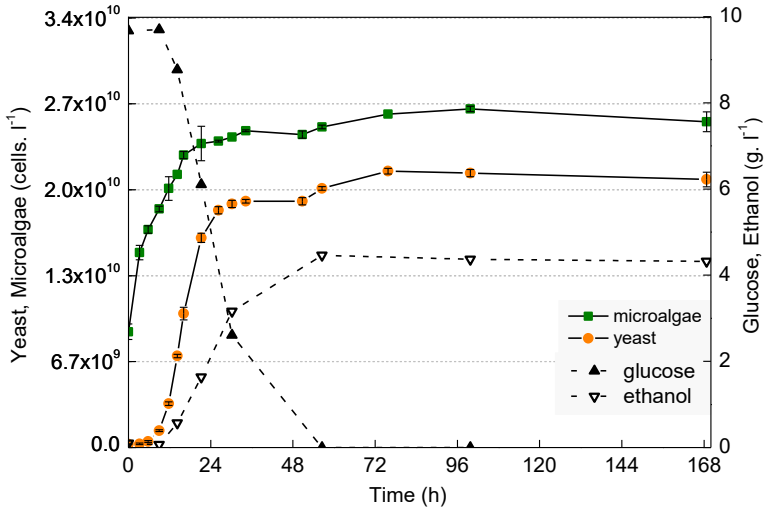

Figure 64. Mixed culture 1 of *C. vulgaris* and *S. cerevisiae* in closed and non-aerated PBR using MBM-GP medium. The yeast and microalgae inocula were both prepared in Mix medium.

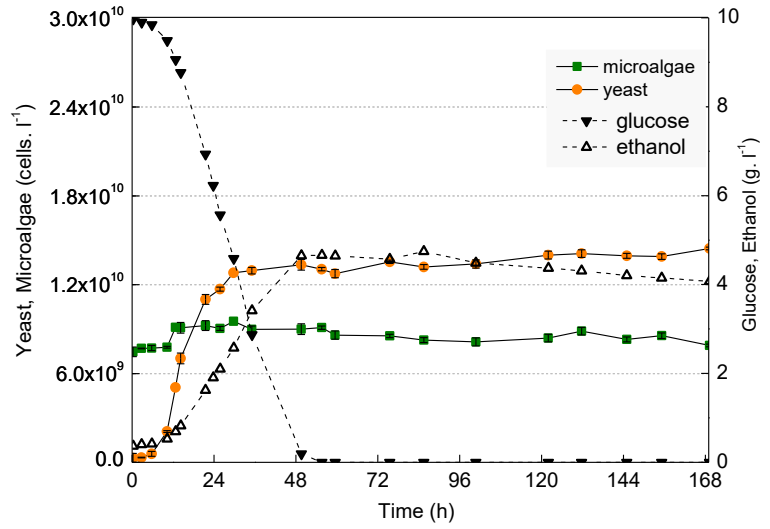

Figure 65. Mixed culture 2 of *C. vulgaris* and *S. cerevisiae* in closed and non-aerated PBR using Mix medium. The yeast inoculum was prepared using Mix medium while the microalgae inoculum was prepared using autotrophic MBM medium.

In the mixed culture 2, the yeast inoculum was prepared in the Mix medium while the microalgae inoculum was prepared in autotrophic MBM medium (Figure 65); in other words, the media used for the growth of the inocula and the photo-bioreactor culture were different. The yeast population yield was lower than in mixed culture 1 (Figure 64) and in the reference

yeast monoculture (1.3×10^{10}, 1.8×10^{10}, 1.9×10^{10} cells. l^{-1} respectively). The *C. vulgaris* growth in this mixed culture 2 was low compared to the mixed culture 1 and the reference microalgae monoculture (Chapter 4). The microalgae population only slightly increased from 7×10^{9} to 9×10^{9} cells. l^{-1} within the first 13 hours and remained mainly constant until the end of incubation (168 hours). The yeast and microalgae maximal population were similar but the mixed culture 2 could not be considered as a co-dominant since the majority of the microalgae population corresponds to the microalgae inoculum.

As the non-interference of the two organisms in mixed culture had been previously observed (mixed culture 1), this behavior is likely due to competition for nutrients between the two organisms. In both mixed culture 1 and 2, the glucose was completely assimilated within the first 48 hours as it had been observed in the reference yeast monoculture (Chapter 4). Despite the lower yeast population yield in mixed culture 2, the ethanol yield coefficient on glucose was the same for the two mixed cultures and for the yeast reference monoculture (Figure 66), which could indicate the same fermentation activity as also observed in Chapter 3. The observed ethanol production rate and glucose uptake rate for the three cultures supports the hypothesis that the fermentation activity was the same in the three cultures (Figure 66) hence, the glucose was only used by yeast in both mixed cultures. Since no glucose was available for the microalgae, *C. vulgaris* grew fully photosynthetically in both mixed culture 1 and 2.

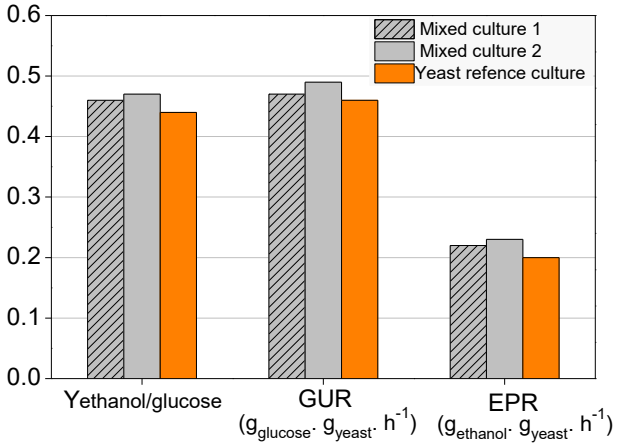

Figure 66. Ethanol yield coefficient on glucose Yethanol/glucose, ethanol production rate (EPR) and glucose uptake rate (GUR) in mixed culture 1 and 2 and yeast reference monoculture.

According to Chapter 3, peptone components (NH_4^+, individual amino acids and small peptides) were the first limiting yeast growth factor when using Mix medium. In mixed culture 2, the yeast population yield decreased in other words, yeast assimilated less nitrogenous components from peptone than in mixed culture 1. Surprisingly, this statement suggests that the

preparation of the microalgae inoculum in autotrophic MBM medium lead to a decrease in yeast growth. Nitrogenous components from peptone might have been shared between yeast and microalgae, which would explain why yeast assimilated less of the peptone components and the decrease in yeast yield in mixed culture 2.

The sharing of peptone components in mixed culture 2 provided more nitrogen sources available to microalgae (in addition to nitrate), hence the *C. vulgaris* population yield should have increased or at least reached the same level as microalgae monoculture if it consumed some of the peptone components (Chapter 3). However, the inverse effect was observed: the microalgae population yield in mixed culture 2 was lower than in microalgae reference monoculture. It seems that the assimilation of components of peptone lowered the microalgae population yield.

5.5 Interactions between yeast and microalgae

5.5.1 Nitrogen source sharing

The principal nitrogen sources in Mix medium are individual amino acids, small peptides (one to three units) and ammonium from peptone and nitrate added in the form of salt. Nitrogenous components from peptone and nitrate were only available to the microalgae and amino acids were the preferential nitrogen sources for yeast.

The peptone concentration was the first limiting growth factor for yeast as demonstrated in Chapter 3: the lower the peptone concentration, the lower the FAN (free amino nitrogen), the lower the yeast growth. In mixed culture 1 and yeast reference monoculture, the yeast yield was identical, which means that in both cultures, yeast used the same amount of amino acids from peptone, i.e. none was shared with microalgae.

The lower yeast growth observed in mixed culture 2 compared to the yeast reference monoculture implied that *S. cerevisiae* most probably assimilated only part of amino acids from peptone that it would otherwise have consumed in the reference monoculture. The other part would have been available to the microalgae but the maximal microalgae population in mixed culture 2 was still 2.8 times lower than in mixed culture 1 and in microalgae reference culture (in which *C. vulgaris* did not grow on peptone). As explained in Chapter 2, the peptone was not the microalgae limiting growth factor since *C. vulgaris* had also access to nitrate.

According to Scherholz and Curtis (2013), when microalgae grow in a medium containing ammonium, nitrate and amino acids, the microalgae firstly use ammonium, preventing the nitrate assimilation and they start using nitrate as soon as ammonium is depleted (Figure 67). They also noted that the apparent yields on nitrogen are much lower for ammonium than for nitrate (7.13 gDW/gN-NH_4^+ and 14.5 gDW/gN-NO_3^- respectively). They explained that the ammonium accumulation within the cell for reserve was preferred over its use for growth, yielding a lower biomass. In mixed culture 2 and during *C. vulgaris* growth (first 12 hours), the amount of nitrate used was almost zero, therefore, this weak microalga growth was probably due to the use of ammonium from peptone.

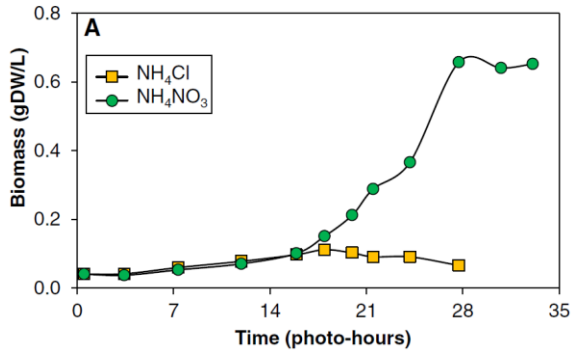

Figure 67. Photoautotrophic *C. vulgaris* cultures were grown in 1.5-L loop air-lift photobioreactors on 0.0135 gN-$NH4^+$. l^{-1} with chloride and nitrate as the counter-ions. The reactor was supplemented with 5% CO_2 (v/v) in air. The optical density was measured at 550 nm at 3 to 4 hours intervals and was converted to biomass density using a ratio of 0.52 g_{DW}/L/OD_{550}. This graph and the caption were directly taken from Scherholz and Curtis (2013).

In mixed culture 1, microalgae grew exclusively on nitrate from the beginning of the culture in PBR and this is confirmed by the fact the microalgae yield on N-NO_3 (nitrogen from NO_3) in mixed culture 1 was similar to that in microalgae reference monoculture (12 gDW/gN-NO_3^- and 10.4 gDW/gN-NO_3^- respectively): in the latter there was no peptone, so nitrate was the only source of nitrogen (Figure 68). These specific yield coefficients were also coherent with those in Scherholz and Curtis (2013) and Liao et al. (2017) (14.5 and 15.9 gDW/gN-NO_3^- respectively). This statement is coherent with the fact that in mixed culture 1, components from peptone were exclusively used by yeast. Consequently, microalgae grew only on nitrate and yeast on the nitrogenous components present in the peptone. Competition for nitrogen between the two organisms was hence avoided in mixed culture 1.

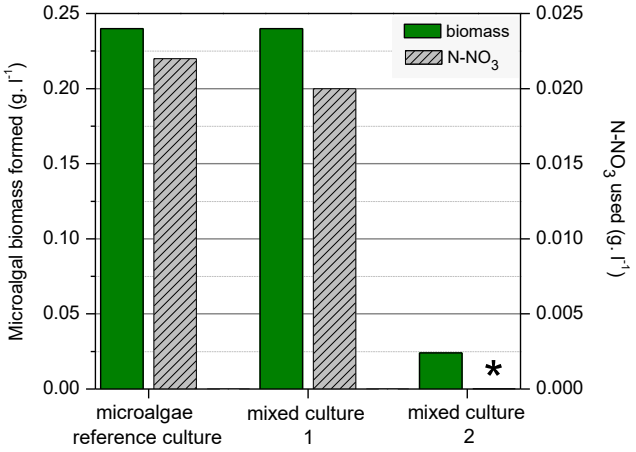

Figure 68. Maximal microalgal biomass formed and nitrate used in mixed culture 1 and 2, and microalgal biomass formed and nitrate used at 120 hours in microalgae reference culture. * means that no nitrate was used.

As the two mixed cultures only differed in the microalgae inoculum preparation (in Mix medium or autotrophic MBM medium), it seems that the latter impacted on the utilization or not of ammonium from peptone by *C. vulgaris*. The microalgae inoculum from mixed culture 1 was prepared in Mix medium, already adapted to the presence of nitrate, ammonium and amino acids, possibly avoiding the repression of nitrate assimilation by ammonium and resulting in microalgae growth exclusively on nitrate from the beginning of the culture in PBR. In mixed culture 2, the microalgae inoculum was prepared in autotrophic MBM medium, hence *C. vulgaris* was not adapted to the presence of ammonium in Mix medium. This first contact with ammonium repressed the utilization of nitrate in favor of a microalgae growth on ammonium and amino acids, lowering the microalgae population yield and that of yeast as less amino acids were available.

Mixed cultures in closed shake flasks were conducted to confirm that the competition of nitrogen was avoided when *C. vulgaris* inoculum was prepared in Mix medium as for mixed culture 1 (Figure 69).

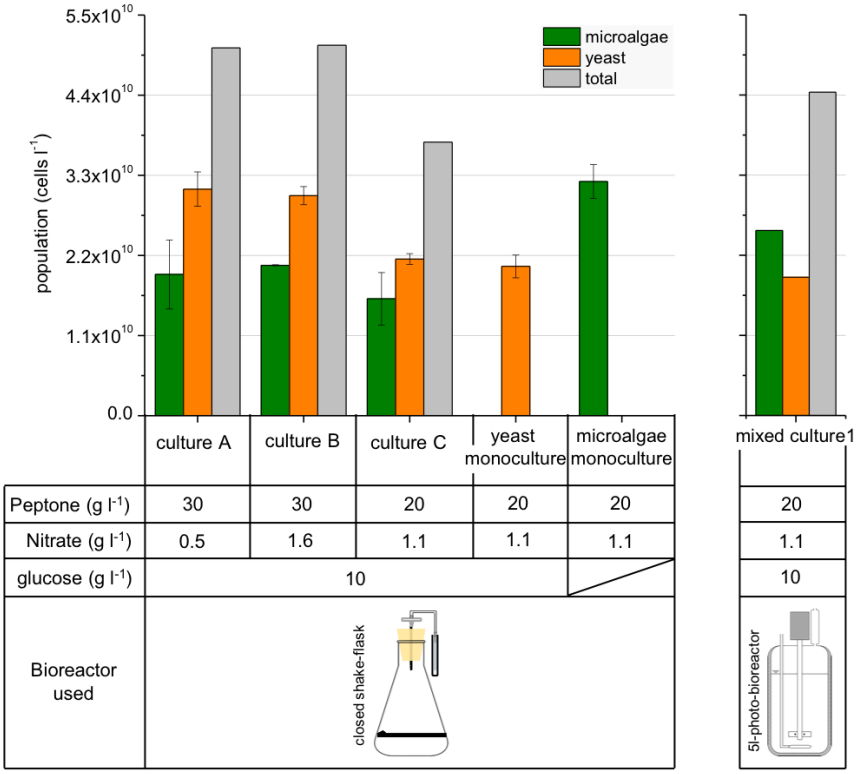

Figure 69. Yeast and microalgae population in mixed cultures according peptone and nitrate concentration in closed shake flasks after 336 hours of incubation. Error bars represent standard deviations of duplicate cultures

In the culture C, yeast reached a maximal population equal to that in yeast monoculture and to that in mixed culture 1 in photo-bioreactor. Moreover, when peptone concentration increased to 30 g. l^{-1} in cultures A and B, yeast population yields also increased and was closed to that obtained in yeast monoculture in shake flask also using 30 g. l^{-1} of peptone (Chapter 3). Peptone contains the limiting growth factor of yeast when grown in Mix medium (Chapter 3), so in the cultures A, B and C, the entire limiting factor present in peptone was used by *S. cerevisiae*.

Since yeast assimilated the limiting factor present in peptone entirely, in the mixed cultures A, B and C, *C. vulgaris* grew exclusively on nitrate as nitrogen source. The maximal microalgae populations in mixed culture A, B and C were similar and also close to that in mixed culture 1 (in PBR). The nitrate concentration did not affect microalgae growth, which could be explained by the fact that nitrate was added in excess even with an initial nitrate concentration of 550 mg. l^{-1} (culture A). For instance, in mixed culture 1 (in photo-bioreactor), only 81 mg. l^{-1}

was assimilated when the maximal microalgae biomass was reached (24 hours). These results confirmed that the microalgae adaptation to this medium is necessary in order to avoid competition for the same nutrients in mixed culture, allowing co-dominant growth of both species.

The microalgae population yield was higher in mixed culture 1 (PBR) than in the mixed culture C (closed shake-flask) (2.5 and 1.6×10^{10} cells. l^{-1}), with the same medium composition. This observation may be explained by pH of the mixed cultures in shake-flask and photo-bioreactor culture. In mixed culture 1 in PBR the pH was maintained at 6.5 while in closed shake flask there was no pH adjustment. Without pH control, the yeast growth acidified the culture medium to 4. Acidic pH values are known to retard *C. vulgaris* growth (Rachlin and Grosso 1991), hence continuous pH adjustment to 6.5 could provide an explanation for the enhanced *C. vulgaris* growth in mixed 1 in photo-bioreactor when compared to shake-flask culture.

5.5.2 Iron source sharing

The preparation of the microalgae inoculum in the Mix medium could explain how the competition in nitrogen source between yeast and microalgae could have been avoided in mixed culture, however, it does not explain the abrupt cessation of microalgae growth at 24 hours in mixed cultures, and iron was suspected to be the microalgae limiting growth factor. In both mixed cultures 1 and 2, *C. vulgaris* should have carried on its growth as nitrate remained in excess in the culture medium. In microalgae reference monoculture, nitrate was also in excess and *C. vulgaris* grew linearly for 336 hours, hence, in mixed culture 1, *C. vulgaris* should have continued to grow on nitrate and in mixed culture 2, microalgae should have switched to a growth on nitrate when ammonium from peptone was depleted. The abrupt cessation of microalgae growth in both mixed cultures outlines the presence of a limiting growth factor for microalgae shared with yeast in mixed culture.

The Mix medium used in mixed cultures was based on the autotrophic MBM medium with glucose and peptone added, and the microalgae reference culture showed that *C. vulgaris* could grow in the MBM medium, without glucose and peptone, linearly for more than 336 hours. Consequently, the microalgae limiting growth factor should have been a component from the autotrophic MBM medium.

After the maximal microalgae population was reached in both mixed cultures, the key factors for *C. vulgaris* growth were quantified and remained in excess (NO_3^+, Mg^+, Ca^+, Cl^-,

SO_4^-, PO_4^-, and K^+). Only iron (FeEDTA) and trace elements were not measured and their impact on microalgae growth was evaluated with experiments in shake flask (Figure 70).

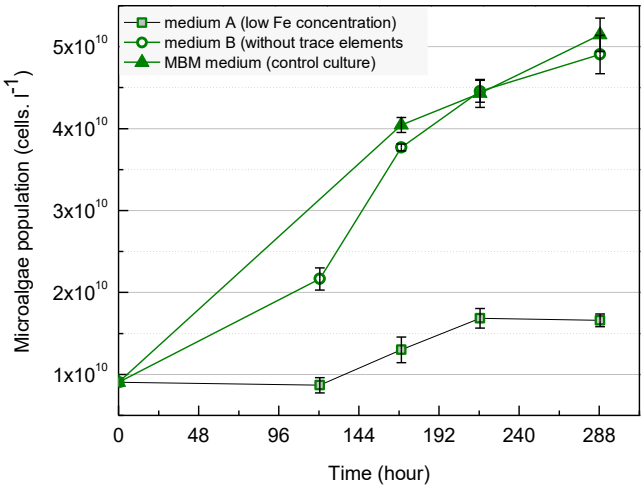

Figure 70. Impact of iron and trace elements on *C. vulgaris* growth in aerated shake flask monocultures. Medium A corresponds to MBM medium with a low concentration of iron (6.5×10^{-4} gFe. l^{-1}) and medium B corresponds to MBM medium without any trace elements and with normal concentration of iron (6.5×10^{-3} gFe. l^{-1}). MBM medium contained iron (6.5×10^{-3} gFe l^{-1}) and trace elements. Cultures were performed in shake flask, in duplicate and were inoculated with the same microalgae concentration as in mixed culture (9×10^9 cells l^{-1}). Error bars represent standard deviations of duplicate cultures.

Iron concentration influenced the microalgae yield. The low iron concentration limited the microalgae population yield, with an iron uptake coefficient of 2.7 mgFe. gDW^{-1}, which is coherent with 2.6 mgFe. gDW^{-1} from Liu et al. (2008). The absence of trace elements had no effect on *C. vulgaris* growth: microalgae growth in the medium without trace elements (medium B) is identical to that in the control culture. Consequently, the first limiting growth factor for *C. vulgaris* in mixed culture is iron. For microalgae, iron is an essential cofactor for several elements of their electron transport system associated with the chloroplast, hence, iron deficiency can lead to a reduction in photosynthetic activity, in energy production finally to growth rate (Andaluz et al. 2006; Xia et al. 2014).

Iron would have been used by both organisms, hence partly by yeast. To explain the *C. vulgaris* growth limitation in mixed culture, the effect of iron on yeast growth was also assessed: the metal had no effect on *S. cerevisiae* growth since yeast growth in Mix medium with and without iron were identical (Figure 71). Iron is also an essential element of the yeast respiration (Kaplan et al. 2006), however as shown previously, the principal activity of *S. cerevisiae* is fermentation whether in monoculture or mixed culture using Mix medium.

Respiration was little involved, hence small amount of iron was required for yeast growth. In theorical absence of iron in the culture, few quantities of iron could have been provided through inoculation.

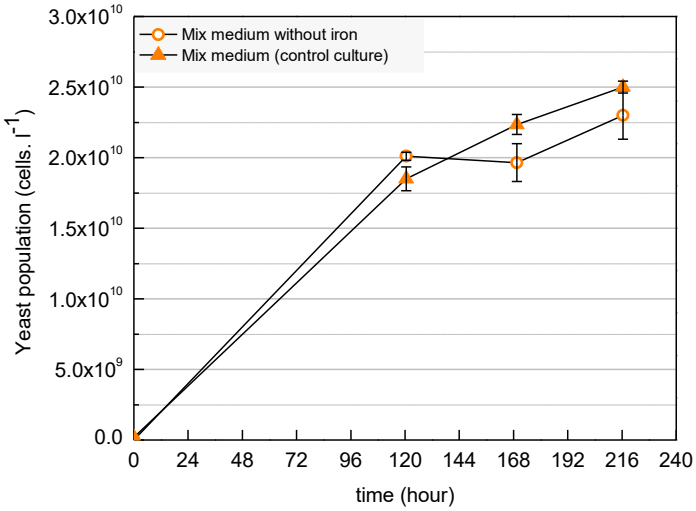

Figure 71. Impact of iron on *S. cerevisiae* growth in aerated shake flask. Mix medium (control culture) contained iron (6.5×10^{-3} gFe. l^{-1}). Cultures were performed in shake flask and error bars represent standard deviations of duplicate cultures.

Even if iron was not a limiting growth factor for yeast, iron could have been sequestered into the yeast vacuole to prevent toxicity or for later use (De Freitas et al. 2003; Holmes-Hampton et al. 2013), which could explain the utilization of iron by yeast in mixed culture. This would have reduced iron concentration available to microalgae limiting the population yield of the latter.

To conclude, there was a competition for iron between *C. vulgaris* and *S. cerevisiae* in mixed culture, but the iron requirement differed between both: iron was used by microalgae for growth while yeast simply stored the iron. For future studies, the initial iron concentration may be increased to enhance microalgae growth.

5.5.3 Ethanol impact on microalgae

To test the impact of ethanol on *C. vulgaris* growth, ethanol was added to four *C. vulgaris* shake-flask cultures when the population reached 7×10^9 cells. l^{-1} (corresponding to the initial *C. vulgaris* population in the mixed culture). Four ethanol concentrations (0, 2, 4, 6 g. l^{-1}) were chosen according to the range of ethanol concentrations that could be produced by *S. cerevisiae*

in monoculture and mixed culture (Figure 72) from 10 g. l^{-1} glucose. The *C. vulgaris* growth profile was the same in all cultures, including the control without any ethanol. Moreover, cell viability of the four cultures was broadly constant at around 98 %. This experiment with monocultures of *C. vulgaris* in shake-flask cultures with external ethanol addition confirms that in mixed photo-bioreactor mixed cultures the presence of ethanol was not limiting *C. vulgaris* growth.

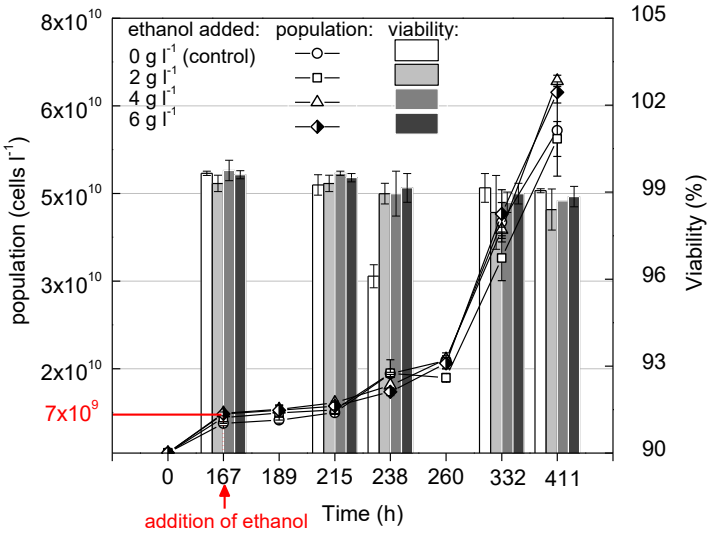

Figure 72. Impact of different ethanol concentration on *C. vulgaris* growth in shake flask culture using autotrophic MBM medium. Ethanol was added to the cultures after 7 days reflecting the initial cell concentration of microalgae in PBR mixed cultures. The different symbols connected by solid line represents the microalgae population concentration in the different cultures. The bar graph represents the microalgae population viability in the cultures. Error bars represent standard deviations of data from duplicate experiments.

5.5.4 Gas exchange between yeast and microalgae in mixed culture 1

The sections 5.5.4.1 and 5.5.4.2 are from La et al. (2018) published in the journal Applied Microbiology and Biotechnology.

5.5.4.1 CO_2 production by yeast in monoculture

In monoculture of *S. cerevisiae* using MBM-GP medium, yeast biomass, ethanol and CO_2 were produced during growth, the latter resulting in the acidification of the culture medium (Chapter 4). Since a stable pH was specified for the fermentation, the acidification of the culture resulted in the automatic addition of KOH in step with yeast growth during the first 41 h of the culture. Ethanol (3.95 g. l^{-1}) was produced and CO_2 (3.80 g. l^{-1}) was released. The CO_2

concentration was calculated for 100 g of yeast biomass by adopting the stoichiometric fermentation Reaction 9 (Verduyn et al. 1990b) using the ethanol yield (3.95 g. l^{-1}) of the yeast monoculture in MBM-GP medium:

$8.98\ C_6H_{12}O_6 \rightarrow 1\ C_{3.75}H_{6.6}N_{0.63}O_{2.1} + 15.4\ C_2H_6O + 16\ CO_2 + 1.1C_3H_8O_3 + 0.8\ H_2O$ **Reaction 12**

The CO_2 released into the culture medium reacts with water to form carbonic acid H_2CO_3 and then dissociates into H^+ and HCO_3^- (Peña et al. 2015) acidifying the culture medium. Under the pH-control regime, the KOH solution is added to maintain the pH at 6.5. The stoichiometry of the reaction between CO_2 and KOH is 1:1. A total KOH volume of 337 ml was added during the yeast growth phase, which corresponded to 0.337 mole of KOH added to the 5-liter culture medium. For ease of the mass balance calculation, the amount of KOH added was expressed as a concentration (6.74×10^{-2} mole. l^{-1}):

$$[\mathrm{KOH}] = \frac{V_{KOH} \times C_{KOH}}{V} \quad (33)$$

with:
[KOH]: base KOH concentration in the culture medium (mole. l^{-1})
V_{KOH}: volume of KOH added to the culture medium (l)
C_{KOH}: concentration of the KOH solution added to the photo-bioreactor (mole. l^{-1})
V: working volume (5 l)

Assuming that the KOH reacted exclusively with the H^+ from the hydration of the CO_2 produced, 6.74×10^{-2} mole. l^{-1} of KOH was used for pH adjustment:

$CO_2 + H_2O \rightarrow H_2CO_3 \rightarrow H^+ + HCO_3^-$ **Reaction 13**

The CO_2 concentration produced by yeast and neutralized by the KOH was 2.97 g. l^{-1} and was calculated as:

$$[CO_2]_{KOH} = [KOH] \times M_{CO_2} \quad (34)$$

with:

$[CO_2]_{KOH}$: concentration of CO_2 produced by yeast and reacted with KOH (g. l^{-1})

$[KOH]$: base KOH concentration in the culture medium (mole. l^{-1})

M_{CO_2}: molar mass of CO_2 (44 g. $mole^{-1}$)

From the above calculation, 3.80 g. l^{-1} of CO_2 would have been produced during yeast monoculture but only 2.97 g. l^{-1} of CO_2 was measured based on the KOH used. This means that 0.83 g. l^{-1} of CO_2 remained in solution and/or passed into gaseous phase (Figure 73).

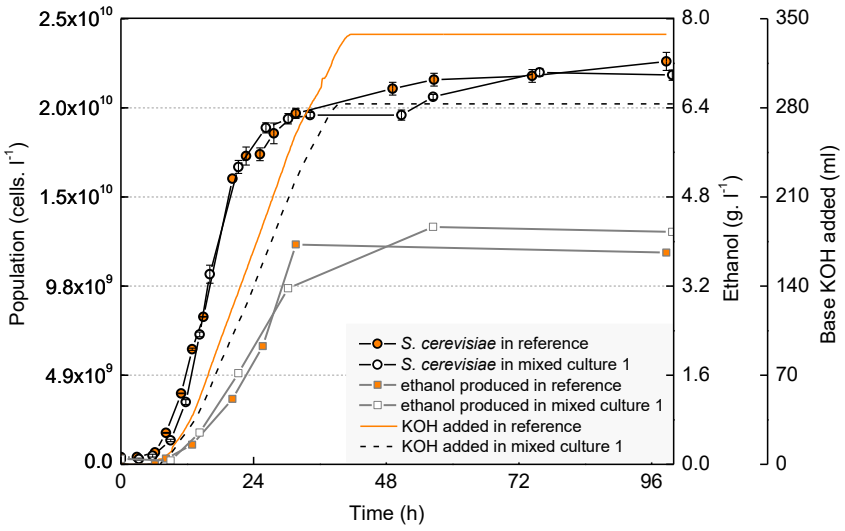

Figure 73. Automatic addition of base KOH solution in *S. cerevisiae* monoculture and in mixed culture. Error bars represent standard deviations of duplicate analyses of yeast population concentration.

5.5.4.2 CO_2 mass balance for yeast and microalgae

The CO_2 production and biofixation was studied only in mixed culture 1 since the dominance between microalgae and yeast was reached in this mixed culture and not in mixed culture 2.

In mixed culture 1, the KOH solution was added during the first 39 h of culture corresponding to yeast growth. As explained above, the *S. cerevisiae* behavior was similar in both mixed culture 1 and in the reference yeast monoculture (Figure 73); again, the assumption was made that the KOH solution was mainly added to the mixed culture 1 to compensate for the medium acidification by the CO_2 release by the yeast. KOH (283 ml) was added during the

growth phase of the yeast corresponding to 5.7×10^{-2} mole. l^{-1} of CO_2 equivalent to 2.49 g. l^{-1} of CO_2 (equations 33 and 34).

In the yeast reference monoculture 2.97 g. l^{-1} of CO_2 reacted with KOH whereas in mixed culture 1 only 2.49 g. l^{-1}, of CO_2 reacted with KOH. The difference in CO_2 concentration most likely corresponds to the amount of CO_2 assimilated by microalgae in the mixed culture: 0.48 g. l^{-1} of CO_2 i.e. 0.13 g. l^{-1} of carbon. This concentration of carbon is coherent with the concentration of carbon required for the *C. vulgaris* biomass measured in mixed culture 1; 1.5×10^{10} cells. l^{-1} of *C. vulgaris* was produced corresponding to a dry weight of 0.23 g. l^{-1} or 8.8×10^{-3} mol. l^{-1} (the microalgae composition is $C_1H_{1.78}N_{0.165}O_{0.495}$ according to Scherholz and Curtis (2013), and consequently 0.11 g. l^{-1} of carbon was required for the microalgae biomass production. Hence, the amount of carbon fixed by microalgae was determined by two different methods; the carbon fixation by *C. vulgaris* calculated from the microalgae biomass concentration corresponded to 85% of that calculated from the KOH consumption. To conclude, *C. vulgaris* grew on the CO_2 produced by *S. cerevisiae* as there was no other source of CO_2. Of the CO_2 produced by *S. cerevisiae* in mixed culture 1, 12.6 % was consumed directly by *C. vulgaris*, and the 64% of CO_2 captured by the KOH was in the HCO_3^- form and still available to the microalgae for utilization, then 24% remained in solution and/or passed into gaseous phase (Figure 74).

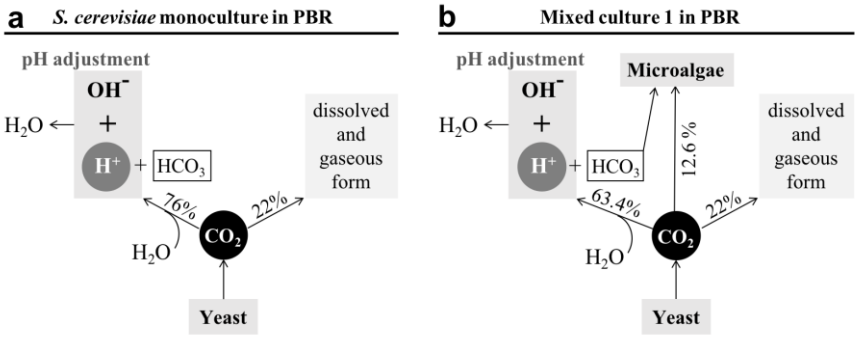

Figure 74. Repartition of CO_2 produced by *S. cerevisiae* in yeast monoculture (a) and mixed culture 1 (b).

5.5.4.3 CO_2 production and biofixation rate in mixed culture 1 and microalgae reference culture

In yeast reference mixed culture, the KOH solution was added within 35 hours (during yeast fermentation) so the CO_2 production rate was 0.085 gCO_2. l^{-1} h^{-1}. In mixed culture 1, the CO_2 production rate should have been the same since the fermentation activity was the same in the two cultures.

In mixed culture 1, the CO_2 biofixation rate by *C. vulgaris* was calculated to be 0.014 gCO_2. l^{-1} h^{-1}, which was higher than that in microalgae reference monoculture (0.002 gCO_2. l^{-1} h^{-1}). The latter was conducted without any CO_2 supply and the mixed culture 1 was fed in CO_2 through yeast fermentation, hence this contribution should have improved CO_2 biofixation rate. In Adamczyk et al. (2016), the CO_2 biofixation rate was 0.023 gCO_2. l^{-1} h^{-1} in a *C. vulgaris* culture enriched with 8 % of CO_2 and 0.033 gCO_2. l^{-1} h^{-1} with 13 % of CO_2 in Clément-Larosière et al. (2014): these CO_2 biofixation rates were coherent with that obtained in mixed culture 1. In Wang et al. (2016) a mixed culture of yeast *S. cerevisiae* and microalgae *S. obliquus* also showed an increase in CO_2 biofixation rate compared to the microalgae monoculture (0.020 and 0.019 gCO_2. l^{-1} h^{-1}).

5.5.4.4 O_2 mass balance

In mixed culture 1, *C. vulgaris* grew from the beginning using CO_2, hence producing O_2 through photosynthesis. The pO_2 measurements indicated an increase of 7×10^{-4} g. l^{-1} of O_2 (Figure 75). This amount is negligible but did not represent the net O_2 production by *C. vulgaris* as *S. cerevisiae* grew at the same time using O_2.

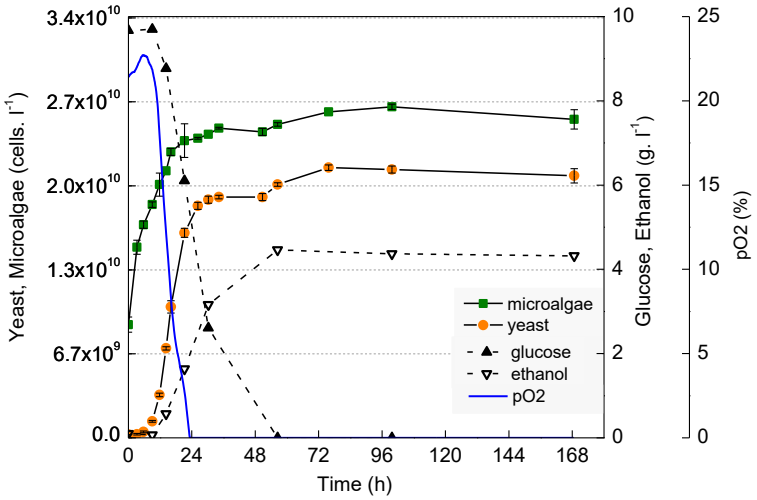

Figure 75. *S. cerevisiae* and *C. vulgaris* growth profiles in mixed culture 1 with evolution of pO_2.

The amount of O_2 produced by *C. vulgaris* can be estimated by the molar stoichiometric relation between CO_2 and O_2 during photosynthesis:

$6\ CO_2 + 6\ H_2O \rightarrow C_6H_{12}O_6 + 6\ O_2$ **Reaction 14**

In mixed culture 1, *C. vulgaris* used 0.48 g. l^{-1} of CO_2 by the end of the culture period (section 5.5.4.2), hence 0.35 g. l^{-1} of O_2 (1.75 g in total) would have been produced by the microalgae. This amount was not negligible as it was around 4 times higher than the initial amount of O_2 available in the PBR (liquid and gaseous phase). Although this increase in O_2 did not enhance the yeast yield as the *S. cerevisiae* growth was limited by nitrogenous compounds from peptone, it would favor yeast growth if the initial peptone concentration were to be increased.

5.5.5 Gas exchange between yeast and microalgae in mixed culture 2

Within the first 48 hours of mixed culture 2 the increase in pCO_2 and the decrease in pO_2 (Figure 76) were directly linked to the yeast fermentation activity and growth (Figure 65). From 48 h to 168 h, dissolved CO_2 concentration gradually decreased from 16 % to 0 % at the end of the experiment.

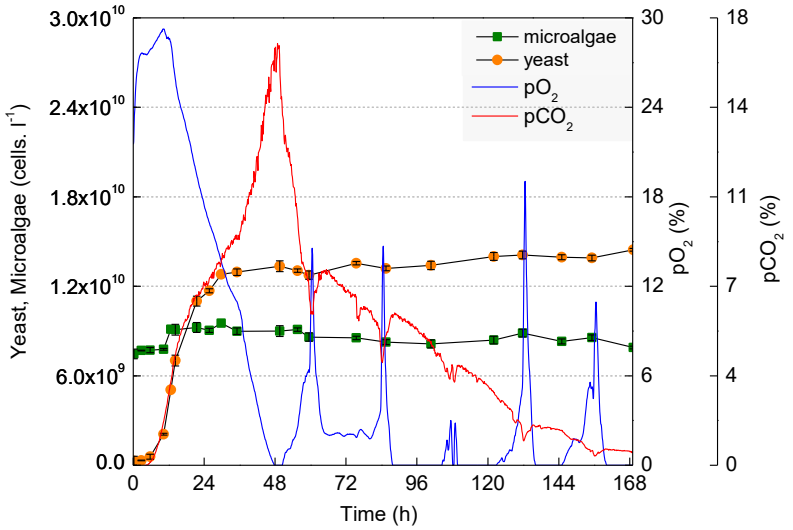

Figure 76. Evolution of pO_2 and pCO_2 in Mixed culture 2 Mixed culture 2 of *C. vulgaris* and *S. cerevisiae* in closed and non-aerated PBR using Mix medium.

Although the *C. vulgaris* population was low, the microalgal cells remained active during the entire experiment (168 hours). During the latter phases of the experiment, there were instances where the sun shone directly on the PBR; intermittent negative pCO_2 troughs and concomitant positive pO_2 peaks were observed during these transient periods. This can be

considered as a strong indicator that both organisms in the mixed culture were metabolically active and that synergy effects between yeast and microalgae occurred. The final pCO_2 concentration reached almost its initial level indicating that in principle, *in situ* CO_2 mitigation in mixed culture is feasible, although the efficiency of the process remains to be improved.

5.6 Conclusion

In conclusion, in order to encourage mutual symbiosis, we developed a mixed culture of *C. vulgaris* and *S. cerevisiae* in PBR in a way that neither organism dominated the other in terms of population concentration. The method developed for simultaneous cell enumeration with flow cytometry permitted to rigorously monitor the two populations in the mixed culture. The results indicated that the medium design, the culture conditions, the inoculum ratio and the *C. vulgaris* inoculum preparation all contributed for co-dominance of the two species. By comparing the physiological behavior of microalgae and yeast in monoculture and mixed culture, co-dominance and a mutual symbiosis based on *in situ* gas exchange were demonstrated. There is no evidence that the two organisms interfere one with the other, except in terms of competition for nutrients. This work opens the perspective for *in situ* CO_2 mitigation, full utilization of the organic substrate and a reduction in aeration costs of biotransformation processes.

Chapter 6. Yeast and microalgae growth model

This chapter describes a predictive yeast model based on components, energy and electron carrier balances. The yeast individual model is presented as a pre-submitted version to journal. A second model is described to predict yeast and microalgae growth in mixed culture. This model is based on the combination of the yeast and microalgae individual model.

Contents

6.1 A predictive dynamic yeast model based on component, energy and electron carrier balances

Angéla La[a,b], Huan Du[b], Behnam Taidi[a,b], Patrick Perré[a,b]

[a] LGPM, CentraleSupélec, Université Paris-Saclay, 8-10 rue Joliot-Curie, 91 190 Gif-sur-Yvette, France
[b] LGPM, CentraleSupélec, Centre Européen de Biotechnologie et de Bioéconomie (CEBB), 3 rue des Rouges Terres, 51 110 Pomacle, France

6.1.1 Abstract

This study presents a novel yeast model for the prediction of yeast fermentation. The model takes into account the possible yeast metabolic pathways. For each pathway, the time evolution of components, energy (ATP/ADP) and electron carriers (NAD^+/NADH) are expressed with limitation factors for all quantities consumed by this pathway. In this manner, the model can predict the partition of these pathways, depending on the growth conditions and their evolution in time. The several biological pathways and their stoichiometric coefficients are well known from literature. It is important to note that most of the kinetics parameters have no effect as the actual kinetics are controlled by the balance of the limiting factors. The few remaining parameters were adjusted and compared with literature when dataset was available. The model fits our experimental data, obtained from yeast fermentation on glucose in a non-aerated batch system. The predictive ability of the model and its capacity to represent the intensity of each pathway versus time, allows a better understanding of interactions between the pathways. The key role of energy (ATP) and the electron carrier (NAD^+) in the yeast growth is highlighted and the involvement of mitochondrial respiration not associated with Krebs cycle is showed.

Keywords: energy balance, fermentation, Krebs cycle, metabolic pathway, respiration

6.1.2 Introduction

Yeast fermentation of organic substrates is one of the oldest and main metabolic process used in biotechnological processes, such as beer brewing, wine making and biofuel fermentations (Dashko et al. 2014). *Saccharomyces cerevisiae* is commonly used for its

capacity to rapidly convert sugars to ethanol and carbon dioxide under both anaerobic and aerobic conditions (Hagman et al. 2014). Under aerobic conditions, the respiration can occur with molecular oxygen as the final electron acceptor, however, *S. cerevisiae* also produces ethanol when the glucose concentration exceeds 0.10 – 0.15 $g.l^{-1}$ (Verduyn et al. 1984), reducing the respiration process. This phenomenon is called Crabtree effect (De Deken 1966) and its emergence is likely due to the increased rate of ATP production through fermentation (Pfeiffer and Morley 2014).

The fermentation activity in yeast depends on the biomass yield. Cramer et al. (2002) describes the ethanol production as completely proportional to the amount of biomass formed and not as growth-associated stoichiometric bioconversion of sugar to ethanol. Therefore, a decrease in yeast yield can lead to a reduction in fermentation activity rate (sluggish fermentation) and worse, to a premature cessation of ethanol production, with more than 0.4% (w/v) residual sugar remaining in the medium (stuck fermentation) (Bisson 1999; Coleman et al. 2007). These phenomena are often observed in wine making process bringing about significant economic issues (Chaney et al. 2006) and the main cause is nitrogen and/or oxygen limitation. Nitrogen is an essential element in *S. cerevisiae* composition as it is mandatory for protein synthesis and represents 9% (w/w) of yeast biomass (Verduyn et al. 1990a). Oxygen is required to regenerate NAD^+ used in the glycolytic pathway of biomass formation, closing the redox balance for the co-enzyme system NAD^+/NADH. The oxidation of cytosolic NADH into NAD^+ can occur through the mitochondrial respiration, with the external NADH dehydrogenase (Overkamp et al. 2000; Bakker and Overkamp 2001). Oxygen is also important for the synthesis of yeast membrane compounds (sterols and unsaturated fatty acids) (Sablayrolles J.M. 1986), but this process can be neglected as the required amount is very weak, between 0.3 and 1.5 $mg_{O2}.\ g_{yeast}^{-1}$ (Rosenfeld et al. 2003).

Consequently, the fermentation activity hinged on the yeast biomass production, which is limited by nitrogen, organic carbon and oxygen. The latter can be used for strict respiration pathway (including Krebs cycle) producing ATP, and/or to close the NAD^+/NADH system for the biomass glycolytic pathway. Fermentation of glucose is also an ATP source for biomass formation.

To our knowledge, none publication has described a yeast model that connects the possible pathways of glucose utilization (ethanol, glycerol, biomass and Krebs cycle) and mitochondrial respiratory chain, according nutrients (nitrogen, carbohydrates and oxygen), energy and electron carrier balances. Moreover, most of models indirectly linked cell growth and ethanol production through a Monod-like function (Holzberg et al. 1967; Aiba et al. 1969;

Bovee et al. 1984; López and Secanell 1992; Giovanelli et al. 1996) with the exception of models from Cramer et al. (2002) and Coleman et al. (2007), in which ethanol production rate depends on the *S. cerevisiae* biomass yield and not on the growth. However, these models could be criticized as glucose is not integrated in the model as a limiting growth factor. In Liu et al. (2011), ethanol is both associated to *S. cerevisiae* growth and yeast biomass concentration, but the model could also be partly disapproved as yeast growth is not limited by nitrogen.

The aim and the novelty of this work is to develop a yeast model that predicts the partition between several metabolic pathways based on nutrients, energy and electron carrier balances (Figure 77). The model is then compared to experimental results and simultaneously on a full set of data.

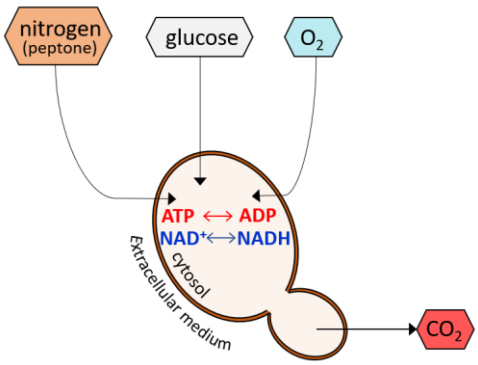

Figure 77. A schematic diagram of yeast cell and its growth limitations

6.1.3 Materials and method

6.1.3.1 Yeast fermenter

S. cerevisiae strain ID YLR249W was supplied by Life Technologies-University of California San Francisco. The yeast fermenter was conducted in a non-aerated and closed 5l-bioreactor, with temperature and pH adjusted at 25°C and 6.5, and dissolved oxygen in the liquid phase was measured with an internal probe (La et al. 2019).

6.1.3.2 Medium composition

The culture medium was composed of glucose (10 g. l^{-1}), peptone 20 (g. l^{-1}) and mineral salts. This medium was previously designed in La et al. (2018). The nitrogen content in peptone

was estimated from the free amino nitrogen content (FAN). FAN in the medium was 5.4×10^{-1} g. l^{-1}, assuming that the average molar mass of an amino acid is 118.9 g. $mole^{-1}$ (Hachiya et al. 2007) and that an amino acid contains one nitrogen element, the concentration of nitrogen available to yeast was 5.5×10^{-2} g. l^{-1}.

6.1.3.3 Dry weight

Yeast growth was followed by cell concentration *N* measurements through flow cytometer and the corresponding dry weight *DW* was obtained applying the correlation between *N* (cells. l^{-1}) and *DW* (g. l^{-1}):

$$\mathrm{DW} = 3.25 \times 10^{-11} \times \mathrm{N} \quad (35)$$

6.1.3.4 Glucose, ethanol and glycerol measurements

Glucose, ethanol and glycerol concentration were measured by high-pressure liquid chromatography (HPLC) according to La et al. (2018).

6.1.4 The yeast model

6.1.4.1 Pathways

The metabolic pathways considered in the model are depicted in figure (Figure 78). Seven biological pathways emerge, and all ratios depicted in this diagram are expressed in moles and respect the carbon balance. The composition and molar mass of the main molecules are summarized in table (Table 9).

The kinetics of each pathway is expressed as a kinetics parameter times the yeast population, together with one or several factors accounting for possible limitations. Three compartments are considered in the model: the bioreactor liquid (substrate), the inner cell (cytosol) and mitochondrion. In order to ease the stoichiometric balances, all concentrations are expressed as mole per liter of substrate. However, the limiting factors should be expressed in relevant quantities: *mole/liter* in the substrate and *mole/mole of biomass* for quantities inside the cell or mitochondrion (quota). Regarding the ATP/ADP and NAD^+/NADH balances, in addition to the source/sink terms tied to metabolic pathways, source terms have also to be implemented to maintain a constant ratio per quantity of yeast. Indeed, literature reports that

[NADH]+[NAD$^+$] ~6 µmole/g of biomass and [ATP]+[ADP] ~5 µmole/g of biomass (Suomalainen et al. 1965; Sakai et al. 1973; Sato et al. 2000; Koç et al. 2004; Thomsson et al. 2005).

Table 9. Composition and molar mass of the main molecules involved in the metabolic pathways.

Molecule	Composition	Molar mass (g. l^{-1})
glucose	$C_6H_{12}O_6$	180
G3P	$C_3H_7O_6P$	170
pyruvate	$C_3H_4O_3$	88
ethanol	C_2H_6O	46
glycerol	$C_3H_8O_3$	92
carbon dioxide	CO_2	44
biomass	$CH_{1.76}N_{0.17}O_{0.56}$ + …	27

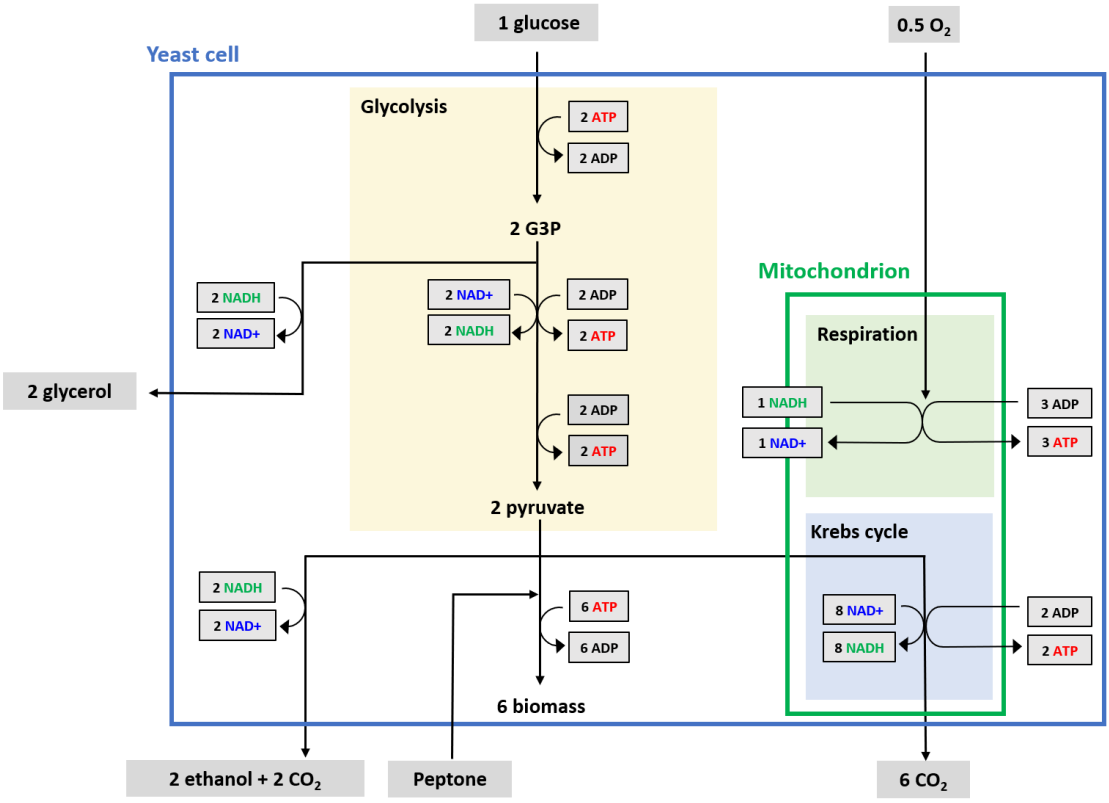

Figure 78. A schematic diagram of the metabolic pathways implemented in the present modelling approach. All numeric ratios are in moles.

Each constituent C consumed by a biological reaction is likely to induce limitation when its relevant concentration $[C]$ (mole per liter or mole per mole depending of the compartment of

this constituent) becomes too small. We also implemented the possibility to activate a reaction likely to produce a limiting resource, even though this possibility was not applied in the present work. The classical Monod-like function is applied to all resources present in the substrate. Its asymptotic behavior shape is indeed well adapted to resources that can be initially much higher than the limiting concentration (Figure 79). The case of ATP/ADP and NAD^+/NADH balances is quite different: as the accumulation of these quantities remains very low (some µmoles per gram of biomass), the limiting function should behave as a switch function, which is represented by a smoothed stepwise function (Figure 79). The two functions used to express the limiting effects read as follows:

A Monod-like functions

$$M([C]) = \frac{[C]}{k_C + [C]} \tag{36}$$

In these equations, the term k_C defines the steepness of the function near zero. The rate is divided by 2 when $[C] = k_C$.

A smooth stepwise function

$$S([C]) = \frac{1 + tanh\left(\alpha([C]/\Delta_C - 1)\right)}{2} \tag{37}$$

Each function is defined by two parameters. The shift value Δ_C defines the concentration value at which transition occurs and α the steepness of this transition. Figure 79 depicts example of functions shapes with different parameter sets. The additional parameter of function *Step* allows the sharpness of transition to be tuned.

In the metabolic pathways described in Figure 78, the three compartments should be respected. As the ATP/ADP molecules are likely to path through the mitochondrion wall, one unique stock of these constituents should be considered in the model. On the contrary, the $[NAD^+]$ to [NADH] transfer involved in the Krebs cycle should be balanced inside the mitochondrion by respiration. Therefore, a specific stock of these molecules should be considered inside the mitochondrion (superscript ^{M}). Finally, ten quantities are involved as inhibition effects. For each metabolic pathway, each constituent consumed by the reaction is systematically involved as limiting factor (Table 10).

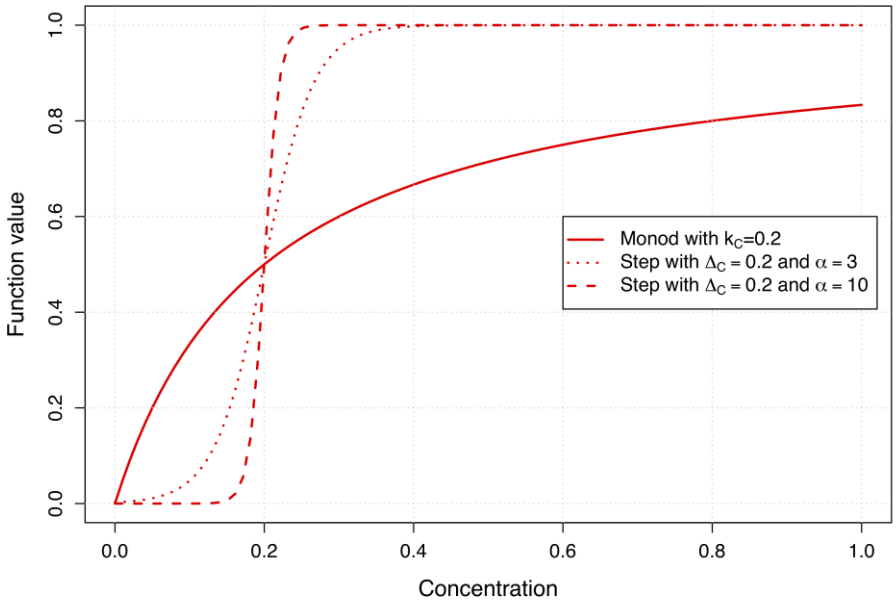

Figure 79. Shape of the functions used to affect the reaction rates.

Table 10. Expression of the limiting factors involved in the seven metabolic pathways (M for Monod-like function and S for stepwise function).

Pathway	ATP	ADP	NAD^+	NADH	NAD^+ M	Glu	G3P	Pyr	N	O_2
G3P	S					M				
Glycerol				S			M			
Pyruvate		S	S				M			
Ethanol				S				M		
Biomass	S							M	M	
Krebs		S			S			M		
Respiration		S		S						M

With this rule, the set of kinetics takes the following form:

First step

$$\frac{d[G3P]}{dt} = \mu_{yeast} \times \left(\frac{[ATP]}{[yeast]}\right) \times M([G]) \times [yeast] \quad (38)$$

Second step

$$\frac{d[Gly]}{dt} = \lambda_{Gly} \times S\left(\frac{[NADH]}{[yeast]}\right) \times M\left(\frac{[G3P]}{[yeast]}\right) \times [yeast] \quad (39)$$

$$\frac{d[Pyr]}{dt} = \lambda_{Pyr} \times S\left(\frac{[NAD^+]}{[yeast]}\right) \times S\left(\frac{[ATP]}{[yeast]}\right) \times M\left(\frac{[G3P]}{[yeast]}\right) \times [yeast] \quad (40)$$

Third step

$$\frac{d[E]}{dt} = \lambda_{E} \times S\left(\frac{[NADH]}{[yeast]}\right) \times M\left(\frac{[Pyr]}{[yeast]}\right) \times [yeast] \quad (41)$$

$$\frac{d[yeast]}{dt} = \lambda_{yeast} \times S\left(\frac{[ATP]}{[yeast]}\right) \times M\left(\frac{[Pyr]}{[yeast]}\right) \times M([N]) \times [yeast] \quad (42)$$

$$\frac{d[Krebs]}{dt} = \lambda_{Krebs} \times S\left(\frac{[ADP]}{[yeast]}\right) \times S\left(\frac{[NAD^{+M}]}{[yeast]}\right) \times M\left(\frac{[Pyr]}{[yeast]}\right) \times [yeast] \quad (43)$$

Mitochondrial respiration

$$\frac{d[Resp]}{dt} = \mu_{Resp} \times S\left(\frac{[ATP]}{[yeast]}\right) \times S\left(\frac{[NADH]}{[yeast]}\right) \times M([O_2]) \times [yeast] \quad (44)$$

6.1.4.2 Productions

As depicted in Figure 78, each biological pathway involves sink or source terms. Besides, the [NADH] to [NAD^+] transfer assured by respiration can be used either in the cytosol or in the mitochondrion. This fact rises the important question of allocation of this transfer between these two compartments. This question has not been addressed yet. Instate, we simply assumed that, due to the Crabtree effect, the Krebs cycle is not active. The balance inside the mitochondrion was therefore discarded so far. The remaining stoichiometric coefficients can be summarized in a rectangular matrix, as defined in equations 45 and 46.

$$\frac{d}{dt}\begin{bmatrix}[ATP]\\[ADP]\\[NAD^+]\\[NADH]\\[CO_2]\\[O_2]\\[N]\\[G]\end{bmatrix} = A\frac{d}{dt}\begin{bmatrix}[G3P]\\[Gly]\\[Pyr]\\[E]\\[yeast]\\[Krebs]\\[Resp]\end{bmatrix} + \begin{bmatrix}S_{ATP}\\S_{ADP}\\S_{NAD+}\\S_{NADH}\\0\\0\\0\\0\end{bmatrix} \tag{45}$$

$$A = \begin{bmatrix}-1 & 0 & 2 & 0 & -1 & 1 & 3\\ 1 & 0 & -2 & 0 & 1 & -1 & -3\\ 0 & 1 & -1 & 1 & 0 & -4 & 1\\ 0 & -1 & 1 & -1 & 0 & 4 & -1\\ 0 & 0 & 0 & 1 & 0 & 3 & 0\\ 0 & 0 & 0 & 0 & 0 & 0 & -0.5\\ 0 & 0 & 0 & 0 & -0.17 & 0 & 0\\ -0.5 & 0 & 0 & 0 & 0 & 0 & 0\end{bmatrix} \tag{46}$$

The last right-hand vector of equation 45 represents the source terms required to insure a constant concentration of [*ATP*] + [*ADP*] and [NAD^+] + [*NADH*] per gram of yeast. For example, the source term of ATP read as follows:

$$S_{ATP} = \frac{[ATP]}{[yeast]} \times \frac{d[yeast]}{dt} \tag{47}$$

6.1.4.1 Oxygen balance

The total bioreactor volume is the sum of the liquid volume V_{liq} and the upper gaseous volume V_{gas}, both contains an initial quantity of oxygen. As the bioreactor is closed during the culture, an oxygen balance equation is needed to know how the initial stock can be used by biological activity.

The sink term S_{O2} is solely due to mitochondrial respiration. According to the stoichiometric coefficients (see equation 46), the oxygen consumption reads as:

$$S_{O_2} = -0.5\frac{d[Resp]}{dt} \times V_{liq} \qquad (mole.s^{-1}) \tag{48}$$

The time derivative of the oxygen contained in the liquid phase should account for this biological sink term, but also for the exchange between the liquid and gaseous phase. This mass flux q_{O2} is expressed using a mass transfer coefficient h_m. This flux is expressed in *kg/s*:

$$q_{O_2} = h_m \frac{S}{RT}\left(P_{O_2} - hM_{O_2}[O_2]\right) \qquad (mole.s^{-1}) \tag{49}$$

Combining the two previous equations allows the time evolution of the oxygen in liquid to be obtained:

$$\frac{d[O_2]}{dt} = \frac{q_{O_2} + S_{O_2}}{V_{liq}} \qquad (mole.m^{-3}s^{-1}) \tag{50}$$

Finally, one must account for the decrease of partial pressure of oxygen in the gaseous phase induced by the flux q_{O2}:

$$\frac{dP_{O_2}}{dt} = -q_{O_2}\frac{RT}{V_{gas}} \qquad (Pa.s^{-1}) \tag{51}$$

6.1.4.1 Model parameters

The model described in the previous section contains several parameters that must be supplied to the computational code. The parameters h_m, S, T, V_{gas} and V_{liq} are specific to the bioreactor used for the experimental part (Table 11). All stoichiometric coefficients, as reported in Figure 78, are supplied to the code as the matrix A of equation 46. Finally, two sets of parameters remain to be defined: the kinetics parameters and the threshold values of the limiting factors.

The kinetics parameters were defined as follows: assuming the collection of sugar from the substrate to be the most difficult task for yeast, the observed maximum growth rate μ_{max}, defined during the exponential growth, was allocated to the first step of glycolysis. Somehow, this assumption is consistent with the concept of harvesting volume proposed in Quéméner and Bouchez (2014). All other kinetics parameters involving pathways inside the cell are assumed to be fast: 20 times μ_{max}. The kinetics of respiration was adjusted from the measured variation of

O_2 in the substrate. The fitted value is in good agreement with literature data (Hagman and Piškur 2015).

Table 11. Bioreactor configuration

Parameter	Value
h_m	1×10^{-2} (m. s^{-1})
S	2×10^{-2} (m^2)
T	293 (K)
V_{gas}	1.3 (l)
V_{liq}	5 (l)

Regarding the threshold values of the Monod-like functions, again the classical value (0.1 g per liter) was adopted for the first step of glycolysis. The Monod constants K_C for other components are very small (namely for the intermediate components ATP, G3P, NAD^+, and Pyr), meaning that these components are rapidly consumed after being produced knowing that these values have very little effect on the kinetics. The parameter values of the stepwise functions were determined to obtain a rapid switch when the concentration becomes low with regard to the sum per gram of cells (tot_{NAD} = [NADH]+[NAD^+] = 6 µmole/g of yeast and tot_{ATP} = [ATP]+[ADP] = 5 µmole/g of yeast. Δ_C was taken as 5% of this total content. α was set to 5 to ensure that the function equals zero at zero concentration. For these balances, the total content per cell is so small that the value of Δ_C has absolutely no effect of the model results: the time-evolution equation is indeed forced to balance the source and sink terms at any time. The full set of parameters are reported in Table 12 and Table 13.

Table 12. Kinetics parameters associated to metabolic pathways. Values in bold style are adjusted parameters.

Parameters	Value (h^{-1})	Literature value
μ_{yeast}	0.30	0.27 (our exp. Data)
λ_{Gly}	**0.012**	0.01 - 0.03 (Yalçin and Özbas 2004)
λ_{Pyr}	$20\times\mu_{yeast}$	-
λ_E	**10**$\times\mu_{yeast}$	0.3 (Cramer et al. 2002)
λ_{yeast}	$20\times\mu_{yeast}$	-
λ_{Krebs}	$20\times\mu_{yeast}$	-
μ_{Resp}	$\mathbf{7.7\times10^{-2}}$	9.6×10^{-2} (Hagman and Piškur 2015)

Table 13. Threshold constants of the limiting functions (K_C or Δ_C). Values in bold style are adjusted parameters.

Parameters	Value	Literature value
K_{ATP}	$0.05 \times tot_{ATP}$	-
K_{ADP}	$0.05 \times tot_{ATP}$	-
K_{NAD^+}	$0.05 \times tot_{NAD}$	-
K_{NADH}	$0.05 \times tot_{NAD}$	-
K_G	1.8×10^{-1} g. l^{-1}	1.8×10^{-1} g. l^{-1} (van Dijken et al. 1993)
K_{G3P}	2×10^{-5} mole. $mole^{-1}$	-
K_{Pyr}	2×10^{-5} mole. $mole^{-1}$	-
K_N	4×10^{-3} mole. l^{-1}	7×10^{-4} mole. l^{-1} (Cramer et al. 2002)
K_{O2}	3×10^{-3} mole. l^{-1}	-

Despite these restrictive parameters, the partition of each concurrent pathways can be predicted thanks to the limitation factors and the stoichiometric coefficients that are well-known from literature. Among the whole set of model parameters, only 4 parameters were unknown with significant effect on the modelling results. These parameters were highlighted in bold style in Table 12 and Table 13:

- λ_{Gly} was adjusted to get the measured concentration of glycerol at the end of the experiment. This parameter has however a quite moderate effect as this pathway is activated just at the end when the G3P content becomes significant due to the limitation of the pyruvate pathway. The adjusted value is consistent with literature data,

- λ_E needed to be different from the biomass pathway to give a certain priority to biomass production in the use of pyruvate. The obtained value cannot be directly compared to literature data as our model accounts for sequential pathways,

- μ_{Resp} was fitted to get the experimental decrease of dissolved oxygen. This kinetics is very important at the beginning of growth as it provides the cell with ATP and NAD+ and allows the fast increase of biomass to be obtained,

- The initial value of K_N, as taken from literature data, gave a too low reduction in growth when nitrogen is depleted. We increased this parameter up to 4×10^{-3} mole. l^{-1}.

We had also to increase μ_{yeast} by 10% (0.30 instead of 0.27) for the modelled growth curve to lie exactly on the experimental curve. This is however not necessary to claim the model

to be predictive: we did it for the reader to be able to compare more easily the kinetics of yeast population and the kinetics of ethanol production. In addition, as μ_{yeast} is applied to the first step of glycolysis, the successive pathways in series are likely to affect slightly the global dynamic of yeast population.

6.1.5 Results and discussion

6.1.5.1 Comparison with experimental data

The first simulation accounts for the formulation with the full set of limiting factors (Figure 80). In order to obtain a time-evolution in agreement with our experimental data, we were obliged to scale all kinetics parameters of Table 12 by a factor 2. At the beginning of the culture, the available oxygen is used for respiration, which produces ATP and NAD^+. NAD^+ is needed to activate the pyruvate pathway. However, this path way is also very efficient to produce ATP. As a result, the level of ADP decreases and eventually limits the pyruvate pathway. Throughout the culture, the low pyruvate kinetics is not able to balance the G3P production. The high and unrealistic level of G3P activates the glycerol pathway, which is required to produce NAD^+ as the ethanol pathway is not very active due to a limited concentration in pyruvate. At 25 hours, the lack of ADP completely blocks the pyruvate pathway and the lack of NADH blocks the glycerol pathway. This explains why the G3P level remains at its unrealistic value. In turn, the ethanol production is blocked as well, and the final level is by far lower than the experimental value.

It seems unrealistic that an excess in energy blocks the main path towards biomass production. Assuming that the excess of ATP could be used to produce internal reserves, we add a sink term of ATP to mimic this possibility. The sink term is activated when the level of ADP is too low. The yeast model now nicely predicts the experiment, regarding the comprehensive set of experimental data (Figure 81). This indicates that the limitation factors (except ADP) and the stoichiometric coefficients could be used in the current experimental results to predict glucose, biomass, ethanol, glycerol and oxygen profiles. The prediction of components that were not measured experimentally (ATP, NAD^+, G3P, Pyruvate and nitrogen), helped in interpreting and understanding of the biological activity.

S. cerevisiae growth can be divided into three distinct stages and the transition from one phase to the next is explained by changes of limiting components.

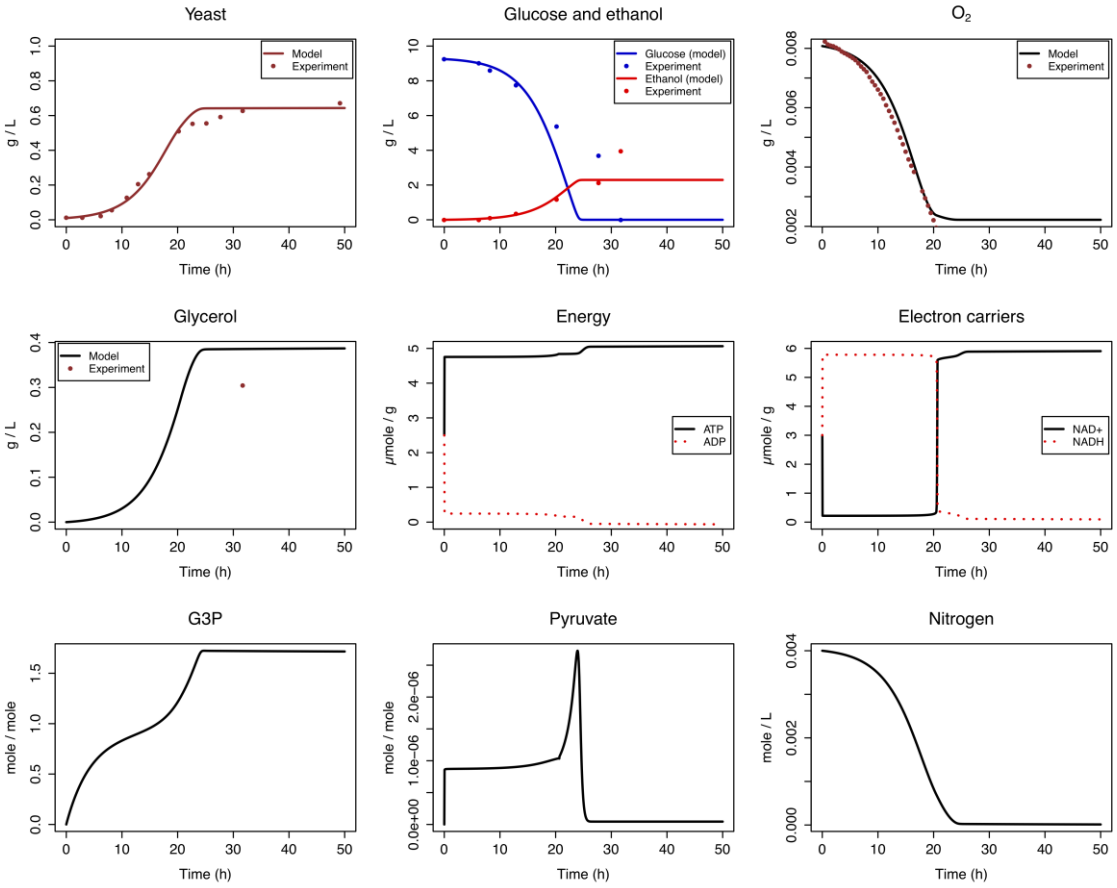

Figure 80. Simulation results with the modelling strategy described in previous section. All kinetics were multiplied by a factor 2 to get a proper time-evolution.

The first stage occurred during the first 20 hours. Oxygen content is enough to keep the mitochondrial respiration pathway active, producing enough ATP and NAD^+ to activate the biomass pathways (*Glucose* → *G3P* → *Pyruvate* → *biomass*). Respiration allows the yeast population to increase exponentially at a rate similar to the experimental results. It is noteworthy to mention that this correct kinetics is obtained solely by supplying the experimental value of μ_{max} to the first step of glycolysis. Although the respiration pathway is the main booster of the biomass pathways during this first stage, the ethanol pathway is also active and produce additional NAD^+ needed for the pyruvate pathway. As already said in paragraph 3, we had to limit the kinetics of fermentation (2 times slower than the biomass pathway) to obtain the experimental delay between yeast and ethanol: the yeast population increases clearly before ethanol. During this phase, the glycerol pathway remains slow due to the low level of G3P.

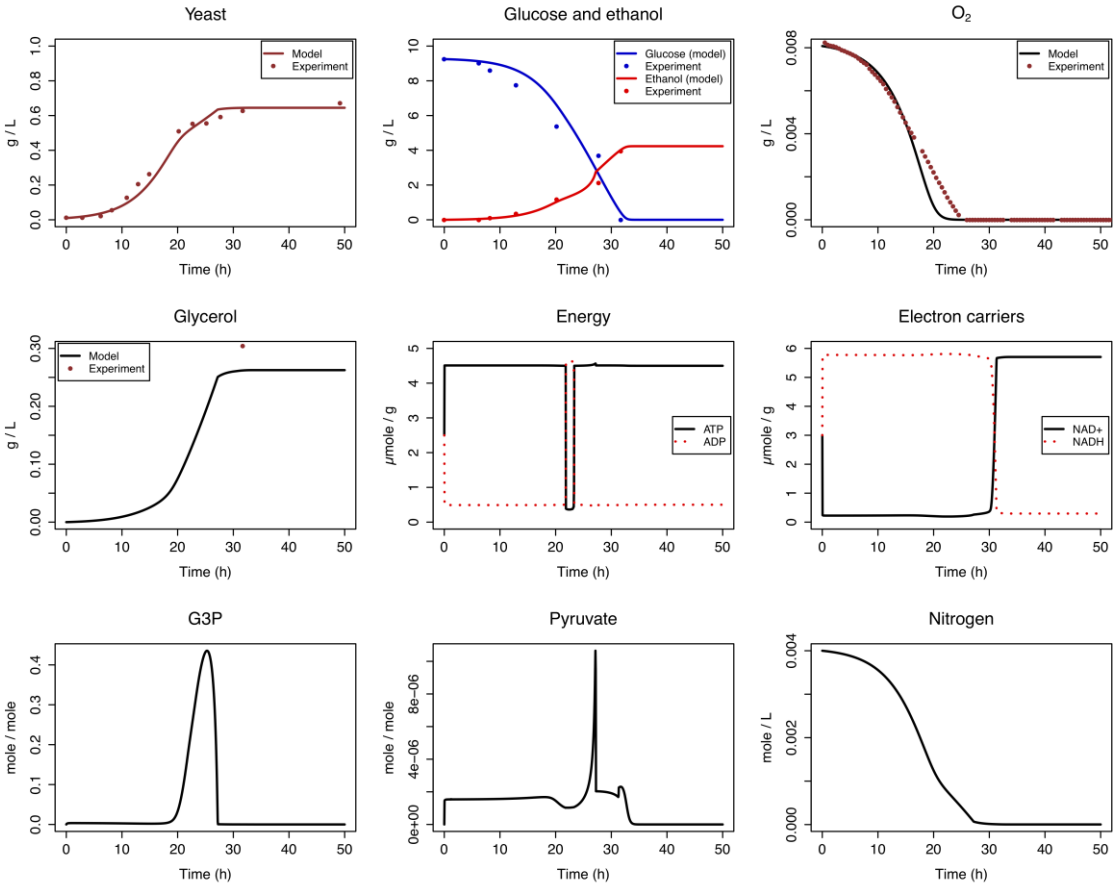

Figure 81. Simulation results with a sink term of ATP to avoid ADP depletion. Comparison with experimental data.

Once oxygen depletion occurs, the lack of ATP and NAD^+ produced by mitochondrial respiration activity reduces the biomass production. During the second stage (20-30 hours), oxygen was completely depleted and the production NAD^+ is only ensured by the ethanol and glycerol pathways with a smaller production rate, resulting in smaller growth of yeast population. The slight decrease in NAD^+ visible after 20 hours has a great effect of the Step function and reduces the pyruvate pathway. This is confirmed by the accumulation of G3P during this period. The higher level of G3P triggers the glycerol pathway, as proven by a fast increase of the glycerol concentration. This trend is in good agreement with our experimental data: the glycerol level was too low to be detected for most of samples collected throughout the culture. Besides, the production of ATP is now solely ensured by the pyruvate pathway which is slow. The ATP graph depicts a short time interval, just after 20 hours, during which ATP is depleted.

After 30 hours (third stage), the yeast growth stopped despite ATP and NAD^+ was still available to *S. cerevisiae*. The nitrogen plot from simulation results tells us that the depletion of nitrogen is responsible for the inhibition of the biomass pathway. Nitrogen is therefore the second and ultimate limiting yeast growth factor. The short period of ATP depletion ends just because the biomass pathway is the most demanding in ATP. The final yeast population was consistent with the experiment, which is simply consistent as we entered in the model the same initial value of nitrogen as in the experiment. In response to nutrient limitation, yeast generally accumulates glycogen and trehalose during fermentation and at the end, the excess of ATP and NAD^+ could be subsequently involved in the degradation of these internal reserves for cell maintenance (François 2002; Lillie and Pringle 2006). This process was not integrated in our model.

In order to further analyze the intricate coupling formulated in our model, two additional simulations were performed: one simulation without respiration and one simulation without the NAD^+/NADH balance.

6.1.5.2 Simulation without mitochondrial respiration

The same test was run but without the mitochondrial respiration pathway. This pathway was simply blocked in the model. Consequently, oxygen was not used and the NAD^+ production through the respiration pathway could not occur. This lack of electron carrier provides the biomass pathway to be boosted, limiting the yeast growth almost completely. Therefore, the mitochondrial respiration is mandatory to ensure yeast growth. In order to obtain realistic kinetics in the simulation, we had to accelerate all kinetics by a factor 1.3 and, in addition to that, the glycerol pathway by a factor 10. Doing so, the glycerol pathway is able to produce enough NAD^+ to activate the pyruvate pathway and subsequently the biomass pathway (Figure 82). As a consequence of these factor changes, the glycerol content at the end of simulation is much larger than the experimental measurement.

Without the boosting factors, the yeast growth limitation turns into a premature cessation of fermentation activity, resulting in remaining glucose in the medium. This is a common phenomenon in wine-making, called stuck fermentation, and the oxygen limitation is generally described as a cause of the deficiency in cell membrane synthesis and so, the yeast growth (Sablayrolles et al. 1996; Bisson 1999; Julien et al. 2000; Blateyron and Sablayrolles 2001). However, by removing the respiration pathway in the simulation, it seems that the lack of oxygen for respiration process should also be considered as a limiting factor for yeast growth in stuck fermentation.

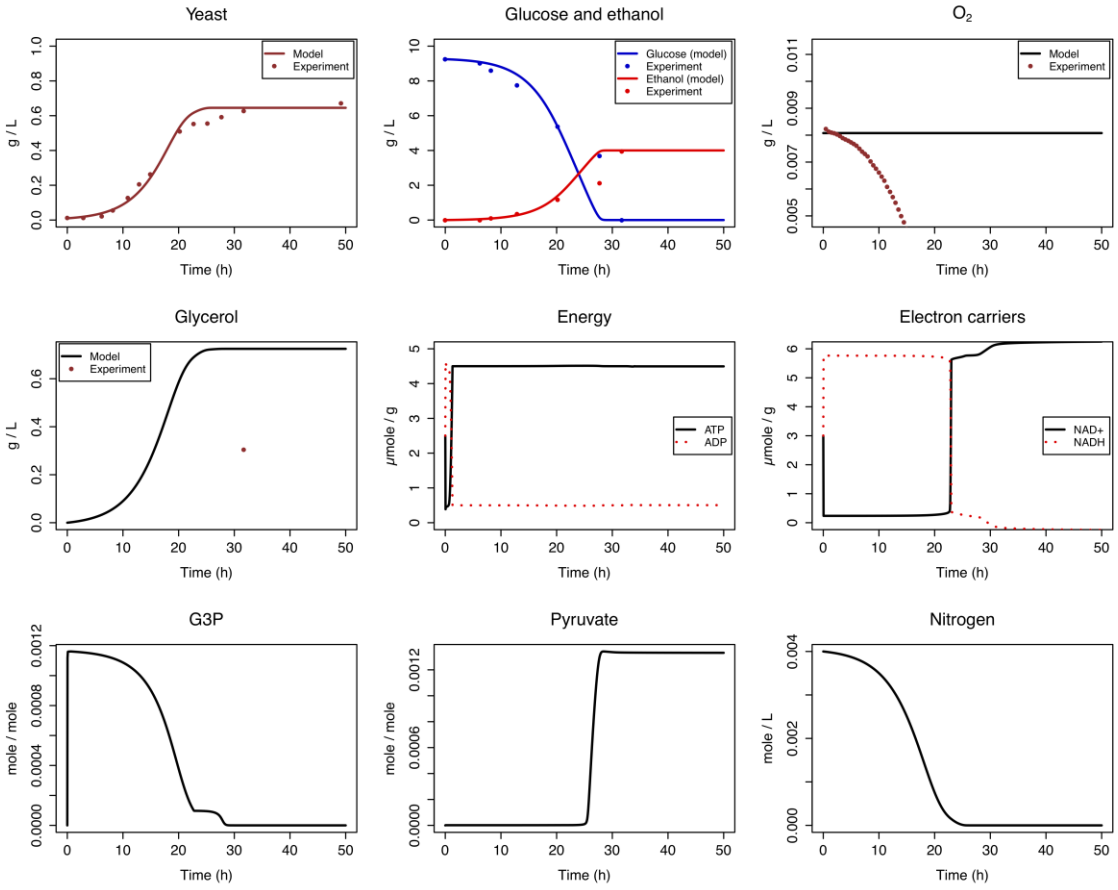

Figure 82. Simulation results, without respiration: the glycerol kinetics was multiplied by a factor 12 and all kinetics by a further factor 1.3 to get a proper time-evolution.

6.1.5.3 Simulation without limiting effects of NAD^+

Finally, we performed a test in which we cancelled any effect of NAD^+. This configuration was implemented in the simulation code by modifying the NAD^+/NADH balance in such a way to keep both concentrations equal to 0.5 * tot_{NAD}×[yeast]. In addition to the availability of reactants, the kinetics were therefore controlled only by the ATP content. In this case, no correction needed to be applied to the kinetics. One can observe on Figure 83 that the main trends remain quite good, except the glycerol pathway, which is much smaller in this case (10 times smaller than in the experiment). Because the *G3P* → *pyruvate* pathway is not any more limited by the availability in NAD^+, G3P is more devoted to the pyruvate pathway than towards glycerol. The glycerol pathway has not to be promoted anymore to produce NAD^+.

The respiration and the ethanol pathways supplied enough ATP, and NAD^+ had no limiting effect on biomass pathways, hence nitrogen was the only limiting growth factor. By reducing the number of yeast limiting growth factors to one, the specific growth rate is slightly higher than the experimental results. One can also remark that the ethanol production appears sooner, with a reduced delay between yeast growth and ethanol production.

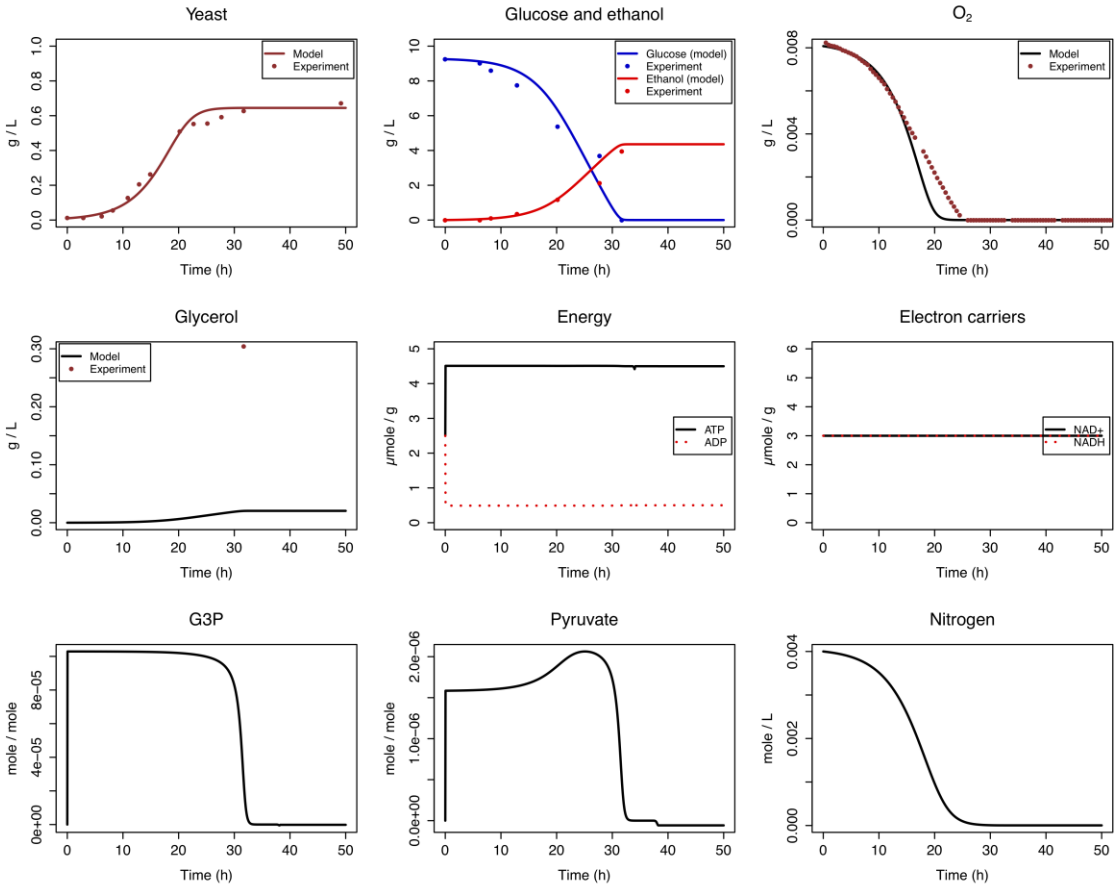

Figure 83. Simulation results, without any limiting effects of NAD^+. Comparison with experimental data.

6.1.6 Conclusion

The model developed in the present work has successfully proven its prediction potential of yeast fermentation. Resources allocation was consistent with experimental results just thanks to the limiting factor of the seven metabolic pathways. The model was built in such a way to be able to save and plot the intensity of each component and the rates of reaction versus time, making this model an essential tool to understand the interactions between the different metabolic pathways. This model pinpoints the key role of ATP and the electron carrier NAD^+ in

the yeast growth and so, revealed the crucial role of oxygen and mitochondrial respiration (without Krebs cycle) on the dynamic of yeast population.

Further developments of this model are currently in progress in our team, including the implementation of Krebs cycle, which will require a new NAD^+/NADH balance to be added in the mitochondrion. The present version is solely driven by limiting factors. The question of possible promoting effects, that could be tuned based on a global optimization of resources, is also part of our works under progress.

6.2 Microalgae individual model

6.2.1 Formulation

It has been proved that *C. vulgaris* growth in the co-dominant mixed culture was photo-autotrophic (Chapter 5). Therefore, the microalgae model developed in this study was only based on the photosynthetic activity of microalgae; the heterotrophic metabolism is not taken account. With a photo-autotrophic metabolism, the microalgae growth is limited by CO_2, nitrogen in the form of nitrate ($N\text{-}NO_3^-$), iron and light (Figure 84).

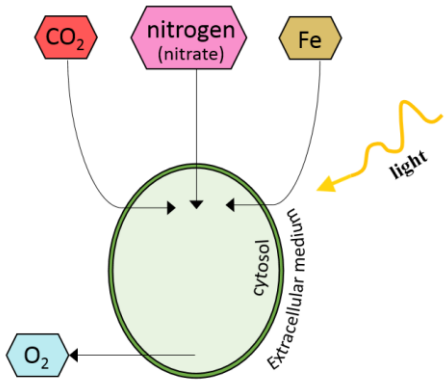

Figure 84. A schematic diagram of microalgae cell and its growth limitations with photo-autotrophic metabolism.

The configuration of the photo-bioreactor allows all its surface to be lit (Figure 85A). The light intensity I in the bioreactor follows the Beer-Lambert law: for an incident light I_0, coming

in the bioreactor, I decreases as the length of the light path r increases (Figure 85B). The lowest I value would be when r equals the radius of the bioreactor.

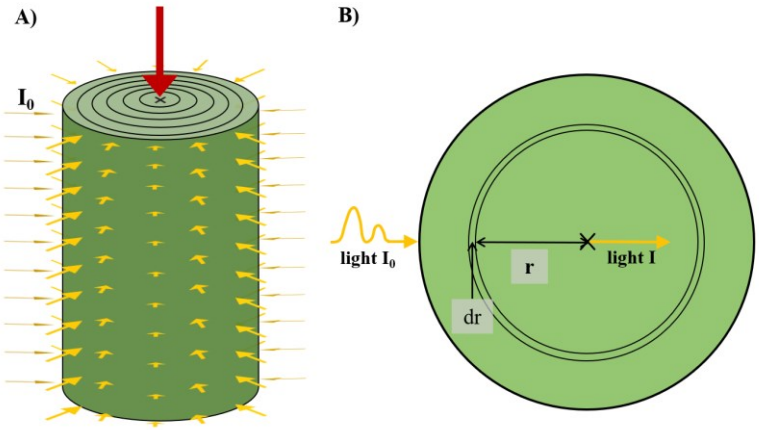

Figure 85. Light through the photo-bioreactor.

The light intensity I, previously described by Bernard and Rémond (2012), with μ_{max_algae} the maximal specific growth rate, α the initial slope of the light response curve and I_{opt} the light intensity for which growth is maximal:

$$\mu(I) = \mu_{max\_algae} \frac{I}{I + \frac{\mu_{max\_algae}}{\alpha}\left(\frac{I}{I_{opt}} - 1\right)^2} \tag{52}$$

I is calculated according the length of the light path r and the microalgal population:

$$I(r) = I_0 \, exp^{(-b\,(R-r)\,[algae])} \tag{53}$$

The decrease in I leads to a decrease in the growth rate μ, i.e. the higher r is, the lower μ is. Therefore, the average μ was calculated as the mean of growth rates across the bioreactor:

$$\mu_{mean} = \frac{\int_0^R \mu\big(I(r)\big)\, 2\pi\, r dr}{\pi\, R^2} \tag{54}$$

CO_2, Fe and $N\text{-}NO_3^-$ limitation are added to the light limitation, resulting in the microalgae growth rate μ_{algae} and the algal biomass formed can be predicted:

$$\mu_{algae} = \mu_{mean} \frac{[CO_2]}{K_{CO_2} + [CO_2]} \frac{[Fe]}{K_{Fe} + [Fe]} \frac{[N - NO_3]}{K_{N\_algae} + [N - NO_3]} \quad (55)$$

$$\frac{d[algae]}{dt} = \mu_{algae}[algae] \quad (56)$$

CO_2 is supplied to the photo-bioreactor at atmospheric concentration through continuous aeration. The CO_2 mass balance is carried out with the volumetric gas transfer K_La, taking account the consumption by microalgae:

$$\frac{d[CO_2]}{dt} = K_L a([CO_2]^* - [CO_2]) - \beta_{CO_2} \frac{d[algae]}{dt} \quad (57)$$

The photosynthetic activity leads to a production of O_2:

$$\frac{d[O_2]}{dt} = \beta_{O_2} \frac{d[algae]}{dt} \quad (58)$$

Fe is consumed by microalgae, so its concentration decreases as microalgae is growing:

$$\frac{d[Fe]}{dt} = -\gamma \frac{d[algae]}{dt} \quad (59)$$

The $N\text{-}NO_3^-$ evolution depends on the microalgae growth. The microalgal biomass is composed of 9% (w/w) nitrogen, hence the nitrogen (from nitrate) consumption reads as:

$$\frac{d[N - NO_3]}{dt} = -0.09 \frac{d[algae]}{dt} \quad (60)$$

6.2.2 Parameters

The microalgae model parameters were calculated from experimental data or adjusted from literature studies. Parameters from experiment can easily be compared to literature (Table 14).

Table 14. Microalgae model parameters from experimental date or adjusted from literature studies.

Parameters	Value	Unit	Literature review
μ_{max_algae}	0.04	h^{-1}	experimental data (0.04 [(a)] 0.036 [(b)])
α	2.1×10^{-3}	h^{-1}	2.1×10^{-3} [(c)]
I_{opt}	275	µmole. s^{-1} m^{-2}	275 [(d)]
K_{CO2}	9.2×10^{-6}	g. l^{-1}	9.2×10^{-6} [(e)]
K_{Fe}	9.0×10^{-6}	g. l^{-1}	9.5×10^{-6} [(f)]
K_{N_algae}	1.2×10^{-2}	g. l^{-1}	1.2×10^{-2} [(g)] 3.2×10^{-2} [(h)]
K_La	9.98	h^{-1}	experimental data
CO_2^*	3×10^{-4}	g. l^{-1}	experimental data
β_{CO2}	1.6	g. g^{-1}	experimental data
β_{O2}	1.2	g. g^{-1}	calculated from experimental data
γ	2.1×10^{-3}	g. g^{-1}	experimental data (2.6×10^{-3} [(i)])
I_0	1830	µmole. s^{-1} m^{-2}	experimental data
b	143	l. g^{-1} m^{-1}	experimental data (Appendix 7)

[a] Clément-Larosière et al. (2014); [b] Chang et al. (2016); [c,d] Bernard and Rémond (2012); [e] Lee et al. (2015); [f] Concas et al. (2014); [g] Xin et al. (2010), [h] Aslan and Kapdan (2006); [i] Liu et al. (2008)

The maximal growth rate μ_{max_algae} was calculated as the slope of the linear part of the logarithm of cell concentration plotted versus time. The extinction coefficient b was determined experimentally by measuring the absorbance at 600 nm of *C. vulgaris* solutions containing different concentration. Concerning CO_2 evolution, β_{CO2} is determined by assuming that the carbon content (46% w/w) of microalgae is provided from CO_2 and β_{O2} is calculated through the stoichiometric relation between CO_2 and O_2 under photo-autotrophic metabolism: a mole of CO_2 used allows to generate a mole of O_2.

6.2.3 Results

The microalgae model considers the light absorbance according to the distance from the photo-bioreactor edge and the concentration of microalgae (Figure 86). For a microalgae concentration fixed, the further from the edge the lower the light intensity. From microalgae

concentration of 0.3 g. l^{-1}, light is almost completely absorbed at the photo-bioreactor center (dr = 0.08). The model is valid when the population is dense enough, as the photo-bioreactor is illuminated all around.

The model also links the microalgae growth rate and the distance from the photo-bioreactor edge (Figure 86). Microalgae population close to the light source is photo-inhibited, hence the growth rate is lower than the maximal specific growth rate (0.04 h^{-1}). In moving away from the light source, the microalgae specific growth rate increases reaching at some point, the maximal growth rate. The higher the microalgae concentration, the lower the distance to reach the maximal specific growth rate. After the latter reached, the specific growth rate decreases because the light intensity is decreasing.

The growth model nicely predicts the microalgae growth (Figure 87). First, the growth was exponential and very quickly, became almost linear (from 70 hours). The beginning of the pseudo-linear growth was concomitant with the start of CO_2 limitation. The pseudo-linear growth was maintained thanks to the continuous and constant CO_2 supply through aeration and continuous light supply. At 70 hours, the microalgae population was 0.07 g. l^{-1} and the light intensity is zero in the center of the photo-bioreactor (Figure 86), hence light intensity could also have been the limiting factor responsible of the switch to the pseudo-linear growth.

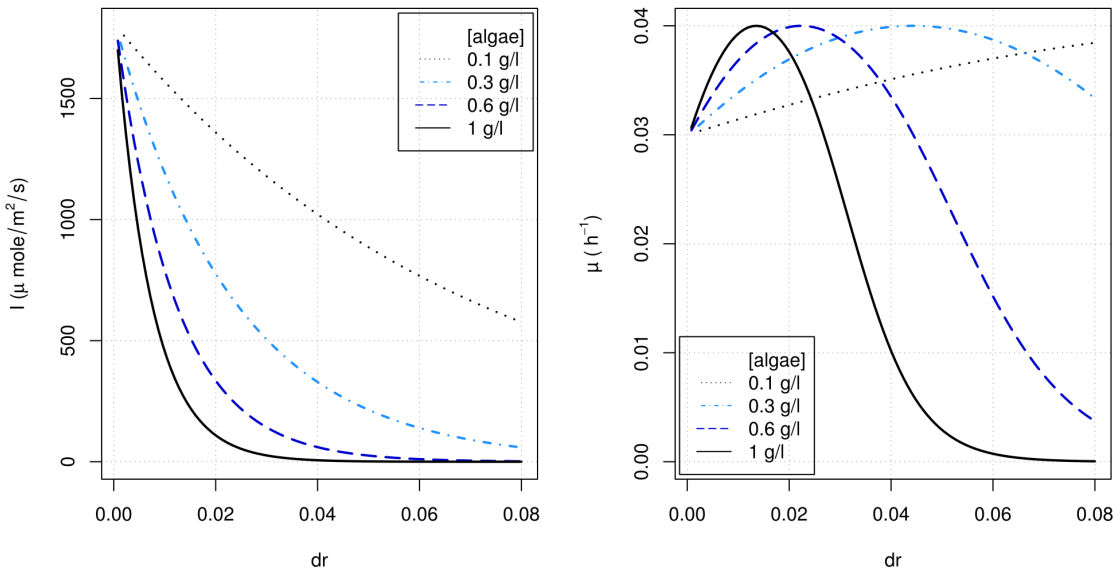

Figure 86. Light intensity (I) and growth rate (μ) according distance from the edge to the center of the photo-bioreactor (dr) and the microalgae concentration.

To determine which of CO_2 or light is the first limiting nutrient, a test was run by deleting the limiting growth effect by light (Figure 88). With CO_2, Fe and N-NO_3^- as the only limiting growth factors, the microalgae growth is identical to that when light is also considered as a limiting growth factor. Another test was run without the limiting effect of CO_2, hence light, Fe and N-NO_3^- are the only limiting factors. The microalgae growth increases very quickly within the first 200 hours and stops when Fe is depleted and at this stage, nitrogen from nitrate is still available. From these two tests, we can conclude that the first limiting growth factor is CO_2, the second is Fe, the third is N-NO_3^- and the last one is light.

Although the model predicts correctly the microalgae growth, the CO_2 prediction is not as accurate. The predicted CO_2 profile has a relatively close trend to the experimental data, but the values are lower, hence either a parameter adjustment is needed, or the sensitivity of the CO_2 probe has to be called into question.

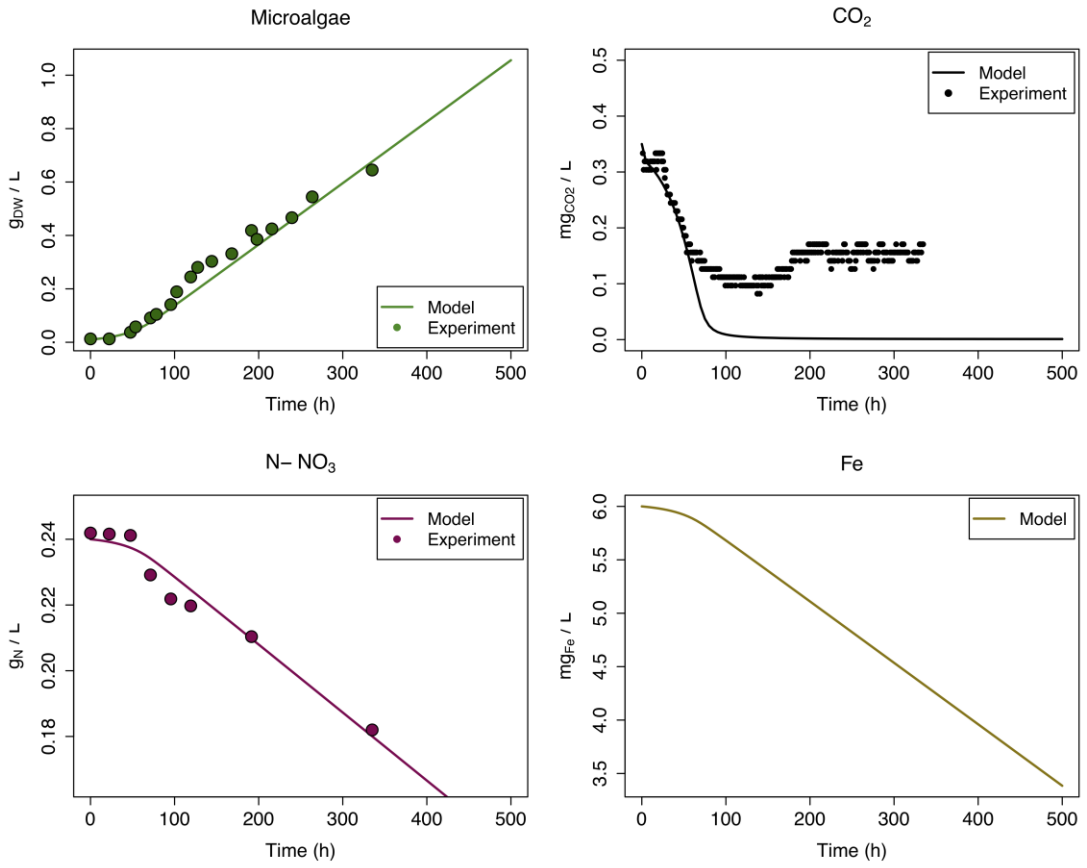

Figure 87. Simulation results of microalgae individual model.

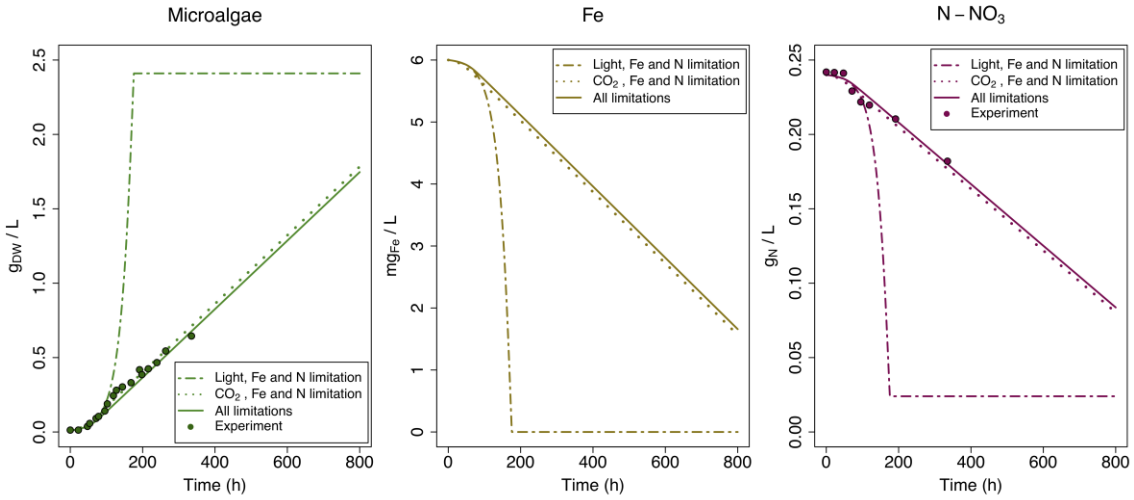

Figure 88. Effects of CO_2 and light limitation on microalgae growth.

6.3 Yeast and microalgae model in mixed culture.

6.3.1 Formulation and parameters

The development strategy of the yeast and microalgae model in mixed culture is based on the combination of the respective individual growth model. The microalgae model developed was only based on the photosynthetic activity of microalgae; the heterotrophic metabolism is not taken into account. With a photo-autotrophic metabolism, the microalgae growth is limited by CO_2, nitrogen in the form of nitrate NO_3^-, Fe and light intensity (Figure 84). The yeast model involved nitrogen (from peptone), glucose and O_2 as limiting growth factors. The model also considers the ADP/ATP and NAD^+/NADH balances as key point for yeast growth (Figure 77). The interactions between yeast and microalgae are based on CO_2/O_2 exchanges and light is attenuated by both yeast and microalgae growing population (Figure 89). The parameters are those used in yeast and microalgae individual model and the values remain unchanged.

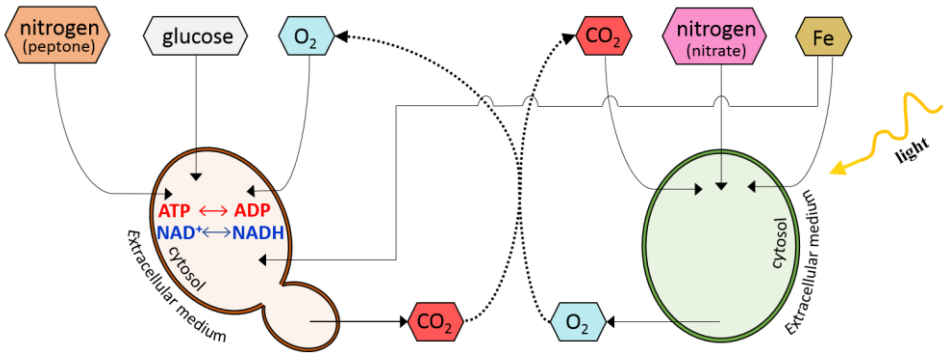

Figure 89. Yeast and microalgae growth limitation and interactions in mixed culture.

A Fe competition is also considered to simulate the rapid microalgae growth limitation in mixed culture. Fe is not only used by microalgae. Yeast also assimilates Fe to prevent from toxicity during growth and it was proved that this component was not a limiting growth factor for yeast (Chapter 5). The Fe utilization by yeast was added to the Fe balance with a coefficient ϵ (8.5×10^{-3} g. g^{-1}), adjusted from literature study (13×10^{-3} g. g^{-1} in Paš et al. 2007):

$$\frac{d[Fe]}{dt} = -\gamma\frac{d[algae]}{dt} - \epsilon\frac{\mathrm{d[yeast]}}{\mathrm{dt}} \tag{61}$$

The CO_2 balance depends on the CO_2 production by yeast (through ethanol production and Krebs cycle) and consumption by microalgae (through photosynthetic activity). The mixed culture process is not aerated, hence the CO_2 supply through continuous aeration is not taken account. Moreover, part of CO_2 produced by yeast reacts with KOH for pH adjustment and according to the study of experimental data, 60% of CO_2 produced by yeast reacted with KOH:

$$\frac{dKOH}{dt} = 0.6\frac{d[CO_2]}{dt} \tag{62}$$

$$\frac{d[CO_2]}{dt} = \frac{d[E]}{dt} + 3\frac{d[Krebs]}{dt} - \beta_{CO_2}\frac{d[algae]}{dt} - \frac{dKOH}{dt} \tag{63}$$

The time derivative of O_2 contained in the liquid phase V_{liq} depends on the mitochondrial respiration of yeast and the mass flux q_{O2} from gaseous to liquid phase (equation 50). The

photosynthetic activity also provides additional O_2 to the liquid phase and the additional yeast population decreases the light intensity:

$$\frac{d[O_2]}{dt} = -0.5\frac{d[Resp]}{dt} + \frac{q_{O_2}}{V_{liq}} + \beta_{O_2}\frac{d[algae]}{dt} \quad (64)$$

$$I(r) = I_0\, exp^{(-b\,(R-r)\,[algae+yeast])} \quad (65)$$

6.3.2 Results and discussion

The simulation results fit with the yeast and microalgae populations from experimental data. The yeast and microalgae growth stop when their respective limiting nutrient is depleted (nitrogen from peptone for yeast and iron for microalgae). Iron is used by both species and with the high yeast growth rate, the microalgae population is rapidly limited at around 0.4 g. l^{-1}, leaving a high excess of nitrate in the medium (Figure 90).

The fermentation activity of yeast is also nicely predicted: the content of ethanol and glucose fit with experimental data. Through fermentation, CO_2 is produced and partly used by microalgae and more than half reacts with alkaline KOH to maintain pH constant at 6.5. When ethanol production stops, the CO_2 content remains constant at around 1.5 g. l^{-1}; the CO_2 concentration does not decrease since the microalgae growth and CO_2 consumption stop earlier at around 20 hours (Figure 90).

The glycerol kinetics was multiplied by 70 to boost glycerol pathway and obtain a prediction of glycerol content coherent with experimental data (Figure 90). This parameter modification impacts very weakly on the ethanol content and the yeast biomass. Without this kinetics increase, the model predicts a very small glycerol production (close to 0 g. l^{-1}), just enough to supply NAD^+ required for yeast growth at the beginning. A stop of glycerol production is rapidly predicted because microalgae produce high amount of O_2 for yeast to generate NAD^+ through mitochondrial respiration (Appendix 8).

The O_2 prediction is overestimated compared to experimental data, although the simulation trend is coherent with experiments (Figure 90). Results from both simulation and experiment show three stages of O_2 evolution. The first stage (0-20 hours) is represented by an increase in O_2 content; as microalgae is growing, the microalgae photosynthesis activity is higher than the yeast respiration. The O_2 concentration decreases during the second phase (20-

30 hours), which means that the yeast respiration activity is higher than the photosynthetic activity of microalgae. In the third stage (from 30 hours), the yeast and microalgae growth stop: the microalgae photosynthetic activity stops and no O_2 is produced, also yeast respiration ceases with an arrest of O_2 consumption. The first stage of O_2 increase with simulation is higher than with experiment and the O_2 content does not reach 0 like in experiment and remains constant at around 0.014 g. l^{-1}.

According to simulation results, all O_2 produced by microalgae is not reused by yeast and the excess of O_2 could be due to a too great proportion of the microalgae photosynthetic activity as an iron limitation for microalgae reduces the photosynthetic activity (Glaesener et al. 2013). The heterotrophic metabolism of microalgae could also explain the low O_2 production in experiment.

The overestimation of O_2 could also be explained by disability of yeast to respire the additional O_2 produced by microalgae. The mitochondrial respiration requires NADH, but the latter is primarily used for glycerol production. When glycerol production ends, no more NADH remains available, then the O_2 consumption stops, which explains the constant O_2 value from 30 hours. The yeast Krebs cycle was not implemented in this model, but its involvement could regenerate NADH from NAD^+ in excess, allowing then the mitochondrial respiration. To use all remaining O_2 (0.014 g. l^{-1}), 8.8×10^{-4} mole. l^{-1} of NADH is required and this amount of co-factor can be regenerated through Krebs cycle by using 2.0×10^{-2} g. l^{-1} of glucose, i.e. 0.2% of total glucose amount available in the culture, a very low value that should not impact on the ethanol, biomass and glycerol content.

Although the overestimation of O_2 can be explained by a metabolic approach, the assumption of some O_2 loss toward the gaseous phase or even outside the photo-bioreactor cannot be ruled out.

According to the yeast individual model, the amount of O_2 available in the liquid and the gaseous phase is enough to ensure the yeast growth, therefore the additional O_2 produced by microalgae has a limited influence on yeast growth in the conditions of the mixed culture. However, CO_2 produced by yeast boost the microalgae growth, allowing *C. vulgaris* biomass to increase by 0.2 g. l^{-1} within 20 hours against 100 hours when CO_2 is supplied through continuous aeration (microalgae monoculture); the individual microalgae model shows that the *C. vulgaris* growth is firstly dictated by the CO_2 availability.

6.3.3 Conclusion

The combination of yeast and microalgae individual model is proving to be a suitable approach to predict yeast and microalgae growth in mixed culture. However, questions still arise to understand the lower O_2 content in experiment compared to the simulation results:

- reduction of microalgae photosynthetic activity under iron limitation
- involvement of microalgae heterotrophic metabolism
- activation of yeast Krebs cycle

Questions on microalgae photosynthetic activity shows that the microalgae model remains basic and needs to be completed with implementation of heterotrophy and mixotrophy metabolism for better understanding.

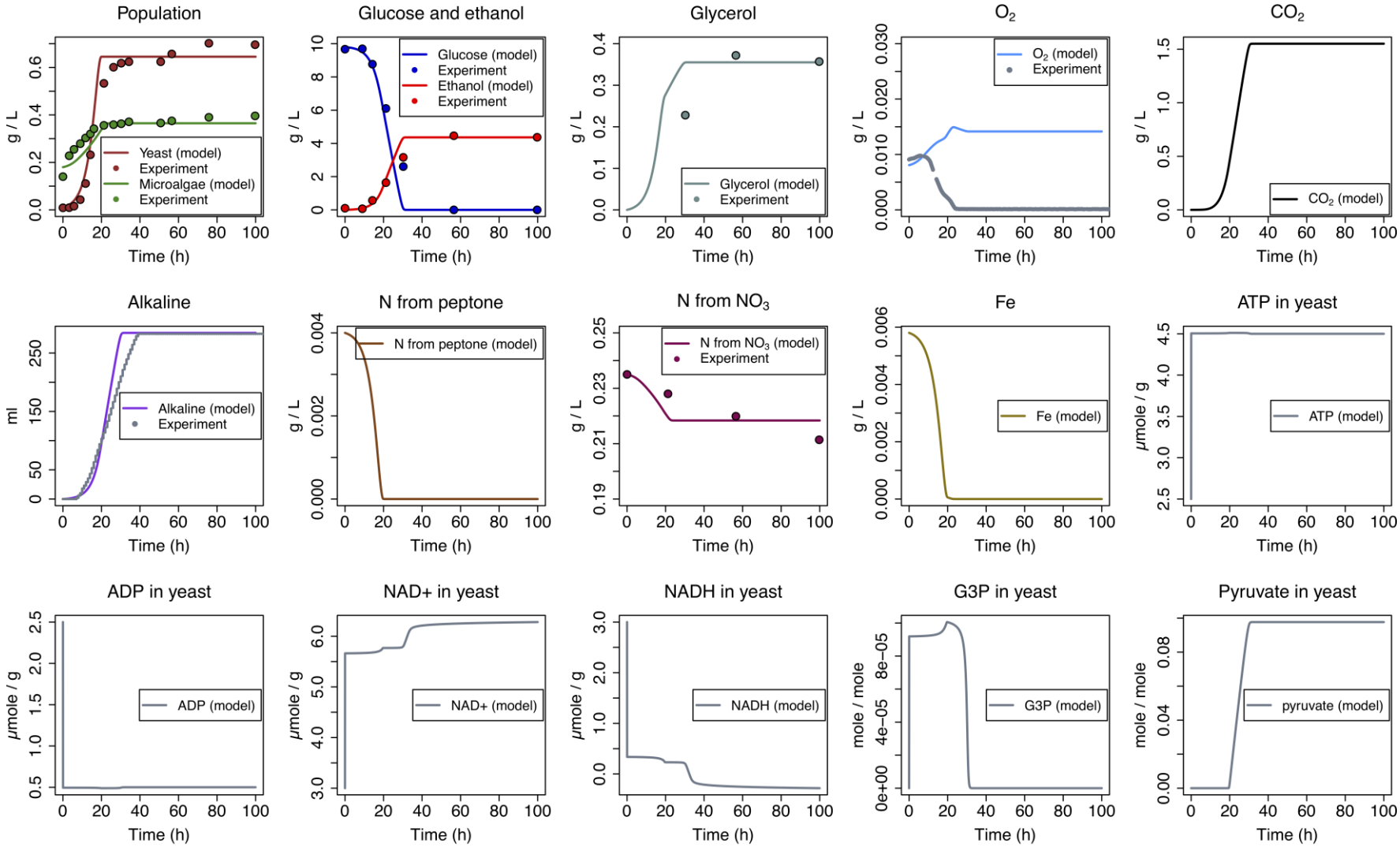

Figure 90. Simulation results of yeast and microalgae growth model in mixed culture **with** an increase of glycerol kinetic factor of 70.

General Conclusion

The aim of our work was to develop a symbiotic mixed culture of *S. cerevisiae* and *C. vulgaris* based on gas exchange in photo-bioreactor. Yeast is a heterotroph that produces CO_2 available to microalgae for photosynthesis and, in turn, microalgae generate O_2 used by yeast for respiration and membrane synthesis.

One of the major difficulties was to develop a deep knowledge on the possible metabolisms of both yeast (fermentation and respiration) and microalgae (photo-autotrophy, heterotrophy and mixotrophy). The yeast metabolisms and their occurrences are well-documented while such information concerning microalgae is less available. This complicated the construction of the symbiotic mixed culture and the identification of the metabolisms in action in the process conditions.

A literature review on cultures based on the association of yeast and microalgae allowed us to identify two process types: the coupled culture and the mixed culture process. We postulated on the advantage of the mixed culture process over the other one because both species can take advantage of the dissolved gases produced *in situ*. Then, a deep literature study on mixed cultures underlined the constant dominance of one organism over the other one in such processes. The activities of yeast and microalgae population must be balanced to ensure CO_2/O_2 balance and favor mutual symbiosis between the two populations. Consequently, in order to encourage mutual symbiosis based on gas exchanges, the mixed culture was developed in photo-bioreactor in a way that neither organism dominated the other in terms of population concentration.

The co-dominance between *S. cerevisiae* and *C. vulgaris* population was established thanks to the design of an appropriate medium, that limits yeast but promotes microalgae growth: the Mix medium. This medium was the combination between the standard autotrophic medium MBM (Modified Bristol Medium) with glucose and peptone from the standard YPG medium added for yeast (Yeast extract Peptone Glucose). The competition between the organisms in using each component of the medium influenced the biomass production yield of the two species and by comparing the physiological behavior of microalgae and yeast in monoculture and mixed culture, co-dominance and a mutual symbiosis based on *in situ* gas exchange were demonstrated. In mixed culture, the high growth rate of yeast conducted to an exclusive used of glucose and peptone by *S. cerevisiae* and *C. vulgaris* grew on a photo-autotrophic metabolism using nitrate and CO_2 for its growth. The yeast growth was limited by

amino acids and short peptides from peptone while the microalgae growth was limited by iron, a component also used by yeast not for growth but to prevent iron toxicity.

The strategy for a co-dominant mixed culture also implies the preparation of the microalgae inoculum in the Mix medium, the adjustment of the microalgae:yeast inoculum ratio to 30:1, the definition of the culture parameters in photo-bioreactor. The dissolved O_2 and CO_2 probes brought relevant measurements that allowed us to follow gas profiles. Moreover, the method developed for simultaneous cell enumeration with flow cytometry permitted to rigorously monitor the two populations in the mixed culture.

The development of the symbiotic mixed culture of *S. cerevisiae* and *C. vulgaris* was accompanied by the construction of yeast and microalgae growth models as a tool to better understand their respective metabolisms in monoculture and in mixed culture.

The yeast model developed here has successfully proven prediction potential of yeast fermentation. The model took account seven possible metabolic pathways involved in yeast, then, a Monod-like function and a smooth stepwise function were used as limiting factors on the metabolic pathways involved in yeast fermentation. Resources allocation was consistent with experimental results just by dint of the limiting factor of the seven metabolic pathways. The model was built in a way to be able to save and plot the intensity of each component versus time, making this model, an essential tool to understand the interactions between the different metabolic pathways. This model revealed the non-negligible impact of molecular oxygen and mitochondrial respiration (without Krebs cycle) on yeast fermentation.

The microalgae model developed in this study only took into account the photo-autotrophic metabolism of *C. vulgaris* with CO_2 and light as limiting growth factor. The heterotrophic and mixotrophic metabolisms were neglected as a deep study of *C. vulgaris* behavior when grown in mixed culture, allowed us to rule on the photo-autotrophic growth of microalgae. The model fit with experimental data from the *C. vulgaris* monoculture in photo-autotrophic conditions.

The yeast and microalgae model were combined in order to construct the model of yeast and microalgae growth in mixed culture. The simulation results were consistent with the experimental data and the comparison between experimental and simulations results is a key way to understanding the behavior of each species when grown alone and in mixed culture.

With the experimental work and the modelling part, the synergy based on gas exchange in the mixed culture process has been shown with a greater benefit for microalgae than for yeast: CO_2 from yeast highly boosted the microalgae growth while O_2 from microalgae photosynthesis had a limited positive impact on yeast growth.

Various perspectives emerge from this work, either to better understand and optimize the mixed culture process of *S. cerevisiae* and *C. vulgaris* or to refine the model proposed.

For the experimental aspects, the design of a medium whose nitrogen source available to yeast is better-defined, could allow to monitor the nitrogen utilization precisely. The peptone could be replaced by a mixture of amino-acids and ammonium. The choice of amino acids should depend on the preferred amino acids assimilable by yeast and their concentration should always be defined by ensuring co-dominance between yeast and microalgae. For the latter, nitrate could be kept as a nitrogen source exclusively available to microalgae.

Iron utilization by yeast and microalgae deserves to be thoroughly studied to allow an optimization of the medium by adjusting the iron concentration. Iron utilization in both yeast and microalgae monoculture could be firstly monitored and compared to that in mixed culture. This approach is mostly important to understand the microalgae photosynthetic activity in iron limitation conditions.

Continuous culture could be imagined for the mixed culture process to ensure the co-dominance between yeast and microalgae. With the continuous system, the culture is carried out in an open fermenter, with nutrients added and products removed at a steady rate throughout. In this configuration, the cell density remains constant by maintaining defined and constant dilution and flow rate, hence the co-dominance of yeast and microalgae could be optimized. The Steady-state continuous culture is a perspective that could be interesting for industrial applications as it allows continuous reaction with no idle time, to reduce labor time and to increase the productivity. However, the disadvantage of continuous culture is that there is a higher risk of contamination due to the constant adjustments and the strains should also be genetically stable.

The yeast and microalgae individual growth model could be enhanced to be more predictive. The Krebs cycle could be implemented in the yeast model and the strategy used to construct yeast model could be applied to the microalgae. In this manner, all the pathways involved in photo-autotrophy, heterotrophy and mixotrophy metabolism could be integrated in the model and kinetics factors should be imposed to predict the partition of the pathways.

In conclusion, this study was conducted with *S. cerevisiae* and *C. vulgaris*, two model species and all strategy developed can be adapted to any heterotroph and autotroph for the construction of symbiotic mixed culture process based on gas exchanges. Hence, this work and the proposed enhancement open the perspective for *in situ* CO_2 mitigation, full utilization of the organic substrate and a reduction in aeration costs of biotransformation processes.

References

A W Hom EFYM (2015) Niche Engineering Demonstrates a Latent Capacity for Fungal- Algal Mutualism. Science (80-) 345:94–98 . doi: 10.1126/science.1253320.Niche

Abinandan S, Shanthakumar S (2016) Evaluation of photosynthetic efficacy and CO_2 removal of microalgae grown in an enriched bicarbonate medium. 3 Biotech 6:1–9 . doi: 10.1007/s13205-015-0314-5

Adamczyk M, Lasek J, Skawińska A (2016) CO_2 Biofixation and Growth Kinetics of *Chlorella vulgaris* and Nannochloropsis gaditana. Appl Biochem Biotechnol 179:1248–1261 . doi: 10.1007/s12010-016-2062-3

Aiba S, Shoda M, Nagatani M (1969) Kinetics of product inhibition in alcohol fermentation-temperature effect in the “sake” brewing. Biotechnol Bioeng 11:1285–1287 . doi: 10.1002/bit.260110621

Albers E, M. Bakker B, Gustafsson L (2002) Modeling response of glycolysis in *S. cerevisiae* cells harvested at diauxic shift. Mol Biol Rep 119–123

Aldiguier AS, Alfenore S, Cameleyre X, Goma G, Uribelarrea JL, Guillouet SE, Molina-Jouve C (2004) Synergistic temperature and ethanol effect on *Saccharomyces cerevisiae* dynamic behaviour in ethanol bio-fuel production. Bioprocess Biosyst Eng 26:217–222 . doi: 10.1007/s00449-004-0352-6

Alexander MA, Jeffries TW (1990) Respiratory efficiency and metabolite partitioning as regulatory phenomena in yeasts. Enzyme Microb Technol 12:2–19 . doi: 10.1016/0141-0229(90)90173-N

Andaluz S, López-Millán AF, De Las Rivas J, Aro EM, Abadía J, Abadía A (2006) Proteomic profiles of thylakoid membranes and changes in response to iron deficiency. Photosynth Res 89:141–155 . doi: 10.1007/s11120-006-9092-6

Arumugam A, Sandhya M, Ponnusami V (2014) Biohydrogen and polyhydroxyalkanoate co-production by *Enterobacter aerogenes* and *Rhodobacter sphaeroides* from *Calophyllum inophyllum* oil cake. Bioresour Technol 164:170–176 . doi: 10.1016/j.biortech.2014.04.104

Aslan S, Kapdan IK (2006) Batch kinetics of nitrogen and phosphorus removal from synthetic wastewater by algae. Ecol Eng 28:64–70 . doi: 10.1016/j.ecoleng.2006.04.003

Baba M, Shiraiwa Y (2007) High-CO_2 Response Mechanisms in Microalgae. Adv Photosynth - Fundam Asp 2:299–320 . doi: 10.5772/27737

Bakker B, Overkamp K (2001) Stoichiometry and compartmentation of NADH metabolism in *Saccharomyces cerevisiae*. FEMS Microbiol Rev 15–37

Beck C, Kaspar von Meyenburg H (1968) Enzyme Pattern and Aerobic Growth of

Saccharomyces cerevisiae Under Various Degrees of Glucose Limitation Enzyme Pattern and Aerobic Growth of *Saccharomyces cerevisiae* Under Various Degrees of Glucose Limitation. J Bacteriol 96:479–486

Ben Amor-Ben Ayed H, Taidi B, Ayadi H, Pareau D, Stambouli M (2015) Effect of magnesium ion concentration in autotrophic cultures of *Chlorella vulgaris*. Algal Res 9:291–296 . doi: 10.1016/j.algal.2015.03.021

Ben Amor-Ben Ayed H, Taidi B, Ayadi H, Pareau D, Stambouli M (2017) The Use of *Chlorella vulgaris* to Accumulate Magnesium under Different Culture Conditions. J Appl Biotechnol Bioeng 2:180–185

Bernard O, Rémond B (2012) Validation of a simple model accounting for light and temperature effect on microalgal growth. Bioresour Technol 123:520–527 . doi: 10.1016/j.biortech.2012.07.022

Bhola V, Desikan R, Santosh SK, Subburamu K, Sanniyasi E, Bux F (2011) Effects of parameters affecting biomass yield and thermal behaviour of *Chlorella vulgaris*. J Biosci Bioeng 111:377–382 . doi: 10.1016/j.jbiosc.2010.11.006

Bisson LF (1999) Stuck and Sluggish Fermentations. Am J Enol Vitic 50:107–119

Blateyron L, Sablayrolles J-M (2001) Stuck and Slow Fermentations in Enology: Statistical Study of Causes and Effectiveness of Combined Additions of Oxygen and Diammonium Phosphate. J Biosci Bioeng 91:184–189 . doi: https://doi.org/10.1016/S1389-1723(01)80063-3

Boulton C, Quain D (2001) Brewing Yeast and Fermentation, The Instit. Blackwell Science (UK)

Bovee JP, Strehaiano P, Goma G, Sevely Y (1984) Alcoholic fermentation: Modelling based on sole substrate and product measurement. Biotechnol Bioeng 26:328–334 . doi: 10.1002/bit.260260406

Boyle NR, Morgan JA (2009) Flux balance analysis of primary metabolism in *Chlamydomonas reinhardtii*. BMC Syst Biol 3:1–14 . doi: 10.1186/1752-0509-3-4

Cai S, Hu C, Du S (2007) Comparisons of growth and biochemical composition between mixed culture of alga and yeast and monocultures. J Biosci Bioeng 104:391–397 . doi: 10.1263/jbb.104.391

Chaney D, Rodriguez S, Fugelsang K, Thornton R (2006) Managing high-density commercial scale wine fermentations. J Appl Microbiol 100:689–698 . doi: 10.1111/j.1365-2672.2006.02839.x

Chang HX, Huang Y, Fu Q, Liao Q, Zhu X (2016) Kinetic characteristics and modeling of microalgae *Chlorella vulgaris* growth and CO_2 biofixation considering the coupled effects of light intensity and dissolved inorganic carbon. Elsevier Ltd

Charoenbhakdi S, Dokpikul T, Burphan T, Techo T, Auesukaree C (2016) Vacuolar H^+-ATPase Protects Saccharomyces cerevisiae Cells against Ethanol-Induced Oxidative and

Cell Wall Stresses. Appl Environ Microbiol 82:3121–3130 . doi: 10.1128/AEM.00376-16

Cheirsilp B, Kitcha S, Torpee S (2011a) Co-culture of an oleaginous yeast *Rhodotorula glutinis* and a microalga *Chlorella vulgaris* for biomass and lipid production using pure and crude glycerol as a sole carbon source. Ann Microbiol 62:987–993 . doi: 10.1007/s13213-011-0338-y

Cheirsilp B, Suwannarat W, Niyomdecha R (2011b) Mixed culture of oleaginous yeast *Rhodotorula glutinis* and microalga *Chlorella vulgaris* for lipid production from industrial wastes and its use as biodiesel feedstock. N Biotechnol 28:362–368 . doi: 10.1016/j.nbt.2011.01.004

Chen CY, Yeh KL, Aisyah R, Lee DJ, Chang JS (2011) Cultivation, photobioreactor design and harvesting of microalgae for biodiesel production: A critical review. Bioresour Technol 102:71–81 . doi: 10.1016/j.biortech.2010.06.159

Cho BH, Sauer N, Komor E, Tanner W (1981) Glucose induces two amino acid transport systems in *Chlorella*. Proc Natl Acad Sci U S A 78:3591–4 . doi: 10.1073/pnas.78.6.3591

Clément-Larosière B, Lopes F, Taidi B, Benedetti M, Minier M, Pareau D (2014) Carbon dioxide biofixation by *Chlorella vulgaris* at different CO_2 concentrations and light intensities. Eng Life Sci 14: . doi: https://doi.org/10.1002/elsc.201200212

Coleman MC, Fish R, Block DE (2007) Temperature-dependent kinetic model for nitrogen-limited wine fermentations. Appl Environ Microbiol 73:5875–5884 . doi: 10.1128/AEM.00670-07

Concas A, Steriti A, Pisu M, Cao G (2014) Comprehensive modeling and investigation of the effect of iron on the growth rate and lipid accumulation of *Chlorella vulgaris* cultured in batch photobioreactors. Bioresour Technol 153:340–350 . doi: 10.1016/j.biortech.2013.11.085

Cramer AC, Vlassides S, Block DE (2002) Kinetic model for nitrogen-limited wine fermentations. Biotechnol Bioeng 77:49–60 . doi: 10.1002/bit.10133

Cullen JJ, Yang X, MacIntyre HL (1992) Nutrient limitation of marine photosynthesis. Prim Product Biogemichal Cycles Sea 69–88 . doi: 10.1007/978-1-4899-0762-2_5

da Silva Ferreira V, Sant'Anna C (2017) Impact of culture conditions on the chlorophyll content of microalgae for biotechnological applications. World J Microbiol Biotechnol 33: . doi: 10.1007/s11274-016-2181-6

Dashko S, Zhou N, Compagno C, Piškur J (2014) Why, when, and how did yeast evolve alcoholic fermentation? FEMS Yeast Res. 14:826–832

de-Bashan LE, Bashan Y, Moreno M, Lebsky VK, Bustillos JJ (2002) Increased pigment and lipid content, lipid variety, and cell and population size of the microalgae *Chlorella* spp. when co-immobilized in alginate beads with the microalgae-growth-promoting bacterium *Azospirillum brasilense*. Can J Microbiol 48:514–521 . doi: 10.1139/w02-051

De Deken RH (1966) The Crabtree Effect: A Regulatory System in Yeast. J Gen Microbiol

44:149–156 . doi: 10.1099/00221287-44-2-149

De Freitas J, Wintz H, Kim JH, Poynton H, Fox T, Vulpe C (2003) Yeast, a model organism for iron and copper metabolism studies. BioMetals 16:185–197 . doi: 10.1023/A:1020771000746

Dillschneider R, Schulze I, Neumann A, Posten C, Syldatk C (2014) Combination of algae and yeast fermentation for an integrated process to produce single cell oils. Appl Microbiol Biotechnol 98:7793–7802 . doi: 10.1007/s00253-014-5867-4

Dong QL, Zhao XM (2004) In situ carbon dioxide fixation in the process of natural astaxanthin production by a mixed culture of *Haematococcus pluvialis* and *Phaffia rhodozyma*. Catal Today 98:537–544 . doi: 10.1016/j.cattod.2004.09.052

Edwards TJ, Maurer G, Newman J, Prausnitz JM (1978) Vapor-liquid equilibria in multicomponent aqueous solutions of volatile weak electrolytes. AIChE J 24:966–976 . doi: 10.1002/aic.690240605

Endo H, Sansawa H, Nakajima K (1977) Studies on *Chlorella regularis* Heterotrophic Fast Growing Strain Part 2 Mixotrophic Growth in Relation To Light Intensity and Acetate Concentration. Plant Cell Physiol 18:199–205

Falkowski PG, Raven JA (2007) An Introduction to Photosynthesis in Aquatic Systems. Aquat Photosynth 1–44 . doi: 10.1017/CBO9781107415324.004

Fiechter A, Seghezzi W (1992) Regulation of glucose metabolism in growing yeast cells. J Biotechnol 27:27–45 . doi: 10.1016/0168-1656(92)90028-8

François J (2002) Reserve carbohydrates metabolism in the yeast *Saccharomyces cerevisiae*. FEMS Microbiol Rev 25:125–145 . doi: 10.1016/s0168-6445(00)00059-0

Franzén CJ (2003) Metabolic flux analysis of RQ-controlled microaerobic ethanol production by *Saccharomyces cerevisiae*. Yeast 20:117–132 . doi: 10.1002/yea.956

Gancedo C, Gancedo JM, Sols A (1968) Glycerol metabolism in yeasts pathways of utilization and production. Can J Biochem 5:165–17214 . doi: 10.1139/o68-165

Garcia-Ochoa F, Gomez E, Santos VE, Merchuk JC (2010) Oxygen uptake rate in microbial processes: An overview. Biochem Eng J 49:289–307 . doi: 10.1016/j.bej.2010.01.011

Gargas A, DePriest PT, Grube M, Tehler A (1995) Multiple origins of lichen symbioses in fungi suggested by SSU rDNA phylogeny. Science (80-) 268:1492–1495

Gervais P, de Marañon IM (1995) Effect of the kinetics of temperature variation on *Saccharomyces cerevisiae* viability and permeability. BBA - Biomembr 1235:52–56 . doi: 10.1016/0005-2736(94)00299-5

Giovanelli G, Peri C, Parravicini E (1996) Kinetics of grape juice fermentation under aerobic and anaerobic conditions. Am J Enol Vitic 47:429–434

Girard JM, Roy ML, Hafsa M Ben, Gagnon J, Faucheux N, Heitz M, Tremblay R, Deschênes JS

(2014) Mixotrophic cultivation of green microalgae *Scenedesmus obliquus* on cheese whey permeate for biodiesel production. Algal Res 5:241–248 . doi: 10.1016/j.algal.2014.03.002

Glaesener AG, Merchant SS, Blaby-Haas CE (2013) Iron economy in *Chlamydomonas reinhardtii*. Front Plant Sci 4:1–12 . doi: 10.3389/fpls.2013.00337

Goldman JC (1977) Biomass production in mass cultures of marine phytoplankton at varying temperatures. J Exp Mar Bio Ecol 27:161–169 . doi: 10.1016/0022-0981(77)90136-8

Gomez JA, Höffner K, Barton PI (2016) From sugars to biodiesel using microalgae and yeast. Green Chem 18:461–475 . doi: 10.1039/c5gc01843a

Griffiths DJ, Thresher CL, Street HE (1960) The heterotrophic nutrition of *Chlorella vulgaris*. Annu Bot 2:1–11

Großkopf T, Soyer OS (2014) Synthetic microbial communities. Curr Opin Microbiol 18:72–77 . doi: 10.1016/j.mib.2014.02.002

Hachiya T, Terashima I, Noguchi KO (2007) Increase in respiratory cost at high growth temperature is attributed to high protein turnover cost in Petunia ¥ hybrida petals. Plant, Cell Environ 30:1269–1283 . doi: 10.1111/j.1365-3040.2007.01701.x

Haggstrom MH, Dostalek M (1981) Regulation of a mixed culture of Streptococcus lactis and Saccharomycopsis fibuliger. Eur J Appl Microbiol Biotechnol 12:216–219 . doi: 10.1007/BF00499490

Hagman A, Piškur J (2015) A study on the fundamental mechanism and the evolutionary driving forces behind aerobic fermentation in yeast. PLoS One 10:1–24 . doi: 10.1371/journal.pone.0116942

Hagman A, Säll T, Piškur J (2014) Analysis of the yeast short-term Crabtree effect and its origin. FEBS J 281:4805–4814 . doi: 10.1111/febs.13019

Henschke PA (1997) Stuck fermentation: causes, prevention and cure. Allen, M, Leske, P, Baldwin, G (Eds), Adv juice clarification yeast inoculation Proc ASVO oenology Semin Melbourne, Victoria (Australian Soc Vitic Oenology Adelaide, SA), 41:30–38

Herman PK (2002) Stationary phase in yeast. Curr Opin Microbiol 5:602–607 . doi: 10.1016/S1369-5274(02)00377-6

Holmes-Hampton GP, Jhurry ND, McCormick SP, Lindahl PA (2013) Iron content of *Saccharomyces cerevisiae* cells grown under iron-deficient and iron-overload conditions. Biochemistry 52:105–114 . doi: 10.1021/bi3015339

Holzberg I, Finn RK, Steinkraus KH (1967) A kinetic study of the alcoholic fermentation of grape juice. Biotechnol Bioeng 9:413–427 . doi: 10.1002/bit.260090312

Hong S-J, Lee C-G (2007) Evaluation of central metabolism based on a genomic database of *Synechocystis* PCC6803. Biotechnol Bioprocess Eng 12:165–173

Hu ZC, Zheng YG, Wang Z, Shen YC (2005) Effect of sugar-feeding strategies on astaxanthin production by *Xanthophyllomyces dendrorhous*. World J Microbiol Biotechnol 21:771–775 . doi: 10.1007/s11274-004-5566-x

Johnson EA, An GH (1991) Astaxanthin from microbial sources. Crit Rev Biotechnol 11:297–326 . doi: 10.3109/07388559109040622

Jouhten P, Rintala E, Huuskonen A, Tamminen A, Toivari M, Wiebe M, Ruohonen L, Penttilä M, Maaheimo H (2008) Oxygen requirements for formation and activity of the squalene epoxidase in <i>Saccharomyces cerevisiae/i>. BMC Syst Biol 60:1–19 . doi: 10.1186/1752-0509-2-60

Julien A, Roustan JL, Dulau L, Sablayrolles JM (2000) Comparison of nitrogen and oxygen demands of enological yeasts: Technological consequences. Am J Enol Vitic 51:215–222

Kaplan J, McVey Ward D, Crisp RJ, Philpott CC (2006) Iron-dependent metabolic remodeling in *S. cerevisiae*. Biochim Biophys Acta - Mol Cell Res 1763:646–651 . doi: 10.1016/j.bbamcr.2006.03.008

Käppeli O, Arreguin M, Rieger M (1985) The respirative breakdown of glucose by *Saccharomyces cerevisiae*: an assessment of a physiological state. J Gen Microbiol 131:1411–6

Klein C, Olsson L, Nielsen J (1998) Glucose control in *Saccharomyces cerevisiae* : the role of M/G7 in metabolic functions. Int J Syst Evol Microbiol 13–24

Kobayashi M, Kakizono T, Yamaguchi K, Nishio N, Nafai S (1992) Growth and Astaxanthin Formation of *Haematococcus pluvialis* in Heterotrophic and Mixotrophic Conditions. J Ferment Bioeng 74:17–20

Koç A, Wheeler LJ, Mathews CK, Merrill GF (2004) Hydroxyurea Arrests DNA Replication by a Mechanism that Preserves Basal dNTP Pools. J Biol Chem 279:223–230 . doi: 10.1074/jbc.M303952200

Kojima E, Zhang K (1999) Growth and hydrocarbon production of microalga *Botryococcus braunii* in bubble column photobioreactors. J Biosci Bioeng 87:811–815 . doi: 10.1016/S1389-1723(99)80158-3

Kröger M, Müller-Langer F (2011) Impact of heterotrophic and mixotrophic growth of microalgae on the production of future biofuels. Biofuels 2:145–151 . doi: 10.4155/bfs.11.5

Kumar A, Ergas S, Yuan X, Sahu A, Zhang Q, Dewulf J, Malcata FX, van Langenhove H (2010) Enhanced CO_2 fixation and biofuel production via microalgae: Recent developments and future directions. Trends Biotechnol 28:371–380 . doi: 10.1016/j.tibtech.2010.04.004

La A, Perré P, Taidi B (2019) Process for symbiotic culture of *Saccharomyces cerevisiae* and *Chlorella vulgaris* for in situ CO_2 mitigation. Appl Microbiol Biotechnol 103:731–745 . doi: 10.1007/s00253-018-9506-3

Lalibertè G, de la Noüie J (1993) Auto-, Hetero-, and Mixotrophic Growth of *Chlamydomonas Humicola* (Chlorophyceae) on Acetate. J. Phycol. 29:612–620

Lannig R (2015) Impact du dioxyde de carbone sur la levure Saccharomyces cerevisiae : caractérisation du transfert liquide/gaz et implications sur les métabolismes énergétiques. Toulouse

Larsson C, Axelsson L (1999) Bicarbonate uptake and utilization in marine macroalgae. Eur J Phycol 34:79–86 . doi: 10.1080/09670269910001736112

Lebsky VK, Gonzalez-Bashan LE, Bashan Y (2001) Ultrastructure of interaction in alginate beads between the microalga *Chlorella vulgaris* with its natural associative bacterium *Phyllobacterium myrsinacearum* and with the plant growth-promoting bacterium *Azospirillum brasilense*. Can J Microbiol 47:1–8 . doi: 10.1139/cjm-47-1-1

Lee E, Jalalizadeh M, Zhang Q (2015) Growth kinetic models for microalgae cultivation: A review. Algal Res 12:497–512 . doi: 10.1016/j.algal.2015.10.004

Lee YK, Lim BS, Kim CW (2004) Influence of illuminating and viewing aperture size on the color of dental resin composites. Dent Mater 20:116–123 . doi: 10.1016/S0109-5641(03)00072-1

Leesing R, Baojungharn R, Papone T (2012) Microbial Oil Production by Mixed Culture of Microalgae *Chlorella sp.* KKU-S2 and Yeast *Torulaspora maleeae* Y30. Int J Biol Biomol Agric Food Biotechnol Eng 6:247–250

Liang Y, Sarkany N, Cui Y (2009) Biomass and lipid productivities of *Chlorella vulgaris* under autotrophic, heterotrophic and mixotrophic growth conditions. Biotechnol Lett 31:1043–1049 . doi: 10.1007/s10529-009-9975-7

Liao Q, Sun Y, Huang Y, Xia A, Fu Q, Zhu X (2017) Simultaneous enhancement of *Chlorella vulgaris* growth and lipid accumulation through the synergy effect between light and nitrate in a planar waveguide flat-plate photobioreactor. Bioresour Technol 243:528–538 . doi: 10.1016/j.biortech.2017.06.091

Lillie SUEH, Pringle JR (2006) Reserve Carbohydrate Metabolism in *Saccharomyces cerevisiae*: Responses to Nutrient Limitation. J Bacteriol 143:1–11

Liu CG, Lin YH, Bai FW (2011) A kinetic growth model for *Saccharomyces cerevisiae* grown under redox potential-controlled very-high-gravity environment. Biochem Eng J 56:63–68 . doi: 10.1016/j.bej.2011.05.008

Liu ZY, Wang GC, Zhou BC (2008) Effect of iron on growth and lipid accumulation in *Chlorella vulgaris*. Bioresour Technol 99:4717–4722 . doi: 10.1016/j.biortech.2007.09.073

López A, Secanell P (1992) A simple mathematical empirical model for estimating the rate of heat generation during fermentation in white-wine making. Int J Refrig 15:276–280 . doi: 10.1016/0140-7007(92)90042-S

Macy JM, Miller MW (1983) Anaerobic growth of *Saccharomyces cerevisiae* in the absence of

oleic acid and ergosterol? Arch Microbiol 134:64–67 . doi: 10.1007/BF00429409

Magdouli S, Brar SK, Blais JF (2016) Co-culture for lipid production: Advances and challenges. Biomass and Bioenergy 92:20–30 . doi: 10.1016/j.biombioe.2016.06.003

Marquez FJ, Ken S, Kakizono T, Nishio N, Nagap S (1993) Growth Characteristics of *Spirulina platensis* in Mixotrophic and Heterotrophic Conditions. J Ferment Bioeng 76:408–410

Martinez F, Ascaso C, Orus MI (1991) Morphometric and Stereologic Analysis of *Chlorella vulgaris* under Heterotrophic Growth-Conditions. Ann Bot 67:239–245 . doi: 10.1093/oxfordjournals.aob.a088128

Masojídek J, Torzillo G, Koblížek M (2013) Photosynthesis in Microalgae. Handb Microalgal Cult Appl Phycol Biotechnol 21–36 . doi: 10.1002/9781118567166.ch2

Matsuda Y, Hara T, Colman B (2001) Regulation of the induction of bicarbonate uptake by dissolved CO_2 in the marine diatom, Phaeodactylum tricornutum. Plant, Cell Environ 24:611–620 . doi: 10.1046/j.1365-3040.2001.00702.x

McAuley PJ (1987) Planta Nitrogen limitation and amino-acid metabolism. Planta 171:532–538

Meijer MMC, Boonstra J, Verkleij AJ, Verrips CT (1998) Glucose repression in *Saccharomyces cerevisiae* is related to the glucose concentration rather than the glucose flux. J Biol Chem 273:24102–24107 . doi: 10.1074/jbc.273.37.24102

Milledge JJ, Heaven S (2013) A review of the harvesting of micro-algae for biofuel production. Rev Environ Sci Biotechnol 12:165–178 . doi: 10.1007/s11157-012-9301-z

Mitra D, van Leeuwen J (Hans), Lamsal B (2012) Heterotrophic/mixotrophic cultivation of oleaginous *Chlorella vulgaris* on industrial co-products. Algal Res 1:40–48 . doi: 10.1016/j.algal.2012.03.002

Molina Grima E, Garcia Carnacho F, Sanchez Perez J a, Fernandez Sevilla JM, Acien Fernandez FG, Contreras Gomez a (1994) in Light-Limited Chemostat Culture. J Chem Technol Biotechnol 61:167–173 . doi: 10.1002/jctb.280610212

Muñoz-Blanco J, Hidalgo-Martínez J, Cárdenas J (1990) Extracellular deamination of amino acids by *Chlamydomonas reinhardtii* cells. Planta 182:194–198 . doi: 10.1007/BF00197110

Murphree CA, Dums JT, Jain SK, Zhao C, Young DY, Khoshnoodi N, Tikunov A, Macdonald J, Pilot G, Sederoff H (2017) Amino Acids Are an Ineffective Fertilizer for *Dunaliella spp.* Growth. Front Plant Sci 8:847 . doi: 10.3389/fpls.2017.00847

Neilson AH, Lewin RA (1974) The uptake and utilization of organic carbon by algae : an essayin comparative biochemistry. Phycologia 13:227–264 . doi: 10.2216/i0031-8884-13-3-227.1

Nissen TL, Schulze U, Nielsen J, Villadsen J (1997) Flux distributions in anaerobic, glucose-limited continuous cultures of *Saccharomyces cerevisiae*. Microbiology 143:203–218 . doi: 10.1099/00221287-143-1-203

Ogawa T, Aiba S (1981) Bioenergetic analysis of mixotrophic growth in *Chlorella vulgaris* and *Scenedesmus acutus*. Biotechnol Bioeng 23:1121–1132 . doi: 10.1002/bit.260230519

Otterstedt K, Larsson C, Bill RM, Ståhlberg A, Boles E, Hohmann S, Gustafsson L (2004) Switching the mode of metabolism in the yeast *Saccharomyces cerevisiae*. EMBO Rep 5:532–537 . doi: 10.1038/sj.embor.7400132

Oulhen N, Schulz BJ, Carrier TJ (2016) English translation of Heinrich Anton de Bary's 1878 speech, 'Die Erscheinung der Symbiose' ('De la symbiose'). Symbiosis 69:131–139 . doi: 10.1007/s13199-016-0409-8

Overkamp KM, Bakker BM, Ko P, P J, Pronk JT (2000) In Vivo Analysis of the Mechanisms for Oxidation of Cytosolic NADH by *Saccharomyces cerevisiae* Mitochondria. Society 182:2823–2830 . doi: 10.1128/JB.182.10.2823-2830.2000.Updated

Pagnanelli F, Altimari P, Trabucco F, Toro L (2014) Mixotrophic growth of *Chlorella vulgaris* and *Nannochloropsis oculata*: Interaction between glucose and nitrate. J Chem Technol Biotechnol 89:652–661 . doi: 10.1002/jctb.4179

Papone T, Kookkhunthod S, Paungbut M, Leesing R (2016a) Producing of Microbial Oil by Mixed Culture of Microalgae and Oleaginous Yeast Using Sugarcane Molasses as Carbon Substrate. J Clean Energy Technol 4:253–256 . doi: 10.7763/JOCET.2016.V4.292

Papone T, Kookkhunthod S, Paungbut M, Leesing R (2016b) Microbial Oil Production by Monoculture and Mixed Cultures of Microalgae and Oleaginous Yeasts using Sugarcane Juice as Substrate. J Clean Energy Technol 4:253–256 . doi: 10.7763/JOCET.2016.V4.292

Paš M, Piškur B, Šuštarič M, Raspor P (2007) Iron enriched yeast biomass - A promising mineral feed supplement. Bioresour Technol 98:1622–1628 . doi: 10.1016/j.biortech.2006.06.002

Peña A, Sánchez NS ilvi., Álvarez H, Calahorra M, Ramírez J (2015) Effects of high medium pH on growth, metabolism and transport in *Saccharomyces cerevisiae*. FEMS Yeast Res 15:1–13 . doi: 10.1093/femsyr/fou005

Perez-Garcia O, De-Bashan LE, Hernandez JP, Bashan Y (2010) Efficiency of growth and nutrient uptake from wastewater by heterotrophic, autotrophic, and mixotrophic cultivation of *Chlorella vulgaris* immobilized with *azospirillum brasilense*. J Phycol 46:800–812 . doi: 10.1111/j.1529-8817.2010.00862.x

Pfaffinger CE, Schöne D, Trunz S, Löwe H, Weuster-Botz D (2016) Model-based optimization of microalgae areal productivity in flat-plate gas-lift photobioreactors. Algal Res 20:153–163 . doi: 10.1016/j.algal.2016.10.002

Pfeiffer T, Morley A (2014) An evolutionary perspective on the Crabtree effect. Front Mol Biosci 1:1–6 . doi: 10.3389/fmolb.2014.00017

Pisman TI, Somova LA (2003) Interaction of a mixed yeast culture in an "autotroph-heterotroph" system with a closed atmosphere cycle and spatially separated components. Adv Sp Res 31:1751–1756 . doi: 10.1016/S0273-1177(03)00116-9

Porra RJ (1990) The assay of chlorophylls a and b converted to their respective magnesium-rhodochlorin derivatives by extraction from recalcitrant algal cells with aqueous alkaline methanol: Prevention of allomerization with reductants. BBA - Bioenerg 1015:493–502 . doi: 10.1016/0005-2728(90)90083-G

Pragya N, Pandey KK, Sahoo PK (2013) A review on harvesting, oil extraction and biofuels production technologies from microalgae. Renew Sustain Energy Rev 24:159–171 . doi: 10.1016/j.rser.2013.03.034

Puangbut M, Leesing R (2012) Integrated Cultivation Technique for Microbial Lipid Production by Photosynthetic Microalgae and Locally Oleaginous Yeast. World Acad Sci Eng Technol 64:975–979 . doi: 10.1016/S0022-5320(69)90089-6

Qiang H, Richmond A (1996) Productivity and photosynthetic efficiency of *Spirulina platensis* as affected by light intensity, algal density and rate of mixing in a flat plate photobioreactor. J Appl Phycol 8:139–145 . doi: 10.1007/BF02186317

Quéméner ED Le, Bouchez T (2014) A thermodynamic theory of microbial growth. ISME J 8:1747–1751 . doi: 10.1038/ismej.2014.7

Rachlin JW, Grosso A (1991) The Effects of pH on the Growth of *Chlorella vulgaris* and its Interactions with Cadmium Toxicity. Arch Environ Contam Toxicol 20:505–508 . doi: 10.1007/BF01065839

Rai PK, Singh SP, Asthana RK (2012) Biohydrogen production from cheese whey wastewater in a two-step anaerobic process. Appl Biochem Biotechnol 167:1540–1549 . doi: 10.1007/s12010-011-9488-4

Richmond A (ed) (2017) Handbook of Microalgae Culture: Biotechnology and Applied Phycology. Blackwell Science

Rosenfeld E, Beauvoit B, Blondin B, Salmon J (2003) Oxygen Consumption by Anaerobic *Saccharomyces cerevisiae* under Enological Conditions: Effect on Fermentation Kinetics. Appl Environ Microbiol 69:113–121 . doi: 10.1128/AEM.69.1.113

Sablayrolles J.M. BP (1986) Evaluation des besoins en oxygène des fermentations alcooliques en conditions oenologiques simulées. Sci des Aliment n°6:373–383

Sablayrolles JM, Dubois C, Manginot C, Roustan JL, Barre P (1996) Effectiveness of combined ammoniacal nitrogen and oxygen additions for completion of sluggish and stuck wine fermentations. J Ferment Bioeng 82:377–381 . doi: 10.1016/0922-338X(96)89154-9

Safi C, Zebib B, Merah O, Pontalier PY, Vaca-Garcia C (2014) Morphology, composition, production, processing and applications of *Chlorella vulgaris*: A review. Renew Sustain Energy Rev 35:265–278 . doi: 10.1016/j.rser.2014.04.007

Sakai T, Uchida T, Chibata I (1973) Accumulation of Nicotinamide Adenine Dinucleotide in Baker's Yeast by Secondary Culture. Agric Biol Chem 37:1049–1056 . doi: 10.1080/00021369.1973.10860805

Salmon JM (2006) Interactions between yeast, oxygen and polyphenols during alcoholic

fermentations: Practical implications. LWT - Food Sci Technol 39:959–965 . doi: 10.1016/j.lwt.2005.11.005

Santos CA, Caldeira ML, Lopes da Silva T, Novais JM, Reis A (2013) Enhanced lipidic algae biomass production using gas transfer from a fermentative *Rhodosporidium toruloides* culture to an autotrophic *Chlorella protothecoides* culture. Bioresour Technol 138:48–54 . doi: 10.1016/j.biortech.2013.03.135

Santos CA, Ferreira ME, Lopes Da Silva T, Gouveia L, Novais JM, Reis A (2011) A symbiotic gas exchange between bioreactors enhances microalgal biomass and lipid productivities: Taking advantage of complementary nutritional modes. J Ind Microbiol Biotechnol 38:909–917 . doi: 10.1007/s10295-010-0860-0

Santos CA, Reis A (2014) Microalgal symbiosis in biotechnology. Appl Microbiol Biotechnol 98:5839–5846 . doi: 10.1007/s00253-014-5764-x

Sanz-Luque E, Chamizo-Ampudia A, Llamas A, Galvan A, Fernandez E (2015) Understanding nitrate assimilation and its regulation in microalgae. Front Plant Sci 6: . doi: 10.3389/fpls.2015.00899

Sato K, Yoshida Y, Hirahara T, Ohba T (2000) On-Line Measurement of Intracellular ATP of *Saccharomyces cerevisiae* and Pyruvate during Sake Mashing. J Biosci Bioeng 90:294–301

Sauer N (1984) A general amino-acid permease is inducible in *Chlorella vulgaris*. Planta 161:425–431 . doi: 10.1007/BF00394573

Scanes KT, Hohmann S, Prior B a (1998) Glycerol Production by the Yeast *Saccharomyces cerevisiae* and its Relevance to Wine: A Review. South African J Enol Vitic 19:17–24

Scherholz ML, Curtis WR (2013) Achieving pH control in microalgal cultures through fed-batch addition of stoichiometrically-balanced growth media. BMC Biotechnol 13: . doi: 10.1186/1472-6750-13-39

Schifferdecker AJ, Dashko S, Ishchuk OP, Piškur J (2014) The wine and beer yeast *Dekkera bruxellensis*. Yeast 31:323–332 . doi: 10.1002/yea.3023

Scragg AH, Illman AM, Carden A, Shales SW (2002) Growth of microalgae with increased calorific values in a tubular bioreactor. Biomass and Bioenergy 23:67–73 . doi: 10.1016/S0961-9534(02)00028-4

Shi X-M, Liu H-J, Zhang X-W, Chen F (1999) Production of biomass and lutein by *Chlorella protothecoides* at various glucose concentrations in heterotrophic cultures. Process Biochem 34:341–347 . doi: 10.1016/S0032-9592(98)00101-0

Shu CH, Tsai CC, Chen KY, Liao WH, Huang HC (2013) Enhancing high quality oil accumulation and carbon dioxide fixation by a mixed culture of *Chlorella sp.* and *Saccharomyces cerevisiae*. J Taiwan Inst Chem Eng 44:936–942 . doi: 10.1016/j.jtice.2013.04.001

Silaban A, Bai R, Gutierrez-Wing MT, Negulescu II, Rusch KA (2014) Effect of organic

carbon, C:N ratio and light on the growth and lipid productivity of microalgae/cyanobacteria coculture. Eng Life Sci 14:47–56 . doi: 10.1002/elsc.201200219

Siverio JM (2002) Assimilation of nitrate by yeasts. FEMS Microbiol Rev 26:277–284 . doi: 10.1016/S0168-6445(02)00100-6

Smith RT, Bangert K, Wilkinson SJ, Gilmour DJ (2015) Synergistic carbon metabolism in a fast growing mixotrophic freshwater microalgal species *Micractinium inermum*. Biomass and Bioenergy 82:73–86 . doi: 10.1016/j.biombioe.2015.04.023

Subashchandrabose SR, Ramakrishnan B, Megharaj M, Venkateswarlu K, Naidu R (2011) Consortia of cyanobacteria/microalgae and bacteria: Biotechnological potential. Biotechnol Adv 29:896–907 . doi: 10.1016/j.biotechadv.2011.07.009

Subba Rao DV, Pan Y, Al-Yamani F (2005) Growth and photosynthetic rates of *Chlamydomonas plethora* and *Nitzschia frustula* cultures isolated from Kuwait Bay, Arabian Gulf, and their potential as live algal food for tropical mariculture. Mar Ecol 26:63–71 . doi: 10.1111/j.1439-0485.2005.00043.x

Suomalainen H, Bjorklund A, Vihervaara K, Oura E (1965) Nicotinic acid and nicotinamide adenine dinucleotide contents of baker's yeast in changing culture conditions. J Inst Brew 71:221–226

Syrett PJ, Morris I (1963) The inhibition of nitrate assimilation by ammonium in *chlorella*. Biochim Biophys Acta - Spec Sect Enzymol Subj 67:566–575 . doi: 10.1016/0926-6569(63)90277-3

Thomsson E, Gustafsson L, Larsson C (2005) Starvation response of *Saccharomyces cerevisiae* grown in anaerobic nitrogen- or carbon-limited chemostat cultures. Appl Environ Microbiol 71:3007–3013 . doi: 10.1128/AEM.71.6.3007-3013.2005

Turpin DH, Elrifi IR, Birch DG, Weger HG, Holmes JJ (1988) Interactions between photosynthesis, respiration, and nitrogen assimilation in microalgae. Can J Bot 66:2083–2097 . doi: 10.1139/b88-286

van Dijken JP, Weusthuis RA, Pronk JT (1993) Kinetics of growth and sugar consumption in yeasts. Antonie Van Leeuwenhoek 63:343–352 . doi: 10.1007/BF00871229

Verduyn C, Postma E, Scheffers A, Dijken J (1990a) Energetics of *Saccharomyces cerevisiae* in anaerobic glucose-limited chemostat cultures. Biotechnol Bioeng 405–412

Verduyn C, Postma E, Scheffers WA, van Dijken JP (1990b) Physiology of *Saccharomyces cerevisiae* in Anaerobic Glucose-Limited Chemostat Cultures. J Gen Microbiol 136:395–403 . doi: 10.1099/00221287-136-3-395

Verduyn C, Zomerdijk TPL, Dijken JP, Scheffers WA (1984) Continuous measurement of ethanol production by aerobic yeast suspensions with an enzyme electrode. Appl Microbiol Biotechnol 19:181–185 . doi: 10.1007/BF00256451

Walker G, Stewart G (2016) *Saccharomyces cerevisiae* in the Production of Fermented Beverages. Beverages 2:30 . doi: 10.3390/beverages2040030

Wang J, Yang H, Wang F (2014) Mixotrophic cultivation of microalgae for biodiesel production: Status and prospects. Appl Biochem Biotechnol 172:3307–3329 . doi: 10.1007/s12010-014-0729-1

Wang R, Tian Y, Xue S, Zhang D, Zhang Q, Wu X, Kong D, Cong W (2016) Enhanced microalgal biomass and lipid production via co-culture of *Scenedesmus obliquus* and *Candida tropicalis* in an autotrophic system. J Chem Technol Biotechnol 91:1387–1396 . doi: 10.1002/jctb.4735

Weber FJ, Bont JAM De (1996) Adaptation mechanisms of microorganisms to the toxic effects of organic solvents on membranes. Biochim Biophys Acta 1286:225–245 . doi: http://dx.doi.org/10.1016/S0304-4157(96)00010-X

Werner-Washburne M, Braun E, Johnston GC, Singer RA (1993) Stationary phase in the yeast *Saccharomyces cerevisiae*. Microbiol Rev 57:383–401 . doi: 10.1093/nar/gkr782

Wilhelm C, Büchel C, Fisahn J, Goss R, Jakob T, LaRoche J, Lavaud J, Lohr M, Riebesell U, Stehfest K, Valentin K, Kroth PG (2006) The Regulation of Carbon and Nutrient Assimilation in Diatoms is Significantly Different from Green Algae. Protist 157:91–124 . doi: 10.1016/j.protis.2006.02.003

Xia J, Oyler GA, Yu G, Wan M, Rosenberg JN, Jin X, Betenbaugh MJ, Nie Z (2014) The effect of iron on growth, lipid accumulation, and gene expression profile of the freshwater microalga *Chlorella sorokiniana*. Appl Microbiol Biotechnol 98:9473–9481 . doi: 10.1007/s00253-014-6088-6

Xin L, Hong-ying H, Ke G, Ying-xue S (2010) Effects of different nitrogen and phosphorus concentrations on the growth, nutrient uptake, and lipid accumulation of a freshwater microalga *Scenedesmus sp.* Bioresour Technol 101:5494–5500 . doi: 10.1016/j.biortech.2010.02.016

Xiong W, Gao C, Yan D, Wu C, Wu Q (2010) Double CO_2 fixation in photosynthesis-fermentation model enhances algal lipid synthesis for biodiesel production. Bioresour Technol 101:2287–2293 . doi: 10.1016/j.biortech.2009.11.041

Xu Z, Jiang Y, Zhou G (2015) Response and adaptation of photosynthesis, respiration, and antioxidant systems to elevated CO_2 with environmental stress in plants. Front Plant Sci 6:1–17 . doi: 10.3389/fpls.2015.00701

Xue F, Miao J, Zhang X, Tan T (2010) A new strategy for lipid production by mix cultivation of *Spirulina platensis* and *Rhodotorula glutinis*. Appl Biochem Biotechnol 160:498–503 . doi: 10.1007/s12010-008-8376-z

Yalçin SK, Özbas ZY (2004) Effects of different substrates on growth and glycerol production kinetics of a wine yeast strain *Saccharomyces cerevisiae* Narince 3. Process Biochem 39:1285–1291 . doi: 10.1016/S0032-9592(03)00252-8

Yamamoto M, Fujishita M, Hirata A, Kawano S (2004) Regeneration and maturation of daughter cell walls in the autospore-forming green alga *Chlorella vulgaris* (Chlorophyta, Trebouxiophyceae). J Plant Res 117:257–264 . doi: 10.1007/s10265-004-0154-6

Yang C, Hua Q, Shimizu K (2002) Integration of the information from gene expression and metabolic fluxes for the analysis of the regulatory mechanisms in Synechocystis. Appl Microbiol Biotechnol 58:813–822 . doi: 10.1007/s00253-002-0949-0

Yang C, Hua Q, Shimizu K (2000) Energetics and carbon metabolism during growth of microalgal cells under photoautotrophic, mixotrophic and cyclic light-autotrophic/dark-heterotrophic conditions. Biochem Eng J 6:87–102 . doi: 10.1016/S1369-703X(00)00080-2

Zhang K, Miyachi S, Kurano N (2001) Evaluation of a vertical flat-plate photobioreactor for outdoor biomass production and carbon dioxide bio-fixation: Effects of reactor dimensions, irradiation and cell concentration on the biomass productivity and irradiation utilization efficiency. Appl Microbiol Biotechnol 55:428–433 . doi: 10.1007/s002530000550

Zhang Z, Ji H, Gong G, Zhang X, Tan T (2014) Synergistic effects of oleaginous yeast *Rhodotorula glutinis* and microalga *Chlorella vulgaris* for enhancement of biomass and lipid yields. Bioresour Technol 164:93–99 . doi: 10.1016/j.biortech.2014.04.039

Zheng H, Gao Z, Yin F, Ji X, Huang H (2012) Effect of CO_2 supply conditions on lipid production of *Chlorella vulgaris* from enzymatic hydrolysates of lipid-extracted microalgal biomass residues. Bioresour Technol 126:24–30 . doi: 10.1016/j.biortech.2012.09.048

Zuccaro G, Steyer JP, van Lis R (2019) The algal trophic mode affects the interaction and oil production of a synergistic microalga-yeast consortium. Bioresour Technol 273:608–617 . doi: 10.1016/j.biortech.2018.11.063

Zuo Z, Rong Q, Chen K, Yang L, Chen Z, Peng K, Zhu Y, Bai Y, Wang Y (2012) Study of amino acids as nitrogen source in *Chlamydomonas reinhardtii*. Phycol Res 60:161–168 . doi: 10.1111/j.1440-1835.2012.00646.x

Appendices

Appendix 1

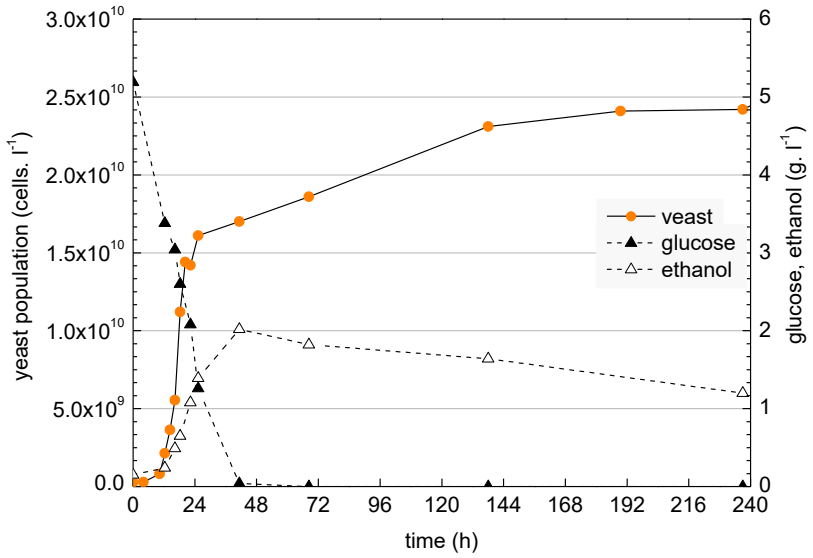

Figure 1.1. Yeast growth in aerated shake flask using Mix medium with **5 g. l^{-1} of glucose**.

Appendix 2

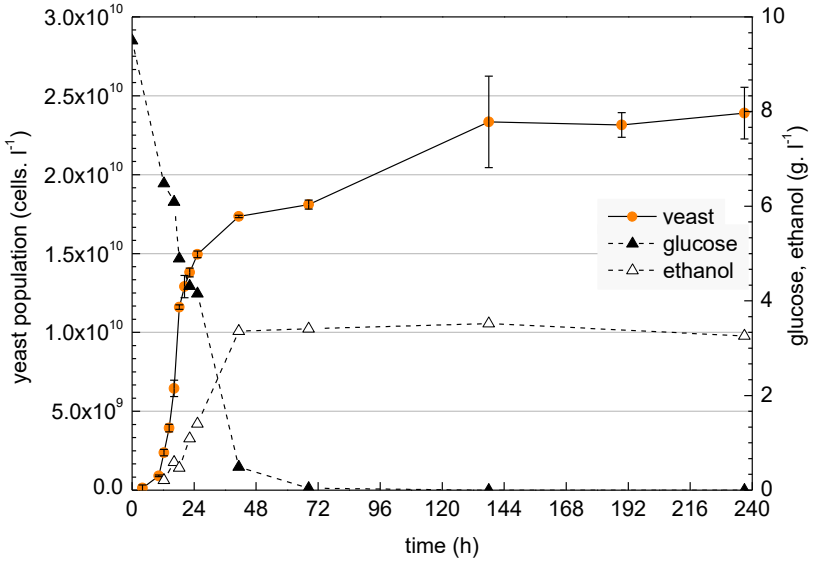

Figure 2.1. Yeast growth in aerated shake flask using Mix medium with **10 g. l^{-1} glucose**. The experiment was performed in duplicate.

Appendix 3

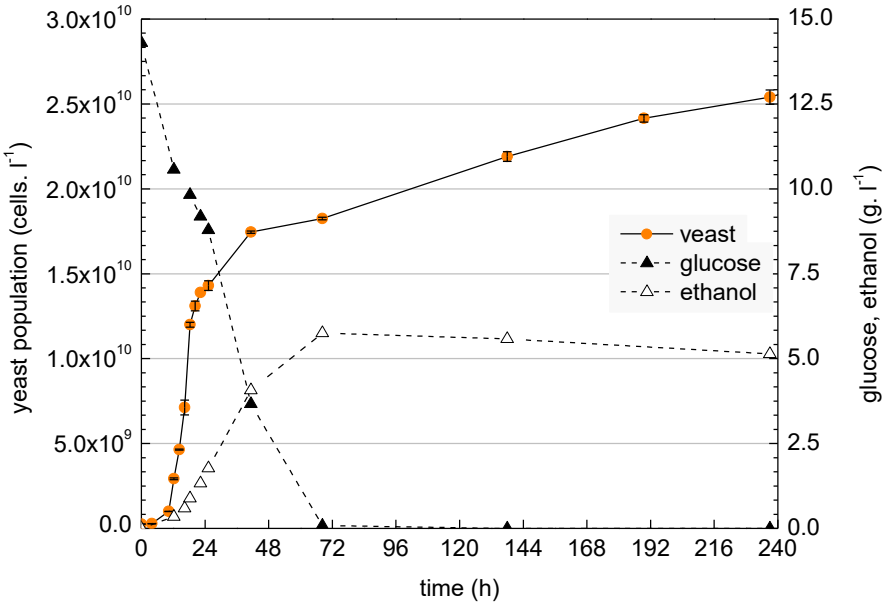

Figure 3.1. Yeast growth in aerated shake flask using Mix medium with **15 g. l-1 glucose**. . The experiment was performed in duplicate.

Appendix 4

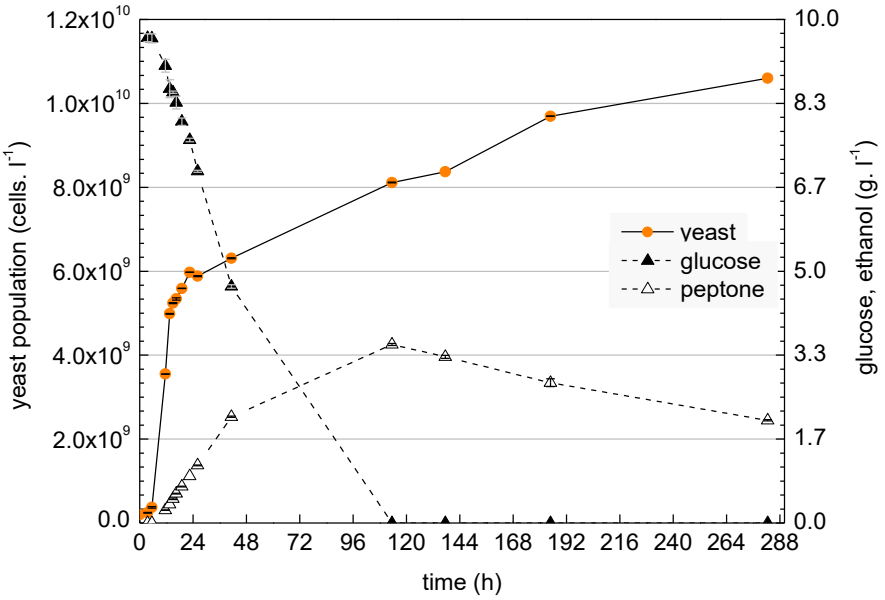

Figure 4.1. Yeast growth in aerated shake flask using Mix medium with **10 g. l^{-1} peptone**. This experiment was performed in duplicate.

Appendix 5

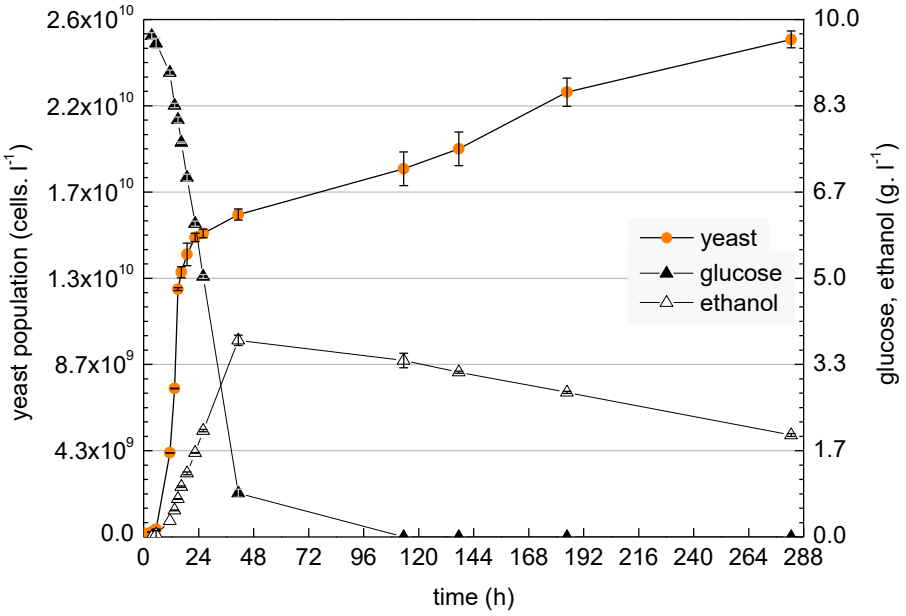

Figure 5.1. Yeast growth in aerated shake flask using Mix medium with **20 g. l^{-1} peptone**. This experiment was performed in duplicate.

Appendix 6

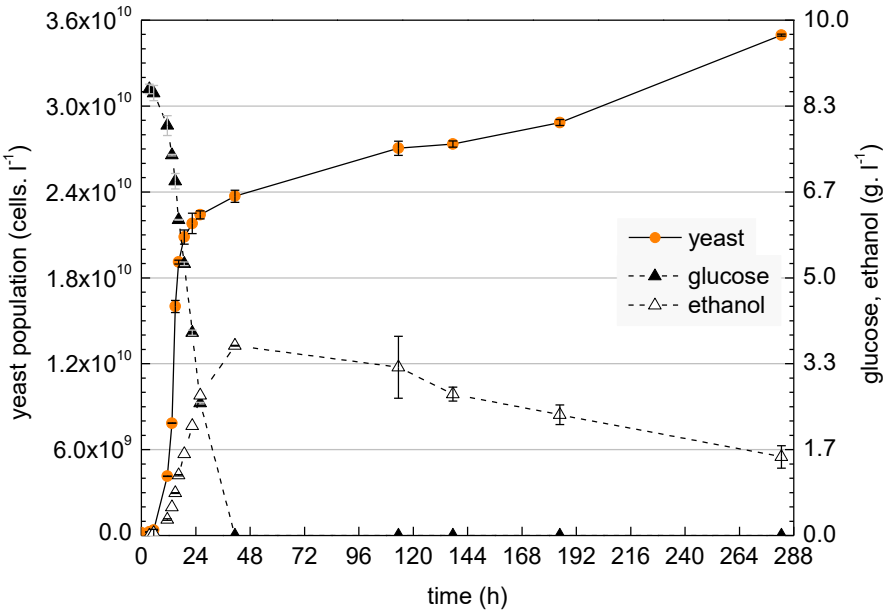

Figure 6.1. Yeast growth in aerated shake flask using Mix medium with **30 g. l^{-1} peptone**. This experiment was performed in duplicate.

Appendix 7

The extinction coefficient b (l. g^{-1} cm^{-1}) of microalgae corresponds to the slope of the linear relation:

$$ln(1 - Absorbance) = 1.43[microalgae]$$

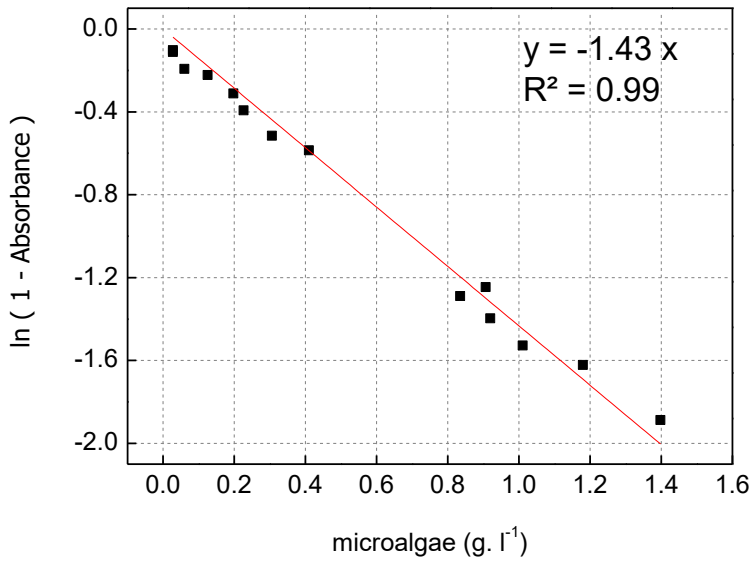

Figure 7.1. Correlation between absorbance and microalgae biomass.

Appendix 8

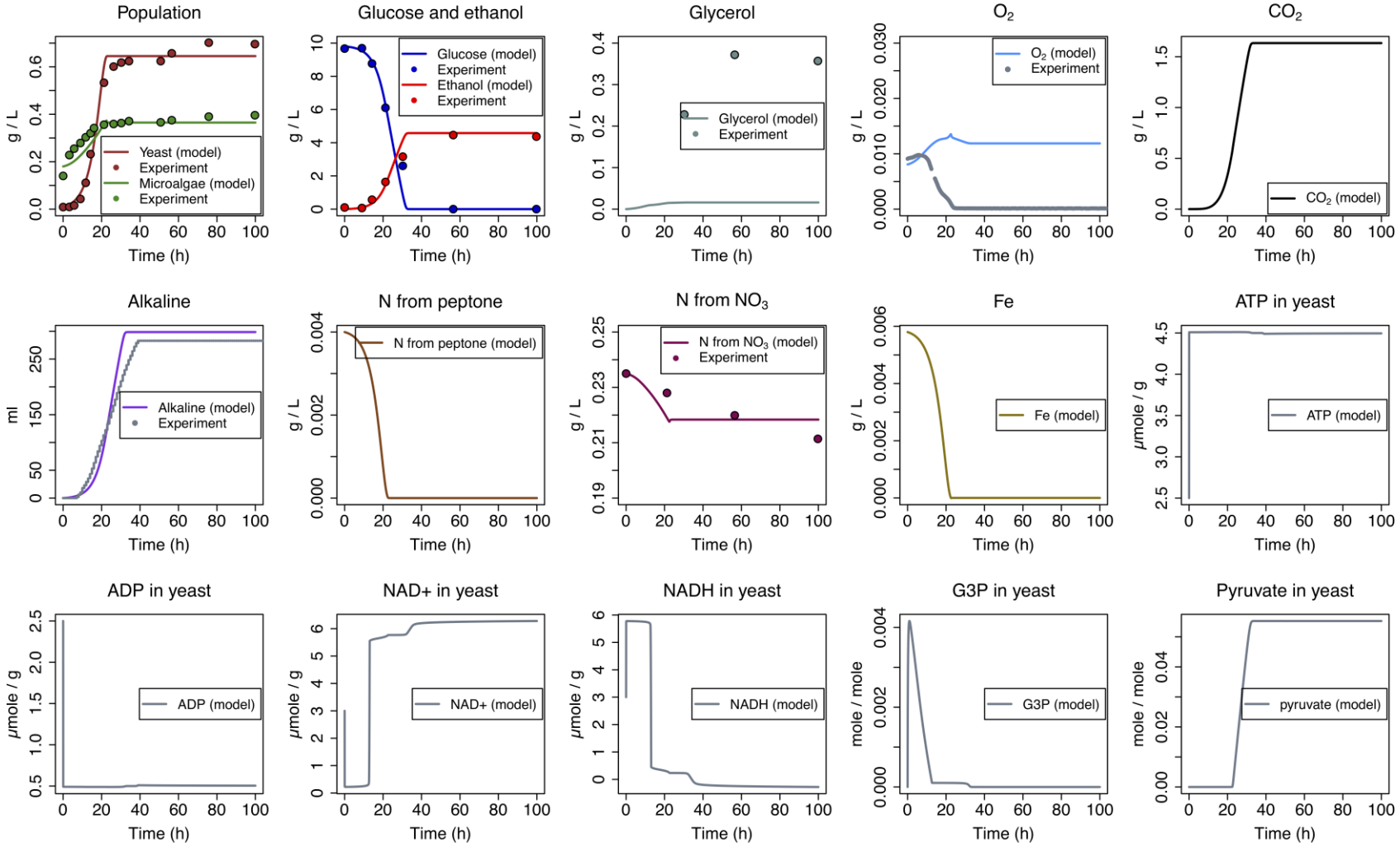

Figure 8.1. Simulation results of yeast and microalgae growth model in mixed culture **without** increase of glycerol kinetic factor of 70.

Appendix 9

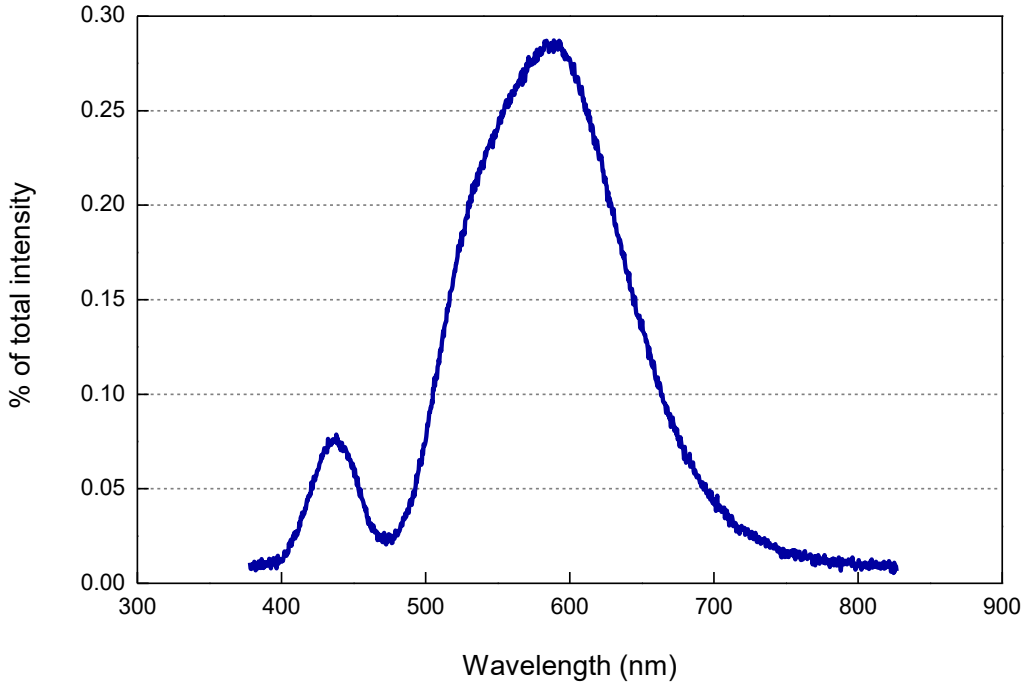

Figure 9.1. Emission spectrum of LED lamp

Appendix 10 - Summary in French

Le monde passe d'une économie linéaire, basée sur le pétrole, à une bioéconomie circulaire agricole. Les effets nocifs du CO_2 anthropique et d'autres gaz à effet de serre sont de plus en plus évidents. Dans ce contexte, le développement de procédés de biotransformation "verts" qui utilisent le moins d'énergie possible de la manière la plus efficace et qui produisent le moins de déchets nocifs est de la plus haute importance. Le CO_2 est produit comme déchet à partir de nombreux processus de biotransformation. Une fois libéré, le CO_2 exerce son influence néfaste avant de pouvoir être à nouveau capté par les cultures agricoles. Les processus chimiques et physiques de captage du CO_2 avant son rejet dans l'atmosphère s'accompagnent d'une consommation de combustibles fossiles. Même la récupération agricole du CO_2 entraîne des coûts énergétiques associés à la culture, à la récolte et à la transformation des cultures. De manière générale, une fois que le CO_2 quitte le bioréacteur, sa capture est toujours associée à l'utilisation d'énergie qui provient souvent de sources de combustibles fossiles et donc à la libération d'une plus grande quantité de CO_2 de sources fossiles. Par conséquent, la séquestration biologique *in situ* de ce gaz a l'avantage potentiel de réduire la libération du carbone fossile dans l'atmosphère et de limiter les dommages environnementaux qui peuvent être causés avant que le CO_2 soit recapturé.

D'un point de vue commercial, la perte d'une partie considérable du substrat sous forme de CO_2 est une pratique inefficace qui ne peut être évitée avec les cultures microbiennes. Avec de nombreux processus de biotransformation, une grande partie du substrat (30-50%) est convertie en CO_2 plutôt qu'en produit d'intérêt. D'un point de vue économique, le producteur "gaspille" près de la moitié de son substrat. La recapture *in situ* du CO_2 pourrait réduire cette perte financière en offrant la possibilité d'utiliser entièrement le substrat, tout en rendant le procédé durable. À cette fin, l'association de la photosynthèse au processus de production normal est la meilleure solution. Ce processus naturel est basé sur des relations symbiotiques entre organismes.

Des systèmes basés sur la symbiose entre espèces microbiennes ont été étudiés pour des applications biotechnologiques dans les bioprocédés et la protection de l'environnement. Le choix des espèces microbiennes (microalgues, bactéries ou levures) dépend des objectifs finaux de la coculture : récolte par bioflocculation, traitement des eaux usées, production de substances polymères extracellulaires ou promotion de croissance et production lipidique. La création et le contrôle de consortiums spécifiques, dotés de l'écologie microbienne souhaitée, est essentielle à l'utilisation de ces consortiums en biotechnologie industrielle.

Le taux de production de CO_2 hétérotrophe est généralement largement supérieur au taux de consommation autotrophe, d'où la nécessité d'équilibrer les populations mixtes du point de vue de l'atténuation du CO_2, de manière à ce que la population photosynthétique puisse supporter le taux de production de CO_2. En d'autres termes, l'activité hétérotrophe doit être en phase avec le taux d'élimination du CO_2. Cet objectif pourrait être atteint grâce à la co-dominance des populations permettant une synergie entre les deux organismes, basée sur les échanges gazeux. Jusqu'à présent, aucune étude scientifique ne présente de travaux dont le l'objectif est de développer des cultures mixtes symbiotiques et co-dominantes.

Les résultats présentés dans ce manuscrit de thèse montrent la faisabilité de développer un procédé qui repose sur la symbiose mutuelle entre la levure *Saccharomyces cerevisiae* et la microalgue *Chlorella vulgaris* autour des échanges de gaz, en imposant une co-dominance en termes de population. Les populations doivent être équilibrées pour que les microalgues puissent gérer la production de CO_2. Le procédé est réalisé en photo-bioréacteur de 5 litres non-aéré et fermé, afin d'éviter les échanges gazeux avec l'environnement externe. Dans cette configuration, le CO_2 est produit sous forme dissoute et directement accessible aux microalgues, évitant les phénomènes de dégazage et de dissolution. Les populations de levures et de microalgues atteignent une concentration égale ($2x10^{10}$ cellules. l^{-1}) au bout de 24 heures de culture, restent stables jusqu'à la fin de la culture (168 heures) et les microalgues recyclent 12% du CO_2 produit par les levures. Un modèle cinétique de la levure et de la microalgue en culture mixte est développé en combinant le modèle individuel de la levure et celui de la microalgue. Le modèle prédictif de la levure prend en compte les possibles voies métaboliques impliquées dans la fermentation et la respiration de ces voies est prédite en y intégrant des facteurs de limitation. Le modèle de la microalgue est basé sur l'activité photosynthétique.

A travers cette étude, nous proposons une méthodologie générale pour le développement et l'étude d'une culture mixte symbiotique et co-dominante d'un hétérotrophe et d'un autotrophe et nous évaluons le succès et les enjeux d'une telle stratégie. Les travaux présentés ici ont été réalisés à partir d'organismes modèles bien connus, mais peuvent servir de base à des études plus appliquées. Le potentiel d'une culture mixte symbiotique est l'autorégulation de la production et de l'utilisation du CO_2. Un tel procédé permettrait de réaliser des économies en limitant l'approvisionnement en gaz et en permettant une utilisation plus complète du substrat, tout en réduisant les émissions de CO_2 dans l'environnement. Le potentiel économique et écologique réside dans la capacité à coordonner la vitesse de bioconversion avec la vitesse de l'activité photosynthétique.

List of figures

List of tables

ÉCOLE DOCTORALE
Sciences mécaniques et énergétiques, matériaux et géosciences (SMEMAG)

Titre : Développement d'un procédé symbiotique entre *Saccharomyces cerevisiae* et *Chlorella vulgaris* en photo-bioréacteur pour une limitation en rejet de CO_2 *in situ*

Mots clés : consortium microbien, culture mixte et co-dominante, échange de gaz, modèle de croissance, photo-bioréacteur, métabolisme

Résumé : La levure et la microalgue sont des microorganismes très étudiés pour la production de composés à haute valeur ajoutée pour des secteurs tels que l'agroalimentaire et l'énergie. Ce travail de thèse propose un procédé de culture mixte entre la levure *Saccharomyces cerevisiae* et la microalgue *Chlorella vulgaris* pour la croissance des deux espèces tout en limitant le rejet en CO_2. Le procédé repose sur la symbiose mutuelle entre les deux organismes autour des échanges de gaz, qui est rendu possible en imposant une co-dominance en termes de population. Les populations doivent être équilibrées pour que les microalgues puissent gérer la production de CO_2. Le procédé est réalisé en photo-bioréacteur de 5 litres non-aéré et fermé, afin d'éviter les échanges gazeux avec l'environnement externe. Dans cette configuration, le CO_2 est produit sous forme dissoute et directement accessible aux microalgues, évitant les phénomènes de dégazage et de dissolution. Les populations de levures et de microalgues atteignent une concentration égale ($2x10^{10}$ cellules. l^{-1}) au bout de 24 heures de culture, restent stables jusqu'à la fin de la culture (168 heures) et les microalgues recyclent 12% du CO_2 produit par les levures. Un modèle cinétique de la levure et de la microalgue en culture mixte est développé en combinant le modèle individuel de la levure et celui de la microalgue. Le modèle prédictif de la levure prend en compte les possibles voies métaboliques impliquées dans la fermentation et la respiration de ces voies est prédite en y intégrant des facteurs de limitation. Le modèle de la microalgue est basé sur l'activité photosynthétique. Les résultats de ce travail montrent la faisabilité du procédé de culture mixte entre hétérotrophe et autotrophe et pourrait apporter les bases pour le développement d'un procédé écologique à faible impact environnemental.

Title : Process development for symbiotic culture of *Saccharomyces cerevisiae* and *Chlorella vulgaris* for in situ CO_2 mitigation

Keywords : microbial consortium, co-dominant mixed culture, gas exchange, growth model, photo-bioreactor, metabolism

Abstract : Yeast and microalgae are microorganisms widely studied for the production of high-value compounds used in food and energy area. This work proposes a process of mixed culture of *Saccharomyces cerevisiae* and *Chlorella vulgaris* for both growth and CO_2 mitigation. The process relies on mutual symbiosis between the two organisms through gas exchange, which is possible by engineering the co-dominance of populations. The two populations must be balanced in such a way so that microalgae can cope with the rate of CO_2 production by the yeast activity. The process is performed in non-aerated 5l-photo-bioreactor fitted with a fermentation lock to prevent gas exchange with the outside atmosphere. With this set-up, the CO_2 is produced in dissolved form and is available to the microalgae avoiding degassing and dissolution phenomena. The two organism populations are balanced at approximately $2x10^{10}$ cells. l^{-1}, 12% CO_2 produced by yeast was reutilized by microalgae within 168 hours of culture. A yeast and microalgae growth model in mixed culture is developed by combining each individual growth model. The predictive yeast model considers the possible metabolic pathways involved in fermentation and respiration and imposes limitation factors on these pathways, in this manner, the model can predict the partition of these pathways. The microalgae individual model is based on the photosynthetic activity. The results of this work show the feasibility of such process and could provide a basis for the development of a green process of low environmental impact.

Université Paris-Saclay
Espace Technologique / Immeuble Discovery
Route de l'Orme aux Merisiers RD 128 / 91190 Saint-Aubin, France